



Strellis, Bethany (2025) *Defining the role of receptor phosphorylation on mGlu5 metabotropic glutamate receptor signal transduction*. PhD thesis.

<https://theses.gla.ac.uk/84922/>

Copyright and moral rights for this work are retained by the author

A copy can be downloaded for personal non-commercial research or study, without prior permission or charge

This work cannot be reproduced or quoted extensively from without first obtaining permission from the author

The content must not be changed in any way or sold commercially in any format or medium without the formal permission of the author

When referring to this work, full bibliographic details including the author, title, awarding institution and date of the thesis must be given

Enlighten: Theses

<https://theses.gla.ac.uk/>
research-enlighten@glasgow.ac.uk

Defining the Role of Receptor Phosphorylation on mGlu₅ Metabotropic Glutamate Receptor Signal Transduction

Bethany Strellis

BSc

Submitted in Fulfilment of the Requirements for the Degree of
Doctor of Philosophy

School of Molecular Biosciences
College of Medical, Veterinary and Life Science
University of Glasgow

September 2024



University
of Glasgow

Abstract

The type 5 metabotropic glutamate receptor (mGlu₅) is a G protein-coupled receptor (GPCR) located on excitatory neurons, and its dysfunction has been linked to multiple neuropathologies such as Alzheimer's disease (Abd-Elrahman et al., 2020). Previous data from our laboratory on phosphoproteomic analysis of the hippocampus of wildtype mice showed that global mGlu₅ phosphorylation increases following a fear conditioning learning and memory test, but the specific role of phosphorylation on signal transduction was not identified. To elucidate the role of mGlu₅ phosphorylation, the aim of this thesis was to dissect the signal transduction pathways downstream of G protein versus phosphorylation dependent pathways.

Phosphodeficient mutants of mGlu₅ were generated by synthesising a mouse ortholog mGlu₅ C-terminus with either all serine residues (mGlu₅-PD), or all serine and threonine residues (total phosphodeficient mutant, mGlu₅-TPD) mutated to alanine. Signal transduction pathways were assessed by generating stable cell lines expressing either wildtype mGlu₅, mGlu₅-PD or mGlu₅-TPD. In β -arrestin 2 recruitment assays, removal of putative phosphorylation sites within the C-terminus of mGlu₅ was found to negatively impact the ability of the receptor to recruit β -arrestin 2. In calcium mobilisation, IP₁ accumulation, and G protein dissociation assays assessing the G α_q dependent transduction pathway, there was no difference in responses between wildtype and phosphodeficient mutant receptors following agonist stimulation. However, the basal activity was reduced with removal of putative C-terminal phosphorylation sites. To further examine G protein activation, a bioluminescent resonance energy transfer (BRET)-based single genetically encoded biosensor was generated to compare the impact of phosphorylation on mGlu₅ G protein activation. Findings with this biosensor revealed a reduced level of G protein activation with the phosphodeficient mutants compared to wildtype receptor.

These results demonstrate that phosphorylation of the mGlu₅ C-terminus appears to predominantly modulate ligand-independent signalling through the G protein-coupled pathway, whilst phosphorylation of C-terminal serine and threonine residues impacts ligand-dependent and ligand-independent β -arrestin 2 recruitment. Therefore, understanding the impact of mGlu₅ phosphorylation on

receptor signalling is likely to be crucial when considering the therapeutic potential of this receptor.

Contents

| | |
|---|------|
| Abstract..... | ii |
| List of Tables..... | viii |
| List of Figures | ix |
| List of Publications | xi |
| Abstracts..... | xi |
| Publications | xi |
| Acknowledgements..... | xii |
| Abbreviations | xiii |
| Author's Declaration..... | xix |
| 1 Introduction..... | 1 |
| 1.1 G Protein-Coupled Receptors..... | 2 |
| 1.1.1 Overview | 2 |
| 1.1.2 Classification of GPCR Families | 2 |
| 1.1.3 G Protein Signalling | 5 |
| 1.1.4 β -Arrestin Signalling and Receptor Internalisation | 7 |
| 1.1.5 Constitutive Activity of GPCRs..... | 9 |
| 1.1.6 Using Biosensors as a Tool to Measure GPCR Activation..... | 10 |
| 1.2 The Pharmacology of Ligands Acting at GPCRs | 13 |
| 1.2.1 The Clinical Potential of Allosteric Modulators | 15 |
| 1.3 Glutamate Receptors..... | 17 |
| 1.3.1 Classification of Metabotropic Glutamate Receptors..... | 17 |
| 1.3.2 Architecture of Metabotropic Glutamate Receptors..... | 20 |
| 1.3.3 Localisation and Subcellular Expression of mGlu Receptors | 24 |
| 1.3.4 Constitutive Activity of the mGlu ₅ Receptor..... | 26 |
| 1.3.5 The Therapeutic Potential of mGlu ₅ in the Central Nervous System... | 27 |
| 1.4 Phosphorylation | 35 |
| 1.4.1 The Role of Direct GPCR Phosphorylation | 35 |
| 1.4.2 Phosphorylation of mGlu ₅ | 36 |
| 1.4.3 Methods to Study Phosphorylation..... | 38 |
| 1.5 Thesis Aims | 45 |
| 2 Materials and Methods | 46 |
| 2.1 Materials | 47 |
| 2.1.1 Pharmacological Compounds | 47 |
| 2.1.2 Primers..... | 47 |
| 2.1.3 Plasmid Constructs | 49 |

| | | |
|-------|---|----|
| 2.1.4 | Antibodies | 51 |
| 2.2 | Molecular Cloning of Plasmid Constructs | 52 |
| 2.2.1 | Generation of Competent <i>Escherichia coli</i> Cells | 52 |
| 2.2.2 | Transformation of Competent Cells by Heat-Shock Method | 52 |
| 2.2.3 | Isolation of Plasmid DNA from Bacterial Cultures | 53 |
| 2.2.4 | Generation of Plasmid DNA | 54 |
| 2.2.5 | mRNA Production | 57 |
| 2.3 | Cell Culture | 58 |
| 2.3.1 | Cell Line Maintenance..... | 58 |
| 2.3.2 | Cryopreservation of Cells..... | 59 |
| 2.3.3 | Transient Transfection | 59 |
| 2.3.4 | Generation of Stably Transfected Flp-In™ T-REx™ 293 Cell Lines ... | 60 |
| 2.3.5 | Primary Neuronal Cultures..... | 61 |
| 2.4 | In-Cell and On-Cell Westerns | 62 |
| 2.5 | Pharmacological and Functional Assays | 63 |
| 2.5.1 | BRET-Based β -Arrestin 2 Recruitment Assay..... | 63 |
| 2.5.2 | NanoBiT Complementation β -Arrestin 2 Recruitment Assay..... | 63 |
| 2.5.3 | Receptor Internalisation Assay | 64 |
| 2.5.4 | Calcium Mobilisation Assay | 65 |
| 2.5.5 | Measurement of Intracellular Calcium in Single Cells using Epifluorescent Microscopy..... | 65 |
| 2.5.6 | IP ₁ Accumulation Assay | 66 |
| 2.5.7 | Measurement of G Protein Dissociation..... | 67 |
| 2.5.8 | Using BRET-based Biosensors to Measure G α -GTP | 68 |
| 2.6 | Western Blotting | 69 |
| 2.6.1 | Sample Preparation | 69 |
| 2.6.2 | SDS-PAGE | 70 |
| 2.6.3 | Western Blot Probing and Detection | 71 |
| 2.6.4 | Quantification of Western Blots..... | 72 |
| 2.7 | Immunocytochemistry | 72 |
| 2.8 | Data Analysis..... | 73 |
| 2.8.1 | Analysis of Pharmacological Parameters..... | 73 |
| 2.8.2 | Statistical Analysis | 73 |
| 3 | Phosphorylation Controls β -Arrestin 2 Recruitment but not Internalisation of the Type 5 Metabotropic Glutamate Receptor | 75 |
| 3.1 | Introduction..... | 76 |
| 3.2 | Aims..... | 78 |

| | | |
|-------|---|-----|
| 3.3 | Results..... | 79 |
| 3.3.1 | Mutation of Serine Phosphorylation Sites in the M1 Acetylcholine Receptor C-Terminus Disrupts β -Arrestin 2 Recruitment | 79 |
| 3.3.2 | Mutation of mGlu ₅ C-Terminal Serine and Threonine Residues to Alanine Disrupts β -Arrestin 2 Recruitment | 83 |
| 3.3.3 | Development of a NanoBiT Assay to Measure β -Arrestin 2 Recruitment to mGlu ₅ | 86 |
| 3.3.4 | G Protein-Coupled Receptor Kinases Play a Role in Basal and Agonist Dependent β -Arrestin 2 Recruitment to mGlu ₅ | 91 |
| 3.3.5 | Mutation of mGlu ₅ C-Terminal Phosphorylation Sites Does Impact Receptor Internalisation | 96 |
| 3.3.6 | Validation of Novel mGlu ₅ Phospho-Site Specific Antibodies..... | 101 |
| 3.4 | Discussion | 109 |
| 3.5 | Conclusion..... | 122 |
| 4 | The Impact of Phosphorylation of the Type 5 Metabotropic Glutamate Receptor on G Protein Signalling..... | 123 |
| 4.1 | Introduction..... | 124 |
| 4.1.1 | The Impact of Phosphorylation on G Protein-Dependent Signalling . | 124 |
| 4.1.2 | Using the Flp-In™ T-REx™ System to Measure Glutamate Receptor Signalling..... | 125 |
| 4.1.3 | Strategies to Measure G Protein-Dependent Signalling..... | 125 |
| 4.2 | Aims..... | 130 |
| 4.3 | Results..... | 131 |
| 4.3.1 | Expression of Wildtype and Phospho-Deficient mGlu ₅ Receptors in Flp-In™ T-REx™ 293 Cells | 131 |
| 4.3.2 | Quantitative Assessment of mGlu ₅ Total and Surface Expression.... | 137 |
| 4.3.3 | The Impact of Doxycycline Concentration on Receptor Expression in Flp-In™ T-REx™ 293 Cells | 144 |
| 4.3.4 | Removal of C-terminal Phosphorylation Sites of the mGlu ₅ Receptor Impacts Intracellular Calcium Mobilisation..... | 153 |
| 4.3.5 | Removal of C-terminal Phosphorylation Sites of the mGlu ₅ Receptor Reduces Ligand-Independent IP ₁ Accumulation | 156 |
| 4.3.6 | Removal of C-terminal Phosphorylation Sites of the mGlu ₅ Receptor Reduces Constitutive Heterotrimeric G Protein Dissociation..... | 163 |
| 4.4 | Discussion | 168 |
| 4.5 | Conclusion..... | 176 |
| 5 | Developing a Genetically Encoded Biosensor to Directly Measure mGlu ₅ G α_q Protein Activation..... | 177 |
| 5.1 | Introduction..... | 178 |
| 5.1.1 | BRET-Based Biosensors | 178 |

| | | |
|-------|--|-----|
| 5.2 | Aims..... | 181 |
| 5.3 | Results..... | 182 |
| 5.3.1 | Generation and Optimisation of a $G\alpha_q$ -Specific Biosensor..... | 182 |
| 5.3.2 | Validating the Biosensors with $G\alpha_q$ Protein-Coupled Receptors | 192 |
| 5.3.3 | Employing a $G\alpha_q$ -Specific Biosensor to Investigate the Effect of Phosphorylation of the mGlu ₅ Receptor | 195 |
| 5.3.4 | Employing a $G\alpha_q$ Biosensor to Measure Endogenous Glutamate Receptor Mediated G Protein Activation..... | 197 |
| 5.4 | Discussion | 201 |
| 5.5 | Conclusions | 206 |
| 6 | Final Discussion | 207 |
| 7 | References | 214 |

List of Tables

| | |
|--|-----|
| Table 2.1: List of primers used for sequencing plasmids. | 47 |
| Table 2.2: PCR primers for the generation of Lyn11-SpNG-GRK2 and Lyn11-iSpNG-GRK2 biosensors..... | 48 |
| Table 2.3: List of plasmid constructs used..... | 49 |
| Table 2.4: List of primary antibodies used for western blots (WB), immunocytochemistry (ICC), or on-cell westerns (OCW). | 51 |
| Table 2.5: List of secondary antibodies used for western blots (WB), immunocytochemistry (ICC), or on-cell westerns (OCW). | 51 |
| Table 2.6: PCR reaction scheme..... | 54 |
| Table 3.1: Mass spectrometry and phosphoproteomics of cell and tissue samples reveals putative phosphorylation sites of the mGlu ₅ C-terminus. | 103 |
| Table 4.1: Peak band intensity, normalised as a percentage to wildtype receptor, of western blots following treatment with 2 ng/mL is significantly lower than treatment with 100 ng/mL doxycycline. | 148 |
| Table 4.2: Western blots from mGlu ₅ -WT, mGlu ₅ -PD and mGlu ₅ -TPD cell lysates demonstrate no significant differences in expression when induced with 2 ng/mL doxycycline. | 148 |
| Table 4.3: The Z' score for IP ₁ accumulation curves at increasing cell seeding densities | 159 |

List of Figures

| | |
|---|-----|
| Figure 1.1: The GRAFs classification of G protein-coupled receptors. | 4 |
| Figure 1.2: The heterotrimeric G protein activation sequence. | 6 |
| Figure 1.3: G protein-dependent signalling pathways following activation of the GPCR. | 7 |
| Figure 3.1: β -arrestin 2 recruitment to the murine M1 receptor is reduced but not eliminated when C-terminal serine residues are mutated to alanine. | 80 |
| Figure 3.2: β -arrestin 2 is recruited to wild type but not phosphodeficient M1 in cultured hippocampal neurons. | 82 |
| Figure 3.3: The phosphodeficient mutant receptors mGlu ₅ -PD and mGlu ₅ -TPD. | 83 |
| Figure 3.4: Constitutive and glutamate dependent β -arrestin 2 recruitment to mGlu ₅ is reduced with removal of putative C-terminal phosphorylation sites. | 85 |
| Figure 3.5: mGlu ₅ demonstrates a much weaker coupling to the β -arrestin 2 pathway compared to the free fatty acid receptor 4. | 87 |
| Figure 3.6: mGlu ₅ -TPD demonstrates reduced β -arrestin 2 recruitment compared to both mGlu ₅ -WT and mGlu ₅ -PD in the NanoBiT complementation assay. | 89 |
| Figure 3.7: Constitutive β -arrestin 2 recruitment to mGlu ₅ measured by a NanoBiT complementation assay is decreased with removal of putative C-terminal phosphorylation sites. | 91 |
| Figure 3.8: β -arrestin 2 recruitment to the mGlu ₅ receptor is eliminated in GRK2/3/5/6 knockout cells. | 94 |
| Figure 3.9: Inhibiting GRK5/6 decreases constitutive β -arrestin 2 recruitment to mGlu ₅ -WT and mGlu ₅ -PD. | 96 |
| Figure 3.10: Treatment with glutamate does not alter mGlu ₅ localisation. | 99 |
| Figure 3.11: Agonist stimulation does not result in internalisation of mGlu ₅ -WT, mGlu ₅ -PD or mGlu ₅ -TPD. | 101 |
| Figure 3.12: Sites in the murine mGlu ₅ C-terminus used to generate novel phospho-site specific anti-sera. | 103 |
| Figure 3.13: Novel phospho-site specific antibodies against mGlu ₅ -WT reveals basal receptor phosphorylation. | 105 |
| Figure 3.14: Immunoprecipitation of mGlu ₅ -WT receptor reveals phosphorylation of Serine1041 and Serine1044 residues. | 108 |
| Figure 4.1: Measurement of the G $\alpha_{q/11}$ protein-coupled receptor activation. | 128 |
| Figure 4.2: Doxycycline induction of Flp-In™ T-REx™ 293 cell lines leads to expression of mGlu ₅ -HA constructs. | 133 |
| Figure 4.3: Western blots to quantify inducible mGlu ₅ receptor expression. | 136 |
| Figure 4.4: Western blot analysis of the structure of mGlu ₅ | 139 |
| Figure 4.5: On-cell and in-cell western analysis can be used to quantify mGlu ₅ surface and total expression. | 143 |
| Figure 4.6: Expression of mGlu ₅ -WT, mGlu ₅ -PD and mGlu ₅ -TPD increases with doxycycline concentration. | 147 |
| Figure 4.7: Cell membrane expression of the mGlu ₅ -WT, mGlu ₅ -PD, and mGlu ₅ -TPD receptors increases with increasing concentration of doxycycline. | 151 |
| Figure 4.8: Quantification of in- and on-cell western analyses of mGlu ₅ receptor expression reveals an increase in membrane expression with increasing concentrations of doxycycline. | 152 |
| Figure 4.9: mGlu ₅ -TPD produces a higher peak Fura-2 ratio in the calcium mobilisation assay than mGlu ₅ -WT and mGlu ₅ -PD. | 154 |
| Figure 4.10: Removal of mGlu ₅ C-terminal phosphorylation sites alters calcium oscillations. | 153 |
| Figure 4.11: Optimisation of cell number in the IP ₁ accumulation assay. | 158 |
| Figure 4.12: Generation of IP ₁ increases with increasing concentration of doxycycline. | 160 |
| Figure 4.13: Mutation of mGlu ₅ C-terminal serine and threonine residues decreases basal IP ₁ release. | 162 |

| | |
|---|-----|
| Figure 4.14: The TRUPATH paradigm can be encoded into a single plasmid, called 'NEWPATH' | 164 |
| Figure 4.15: Mutation of mGlu ₅ C-terminal phosphorylation sites reduces Gα _q constitutive activation | 166 |
| Figure 4.16: Basal BRET ratio from the NEWPATH assay, a measure of constitutive activity, is significantly different with removal of putative C-terminal mGlu ₅ phosphorylation sites | 167 |
| Figure 5.1: The structure of the novel unimolecular biosensors | 183 |
| Figure 5.2: A protein of the expected molecular weight for the iSpNG biosensor is detected by western blotting following transfection into cells..... | 185 |
| Figure 5.3: Increasing the amount of biosensor transfected results in an increase in sensor expression..... | 187 |
| Figure 5.4: Varying receptor expression with doxycycline impacts the signal produced by the biosensor | 189 |
| Figure 5.5: Protocol optimisation for biosensor BRET kinetic reads | 191 |
| Figure 5.6: The SpNG and iSpNG biosensors can detect Gα _q at the M1, FFA1 and mGlu ₅ receptors..... | 191 |
| Figure 5.7: Measuring the impact of mGlu ₅ potential phosphorylation sites on Gα _q activation using a genetically encoded biosensor | 196 |
| Figure 5.8: The mGlu ₅ receptor is endogenously expressed in cortico-hippocampal neurons and produces a functional IP ₁ response | 198 |
| Figure 5.9: Glutamate stimulated endogenous Gα _q protein activation in neurons can be measured with the iSpNG biosensor | 197 |

List of Publications

Abstracts

Strellis, B., Wei, L., Dwomoh, L., Bradley, S. J., & Hudson, B. D. (2023).

Characterising the signal transduction pathway of mGlu₅ to determine the role of receptor phosphorylation. *British Journal of Pharmacology*, 180(4), 499–499.

Publications

Scarpa, M., Molloy, C., Jenkins, L., **Strellis, B.**, Budgett, R. F., Hesse, S., Dwomoh, L., Marsango, S., Tejada, G. S., Rossi, M., Ahmed, Z., Milligan, G., Hudson, B. D., Tobin, A. B., & Bradley, S. J. (2021). Biased M1 muscarinic receptor mutant mice show accelerated progression of prion neurodegenerative disease. *Proceedings of the National Academy of Sciences of the United States of America*, 118(50). <https://doi.org/10.1073/pnas.2107389118>

Acknowledgements

First of all, I would like to express my gratitude to my supervisors: Dr. Brian Hudson and Dr. Sophie Bradley. Sophie, thank you for your inspiration and inception of the mGlu₅ project, and for your support when I was a new PhD student; you gave me such a lovely welcome to Glasgow. Brian, thank you so much for your guidance and encouragement with my project. Your expert knowledge, advice, and feedback made me feel so supported throughout the project. Thank you for helping me think critically about my work and become a better scientist.

Thank you to all the PhD students, postdocs, and technicians in Lab 253/241/441 for always answering my questions and supporting me throughout PhD life across the Wolfson Link Building, Davidson Building, and Advanced Research Centre. Thank you to the friends I have made in Glasgow, especially Kat, Dom, Euan, Kelly, and Olivia. Your laughs in the lab have made this PhD so fun and I'm so grateful to you all. Thank you to Becca for being part of Team mGlu₅ and helping me so much. Thank you to Solasta boys Alex and Euan, your encouragement and support was always appreciated. Thank you to my Mum and Dad for always listening to my complaints and supporting me on my academic journey.

I would like to give my thanks to Molly who has been there for me throughout my PhD despite the distance. We did it, we became the Top Scientists we said we would on our first day studying Pharmacology together.

The biggest thanks of all goes to the original Slackers: Luca, Beth and Elaine. Thank you all so much for the caffeine breaks, the laughs, being there for me when things got tough. The bagel Fridays and pub trips will always have a place in my heart, I will never forget those good times. May we always be thriving.

Abbreviations

| | |
|----------------------------|---|
| 5MPEP | 5-methyl-6-(phenylethynyl)-pyridine |
| ACh | Acetylcholine |
| AD | Alzheimer's Disease |
| AKT | Protein kinase β |
| AM | Acetoxymethyl Ester |
| AMPA | α -amino-3-hydroxy-5-methyl-4-isoxazole propionic acid |
| AMs | Allosteric Modulators |
| ANOVA | Analysis of Variance |
| AP2 | Adaptor Protein 2 |
| APS | Ammonium Persulphate |
| AQUA | Advanced Quick Assembly Cloning |
| ATP | Adenosine Triphosphate |
| AUC | Area Under Curve |
| Aβ | β -Amyloid |
| BAPTA | 1,2-bis(o-aminophenoxy)ethane-N,N,N',N'-tetraacetic acid |
| BERKY | BRET biosensor with ER/K linker and YFP |
| BGH | Bovine Growth Hormone |
| BRET | Bioluminescent Resonance Energy Transfer |
| BSA | Bovine Serum Albumin |
| CaMKII | Calmodulin-Dependent Protein Kinase II |
| cAMP | Cyclic Adenosine Monophosphate |
| CDK5 | Cyclin-Dependent Kinase 5 |
| CDPPB | 3-cyano-N-(1,3-diphenyl-1H-pyrazol-5-yl)benzamide |
| CMV | Cytomegalovirus |
| CNS | Central Nervous System |

| | |
|---------------|---|
| CRD | Cysteine Rich Domain |
| CRISPR | Clustered Regularly Interspaced Short Palindromic Repeats |
| CTEP | 2-chloro-4-((dimethyl-1-(4-(trifluoromethoxy)phenyl)-1H-imidazol-4yl)ethynyl)pyridine |
| DAG | Diacylglycerol |
| DAPI | 4',6-diamidino-2-phenylindole |
| DEPC | Deionised diethylpyrocarbonate |
| dFBS | Dialysed Fetal Bovine Serum |
| DHPG | (S)-3,5-dihydroxyphenyl glycine |
| DMEM | Dulbecco's Modified Eagle Medium |
| DMSO | Dimethylsulphoxide |
| DNA | Deoxyribonucleic acid |
| EAAT | Excitatory Amino Acid Transporter |
| ECD | Extracellular Domain |
| ECL | Extracellular Loop |
| EDTA | Ethylenediaminetetraacetic Acid |
| EGTA | Egtazic Acid |
| ELISA | Enzyme Linked Immunosorbent Assay |
| eNOS | Endothelial Nitric Oxide Synthase |
| EPAC | Exchange Proteins Directly Activated by cAMP |
| ER | Endoplasmic Reticulum |
| ERK | Extracellular Signal-Regulated Kinases |
| EVH | Ena/VASP Homology 1 |
| FBS | Fetal Bovine Serum |
| FDA | Food and Drug Administration |
| FFA | Free Fatty Acid |
| FMRP | Fragile X Mental Retardation Protein |

| | |
|-------------------------------|---|
| FRET | Förster Resonance Energy Transfer |
| FRT | Flp Recombination Target |
| FXS | Fragile X Syndrome |
| GABA | γ -aminobutyric acid |
| GAIN | G Protein-Coupled Receptor Autoproteolysis-Inducing |
| GAP | GTPase-activating protein |
| GDP | Guanosine-5'-diphosphate |
| GEF | Guanine Nucleotide Exchange Factor |
| GFP | Green Fluorescent Protein |
| GLAST | Glutamate-Aspartate Transporter |
| GPCR | G Protein-Coupled Receptor |
| GPS | G Protein-Coupled Receptor Proteolysis Site |
| GPT | Glutamate-Pyruvate Transaminase |
| GRK | G Protein-Coupled Receptor Kinase |
| GSK3β | Glycogen Synthase Kinase 3 β |
| GTP | Guanosine-5'-triphosphate |
| HA | Haemagglutinin |
| HBSS | Hank's Balanced Salt Solution |
| HEK | Human Embryonic Kidney |
| HEPES | N-(2-Hydroxyethyl)piperazine-N'-(2-ethanesulfonic acid) |
| HTRF | Homogenous Time-Resolved Fluorescence |
| ICC | Immunocytochemistry |
| ICL | Intracellular Loop |
| ICW | In-Cell Western |
| IMPase | Inositol Monophosphatase |
| IP₁ | Inositol Monophosphate |
| IP₂ | Inositol Diphosphate |

| | |
|-------------------------|--|
| IP₃ | Inositol 1,4,5-Trisphosphate |
| IRES | Internal Ribosome Entry Site |
| IRS1 | Insulin Receptor Substrate 1 |
| kDa | Kilodaltons |
| KO | Knockout |
| LB | Luria-Bertani |
| LC-MS/MS | Liquid Chromatography-Tandem Mass Spectrometry |
| LTD | Long-Term Depression |
| LTP | Long-Term Potentiation |
| MAPK | Mitogen-Activated Protein Kinase |
| mGlu | Metabotropic Glutamate |
| mNG | mNeonGreen |
| MOPS | 3-(N-morpholino)propanesulfonic acid |
| MPEP | 2-methyl-6-(phenylethynyl) pyridine |
| MRI | Magnetic Resonance Imaging |
| MTEP | 3-[(2-methyl-1,3-thiazol-4-yl)ethynyl]pyridine |
| NAc | Nucleus Accumbens |
| NAM | Negative Allosteric Modulator |
| NHERF | Na ⁺ /H ⁺ Exchanger Regulatory Factors |
| Nluc | Nanoluciferase |
| NMDA | N-methyl-D-aspartate |
| NTPs | Nucleoside triphosphates |
| OCW | On-Cell Western |
| OD₆₀₀ | Optical Density at 600 nm |
| ONE-GO | One-Vector G Protein Optical |
| PAM | Positive Allosteric Modulator |
| PBS | Phosphate Buffered Saline |

| | |
|--------------------------------|--|
| PCR | Polymerase Chain Reaction |
| PD | Phosphodeficient |
| PDL | Poly-D-Lysine |
| PEI | Polyethyleneimine |
| PET | Positron Emission Tomography |
| PICK1 | Protein Kinase C Interacting Protein 1 |
| PIP2 | Phosphatidylinositol 4,5-bisphosphate |
| PKA | Protein Kinase A |
| PKC | Protein Kinase C |
| PLC | Phospholipase C |
| PP2Cα | Protein Phosphatase 2C α |
| PSD | Postsynaptic Density |
| RET | Resonance Energy Transfer |
| RGS | Regulator of G Protein Signalling |
| RIPA | Radioimmunoprecipitation Assay |
| Rluc | <i>Renilla</i> Luciferase |
| RNA | Ribonucleic Acid |
| SAM | Silent Allosteric Modulator |
| SDS-PAGE | Sodium Dodecyl Sulphate Polyacrylamide Gel Electrophoresis |
| S.E.M. | Standard Error of the Mean |
| SPASM | Systematic Protein Affinity Strength Modulation |
| TAE | Tris-acetate-EDTA |
| TBS | Tris-Buffered Saline |
| TEMED | N,N,N',N'-tetramethyl ethylenediamine |
| TetR | Tetracycline Repressor |
| TMD | Transmembrane Domain |
| TPD | Total Phosphodeficient |

| | |
|--------------------------------|----------------------------|
| VFT | Venus Flytrap Domain |
| VTA | Ventral Tegmental Area |
| WT | Wildtype |
| YFP | Yellow Fluorescent Protein |
| λ-PP | Lambda Protein Phosphatase |

Author's Declaration

“I declare that, except where explicit reference is made to the contribution of others, this thesis is the result of my own work and has not been submitted for any other degree at the University of Glasgow or any other institution.”

Bethany Strellis

September 2024

1 Introduction

1.1 G Protein-Coupled Receptors

1.1.1 Overview

G protein-coupled receptors (GPCRs) are a superfamily of membrane-bound receptors responding to a variety of stimuli including hormones, peptides, neurotransmitters and transduce these extracellular signals into an intracellular response. There are greater than 800 members of the GPCR superfamily in humans, representing the largest family of proteins targeted by approved drugs (Fredriksson et al., 2003). As of 2017, 33% of all small molecule drugs target a receptor in this superfamily (Santos et al., 2017). Overall, GPCRs still have the continued potential as novel drug targets in a multitude of pathologies.

While GPCRs have relatively little overall sequence identity across the family, they do share a conserved general structure. All GPCRs possess seven transmembrane domains (TMDs), consisting of α -helices spanning the cell membrane (Crasto, 2010). The seven α -helices are linked by three extracellular loops (ECLs), involved in ligand binding and recognition, and three intracellular loops (ICLs), playing a crucial role in coupling the receptor to G proteins and interacting proteins. Whilst the intracellular carboxyl (C)-terminus is relatively conserved in terms of sites of post-translational modifications, the extracellular amino (N)-terminus is highly diverse among the GPCR subtypes.

1.1.2 Classification of GPCR Families

There are two commonly accepted methods to classify GPCRs within the superfamily. In the first classification system, there are six major classes of GPCRs based on common sequence homology and functional properties (Attwood & Findlay, 1994). **Class A** refers to the 'rhodopsin-like' family of receptors, **Class B** includes the adhesion and secretin receptors, and **Class C** accommodates the metabotropic glutamate receptors, γ -aminobutyric (GABA) receptors, calcium sensing receptors and a family of taste receptors. The final class of receptors to exist in humans is **Class F**, the frizzled/smoothed family of GPCRs. **Class D** and **Class E** consist of the fungal pheromone and cyclic adenosine monophosphate (cAMP) receptors respectively, possessing a sequence

sufficiently different to be considered separate classes of receptor family than the Class A group they were previously ascribed to (Attwood & Findlay, 1994; Fredriksson et al., 2003). In the second method to classify human GPCRs, the GRAFS system, receptors are divided based on the phylogenetic tree based on sequencing of the human genome (Fredriksson et al., 2003). The GRAFS system consist of the **G**lutamate family (class C), **R**hodopsin family (class A), **A**dhesion (class B2), **F**rizzled (class F) and **S**ecretin-like (class B1) receptors (Figure 1.1).

Receptors in the **Glutamate receptor family** (consisting of 22 members (Alexander et al., 2021)) possess a characteristically large C-terminal tail and a bulky extracellular domain (ECD) responsible for ligand binding termed the Venus flytrap domain (VFT) (Figure 1.1) (Kunishima et al., 2000). The C-terminus of this receptor family is very large, typically 100-200 amino acids in length, with numerous sites of phosphorylation situated on this sequence. While all GPCR C-terminal tails play roles in receptor regulation, trafficking, and signalling, the C-terminus of the glutamate receptor family is particularly involved in complex regulatory mechanisms due to its length and interaction potential (Enz, 2012). The **'Rhodopsin-like' receptor family** consists of 719 members (Alexander et al., 2021), making up 80% of all GPCRs; structurally, this family possesses the typical seven TMDs forming a ligand binding pocket, in addition to an eighth helix that runs parallel to the cell membrane within the C-terminal tail (Hu et al., 2017; Yang et al., 2021) (Figure 1.1). The C-terminus of Rhodopsin-like GPCRs is typically short, commonly 20-40 amino acids in length, with a conserved palmitoylation site anchoring helix 8 to the cell membrane (Fukata & Fukata, 2010). **Adhesion receptor family** members possess a long extracellular N-terminus with a conserved region close to TMD1, playing a permissive role in ligand binding. This region constitutes two components: a region rich in serine and threonine residues, and a GPCR proteolysis site (GPS) embedded in a GPCR autoproteolysis-inducing (GAIN) domain (Harmar, 2001; Prömel et al., 2013) (Figure 1.1). The **Frizzled/Taste2 receptor family** control cell proliferation and fate during development through mediation of signals from secreted glycoproteins called Wnt, binding to conserved cysteine residues on the N-terminus (Fredriksson et al., 2003) (Figure 1.1). The **Secretin family** of receptors encompass 15 receptor subtypes in humans (Alexander et al., 2021), with the ligands being polypeptide hormones such as glucagon, secretin and glucagon-like peptides (Harmar, 2001). The N-terminus contains conserved cysteine residues key for peptide ligand

binding to the receptor (Fredriksson et al., 2003), whereas the C-terminus often contains several regulatory motifs and phosphorylation sites involved in binding to scaffolding proteins and other regulatory proteins for receptor trafficking and signalling (Miller et al., 2012) (Figure 1.1).

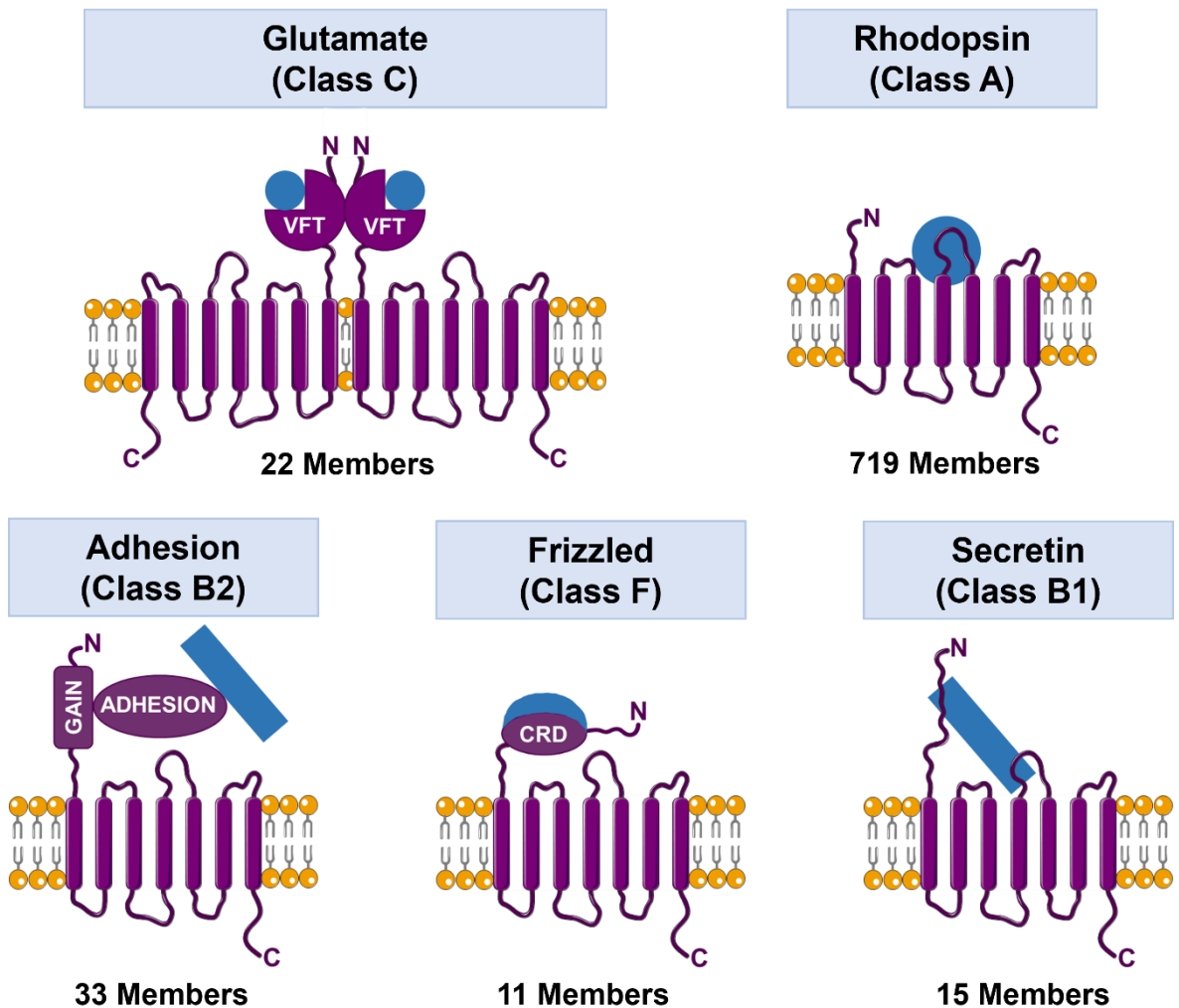


Figure 1.1: The GRAFs classification of G protein-coupled receptors. GPCRs have a common structure consisting of seven α -helical transmembrane domains, intracellular C-terminus that is relatively conserved, and an extracellular N-terminus which is highly diverse. Glutamate receptors exist as constitutive dimers and possess a large Venus flytrap domain (VFT) in the N-terminus to facilitate ligand binding. Conversely, Rhodopsin-like receptors have a small N-terminus as the ligand binding pocket lies deep within the seven transmembrane domains. Adhesion GPCRs feature a GPCR autoproteolysis-inducing (GAIN) domain which acts to catalyse the N-terminus permitting non-covalent association of the adhesion domain, to which ligands bind. Frizzled receptors contain cysteine-rich domains (CRD) to enable ligand binding, whereas secretin receptors are activated through hormone peptide binding domains in the long N-terminus. Blue shapes represent the modes of ligand interaction with each receptor subtype. The number of receptors in each family is listed as reported by Alexander et al., (2021).

1.1.3 G Protein Signalling

The large number of GPCRs requires a highly conserved mechanism of activation and signal transduction. The key protein, from which the receptor superfamily derives its name, is the G protein; this is constituted of $G\alpha$, $G\beta$, and $G\gamma$ subunits which together form a heterotrimeric $G\alpha\beta\gamma$ complex. The $G\alpha$ protein is the principal coordinator in the signalling cascade. In the resting state, $G\alpha$ proteins are bound to guanosine-5'-diphosphate (GDP) and form a high affinity complex with the membrane bound, tightly associated $G\beta\gamma$ proteins (Lambright et al., 1996). Upon agonist binding to the GPCR, a conformational change occurs in the receptor allowing the GPCR to act as a guanine nucleotide exchange factor (GEF) to the G protein. The receptor stimulates exchange of GDP to guanosine-5'-triphosphate (GTP) on the $G\alpha$ subunit, triggering dissociation of the $G\alpha$ from the $G\beta\gamma$ (Neer & Clapham, 1988) (Figure 1.2A). GTP binding prompts GTP- $G\alpha$ to dissociate from $G\beta\gamma$, such that each is then free to activate further downstream signalling effectors (Lambright et al., 1996). Signalling is terminated through intrinsic GTPase activity of the $G\alpha$ subunit, catalysing the hydrolysis of GTP back to GDP (also catalysed by GTPase-activating proteins (GAPs)) promoting re-association of the heterotrimeric $G\alpha\beta\gamma$ complex (Mann et al., 2016) (Figure 1.2A).

$G\alpha$ proteins are divided into four major families: $G\alpha_s$, $G\alpha_{i/o}$, $G\alpha_{q/11}$ and $G\alpha_{12/13}$, each activating distinct effector proteins and second messengers. The $G\alpha_{q/11}$ family consists of $G\alpha_q$, $G\alpha_{11}$, $G\alpha_{14}$, and $G\alpha_{15}$ which stimulate phospholipase C (PLC), catalysing the hydrolysis of phosphatidylinositol 4,5-bisphosphate (PIP_2) to inositol 1,4,5-trisphosphate (IP_3) and diacyl glycerol (DAG) (Sugiyama et al., 1987) (Figure 1.3). DAG activates PKC and triggers release of intracellular calcium through IP_3 receptors located on the endoplasmic reticulum. The $G\alpha_s$ family stimulate adenylyl cyclase, leading to an increase in cAMP, whereas the $G\alpha_{i/o}$ family inhibits adenylyl cyclase therefore decreasing cAMP production (Figure 1.3). The $G\alpha_{12/13}$ family of G proteins activate Rho guanine nucleotide exchange factors (GEFs) (Figure 1.3).

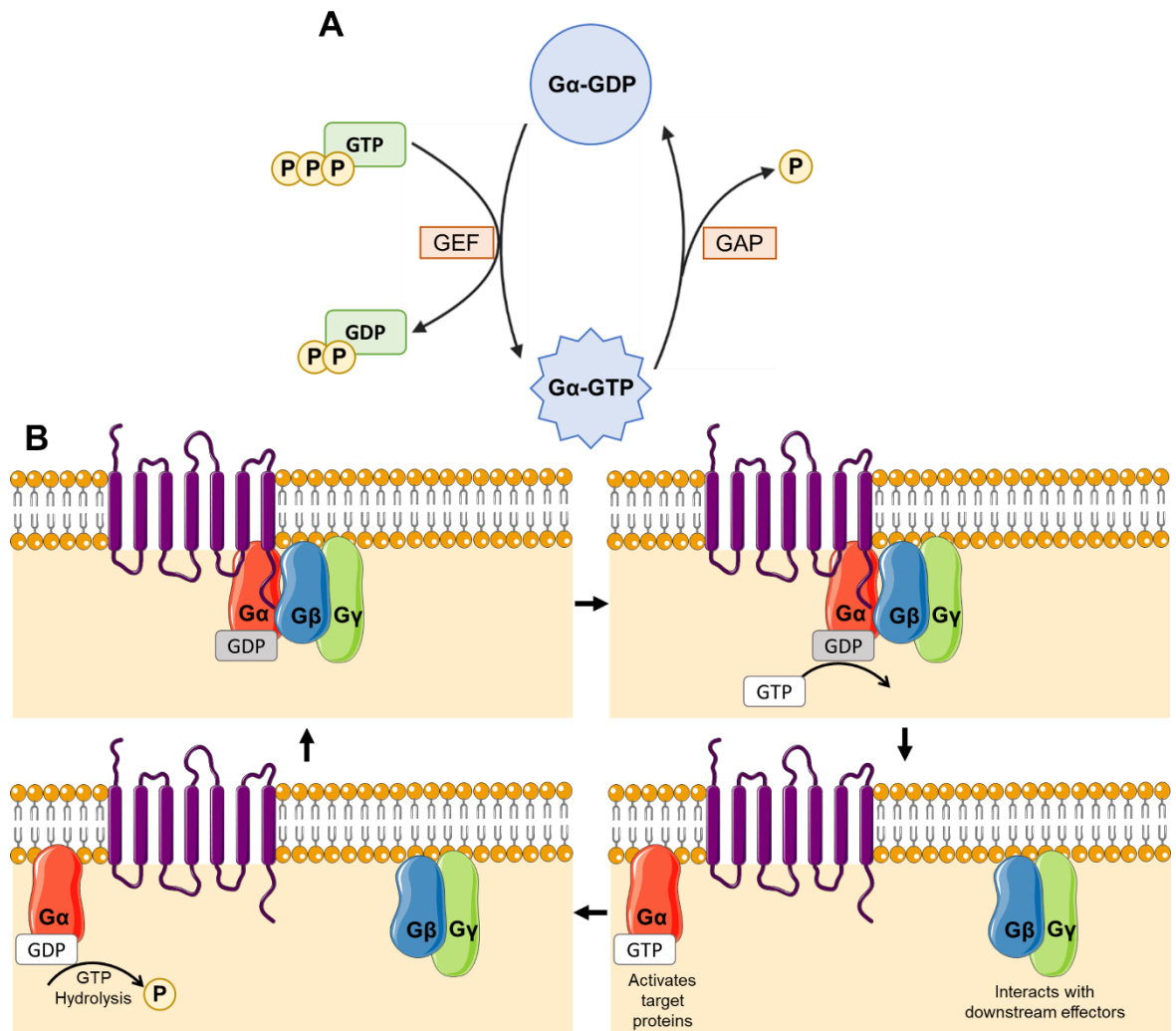


Figure 1.2: The heterotrimeric G protein activation sequence. (A) The GTPase cycle regulates G protein activation. Guanine nucleotide exchange factor (GEF) aids conversion of $G\alpha$ -GDP to $G\alpha$ -GTP, and GTPase activating protein (GAP) reverts this. (B) In resting state, the α , β , and γ subunits of the G protein heterotrimer are anchored to the lipid membrane. When in the active state, GDP is exchanged for GTP causing the GTP- $G\alpha$ complex and the $G\beta\gamma$ subunits to dissociate and activate downstream effectors. Termination of signalling is regulated by intrinsic GTPase activity of the $G\alpha$ subunit, which increases once bound to the effector protein, leading to hydrolysis of GTP to GDP and reassociation of the $G\alpha\beta\gamma$ heterotrimer.

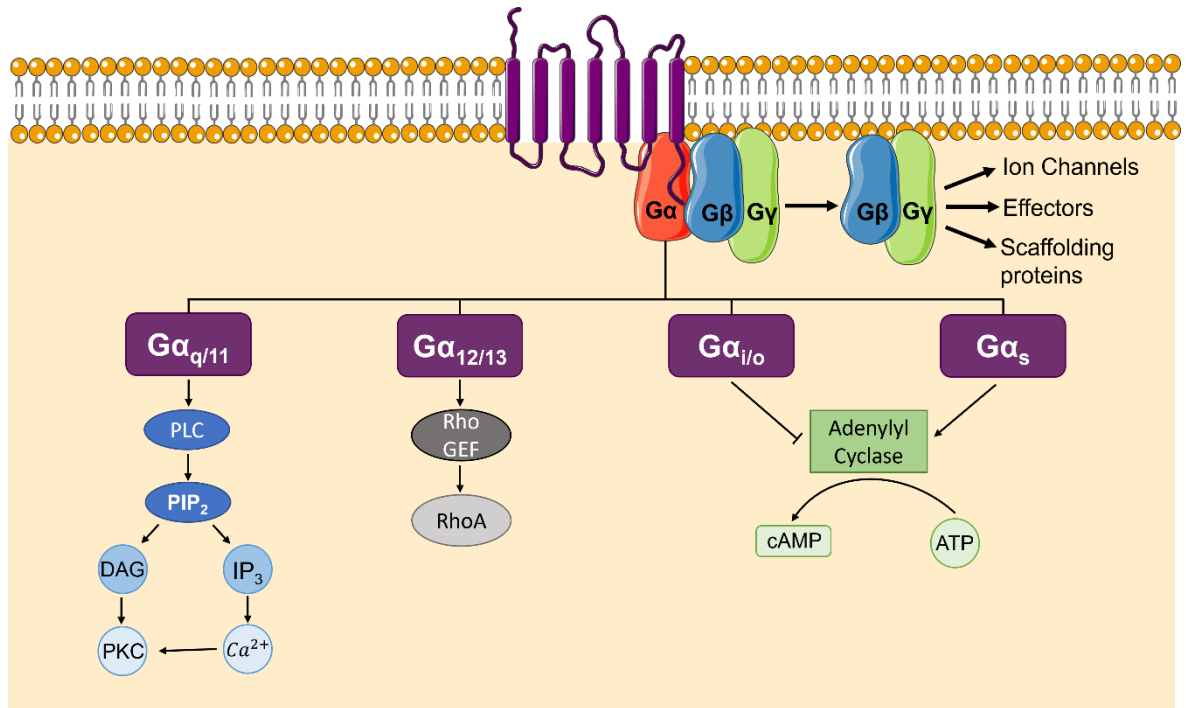


Figure 1.3: G protein-dependent signalling pathways following activation of the GPCR. Subsequent to agonist binding and initiation of a conformational change in the GPCR, guanosine nucleotide exchange is facilitated within the $G\alpha$ subunit stimulating dissociation of the $G\alpha\beta\gamma$ heterotrimer. Distinct $G\alpha$ protein subunits activate specific subsets of second messengers to commence a cascade of downstream signalling effectors. Dissociated $G\beta\gamma$ subunits can engage with further signalling elements in their own right.

Although GPCR activation by ligands is highly specific, the activation of G proteins is less particular and the same intracellular pathway can be activated by multiple GPCRs, or the same GPCR can couple to multiple different G protein families (Neer & Clapham, 1988). It was previously thought that a given receptor was coupled with one specific $G\alpha$ protein, however research in recent years has revealed that many GPCRs are more promiscuous in their couplings; the GPCR- $G\alpha$ pairing may change depending on cellular context, changes of the receptor during activation, or presence of additional proteins outwith the GPCR- $G\alpha$ duo (Masuho et al., 2015).

1.1.4 β -Arrestin Signalling and Receptor Internalisation

GPCRs are subjected to three modes of dampened down signalling: desensitisation, where a receptor becomes insensitive to constant agonist stimuli; sequestration, in which a receptor is internalised and removed from the cell

surface; and downregulation, where the total number of cell surface receptors is decreased (Tian et al., 2013). Following receptor activation, post translational modifications occur on the intracellular surface of GPCRs, including phosphorylation of serine or threonine residues, which then influences the binding affinity for arrestin proteins (Krupnick & Benovic, 1998). GPCRs undergo agonist-dependent phosphorylation by G protein receptor kinases (GRKs), predominantly at serine and threonine residues located either in ICL3 or on the C-terminal tail (Tobin et al., 2008). Phosphorylation of the intracellular receptor surface increases the affinity for the β -arrestin family of adaptor proteins (Carman & Benovic, 1998) (Figure 1.4). β -arrestins inactivate G protein signalling by sterically occluding the G protein binding site, and subsequently facilitate receptor internalisation (Cao et al., 2019). Arrestins are able to scaffold to endocytotic machinery and bind to the β 2 subunit of the clathrin adaptor protein 2 complex (AP2), allowing for clathrin mediated endocytosis of the receptor (Goodman et al., 1996). Following endocytosis, the arrestin dissociates from the GPCR and the receptor is dephosphorylated, permitting the receptor to either be recycled back to the cell membrane or be degraded. In addition to their well-recognised role in turning off GPCR signalling, it is now recognised that arrestins can also signal in their own right by scaffolding to their own effector proteins (Lefkowitz and Shenoy, 2005).

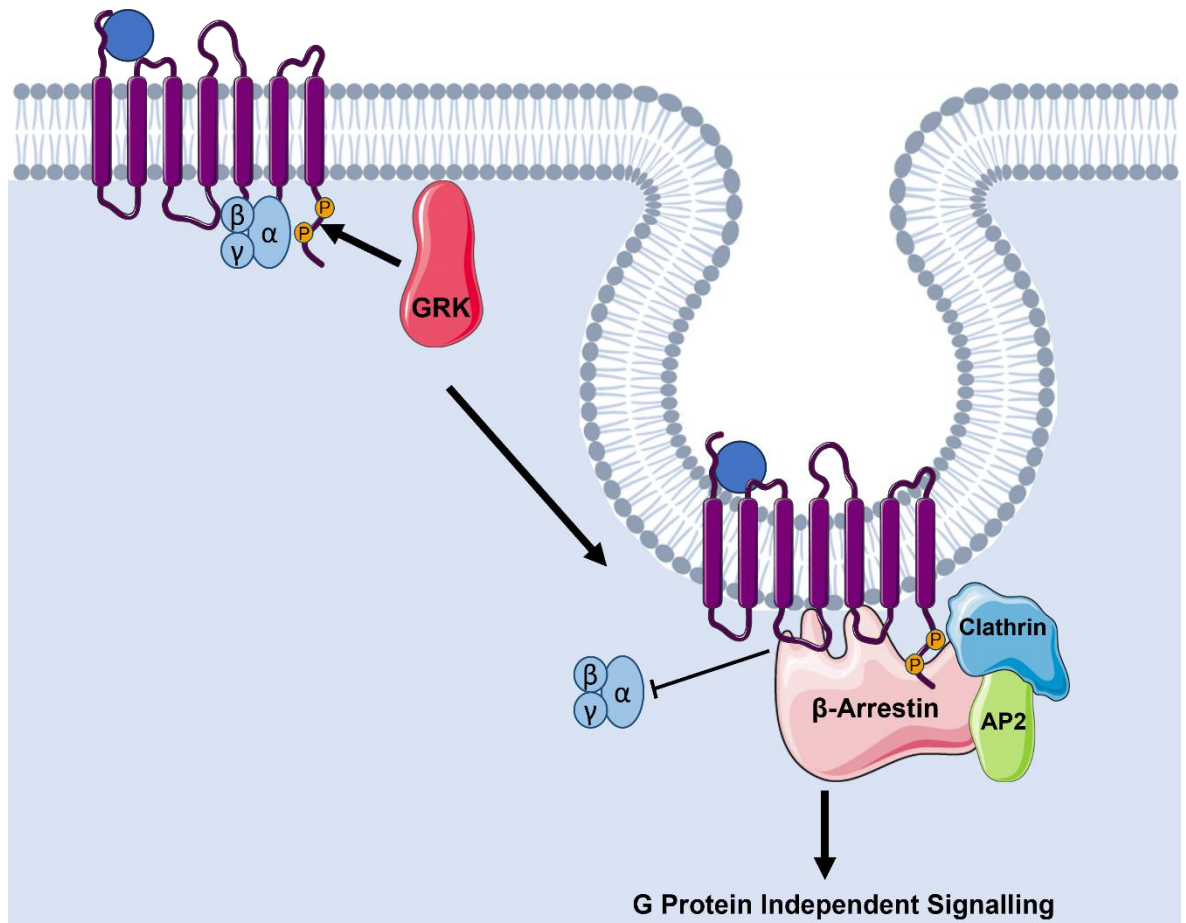


Figure 1.4: The functions of β -arrestin following phosphorylation of the GPCR by GRKs. G protein-coupled receptor kinases (GRKs) can phosphorylate the intracellular surface of a GPCR, which triggers β -arrestin recruitment to the receptor. This protein then triggers receptor internalisation, receptor desensitisation, or signalling in its own right. Figure created using BioRender.

1.1.5 Constitutive Activity of GPCRs

Constitutive activity of GPCRs describes the ability of a receptor to adopt an active conformation and initiate downstream signalling without the presence of an agonist. GPCRs are known to exist in dynamic equilibrium between inactive (R) and active (R^*) states (Black & Leff, 1983). In the classical model, agonist binding stabilises the active conformation (R^*), which in turn activates intracellular G proteins and triggers downstream signalling. In constitutively active GPCRs, however, the receptor can spontaneously shift to the active conformation, resulting in signalling even in the absence of an agonist. This was first reported for the β_2 -adrenoceptor in the 1980s (Cerione et al., 1984), and since reported for a range of other GPCRs (Seifert & Wenzel-Seifert, 2002). Constitutive signalling can lead to

inappropriate cellular responses causing pathologies such as hormone hypersensitivity (Rodien et al., 1998), or obesity (Srinivasan et al., 2004).

The two-state model describes the interaction between three key components: the receptor, the ligand and the G protein, however the extended ternary complex model was developed to account for additional complexities observed in GPCR signalling; in addition to the receptor, ligand, and G protein, this model incorporates the interactions with β -arrestins and other regulatory proteins that modulate receptor activity (Weiss et al., 1996). Upon ligand binding to the receptor, the ligand can either stabilise the inactive state (antagonists or inverse agonists) or the active state (agonists), shifting the equilibrium towards the active receptor conformation, the 'ternary complex'. This model describes the receptor as existing in multiple active states, not just the binary R and R* states. In this model, constitutive activity may result in basal coupling to not only G-proteins but also to β -arrestins or other signalling proteins. This suggests that GPCRs can signal through multiple pathways, even in the absence of a ligand. One remaining key challenge of GPCR research is to better understand the physiological relevance of constitutive activity for different GPCRs and in different tissue contexts.

1.1.6 Using Biosensors as a Tool to Measure GPCR Activation

Given the complexity of GPCR signalling, biosensors have emerged as invaluable tools for measuring GPCR activity with high specificity and sensitivity. Biosensors allow real-time monitoring of receptor activation, downstream signalling, and ligand-receptor interactions in live cells, providing key insights into GPCR function. These biosensors often rely on resonance energy transfer (RET), a naturally occurring process of dipole-dipole non-radiative energy transfer. Fluorescent biosensors rely on Förster RET (FRET); when two fluorophores are in close proximity (<10 nm), the excitation of the donor leads to a transfer of energy to the acceptor, resulting in an emission. The efficiency of the transfer of excited state energy is inversely proportional to the sixth power of the distance between the donor and acceptor pair (Förster, 1960), therefore even very slight changes in the distance between the donor and acceptor proteins will elicit a quantifiable change in FRET. BRET is a chemical reaction, reliant on the transfer of energy between a bioluminescent donor protein (luciferase) and a fluorescent acceptor protein following oxidation of a substrate. The efficiency of the energy transfer, and

thus the signal, is dependent on the distance between the luciferase and fluorescent protein. The main distinction between FRET and BRET is that FRET requires two fluorophores for energy transfer, one of which needing excitation by an external source, whereas BRET takes place following oxidation of a substrate (Pfleger & Eidne, 2006).

Biosensors used for measuring GPCR activity can be broadly classified into two categories: those that detect conformational changes in the receptor, and those that monitor downstream signalling events. For instance, FRET or BRET pairs attached to different domains of a GPCR can report structural rearrangements upon ligand binding (Hudson, 2016), allowing researchers to monitor receptor activation in real time. Additionally, sensors have been employed to measure the dissociation of G protein subunits ($G\alpha$ and $G\beta\gamma$) (Olsen et al., 2020), which occurs after GPCR activation. Fluorescent protein-based biosensors for second messengers such as GCaMP (for calcium ion measurement) (Nakai et al., 2001) and exchange proteins directly activated by cAMP (EPAC)-based cAMP sensors (DiPilato et al., 2004) have been widely used to study GPCR signalling pathways. These biosensors undergo conformational changes upon binding to their target molecules, resulting in changes in fluorescence intensity or wavelength that can be monitored using microscopy or plate readers.

These biosensors serve as tools that can be adapted and employed to measure signalling from endogenously expressed receptors. Measurement of endogenous receptor activity over artificially overexpressed receptors is advantageous predominantly due to the physiological relevance; recording activity from a receptor expressed at natural levels in the appropriate cellular context and interacting with a network of native proteins and signalling pathways reveals a more biologically relevant profile. Progress in GPCR research has been historically hampered by the overreliance on assays that measure GPCR activity indirectly and on a limited number of cell lines which do not necessarily recapitulate GPCR physiological contexts (Janicot et al., 2024). As a result, compounds tested *in vitro* may encounter difficulties in translation to *in vivo* studies. Measuring output from endogenous receptors can be used to provide insights into how GPCR signalling is modulated in different physiological or pathological contexts and bridge the gap between *in vitro* and *in vivo* settings.

Recently, biosensors have been developed to measure endogenous GPCR activation: Maziarz et al. (2020) developed a single peptide biosensor with the capability to measure G α -GTP at endogenously expressed GPCRs. Whilst this biosensor permitted detection of activation of endogenous GPCRs in primary neurons and without compromising with downstream signalling, the small dynamic range and signal window has remained a limitation for the broad applicability of this biosensor. Janicot et al. (2024) developed the one-vector G protein optical (ONE-GO) biosensor system, demonstrated to measure endogenous GPCR activation at a range of receptors. However, this biosensor is limited in its requirement for exogenous G proteins to be expressed. Hence, the field of GPCR biosensors is evolving, whilst multiple limitations and fields for improvement and optimisation exist.

1.2 The Pharmacology of Ligands Acting at GPCRs

Ligands are defined primarily by their pharmacological parameters, efficacy and affinity, which describe how the ligand interacts with the receptor. Efficacy is defined as the ability of a ligand to elicit a response by interaction with its receptor. Affinity is a measure of the ability of the ligand to bind to the receptor, and is typically measured as the K_D dissociation constant, equal to the concentration of the ligand that results in 50% receptor occupancy. Together, efficacy and affinity combine to determine the potency of the ligand, a measure of the concentration of ligand required to produce a given functional response. Potency can be quantitatively measured as the EC_{50} , the effective concentration of an agonist that produces 50% of its maximal effect. To obtain EC_{50} values, functional responses are plotted against the log concentration of the ligand and as a result EC_{50} values are normally distributed on a log scale, and therefore are commonly reported instead as pEC_{50} values (the negative Log_{10} of the EC_{50} value in molar). Unlike affinity, potency and pEC_{50} values are not universal properties of the receptor-ligand interaction, and instead will vary depending on the assay system employed (Kenakin, 2002; Strange, 2008).

Ligands can be divided into categories based on the location on the receptor they bind: orthosteric or allosteric. Orthosteric ligands bind to the same site on the receptor as the endogenous agonist and, depending on their pharmacological characteristics, can be further categorised into full, partial, inverse agonists or neutral antagonists (Figure 1.5). Full agonists stabilise the active conformation (R^*) of the receptor, enhancing signalling, whereas inverse agonists preferentially stabilise the inactive state (R), reducing the constitutive activity by shifting the equilibrium towards the R state (Figure 1.6A). Allosteric ligands bind to a topologically distinct site on the receptor in comparison to the orthosteric binding site of the endogenous ligand. Allosteric modulators (AMs) can work against or in conjunction with orthosteric ligand; AMs can modulate ligand response by increasing or decreasing affinity and/or efficacy of orthosteric ligands. According to their mode of action, AMs can be defined as negative allosteric modulators (NAMs) which reduce orthosteric ligand activity (Figure 1.6B), positive allosteric modulators (PAMs) that enhance orthosteric ligand activity (Figure 1.6C), or silent/neutral allosteric modulators (SAMs) which do not affect the activity of the orthosteric ligand but bind to the allosteric site without eliciting an effect (Figure

1.5). 5-methyl-6-(phenylethynyl)-pyridine (5MPEP) acts on metabotropic glutamate receptors as a neutral allosteric ligand; it binds to the allosteric site yet has no effects alone, however, 5MPEP blocks the effects of both the allosteric antagonist 2-methyl-6-(phenylethynyl)-pyridine (MPEP) and the PAM 3-cyano-N-(1,3-diphenyl-1H-pyrazol-5-yl)benzamide (CDPPB) (Rodriguez et al., 2005). In addition to the pure AMs, some AMs possess intrinsic activity and can signal in their own right. These such ligands are termed PAM-agonists. PAM-agonists are able to potentiate orthosteric ligand affinity and/or efficacy, whilst also possessing intrinsic efficacy themselves (Figure 1.5).

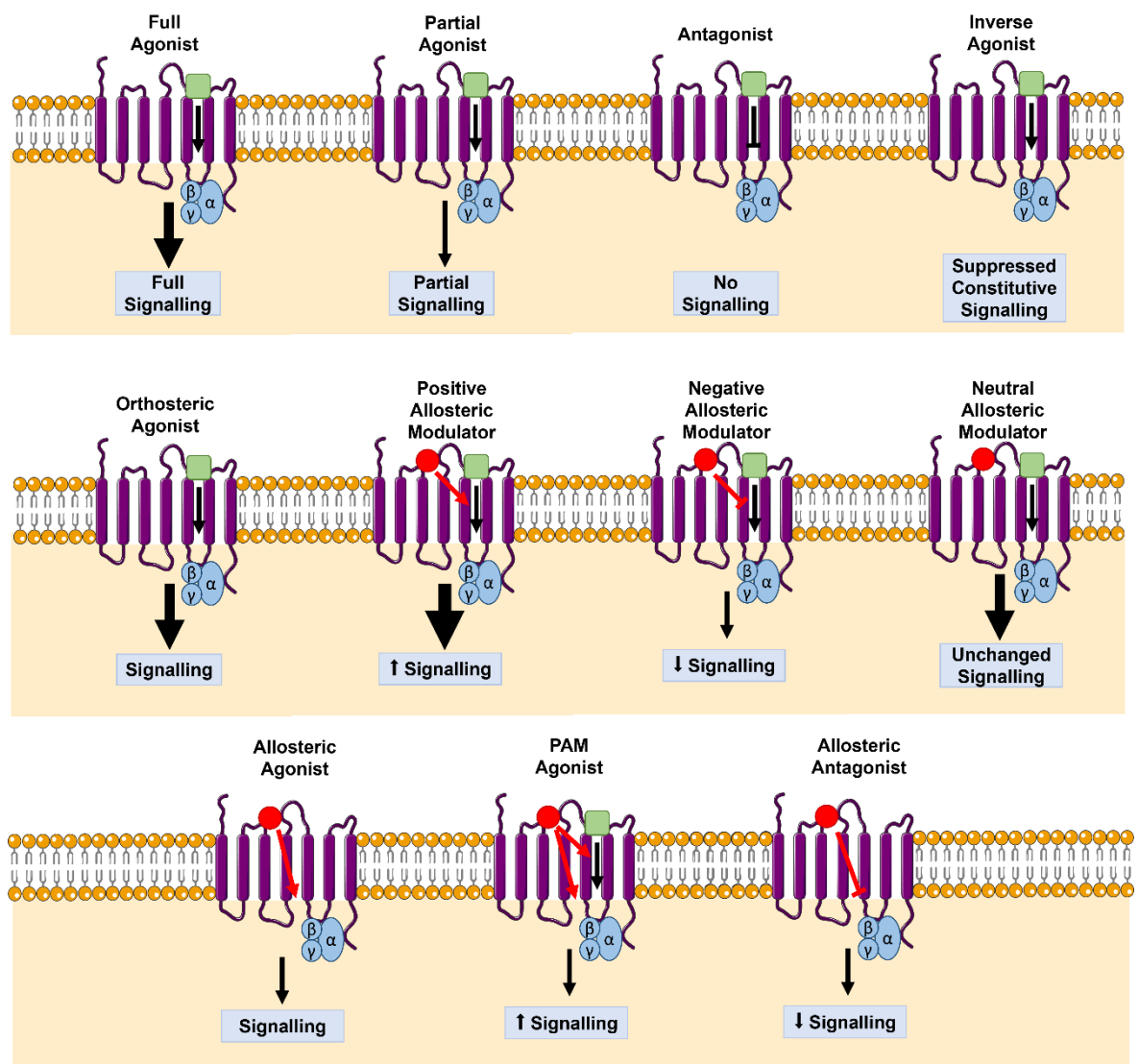


Figure 1.5: The pharmacology of GPCR ligands. Agonists binding at the orthosteric site can be full, partial, or inverse whilst ligands binding at the allosteric site can potentiate, downregulate, or unalter signalling.

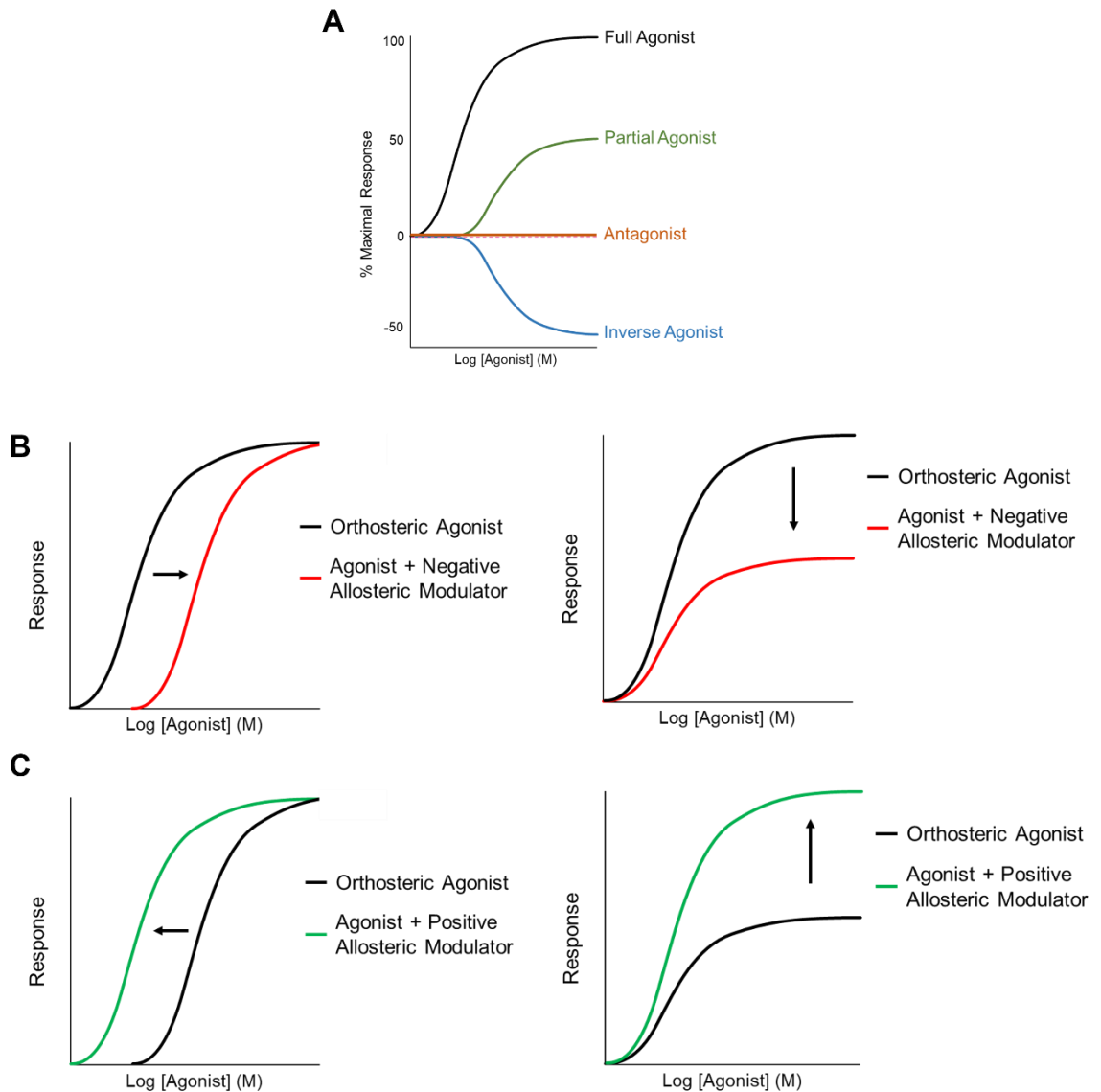


Figure 1.6: The effects of allosteric modulators in response to agonist. (A) A schematic demonstrating the concentration response curves in response to full, partial or inverse agonists or an antagonist. The impact of negative allosteric modulators (B) or positive allosteric modulators (C) affecting either affinity or efficacy of an orthosteric agonist concentration response curve.

1.2.1 The Clinical Potential of Allosteric Modulators

The first model of allosterism was described by Monod, Wyman and Changeux (1965), and since the broad therapeutic potential of allosteric modulators has been taken advantage of by multiple drug development pipelines. Allosteric biased ligands may provide the solution to the failure of many GPCR ligands in clinical trials; the ligand is able to preferentially activate only the clinically desirable subset of effectors and functions from a single receptor, negating the

physiological pathways that result in off target effects. As of 2022, 340 allosteric modulators are in preclinical development, 25 are in clinical trials targeting 12 different GPCRs, and four GPCR allosteric modulators have already been approved by the Food and Drug Administration (FDA) (Persechino et al., 2022).

There are several advantages of employing allosteric modulators in the clinical setting over orthosteric agonists: firstly, there is the preservation of physiological signalling. Pure allosteric modulators that do not signal in their own right and are only active when the endogenous agonist is present, preserving the spatiotemporal aspects of physiological signalling (Persechino et al., 2022). Additionally, biased allosteric ligands provide the opportunity to preferentially activate only the clinically desirable subset of effectors and functions from a single receptor, negating the physiological pathways that result in off target effects (Sengmany et al., 2017; Trinh et al., 2018). Pure allosteric modulators are also saturable, meaning that once the allosteric binding pocket is fully occupied, no other effects are observed due to the orthosteric and allosteric ligand cooperativity reaching a maximal 'ceiling effect' (Persechino et al., 2022). This provides the potential for fine-tuning physiological responses in a positive or negative direction and can safeguard against overdose. Typically, it is challenging to target specific receptors belonging to the same family due to a highly conserved orthosteric site; allosteric sites are less conserved than orthosteric sites, permitting a higher degree of drug selectivity within GPCR families. Development of AMs provide alternative option to target proteins poorly druggable by orthosteric ligands, for example due to wide and deep orthosteric binding pockets (Wootten et al., 2013).

1.3 Glutamate Receptors

Glutamate receptors are integral components of the central nervous system, playing pivotal roles in synaptic transmission, plasticity, and overall brain function. They respond to the endogenous agonist glutamate, the most abundant excitatory neurotransmitter of the central nervous system. Glutamate was described by Krebs in 1935 as a key metabolic regulator in the brain, then later shown through electrophysiology studies to have an excitatory effect in neurons as a direct effect of membrane depolarisation (Curtis & Watkins, 1960).

There are two broad classes of glutamate receptors: ionotropic and metabotropic. The ionotropic glutamate receptor (iGlu receptor) subfamily consists of the kainate, N-methyl-D-aspartate (NMDA), and amino-3-hydroxy-5-methyl-4-isoxazolepropionic acid (AMPA) receptors (Dingledine et al., 1999). Before the mid-1980s, it was thought that glutamate acted exclusively on ionotropic receptors, however it was later discovered that cell exposure to glutamate increased inositol phospholipid hydrolysis, and the metabotropic glutamate (mGlu) receptors were discovered (Sugiyama et al., 1987). While iGlu receptors form ligand-gated ion channels that mediate rapid synaptic transmission, mGlu receptors are GPCRs that modulate neuronal excitability and synaptic plasticity through slower, more complex intracellular signalling pathways, leading to modulation of the strength and efficacy of glutamatergic synapses (Mao & Wang, 2016). The intricate balance and interplay between iGlu receptors and mGlu receptors are crucial for maintaining healthy brain physiology.

1.3.1 Classification of Metabotropic Glutamate Receptors

The eight metabotropic glutamate receptor subtypes (mGlu₁ to mGlu₈) are categorised into three groups based on sequence homology, pharmacology, and G protein coupling (Kolb et al., 2022). The receptors are transcribed from the genes *GRM1-8*.

Group I mGlu receptors, mGlu₁ and mGlu₅, primarily couple to G $\alpha_{q/11}$ proteins to stimulate increases PLC activity. Group I mGlu receptors have also been speculated to couple through G $\alpha_{i/o}$ (Joly et al., 1995; Parmentier et al., 1998) and G α_s (Nasrallah et al., 2018), however other groups have failed to replicate these speculative couplings (Balázs et al., 1997; McCulloch et al., 2023; Minakami et al.,

1997). Both group II mGlu receptors (mGlu₂ and mGlu₃), and group III mGlu receptors (mGlu₄, mGlu₆, mGlu₇ and mGlu₈) predominantly couple to the Gα_{i/o} transduction pathway.

1.3.1.1 Alternative Splicing and Receptor Isoforms

Both members of the group I mGlu receptors have had isoforms identified. mGlu₁ was the first glutamate receptor to have its isoforms cloned, and it was found that the *GRM1* gene encodes four main splice variants: mGlu_{1a}, mGlu_{1b}, mGlu_{1c}, and mGlu_{1d}. These isoforms differ in their C-termini; the mGlu_{1a} isoform has a long C-terminus, involved in synaptic plasticity, whereas the remainder of the isoforms have a shorter C-terminus and have differing signalling properties (Hermans & Challiss, 2001). In *Xenopus* oocytes, it was demonstrated that compared to the rapid transient calcium responses produced by mGlu_{1a} and mGlu_{1c} generates smaller, slower, but long-lasting calcium oscillations (Pin et al., 1992). Additionally, the mGlu_{1b} receptor internalises from the cell surface following agonist stimulation at a faster rate than mGlu_{1a} (Ciruela & McIlhinney, 1997). These observed differences in calcium signalling and internalisation are likely to be due to the differences in the C-termini of the mGlu₁ receptor isoforms.

The type 5 metabotropic glutamate receptor was first cloned in 1992 and was highly homologous to previously cloned mGlu receptors (Abe et al., 1992). The mGlu₅ receptor has two reported isoforms, determined to arise from alternative splicing and not different genes (Minakami et al., 1993). The mGlu_{5b} isoform possesses an insertion of 32 amino acids, 50 residues downstream of TMD7 at the beginning of the C-terminus. This insert contains two putative phosphorylation sites for PKA and PKC (Joly et al., 1995), and is evolutionally conserved between human, rat and mouse (Minakami et al., 1995). When expressed in mammalian cells, no differences in the pharmacological profiles of mGlu_{5a} and mGlu_{5b} were observed (Minakami et al., 1994; Mion et al., 2001), however there has been much documentation on the difference in expression of the isoforms, notably during development. During rat postnatal development, the predominant mGlu₅ isoform switches at postnatal weeks 1 and 2 from mGlu_{5a} to mGlu_{5b} in the hippocampus and cortex (Minakami et al., 1995). In the adult brain, mGlu_{5b} mRNA is expressed at a higher level than mGlu_{5a} and expression of

mGlu_{5b} varies in different brain regions: expression is significantly lower in the olfactory bulb compared to the hippocampus, striatum, and cerebral cortex (Joly et al., 1995; Romano et al., 2002). mGlu_{5b} is also known to regulate the extension of neurites to influence maturation of neurons, whilst mGlu_{5a} hinders neurite outgrowth (Mion et al., 2001).

Currently, there are no identified isoforms from mGlu₂, whereas mGlu₃ undergoes alternative splicing yielding at least four forms of the receptor. *GRM3* encodes for full length mGlu₃, *GRM3Δ2* (missing exon 2), *GRM3Δ2Δ3* (missing exons 2 and 3) and *GRM3Δ4* (missing exon 4). The most abundant of said mGlu₃ isoforms is the isoform lacking in exon 4 (*GRM3Δ4*), expressed in the cerebellum, B lymphoblasts, hippocampus and prefrontal cortex. Exon 4 of *GRM3* encodes for the TMD of the receptor, thus the *GRM3Δ4* isoform is a truncated version of the receptor, retaining an intact N-terminal region. Despite this truncation, *GRM3Δ4* exists as a 60 kDa protein localised to the cell membrane (Sartorius et al., 2006).

Within group III mGlu receptors, there is high diversity due to alternative splicing, particularly within the C-terminus. Two splice variants of mGlu₄ have been identified, with mGlu_{4b} differing from mGlu_{4a} by the last 64 amino acids of the C-terminus being replaced by 135 amino acids (Thomsen et al., 1997). Isoform mGlu_{7b} is generated by replacement of the distal 16 amino acid residues of the C-terminal tail with 23 amino acids compared to mGlu_{7a} (Corti et al., 1998). Three further variants were identified a few years later: mGlu_{7c}, mGlu_{7d} and mGlu_{7e}, which differ in the C-terminal region by substitution of the distal 16 amino acids with 25, 12 and 7 amino acids correspondingly (Schulz et al., 2002). Three isoforms of mGlu₈ exist (mGlu_{8a}, mGlu_{8b}, mGlu_{8c}), with both mGlu_{8a} and mGlu_{8b} showing similar patterns of expression with comparable levels of expression in both fetal and adult brains (Malherbe et al., 1999). The isoform mGlu_{8c} has a 74 base pair out of frame insertion in comparison to mGlu_{8a}, resulting in a 501 amino acid long protein terminated before the TMDs. These truncated forms of the receptors are proposed to be a secreted form of the receptor and potentially act as soluble receptors (Corti et al., 1998; Malherbe et al., 1999).

The human retina expresses two isoforms of *GRM6*, both truncated receptors of 425 and 405 amino acids in length, comprised of the conserved N-terminal region but lacking in the TMDs and C-terminus (Valerio et al., 2001).

1.3.2 Architecture of Metabotropic Glutamate Receptors

1.3.2.1 N-Terminus and Ligand Binding Domain

When mGlu_{1a} was first cloned in 1991, it was noted that the N-terminal region was unusually large for a GPCR, which was later determined to be approximately 65 kDa (Houamad et al., 1991; Romano et al., 1996). Whilst the ligand binding domain is located within a pocket formed by the seven TMDs for the majority of GPCRs, it is not the case for members of the glutamate receptor family. The ligand binding domain is located within the N-terminal Venus fly trap (VFT) domain (Figure 1.7), 100 Å away from the seven TMD (Nasrallah et al., 2021). In all receptors in the glutamate receptor family, with the exception of the GABA_B receptor, a cysteine rich domain (CRD) connects the VFTs to the TMDs (Lee et al., 2015). The CRD contains nine critical cysteine residues, of which eight form intra-subunit disulphide bridges.

The mechanisms by which family C GPCRs communicate their signals across the 120 Å distance from the orthosteric binding site on the VFTs to the TMD has been of long-standing interest to the GPCR field. The globe-like VFT structures were previously thought to have solely three states: open-open (inactive) stabilised by antagonist binding, open-closed (active) and closed-closed (active) conformations stabilised by agonist binding to one or both of the VFTs. The rearrangement of protomers due to the change in activity state results in the CRDs propagating conformational changes to the TMDs, bringing the domains into closer proximity by a degree of 20 Å (Bessis et al., 2002; Koehl et al., 2019). (Figure 1.7). Recent work by Kumar et al. (2023) proposed a sequential activation model following cryo-EM work on the mGlu₅ receptor, demonstrating a sequence of intermediate functional states between the 'inactive' and 'active' conformations. Subsequent to glutamate binding to the VFTs, the dimeric receptor adopts an 'Intermediate 1a' state, in which the VFT lobes are closed but there is a great distance between the protomers, mimicking the inactive conformation (Kumar et al., 2023). This state is different from previously proposed mGlu receptor states, where agonist binds to and activates just one protomer at a time (Liauw et al., 2021; Seven et al., 2021). The Intermediate 1a conformation transitions to the 'Intermediate 2a' active-like configuration, where the VFTs, CRDs, and TMDs are all in close proximity. In the 'Intermediate 2a' configuration, there is a large twisting of VFTs seen, maintaining the orthosteric binding pocket but initiating

rearrangement of the hinge region leading to a reduced distance between the CRDs and TMDs, a notable sign of glutamate receptor family activation (Koehl et al., 2019; Kumar et al., 2023). The 'Intermediate 3a' state resembles that of Intermediate 2a, however there is a difference in the conformation of ICL2. Furthermore, there is evidence of an 'Intermediate 3b' conformation in the presence of the orthosteric agonist L-quisqualic acid and PAM-agonist CDPPB; this state demonstrates similarities to the Intermediate 3a state, but with further reduced inter-protomer distance before the fully active conformation is reached (Kumar et al., 2023). This work was recently replicated and corroborated through single molecule fluorescent resonance energy transfer (smFRET) studies tagging each protomer with FRET donor and acceptor proteins (Latorraca et al., 2024).

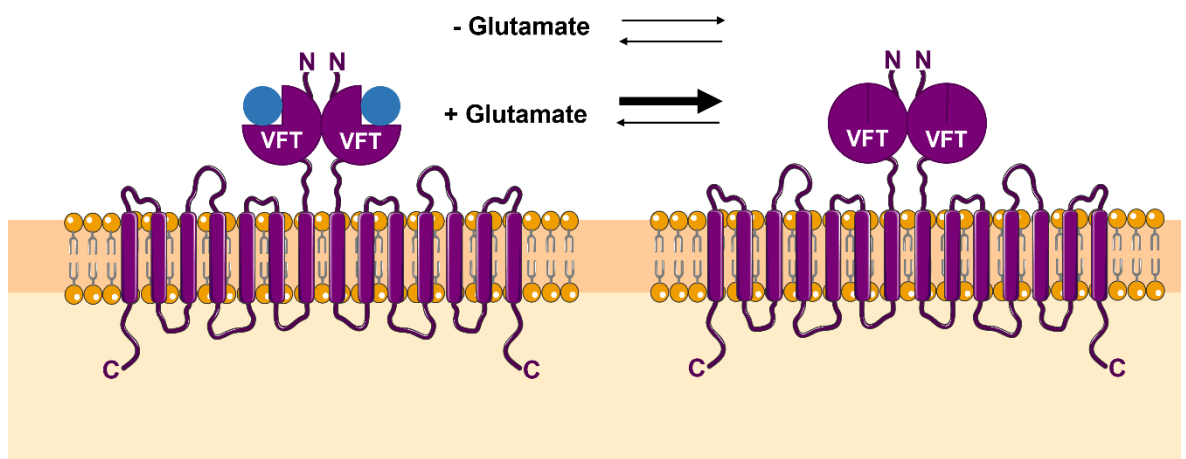


Figure 1.7: The involvement of the Venus flytrap domains of glutamate receptors in agonist activation. The extracellular Venus flytrap domains spontaneously change between open and closed in the absence of a ligand. Binding of the endogenous agonist glutamate to the N-terminal Venus flytrap domains stabilises the closed conformation.

1.3.2.2 C-Terminus

The C-terminal domain of metabotropic glutamate receptors is a vital determinant of their functional properties, influencing receptor localisation, protein-protein interactions, and intracellular signalling pathways. The C-terminal domain of mGlu receptors varies significantly in length and composition among the different receptor subtypes. The C-terminus of GPCRs is rich in serine, threonine and tyrosine residues, all of which are putative targets for protein kinases. This sequence is critical for receptor localisation and trafficking, as it contains motifs that regulate transport of the receptor. Additionally, the C-terminus facilitates

interactions with an array of intracellular proteins such as scaffolding proteins, kinases and phosphatases, each influencing downstream signalling.

Group I mGlu receptors, notably the splice variants mGlu_{1a}, mGlu_{5a}, and mGlu_{5b}, all possess a long C-terminal domain, which interacts with the Ena/VASP Homology 1 (EVH) domain of the scaffolding protein Homer through a proline-rich Homer motif in the distal C-terminus of the receptor (PPXXFr) (Tu et al., 1998). IP₃ receptors also possess this motif, and it is proposed that this allows Group I mGlu receptors and the IP₃ receptors to come in close proximity facilitating a link to intracellular calcium ion stores (Xiao et al., 2000). This group I mGlu receptor C-terminal region also contains multiple phosphorylation sites for kinases like PKC (Gereau IV & Heinemann, 1998) and calmodulin-dependent kinase (Minakami et al., 1997).

The C-terminus of group II mGlu receptors plays a role in coupling to the G $\alpha_{i/o}$ proteins and facilitates interaction with other interacting proteins such as Na⁺/H⁺ exchanger regulatory factors (NHERFs) (Ritter-Makinson et al., 2017). It was found that a specific 50 amino acid region of the C-terminus of mGlu₃ interacts with protein phosphatase 2C α (PP2C α) and alignment of this sequence to mGlu₂ revealed that this region is not conserved between the two receptors within group II (Flajolet et al., 2003). The binding of PP2C α is inhibited by phosphorylation of Ser845 by protein kinase A (PKA) in the C terminus of mGlu₃, however PP2C α is able to dephosphorylate this site (Flajolet et al., 2003).

Group III mGlu receptors have varying lengths of C-termini yet are still typically shorter than those of group I. Protein interactions with the C-termini of group III mGlu receptors are mediated by short linear motifs (Seebahn et al., 2011). It has been proposed by (Dev et al., 2001) that there exists three distinct functionally relevant domains present in the intracellular C-terminus of the mGlu₇ receptor: (1) a proximal intracellular signalling domain that interacts with G protein $\beta\gamma$ -subunits (Okamoto et al., 1994); (2) a central domain thought to provide a signal for axonal targeting, as C-terminal truncation of the receptor was shown to exclude the receptor from axons (Stowell & Craig, 1999); and (3) a terminal PDZ-binding motif that interacts with the protein kinase C interacting protein 1 (PICK1), a component of the presynaptic complex involved in mGlu_{7a} aggregation, presynaptic localisation, and modulation of glutamate neurotransmission (Boudin et al., 2000; El Far et al., 2000). It has been revealed that PKC phosphorylation of Ser862 in the mGlu₇ C-terminus can inhibit the binding of G $\beta\gamma$ subunits; this

incidence may provide a theory by which mGlu₇ has low affinity for glutamate and is predicted to only be activated during periods of intense synaptic activity (Niswender & Conn, 2010). For mGlu₈, there have been several protein interactions identified, including Ran binding protein in the microtubule-organising centre (RanBPM) (Seebahn et al., 2008), a 90 kDa scaffold protein involved in the regulation of the immune and the nervous system (Murrin & Talbot, 2007). In addition, the band 4.1B protein binds to the C-terminal domains of all splice variants of mGlu₈, co-localising with and facilitating their cell surface expression and modulating mGlu₈-mediated reduction of intracellular cAMP concentrations (Rose et al., 2008).

More generally, the C-termini of mGlu receptors play critical roles in synaptic plasticity through interaction with scaffolding proteins and modulation of signalling pathways. A study using chimeric mGlu₂ and mGlu₇ receptors revealed that the C-terminus is a key structural determinant of selection of specific signal transduction pathways in neurons (Perroy et al., 2001).

1.3.2.3 Constitutive Dimerisation of mGlu Receptors

Constitutive dimerisation refers to the inherent tendency of mGlu receptor monomers to form stable dimers without the presence of ligands or other extracellular stimuli. It was recognised shortly after their initial cloning that all mGlu receptors are capable of forming homodimers, however there is also evidence that mGlu receptors form both intra-group (for example mGlu_{1/5}) and inter-group (mGlu_{2/4}) heterodimers (Doumazane et al., 2011). Meng et al. (2022) demonstrated through the use of nanobody-based biosensors that mGlu₄ subunits predominantly exist as heterodimers with other mGlu receptors in most brain regions outside of the cerebellum (Meng et al., 2022). Additionally, group I metabotropic glutamate receptors mGlu₁ and mGlu₅ form a complex in mouse hippocampus and cortex (Pandya et al., 2016). The formation of heterodimers produces unique pharmacological parameters, such as altered affinity and efficacy compared to their respective homodimers (Habrian et al., 2023); these complex behaviours could contribute to the difficulty in selectively targeting individual mGlu receptors and the failure of translating mGlu receptor-specific drugs into a clinical setting.

Stable, covalent metabotropic glutamate receptor dimerisation was first reported for the mGlu₅ receptor (Romano et al., 1996) and shortly after, through crystallography studies (Kunishima et al., 2000). The dimeric arrangement is required for glutamate to activate mGlu receptors (El Moustaine et al., 2012). Each mGlu₅ protomer possesses a large extracellular domain that mediates dimerisation through formation of inter-protomer disulphide bonds at the cysteine rich domain (Romano et al., 1996; Tsuji et al., 2000). The ninth residue of the CRD forms an inter-subunit disulphide bridge with a cysteine residue located in lobe 2 of the VFTs. In addition to the CRD, the seven TMDs and the C-terminus have been shown to contribute to the stabilisation and regulation of mGlu receptor dimerisation (Chang & Roche, 2017).

1.3.3 Localisation and Subcellular Expression of mGlu Receptors

Understanding the precise distribution of mGlu receptors at synapses and other subcellular compartments provides insights into their physiological role in brain function and their contributions to neurological disorders. Group I mGlu receptors are enriched at the post-synapse of excitatory neurons of the hippocampus, cortex and striatum (Shigemoto et al., 1993). The type 5 mGlu receptor is also known to be endogenously expressed in astrocytes and is postulated to play a role in multiple physiological and pathophysiological processes (Figure 1.8) (Bradley & Challiss, 2011).

Group II metabotropic glutamate receptors are distributed pre-synaptically and post-synaptically in various brain regions (Figure 1.8), including the hippocampus, cortex, caudate putamen, thalamus, cerebellum, and basal ganglia (Makoff et al., 1996). The type 3 mGlu receptor is additionally found on astrocytes, alongside mGlu₅ (Figure 1.8) (Schools & Kimelberg, 1999). Pre-synaptically localised group II mGlu receptors regulate neurotransmitter release by modulating voltage-gated calcium channels, neurotransmitter vesicle release machinery, and signalling pathways. Group II mGlu receptors have demonstrated neuroprotective activity (Kingston et al., 1999). The presence of group II mGlu receptors on both pre- and post-synapses indicates that they contribute to the balance of excitatory and inhibitory neurotransmission.

Group III mGlu receptors are predominantly localised pre-synaptically in various brain regions (Figure 1.8): mGlu₄ is expressed predominantly in the cerebellum (Flor et al., 1995), mGlu₇ in the cortex, hippocampus, thalamus, and midbrain (Bradley et al., 1998), and mGlu₈ in the cortex, hippocampus, pons, medulla oblongata, and midbrain (Shigemoto et al., 1997). In the brain, group III receptors play roles in regulating synaptic transmission, synaptic plasticity, and neuronal excitability. The exception, mGlu₆, is expressed only on the post-synapse of ON-bipolar retina cells, where it plays a key role in the detection of light. When glutamate is released from photoreceptors in the dark, it binds to mGlu₆ on the ON-bipolar cells, activating G $\alpha_{i/o}$ proteins (Nomura et al., 1994).

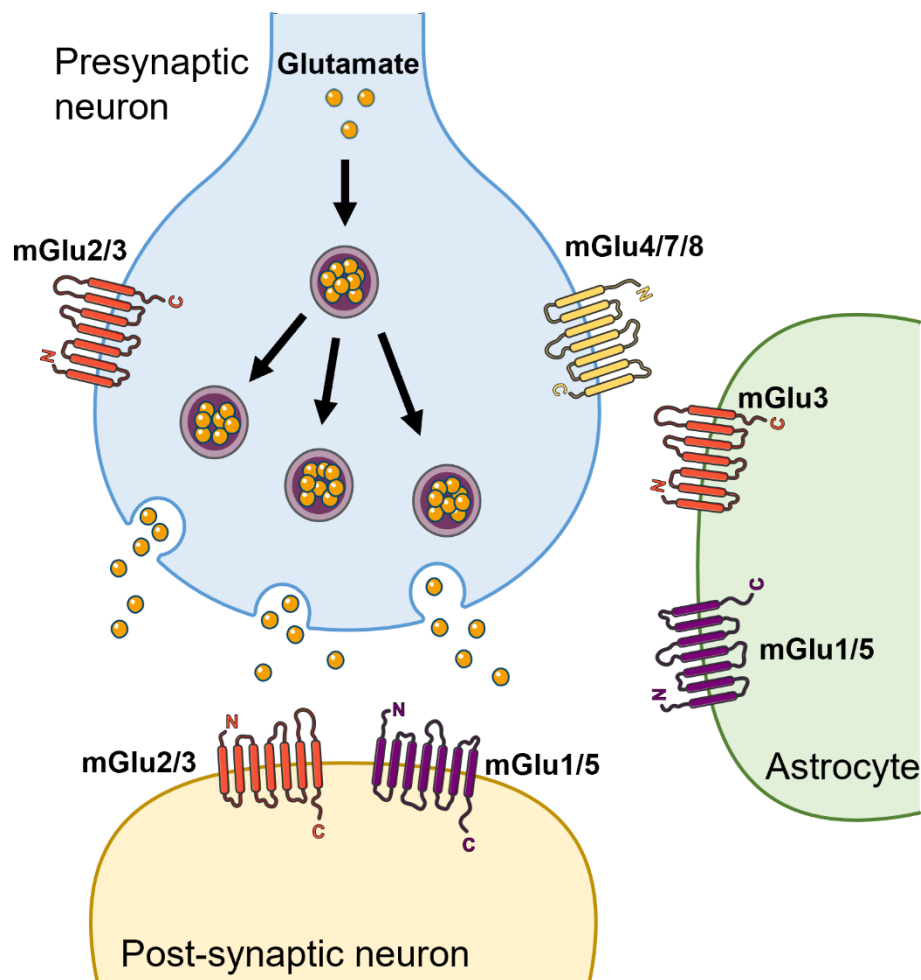


Figure 1.8: The synaptic localisation of metabotropic glutamate receptors. Group I mGlu receptors (mGlu_{1/5}) are predominantly expressed on the post-synapse of neurons, mGlu₂ is expressed pre- and post-synaptically alongside mGlu₃, which is additionally expressed on astrocytes. The receptors mGlu_{4/7/8} are predominantly expressed pre-synaptically.

1.3.4 Constitutive Activity of the mGlu₅ Receptor

With mGlu receptors, constitutive activity manifests as the spontaneous activation of downstream signalling pathways even in the absence of glutamate through ligand-independent conformational changes that stabilise active receptor states that promote G protein coupling. Constitutive activity may contribute to homeostatic regulation of neuronal activity by setting the resting membrane potential and influencing the balance between excitatory and inhibitory neurotransmission (Turrigiano, 2012). Of all the mGlu receptors, constitutive activity has predominantly been reported for the type 5 metabotropic glutamate receptor.

Cells expressing mGlu_{5a} or mGlu_{5b} isoforms were found to have increased PLC activity not dependent on glutamate, as the activity was still high when the glutamate degrading enzyme Glutamate-pyruvate transaminase (GPT) was present, hence this effect was due to high intrinsic activity (Joly et al., 1995). The enzyme glutamate-pyruvate transaminase (GPT) is commonly used in assays, catalysing a reversible reaction converting the substrates glutamate and pyruvate to alanine and α -ketoglutarate (Matthews et al., 2000). Additionally, mGlu₅ internalisation (not mediated by clathrin-coated pits) can occur independently of interaction with endogenous agonist, as it was shown that receptors with mutations in the orthosteric binding site still internalised, determined to be at a rate of 11.7% per minute of the total cell surface receptor pool (Fourgeaud et al., 2003). Later work confirming this constitutive internalisation found that in HEK293 cells, mGlu₅ undergoes constitutive internalisation where receptors are sequestered to the recycling compartment with no lysosomal localisation observed and the majority of mGlu₅ receptors are recycled back to the cell membrane within 3.5 hours following internalisation (Trivedi & Bhattacharyya, 2012).

The Homer family of scaffolding proteins also exert a strong effect on regulating the level of constitutive G protein coupling to mGlu₅. The receptor associating with Homer3 reduces the constitutive activity of mGlu₅, whereas complexes with Homer1a enhances constitutive activity mGlu₅ (Ango et al., 2001), likely through disruption of mGlu₅ association with Homer3 (Fagni et al., 2003).

Constitutive activity of metabotropic glutamate receptors represents an intriguing aspect of receptor function with significant implications for synaptic physiology and pharmacology. It has been shown that disruption of mGlu₅-Homer

complexes leads to phenotypes of neuropathology, specifically an inheritable form of autism named Fragile X Syndrome, indicating a role for Homer scaffolding and regulation of constitutive activity in complex pathologies (Guo et al., 2016).

Both the constitutive activity of the receptor and the abundance of endogenous glutamate in the cells makes this receptor challenging to study *in vitro*. It is difficult to ensure endogenous glutamate is removed from the cells, making it complicated to be certain if assays are measuring constitutive signalling or agonist-dependent signalling. Commonly, glutamate transporters such as the glutamate/aspartate transporter (GLAST) (Desai et al., 1996) (now known as the excitatory amino acid transporter 1 (EAAT1)), or the excitatory amino acid transporter 2 (EAAT2) are co-expressed with mGlu₅ to reduce endogenous glutamate within the cell to prevent excitotoxicity or to ensure cellular responses within assays are solely from exogenously applied glutamate. Transporters have much higher affinities for glutamate than glutamate-degrading enzymes, however enzymes have a higher capacity for glutamate elimination (Matthews et al., 2003). This outlines the challenges in interpreting the constitutive activity of mGlu receptors, as it is typically impossible to remove all endogenous glutamate from the cell assay system.

1.3.5 The Therapeutic Potential of mGlu₅ in the Central Nervous System

Due to the ubiquitous expression of metabotropic glutamate receptors and widespread glutamatergic synapses within the central nervous system, mGlu receptors could provide a promising drug target for a multitude of neurological pathologies. Targeting metabotropic receptors over ionotropic receptors will marginally impact fast synaptic transmission and decrease the likelihood of off-target cognitive effects and causation of a widespread depression of neuronal activity usually associated with ionotropic receptor ligands (Mao & Wang, 2016)

Within the glutamate family of receptors, the orthosteric binding site in the VFT is highly conserved, making targeting of specific mGlu receptors with orthosteric ligands and designing selective drugs very challenging. However, the allosteric site located within the TMDs is generally less conserved, thus targeting

this site permits easier subtype selectivity for drug targets (Wenthur et al., 2014). Allosteric ligands may provide the opportunity to preferentially activate only the clinically desirable subset of effectors and functions from a single mGlu receptor, negating the physiological pathways that result in off target effects (Sengmany et al., 2017; Trinh et al., 2018). To understand which transduction pathways should be potentiated or downregulated, it is important to understand the physiological role of receptor phosphorylation and effects of pharmacological manipulation.

The mGlu₅ receptor is known to play a role in many physiological and pathological processes in the brain including Alzheimer's disease, Fragile X syndrome, anxiety and addiction (Su et al., 2021). Previous work has demonstrated that genetic deletion of mGlu₅ reduced β -amyloid oligomers and rescues learning deficits seen in an APP^{swe}/PS1 Δ E9 mouse model of Alzheimer's disease (Hamilton et al., 2014) and mGlu₅ overactivation contributes to impaired clearance of neurotoxic aggregates (Abd-Elrahman et al., 2018). Modulating the mGlu₅ receptor increases the risk of excitotoxicity; glutamate accumulation in the synaptic cleft over physiological limits is toxic to the cells through potentiation of the ionic glutamate receptors NMDA and AMPA, leading to entry of excessive levels of calcium ions and cell death, a common hallmark of many neurodegenerative disorders (Price et al., 2010). Activation of mGlu₅ has been demonstrated to enhance neuronal toxicity through NMDA-receptor mediated mechanisms (Bruno et al., 1995) suggesting the search for selective antagonists at the mGlu₅ receptor is required. This evidence suggests that mGlu₅ is a potential target for treatment of neurological disorders.

1.3.5.1 Schizophrenia

Schizophrenia affects approximately 1% of the population and is characterised by the following major clinical symptoms: positive symptoms (delusions, hallucinations, and abnormal behaviours) or negative symptoms (blunting of emotional responses, withdrawal from social engagement) (Coyle, 2006). Additional symptoms such as defects in cognitive function (memory and attention span) have also been noted, alongside co-morbidities with anxiety and depression.

There exists the 'glutamate theory of schizophrenia', in which glutamatergic signalling is disturbed and leads to the array of symptoms observed in

schizophrenia patients (Coyle, 1996). The theory suggests that the role of glutamate is predominantly due to hypofunction of NMDA ionotropic glutamate receptor signalling. NMDA receptor antagonists (for example ketamine and phencyclidine) reduce glutamate concentrations in the brain and produce psychotic symptoms (Rang et al., 2007). A common drug-induced mouse model of schizophrenia involves administering noncompetitive NMDA receptor antagonists, demonstrating symptoms stereotypical of schizophrenia (Winship et al., 2019), supporting the glutamate hypothesis of schizophrenia. There is additional involvement of metabotropic glutamate receptors, due to their influence on NMDA receptor function, particularly in brain regions associated with cognitive function. An increase in metabotropic glutamate receptor populations in post-mortem brains of schizophrenia patients has been observed (Ohnuma et al., 1998), indicating a link between this receptor and schizophrenia. Specifically, mGlu₅ receptors can modulate the function of dopamine D2 receptors, which are implicated in the pathophysiology of schizophrenia and the mechanism of action of antipsychotic drugs. Dysregulation of mGlu₅ signalling can affect dopamine through synergism with adenosine A_{2A} receptor interaction (Ferré et al., 2002) contributing to both the positive and negative symptoms of schizophrenia.

Currently, available treatments ameliorate the positive symptoms of schizophrenia, but do not impact the negative or cognitive symptoms. Directly targeting the NMDA receptor results in toxicity due to over-activation of the receptor and excitotoxicity (Hirose & Chan, 1993), thus targeting the mGlu receptors which requires the slower process of G protein-activation in order to enhance NMDA receptor activity reduces the risk of over-activation. Due to the involvement of mGlu₅ and NMDA receptors, positive potentiation of mGlu₅ may reverse the hypofunction of NMDA receptors (Benquet et al., 2002). Recently, it was shown that potentiation of mGlu₅ by the PAM CDPPB attenuated elevations in extracellular glutamate in the medial prefrontal cortex induced by MK-801, an NMDA receptor antagonist (LaCrosse et al., 2024).

Furthermore, mGlu₅ is known to play a role in long-term potentiation (LTP) and long-term depression (LTD) in the brain, supporting the theory that positive allosteric modulation of mGlu₅ may improve the cognitive symptoms seen in schizophrenia (Ayala et al., 2009). Despite this, one risk of directly targeting mGlu₅ with allosteric modulators includes excitotoxicity mediated by the enhanced NMDA receptor activity; mGlu₅ receptor PAMs have previously been shown to induce

seizures and neurotoxicity in rodents (Parmentier-Batteur et al., 2012; Rook et al., 2015). An mGlu₅ PAM has been developed by Conde-Ceide et al. (2015) (VU0409551) with the aim of treating the cognitive symptoms of schizophrenia. This ligand exhibits 'modulation bias', selectively potentiating mGlu₅ coupling to G α_q -mediated signalling but not modulating NMDA receptor currents or NMDA receptor-dependent synaptic plasticity. The efficacy of mGlu₅ specific positive allosteric modulators in animal models of psychosis was previously attributed to potentiation of NMDA receptor function (Rook et al., 2015), therefore the experimentation with this novel compound provides answers to the mechanisms by which mGlu₅ plays a role in schizophrenia. VU0409551 produced robust antipsychotic-like and cognition-enhancing activity in animal models and demonstrated restoration of the balance of excitatory and inhibitory signalling which may underlie the mGlu₅ PAM-mediated correction of cognitive deficits (Brown et al., 2023; Rook et al., 2015). However, recent studies have brought about safety concerns with mGlu₅ PAMs; whilst the PAMs were initially shown to be effective pro-cognitive compounds, studies by Płoska et al. (2024) indicate that CDPBP exaggerated the model of psychosis and enhances endothelial nitric oxide synthase (eNOS) dimer disruption much above the control level, a substance which regulates a variety of biological processes and its dysfunction contributes to multiple brain pathologies. The results indicate serious limitations related to the use of mGlu₅-targeting ligands and indicates that further specificity of ligands is required for drug safety.

1.3.5.2 Substance Abuse

Metabotropic glutamate receptors, specifically mGlu₅, are critically involved in synaptic plasticity mechanisms which are essential for learning and memory (Hagena & Manahan-Vaughan, 2022). Drugs of abuse can hijack these plasticity mechanisms, leading to maladaptive changes in neural circuits that underlie addictive behaviours. High expression of mGlu₅ receptors is observed in the mesolimbic dopamine system, including the nucleus accumbens (NAc) and ventral tegmental area (VTA) (Shigemoto et al., 1993), regions critically involved in reward processing. Activation of mGlu₅ receptors in these regions enhances dopamine release, reinforcing the rewarding effects of drugs. During withdrawal, changes in mGlu₅ receptor function can contribute to negative affective states, such as

anxiety and depression, which drive continued drug use to alleviate these symptoms. Substance abuse can even effect expression of glutamate receptors: it was recently shown by two groups that alcohol-drinking leads to altered expression of glutamate receptors in the hippocampus in a sex-dependent manner (Fabian et al., 2024; Szumlinski et al., 2023).

The mGlu₅ receptor plays a key role in cue-induced relapse, where exposure to drug-related cues triggers craving and drug-seeking behaviour, as mGlu₅ knockout mice was shown to have significantly reduced operant sensation seeking behaviours relative to wildtype mice (Olsen et al., 2010). It was shown that mGlu₅ knockout mice show a lack of cocaine self-administration and did not show hyperlocomotion activity in response to cocaine dosing (Chiamulera et al., 2001), suggesting that mGlu₅ is involved in the behavioural effects of cocaine addiction, however later studies could not replicate these results and found no difference in cocaine self-administration between mGlu₅ knockout mice and wildtype mice (Fowler et al., 2011). It is well established that a decrease in signalling from mGlu₅ via antagonist treatment inhibits cocaine and nicotine seeking behaviours (Bäckström & Hyttiä, 2005; Kenny et al., 2005; Palmatier et al., 2007; Tessari et al., 2004; Vendruscolo et al., 2024), however whilst this downregulation of group I mGlu receptor signalling is shown to reduce drug reward and relapse-related behaviours, positive allosteric modulation of mGlu₅ may reverse some of the cognitive deficits seen following drug abuse (Gass & Olive, 2009).

There is evidence to suggest a link between glutamate receptor post-translational modifications, excitatory synaptic plasticity, and drug-seeking behaviour (as outlined by Mao et al., (2011)). A study by Park et al. (2013) where cocaine was administered to mice demonstrated that this dosing induced both Homer1a expression and phosphorylation of Ser1126 of mGlu₅ in the striatum. The same study also explored the cocaine-stimulated block of D1 dopamine receptor dependent LTD, determining it was dependent on Pin1 acting at mGlu₅ thus inhibitors of Pin1 or allosteric modulators of mGlu₅ that disrupt this complex may be useful in treating drug addiction (Park et al., 2013). Homer2 is phosphorylated on Ser117/Ser216 by calcium-calmodulin kinase II α (CaMKII α), which induces a rapid dissociation of mGlu₅-Homer2 scaffolds; this phosphorylation was recently shown to gate the regulation of mGlu₅ binding following high doses of cocaine (Szumlinski, Beltran, et al., 2023). Together, these

studies suggest that mGlu₅ plays a role in the drug seeking behaviour in addiction and regulation of drug consumption, but not the conditioned associations.

The involvement of mGlu₅ in synaptic plasticity, reinforcement, withdrawal, and relapse highlights their potential as therapeutic targets. Developing mGlu₅-based treatments offers promising avenues for addressing addiction and improving outcomes for individuals struggling with substance abuse disorders, however limitations in directly targeting the receptor exist due to the risk of excitotoxicity.

1.3.5.3 Fragile X Syndrome

Fragile X syndrome (FXS) is the leading genetic cause of autism and is the most common form of inherited intellectual disability. This arises from the amplification of CGG trinucleotide repeat of fragile X mental retardation 1 gene (*FMR1*), encoding the fragile X mental retardation protein (FMRP); the mutation is linked to the methylation of the gene, resulting in silencing of this gene (Pieretti et al., 1991). There is a correlation between the severity of the phenotype and the magnitude of FMRP deficiency. Symptoms include moderate to severe cognitive impairment, susceptibility to seizures, hyperactivity, hypersensitivity to sensory stimulation, anxiety and obsessive-compulsive behaviours (The Dutch-Belgian Fragile X Consortium et al., 1994). Generation of an *FMR1*^{-/-} mouse leads to symptoms consistent with those seen in humans with FXS (Kazdoba et al., 2014).

The metabotropic glutamate receptors have been implicated in FXS: activation of Group I mGlu receptors stimulates FMRP-mediated mRNA transport and protein synthesis near synapses (Di Marco et al., 2021), leading to the functional consequence of long-term depression (LTD) in the hippocampus when FMRP is lost (Bear et al., 2004). Typically, FMRP and Group I mGlu receptors work in physiological opposition, however when FMRP is absent due to the gene silencing, unchecked mGlu receptor-dependent synaptic protein synthesis leads to FXS (Dölen et al., 2007). Additionally, the crossbreeding of an FXS mouse model with an mGlu₅-knockout mouse line results in a phenotype correcting the symptoms seen in FXS (Dölen et al., 2007). It was found that mGlu₅ expression was significantly elevated in cortex of participants with idiopathic autism spectrum disorder but reduced in all brain regions of men with FXS (Brašić et al., 2021). This same pattern of expression was confirmed using Positron emission tomography

(PET) imaging by Mody et al. (2021) and when testing a novel PET tracer for mGlu₅ expression as a biomarker for FXS, patients with FXS were found to have reduced mGlu₅ availability. This led to the hypothesis that chronic downregulation of Group I mGlu receptors may correct the altered development in FXS. A multitude of mGlu₅ antagonists and NAMs have been tested in the clinic (Berry-Kravis et al., 2009; Michalon et al., 2012; Yan et al., 2005). However, these drugs targeting mGlu₅ for FXS have so far been unsuccessful in clinical trials, thus there is a requirement for better understanding of the role of mGlu receptors in FXS to develop treatments.

1.3.5.4 Alzheimer's Disease

Alzheimer's disease (AD) is a progressive neurodegenerative disorder characterized by cognitive decline, memory loss, and changes in behaviour. Pathologically, AD is marked by the accumulation of amyloid-beta (A β) plaques, neurofibrillary tangles, and synaptic dysfunction (Reviewed in (Rajmohan & Reddy, 2017)).

Metabotropic glutamate receptors are expressed throughout the brain in both neurons and microglia, for modulation of excitatory glutamatergic signalling. The expression of mGlu₅ on astrocytes may modulate the release of factors able to influence cell death (Spampinato, et al., 2018), for example through excitotoxicity mediated mechanisms via excessive calcium ion release. An elevation of glutamatergic signalling and excitotoxicity was recently found to be the main common feature of pathogenesis in the 5xFAD amyloidogenic mouse model and in AD patients (Bartas et al., 2024). The mGlu₅ availability correlates with neuropathological biomarkers of AD such as amyloid deposition, confirmed by a recent PET/MRI study (Wang et al., 2024).

A notable hallmark of Alzheimer's disease is synaptic loss and weakening, with A β oligomers which form plaques in the brain being a synaptotoxic trigger (Zhang et al., 2022). Studies have revealed that mGlu₅ acts as a co-receptor for A β oligomers and cellular prion protein, causing activation of the receptor and inducing pathophysiological signalling through release of calcium ions (Abd-Elrahman et al., 2020; Haas et al., 2017; Um et al., 2013). To confirm this, studies on acute A β oligomer treatment to hippocampal slices demonstrated enhancement of mGlu₅-dependent long-term depression and glutamatergic synapse dysfunction

through NMDA receptor dysfunction (Ng et al., 2023). The signalling of mGlu₅ has been shown to be altered in multiple rodent models of AD and it was also found that group I mGlu receptor-mediated calcium ion dyshomeostasis is a potentially pathogenic event in AD (Kaar et al., 2024).

Confusingly, group I mGlu receptor agonists have demonstrated both neuroprotection and neurotoxicity in *in vitro* and *in vivo* models of neurodegeneration (Nicoletti et al., 1999). Recently, mGlu₅ NAMs have been predominant in AD research, based on the principle that the genetic deletion of mGlu₅ reverses learning and memory deficits and reduces A β plaques in a mouse model of neurodegeneration (Hamilton et al., 2014). An mGlu₅ NAM tested in an APP^{swe}/PS1 Δ E9 mouse model reversed cognitive deficits after 24 weeks of treatment, however at 36 weeks of treatment the NAM had no impact on disease pathology (Abd-Elrahman et al., 2023), suggesting mGlu₅ does not drive the late-stage pathogenesis in this model. Despite this, support for mGlu₅ antagonism as therapeutic strategy comes from the observation that mGlu₅ is upregulated in AD patients (Renner et al., 2010). This upregulation in mGlu₅ expression is reduced in both APP^{swe}/PS1 Δ E9 and 3xTg-AD mouse models of AD following chronic inhibition of mGlu₅ using the NAM 2-chloro-4-((2,5-dimethyl-1-(4-(trifluoromethoxy)phenyl)-1H-imidazol-4-yl)ethynyl)pyridine (CTEP) (Abd-Elrahman et al., 2018).

Conversely, there is also evidence to indicate that potentiation of the mGlu₅ receptor is neuroprotective. Recently, A β induced cell death in primary cultures of hippocampal neurons was shown to be prevented by administration of the mGlu₅ PAM CDPPB (Bellozi et al., 2019). However, the same study revealed that the compound did not prevent memory loss in aged transgenic mice.

1.4 Phosphorylation

1.4.1 The Role of Direct GPCR Phosphorylation

Phosphorylation is a prevalent post translational protein modification, involving the transfer of a phosphate group of adenosine 5'-triphosphate (ATP) onto hydroxyl groups of amino acids, catalysed by a family of enzymes called kinases (Burnett & Kennedy, 1954). Upon agonist binding to the orthosteric site of a receptor, intracellular kinases such as G protein-coupled receptor kinases (GRKs) and calmodulin-dependent protein kinase II (CaMKII) phosphorylate the C-terminus (Fagni et al., 2004; L. M. Mao et al., 2008). Phosphorylation is a reversible process; dephosphorylation of proteins is catalysed by another family of enzymes called phosphatases. Approximately 2% of the human genome codes for kinases and phosphatases; there are ~500 kinases and ~100 phosphatases in the human genome (Craig Venter et al., 2001). Phosphorylation occurs on the side chains of predominantly serine, threonine, and tyrosine residues, with the overall percentage of phosphorylation sites distributed as 1.8% tyrosine, 11.8% threonine, and 86.4% serine (Olsen et al., 2006).

Phosphorylation of GPCRs was canonically thought to only lead to arrestin recruitment and receptor internalisation, but it is now understood that receptor phosphorylation plays a much more dynamic role in cell signalling, offering a mechanism to regulate the signalling outcome of a receptor (Chul et al., 2008; Tobin, 2008). Homologous phosphorylation entails phosphorylation of the receptor by a kinase following activation by agonist binding. On the contrary, heterologous receptor phosphorylation involves signalling from one receptor leading to phosphorylation of a different receptor. Homologous phosphorylation requires the receptor to be in the active conformation, however heterologous phosphorylation occurs irrespective of the active state of the receptor (Rang et al., 2007). In the case of GPCRs the main change caused by phosphorylation is the addition of negative charges; these are then recognised by the positively charged residues in the phospho-sensor region in arrestins.

Whilst phosphorylation of GPCRs is most commonly associated with the process of desensitisation, this process can yield a variety of functions. Beyond facilitating downregulation, phosphorylation may also play a crucial role in determining the specificity of signal transduction pathways downstream of the

receptor. Recently, a phosphorylation motif in GPCRs was identified (P-X-P-P), required for β -arrestin interaction to the Lys-Lys-Arg-Arg-Lys-Lys motif in the N-domain of β -arrestins (Maharana et al., 2023). The phosphorylation barcode is a concept in GPCR signalling that refers to the specific pattern or combination of phosphorylation events on the receptor's intracellular domains, especially the C-terminal tail and intracellular loops. This pattern acts like a "barcode," encoding different signalling outcomes by selectively recruiting distinct regulatory proteins. It allows GPCRs to respond to a wide range of extracellular signals through coupling to different intracellular partners based on the cellular context, such as ligand binding and cellular environment. This has been recently begun to be established for the free fatty acid receptor 2 (FFA2); utilising phosphorylation site-specific antisera as biomarkers for constitutive and agonist-regulated phosphorylation revealed differing patterns of phosphorylation in different pathophysiologically relevant tissues (Barki et al., 2023).

Aberrant GPCR phosphorylation has been linked to various diseases, including cancer (Xu et al., 2002), cardiovascular disorders (Rohrer et al., 1996), and neurodegenerative diseases (Janíčková et al., 2013). For example, dysregulation of GPCR phosphorylation by β -arrestins 1 and 2 at the β_2 -adrenoceptor has been implicated in heart failure, where it contributes to disease progression through enhancement of PKA signalling of the receptor (Daaka et al., 1997). Similarly, altered phosphorylation of the dopamine D2 receptor has been associated with schizophrenia (Seeman, 2013) and other psychiatric disorders (Mao & Wang, 2016), pointing to the broader significance of GPCR phosphorylation in disease pathology.

1.4.2 Phosphorylation of mGlu₅

Like other GPCRs, mGlu receptors are subject to phosphorylation on their intracellular surfaces. Phosphorylation plays a key role in desensitisation of GPCRs, and this is no exception for mGlu receptors. For instance, phosphorylation of mGlu₁ by PKC has been shown to recruit arrestins and facilitate its arrestin- and clathrin-dependent internalisation, thereby attenuating receptor signalling (Pula et al., 2004). The internalised receptors can be either recycled back to the plasma membrane or targeted for degradation, depending on

the phosphorylation state and interacting proteins. The majority of mGlu₅ receptors recycle to the membrane rather than become degraded, as shown by Mahato et al. (2015) where most of the agonist-induced internalised mGlu₅ colocalised with the recycling endosome marker Rab11 over the lysosomal marker LAMP1. This receptor recycling process was shown to be completely dependent on protein phosphatase 2A, and the receptors recycle to the membrane within 2.5 hours in HEK293 cells and 3 hours in differentiated N2A cells, a model of neuronal cells (Mahato et al., 2015). This trafficking of mGlu₅ has also been shown to be dependent on PKC (Ko et al., 2012).

A number of serine and threonine residues conserved between group I mGlu receptors that are known to be phosphorylated by PKC have been identified, mediating rapid receptor desensitisation: Thr606, Ser613, Thr665, Thr681, Ser881, Ser890 on mGlu_{5a} (Gereau IV and Heinemann, 1998). It can be inferred that mGlu₅ is regulated by a serine/threonine PKC phosphorylation feedback loop; receptor stimulation leads to PKC activation, and the receptor sequence contains conserved PKC phosphorylation sites mediating desensitisation (Mao & Wang, 2016). Ser870 on mGlu₅ is a direct substrate for PKA phosphorylation; Uematsu *et al.*, demonstrated that phosphorylation of this residue affects the ability of mGlu₅ to induce extracellular signal-regulated kinase (ERK) activation and calcium ion oscillations (Uematsu et al., 2015). Phosphorylation of mGlu₅ at Ser839 by PKC causes decoupling from associated G proteins and dephosphorylation causes reassociation, the balance of phosphorylation and dephosphorylation triggering calcium oscillations (Kim et al., 2005; Bradley and Challiss, 2012). In addition, the regulator of G protein signalling (RGS) homology (RH) domain of GRK2 binds to the second intracellular loop of mGlu₅ at Lys677/Lys678 (Mao et al., 2008). Furthermore, point mutations of mGlu₅ that eliminate phosphorylation at Thr1123/Ser1126 led to excessive alcohol drinking (Campbell et al., 2019), indicating a vital role of C-terminal mGlu₅ phosphorylation.

1.4.3 Methods to Study Phosphorylation

There is an emphasis on understanding the physiological role of protein phosphorylation, as phosphorylation is a post translational modification with a large influence on protein activity. Analysis of phosphorylated proteins is difficult for 5 main reasons according to Mann et al. (2002):

1. Phosphorylation sites on a protein vary. Phosphorylation is very diverse, and proteins can be phosphorylated on more than one site within the protein.
2. Enrichment of the phosphorylated protein is often required before analysis to permit detection, complicating the methodology.
3. Most methods used to detect phosphorylation have limited dynamic range; the techniques are able to identify major sites but sometimes not the minor phosphorylation events.
4. Phosphatases may dephosphorylate proteins in the detection process, so care must be taken to avoid this occurrence.
5. Protein phosphorylation has a low stoichiometry; only a small fraction of the available protein can be phosphorylated at any one moment.

1.4.3.1 Phosphoproteomics

Phosphoproteomics, a mass spectrometry-based technique, is a method used to analyse and quantify the global dynamics of protein phosphorylation. Mass spectrometry is a quantitative method with excellent resolution and sensitivity for proteins; phosphoproteomics can identify a comprehensive profile of phosphorylated proteins *in vivo* and *in vitro* in a single analysis, permitting dual detection of total- and phospho-proteins (Zhang et al., 2022).

One advantage of this methodology is that it provides a wide-ranging global analysis: phosphoproteomics allows for the simultaneous analysis of thousands of phosphorylation sites across the proteome, providing a comprehensive view of the phosphorylation landscape. In 2020, Ochoa et al. generated the largest human phosphoproteome dataset to date, identifying 119,809 human phosphosites. Despite identifying a great number of phosphosites, there still exists a bottleneck in the research: identifying which of said phosphosites are functionally relevant.

Given that phosphorylation can be poorly conserved, it has been suggested that not all phosphorylation is biologically relevant, therefore prioritisation strategies are key to facilitate the discovery of highly relevant sites of phosphorylation (Landry et al., 2009).

Another advantage of employing phosphoproteomics is the high sensitivity and specificity, permitting detection of low abundance phosphoproteins. This was highlighted in a recent study aiming to identify key regulatory phosphorylation sites on low-abundance proteins to delineate the adipocyte signal transduction pathway in insulin signalling. Protein phosphorylation is central to the adipocyte insulin response, but the precise mechanisms by which the adipocyte signalling systems are dysregulated upon insulin resistance is unclear, but the phosphoproteomic study revealed widespread dysregulation of glycogen synthase kinase 3 (GSK3) signalling (Fazakerley et al., 2023).

However, some difficulties arise when analysing phosphopeptides by mass spectrometry. If the peptide fragments are too small, they may not be observed at all. Phosphorylated proteins have a weak signal and are of lower abundance, making it challenging to detect against the high background of non-phosphorylated proteins. Complex sample preparation is required due to the need for protein enrichment to detect these small fragments. This process is expensive, limiting the accessibility of this technique to some laboratories. Additionally, phosphopeptides are hydrophilic and possess a negative charge, meaning they do not bind to columns used for protein purification (Mann et al., 2002), further producing obstacles in the sample preparation process. Other limitations in the phosphoproteome analysis include the temporal resolution; phosphorylation is a highly dynamic process, and capturing rapid changes in phosphorylation status can be difficult with current phosphoproteomics workflows.

Despite the limitations, this strategy has been employed by Nobles et al. (2011) to study the β_2 -adrenoceptor in HEK293 cells, reporting phosphorylation at 13 sites located at ICL3 or the C-terminus following agonist stimulation. Phosphorylation was found to only occur at Ser355 and Ser356 in response to the stimulation with a β -arrestin-biased agonist carvedilol (Nobles et al., 2011). Another study by Butcher et al. (2016) elucidated 14 phosphorylation sites on the M1 muscarinic acetylcholine receptor. Phospho-sites with a low level of basal phosphorylation were significantly upregulated following stimulation with acetylcholine, particularly at the residue Ser228 (Butcher et al., 2016). This

methodology was also previously applied to study putative phosphorylation sites of the free fatty acid receptor 4 (Butcher et al., 2014). Similarly, Ives et al. (2022) utilised middle-down mass spectrometry to quantify states of phosphorylation of the C-terminus of the mGlu₂ receptor and determined that the receptor is subjected to both agonist-induced and basal phosphorylation at up to four sites.

Phosphoproteomics offers significant advantages for studying protein phosphorylation including comprehensive analysis, quantitative information, and high sensitivity. Conversely, it also has disadvantages such as complex sample preparation, high costs, and data complexity. Additionally, limitations in temporal resolution and biological context need to be considered. Despite these challenges, phosphoproteomics remains the best, unbiased approach for advancing our understanding of phosphorylation and its role in cellular regulation, provided that its limitations are acknowledged and addressed in experimental design and data interpretation.

1.4.3.2 Mutagenesis

Site-directed mutagenesis is a technique used to study protein phosphorylation by creating mutations at targeted sites. This approach allows researchers to investigate the functional roles of phosphorylation at individual amino acids within a protein. Mutagenesis studies can be applied to study phosphorylated proteins *in vitro* or *in vivo* through knock-in studies and may target individual or multiple phospho-sites throughout a protein. The paradigm involves the substitution of phosphorylated serine, threonine and tyrosine residues, frequently subsequent to identification by mass spectrometry, to alanine, an amino acid that cannot be phosphorylated.

The advantage of this technique is the specificity of the targeted mutation. The site-directed mutagenesis allows precise modification of individual amino acids, enabling detailed studies of individual phosphorylation sites. This can subsequently be followed by functional studies, investigating the biological consequences of phosphorylation of specific residues on protein stability, activity, cellular localisation and protein-protein interactions. This has been employed to map the signalling pathways of many proteins in a variety of fields, including the insulin receptor substrate-1 to map the insulin signalling pathway (Delahaye et al., 1998), phytochrome A function in plants to identify changes in biological activity

(Stockhaus et al., 1992), and the role of Brca1 phosphorylation in cancer survival (Xu et al., 2002).

However, this amino acid replacement comes with limitations: serine residues are subject to other post-translational modifications (such as N-acetylglucosamine modification), thus mutation of serine to alanine may impact the biochemical phenotype (Chen & Cole, 2015). Site-specific mutations are limited in their dynamic information, the dynamic nature of phosphorylation and dephosphorylation cycles is not captured meaning the temporal dynamics of phosphorylation is not revealed. Additionally, mutation of amino acids comes with the risk of impacting protein folding and stability, for example mutations in the heat shock protein Hsp90 intended to study phosphorylation can inadvertently affect the protein's chaperone activity due to structural perturbations (Mollapour et al., 2011).

Ives et al. (2022) used mutagenesis to explore the impact of the phosphorylation sites found in the mGlu₂ C-terminus using mass spectrometry. This determined that newly identified glutamate-sensitive phosphorylation sites in the C terminus, proximal to the seventh transmembrane domain, affect receptor signalling in a region-specific manner (Ives et al., 2022), supporting the GPCR phosphorylation barcode hypothesis. Site-directed mutagenesis was also employed by Butcher et al. (2014) to investigate the physiological impact of phosphorylation of the free fatty acid receptor 4 (FFA4). Five residues in the C terminal tail were identified through mass spectrometry, then mutagenesis was utilised to observe the phenotype of these residues following pharmacological assays. Single point-mutations of these residues, while not impacting activation of heterotrimeric G proteins, reduced efficacy of agonist-mediated β -arrestin-2 recruitment in addition to impacting the kinetics of this recruitment. Similarly, Bradley et al. (2020) used mutagenesis to create a G protein-biased mutant M1 muscarinic acetylcholine receptor through mutation of 20 serine residues mutated to alanine located in the third intracellular loop and C terminal tail, identified by previous mass spectrometry (Butcher et al., 2016). The phosphorylation-deficient receptor shows robust coupling to $G\alpha_{q/11}$ signalling but reduced β -arrestin-2 recruitment and internalisation (Bradley et al., 2020). This G protein-biased receptor was made into a knock-in mouse model to determine the importance of pharmacologically targetable phosphorylation dependent signalling driving clinically relevant outcomes, finding that M1 ligands promoting phosphorylation

dependent signalling could be neuroprotective against adverse cholinergic effects in the treatment of Alzheimer's disease (Bradley et al., 2020). This same phosphodeficient mutant receptor was also shown to accelerate progression of prion neurodegenerative disease compared to wildtype littermates (Scarpa et al., 2021), thus it can be inferred that M1 phosphorylation and β -arrestin-2 recruitment have neuroprotective effects.

Additional mutation-related paradigms to study phosphorylation include generation of phosphomimetic constructs, whereby amino acid substitution, commonly to aspartate or glutamate, mimic a phosphorylated protein. These negatively charged residues mimic the structure and charge of a phosphate group (Correddu et al., 2020), allowing the study of the functional consequences of phosphorylation without relying on actual phosphorylation events. However, whilst aspartate or glutamate can mimic the negative charge of a phosphate group, they do not exactly replicate the structural or steric effects of phosphorylation therefore phosphomimetic mutants might not fully represent the true functional consequences of phosphorylation (Paleologou et al., 2008). Additionally, phosphorylation is a dynamic and reversible process, and phosphomimetic mutants cannot model this; they represent a static state, which might not fully capture the natural regulation of the protein.

Site-directed mutagenesis offers significant advantages for studying protein phosphorylation, including specificity, functional analysis, and insights into structure-function relationships. However, limitations such as incomplete functional mimicry, context-dependent effects, and off-target consequences need to be considered. Despite these challenges, mutagenesis remains a valuable tool for investigating the roles of phosphorylation in protein function and cellular signalling.

1.4.3.3 Phospho-site Specific Antibodies

Phosphorylation site-specific antibodies can be raised against phosphorylation motifs on target proteins and employed as a tool to study protein phosphorylation using western blotting, immunoprecipitation, immunocytochemistry, or other antibody-based techniques. The use of phospho-site specific antibodies is considered to be the 'gold standard' for the recognition of phospho-proteins due to its wide accessibility.

The first phospho-site specific antibody was described in 1981 by Ross et al. Produced in rabbits following immunisation with benzoyl phosphonate conjugated to keyhole limpet hemocyanin, the antibody broadly recognised phospho-tyrosine independent of the target protein sequence. Ten years later, the work on phospho-site specific antibodies developed into immunising rabbits with synthetic phosphopeptides, based on the sequence flanking a phosphosite of interest (Czernik et al., 1991).

Phospho-site specific antibodies permit the experimental measurement of receptor phosphorylation *in situ* and may be used in overexpressing cell lines or where receptor is expressed at relatively low levels, for example in native tissues (Tobin, Butcher and Kong, 2008). The experimental setup can be used to semi-quantitatively measure both total protein and phospho-protein. Phospho-site specific antibodies demonstrate high specificity and site-specific recognition, distinguishing between the phosphorylated and non-phosphorylated forms of a protein, providing precise information about phosphorylation status. Phospho-site specific antibodies can be employed in studies of the temporal dynamics of phosphorylation, for instance using phospho-Akt antibodies to measure Akt phosphorylation kinetics in response to insulin stimulation (Jin & Ragolia, 2006). The impact of phosphorylation on cellular localisation can also be studied, demonstrated through studies on the agonist-stimulated free fatty acid receptor 2 in Peyer's patches (Barki et al., 2023).

However, detection of the phospho-protein of interest is dependent on affinity and specificity of the antibody; an antibody may cross-react with non-target proteins or fail to detect low levels of phosphorylation, causing misleading results. Antibodies are also costly, marking a significant drawback for large-scale studies. In addition, antibodies also depend on the availability of the epitope: if the epitope is masked through, for instance, protein conformation or other post translational modifications, the recognition of the site is hindered. In a similar scope, the antibody's ability to recognise its target may depend on cellular context and experimental conditions. This may mean that an antibody may produce excellent and clear results in an *in vitro* cell model while conversely showing limited or potentially opposing results *in vivo* due to variations in protein expression and phosphorylation levels. Hence, there is the requirement for extensive validation; each phospho-specific antibody must be extensively validated for specificity and sensitivity under the experimental conditions used. Finally, phospho-site specific

antibodies are limited in their scope by targeting single/dual/triple sites, which may not provide a complete picture of the phosphorylation status of a protein. Phospho-site specific antibodies are limited in their ability to cross cell membranes, so cannot be employed as biosensors to measure function in living cells or to look at kinetics (Hudson, 2016).

This antibody approach has previously been employed to study phosphorylation of the M1 receptor: Butcher et al. (2016) detected phosphorylation of the M1 receptor in the hippocampus of mice following fear conditioning tests and created an antibody to phospho-Ser228 to act as a biosensor specific to receptor phosphorylation. Furthermore, phospho-tau antibodies are commonly used in neuroscience research, with multiple phospho-tau targeting antibodies being commercially available. These can be employed to investigate the role of tau protein phosphorylation in neurodegenerative diseases like Alzheimer's disease, identifying sites such as Ser208 and their role in promoting aggregation and tauopathies in neurodegenerative diseases (Xia et al., 2020). In a similar vein, phospho-site specific antibodies have been used to detect phosphorylated insulin receptor substrate-1 (IRS1) at Ser307, providing insights into insulin resistance mechanisms (Aguirre et al., 2002).

Phospho-site specific antibodies offer significant advantages for studying protein phosphorylation, including high specificity, the ability to conduct dynamic and quantitative analyses, and the capability to visualise subcellular localisation. However, they also have disadvantages such as variable antibody quality, high cost, and potential epitope masking. Additionally, their limitations include a context-dependent binding and the need for extensive validation. Despite these challenges, phospho-site specific antibodies remain invaluable tools for investigating phosphorylation and its role in various cellular processes and diseases.

1.5 Thesis Aims

GPCRs provide an excellent therapeutic target in the clinical setting. Due to the role of phosphorylation in signalling pathways, and the broad involvement of the mGlu₅ receptor in pathophysiology, the broad aims of this thesis was to examine the role of direct mGlu₅ phosphorylation on its signal transduction pathways.

Preliminary data from our laboratory determined through an unbiased phosphoproteomic analysis of the hippocampus of wildtype mice showed that global mGlu₅ phosphorylation increases following a fear conditioning learning and memory test, but the specific phospho-sites in the protein sequence were not identified. This would be of value to study, as a link between memory and mGlu₅ phosphorylation has been demonstrated but not investigated. The precise role of phosphorylation in mGlu₅ signal transduction must be examined. A phospho-deficient form of the mGlu₅ receptor (mGlu₅-PD), in which all putative serine phosphorylation sites are mutated to alanine, was generated. In addition, a second construct was generated with all serine and threonine sites mutated to alanine (mGlu₅-TPD). My aim was to use these constructs to establish the roles of serine and threonine phosphorylation sites in *in vitro* pharmacological assays and through comparison to the wildtype receptor determine the functional impact of direct mGlu₅ C-terminal serine and threonine phosphorylation.

To deliver on this aim, I utilised the phosphodeficient mutant mGlu₅ receptors to conduct the following:

1. Examine the role of direct mGlu₅ receptor phosphorylation on β -arrestin 2 recruitment and receptor internalisation (Chapter 3).
2. Examine the role of direct mGlu₅ receptor phosphorylation on the G protein-dependent signal transduction pathway (Chapter 4).
3. Generate and optimise a biosensor that could be used as a tool to measure how phosphorylation impacts endogenously expressed mGlu₅ mediated G protein signalling (Chapter 5).

2 Materials and Methods

2.1 Materials

2.1.1 Pharmacological Compounds

The group I mGlu receptor agonist **DHPG** ((S)-3,5-dihydroxyphenylglycine) was purchased from Torcris (0342). **Glutamate** (L-Glutamic Acid) was purchased from Sigma (G1251). The FFA4 agonist **TUG-891** (Hudson et al., 2013) was purchased from Torcris (Cat. No. 4601). The muscarinic receptor agonist **acetylcholine** was purchased from Sigma (A6625). The FFA1 agonist **T-3601386** (Ueno et al., 2019) was kindly provided by Associate Professor Elisabeth Rexen Ulven from the University of Copenhagen.

2.1.2 Primers

Table 2.1: List of primers used for sequencing plasmids.

| Primer Name | Sequence |
|-------------|-----------------------|
| CMV Forward | CGCAAATGGGCGGTAGGCGTG |
| BGH Reverse | TAGAAGGCACAGTCGAGG |

Table 2.2: PCR primers for the generation of Lyn11-SpNG-GRK2 and Lyn11-iSpNG-GRK2 biosensors.

| Plasmid | Component | Method | Forward Primer | Reverse Primer |
|------------------|------------------------------|--------------|--|--------------------------|
| Lyn11-SpNG-GRK2 | GRK2 | AQUA Cloning | TCCGGACTCTAGCGT TTAAACTTAAGCTT | GGGCCCTCTAGA TGCATGCT |
| Lyn11-iSpNG-GRK2 | Plasmid (including and GRK2) | AQUA Cloning | CAGCGGAGGAAGTGG CGGATCTGGCTCTTC TCGAGAGAAGTACCT GGAGGAC | CGCGCTGTCTTT CCCTTTTG |
| | Nanoluciferase | | AAAATCAAAGGGAA AGACAGCGCGGGCA GCGGCGGCTCT | CCCACTCCCCC ACTACCA |
| | ER/K | | TTCTGGTGGTAGTGG GGGGAGTGGGGAGG AAGAGGAAAAGAAGA AGCAGCA | TCCGCTTCCGCC TGATCC |
| | mNeonGreen | | CTCTGGGGGATCAGG CGGAAGCGGAGTGAG CAAGGGCGAGGAGG ATAA | GCCAGATCCGCC ACTTCC |

2.1.3 Plasmid Constructs

Table 2.3: List of plasmid constructs used.

| | Plasmid Construct | Insert | Vector | Cloning Method | Source |
|------------------|-----------------------------|---|---------------|---------------------|-------------------------------------|
| Vectors | pcDNA3 | - | - | - | ThermoFisher |
| | pcDNA5/FRT/TO | - | - | - | ThermoFisher |
| Receptors | mGlu₅-WT | Mouse mGlu ₅ receptor with a C-terminal HA tag | pcDNA5/FRT/TO | Restriction Cloning | Unpublished; Made in our Laboratory |
| | mGlu₅-PD | Mouse mGlu ₅ receptor with all C-terminal serine residues mutated to alanine, with a C-terminal HA tag | pcDNA5/FRT/TO | Restriction Cloning | Unpublished; Made in our Laboratory |
| | mGlu₅-TPD | Mouse mGlu ₅ receptor with all C-terminal serine and threonine residues mutated to alanine, with a C-terminal HA tag | pcDNA5/FRT/TO | Restriction Cloning | Unpublished; Made in our Laboratory |
| | M1-WT | Mouse M1 receptor with a C-terminal HA tag | pcDNA3 | Restriction Cloning | (Scarpa et al., 2021) |
| | M1-PD | Mouse M1 receptor with all C-terminal serine residues mutated to alanine, with a C-terminal HA tag | pcDNA3 | Restriction Cloning | (Scarpa et al., 2021) |
| | FFA1 | Human FLAG-FFA1 receptor | pcDNA3 | Restriction Cloning | Unpublished; Made in our Laboratory |

| | | | | | |
|-------------------|---------------------------------------|--|---------------|---------------------|-------------------------------------|
| | FFA4 | Human FLAG-FFA4 with nanoluciferase tagged to the C-terminus | pcDNA5/FRT/TO | Restriction Cloning | Unpublished; Made in our Laboratory |
| Biosensors | Nluc-β-Arr2 | Human β -arrestin 2 with nanoluciferase tagged to the N-terminus | pcDNA3 | Restriction Cloning | (Scarpa et al., 2021) |
| | CAAX-mNeonGreen | mNeonGreen with the CAAX motif tagged to the N-terminus | pcDNA3 Hygro | Restriction Cloning | (Scarpa et al., 2021) |
| | Lyn11-LgBiT | LargeBiT with an N-terminal Lyn11 anchor | pcDNA5/FRT/TO | AQUA Cloning | Unpublished; Made in our Laboratory |
| | SmBiT-β-Arr2 | Bovine β -Arrestin 2 tagged at the N-terminus with SmallBiT | pcDNA3 | Restriction Cloning | Unpublished; Made in our Laboratory |
| | Gα_q NEWPATH | The G α_q protein is tagged with nanoluciferase, with Gy9 tagged with mNeonGreen fluorescent protein, and the G β_3 left untagged | pIRES | AQUA Cloning | Unpublished; Made in our Laboratory |
| | Lyn11-SpNG-GRK2 | Lyn11-mNG-ER/K-Nluc-GRK2 biosensor | pcDNA3 | AQUA Cloning | Made in this Thesis |
| | Lyn11-iSpNG-GRK2 | Lyn11-Nluc-ER/K-mNG-GRK2 biosensor | pcDNA3 | AQUA Cloning | Made in this Thesis |
| | Other | pOG44 | - | pOG44 | - |

2.1.4 Antibodies

Table 2.4: List of primary antibodies used for western blots (WB), immunocytochemistry (ICC), or on-cell westerns (OCW).

| Antigen | Species | Working Dilution | Source |
|--------------------------------|---------|---------------------------|---------------------------|
| Hemagglutinin | Rat | 1:1,000 (WB); 1:500 (ICC) | Roche |
| mGlu ₅ (C-terminus) | Rabbit | 1:1,000 (WB) (OCW) | MilliPore, #AB5675 |
| mGlu ₅ (N-terminus) | Rabbit | 1:1,000 (WB) (OCW) | Alomone Labs, #AGC-007 |
| Nanoluciferase | Mouse | 1:1,000 (WB) (OCW) | R&D Systems |
| pS1018/pS1020 | Rabbit | 1:1,000 (WB) | 7TM Antibodies |
| pS1041/pS1044 | Rabbit | 1:1,000 (WB) | 7TM Antibodies |
| pS871/pS872/pT875 | Rabbit | 1:1,000 (WB) | 7TM Antibodies |
| Sodium-Potassium ATPase | Rabbit | 1:1,000 (WB) | abcam, #ab76020 |

Table 2.5: List of secondary antibodies used for western blots (WB), immunocytochemistry (ICC), or on-cell westerns (OCW).

| Antigen | Working Dilution | Source |
|-------------------------------------|------------------------------|--|
| IRDye® 680LT Donkey anti-Mouse IgG | 1:10,000 (WB); 1:1,000 (OCW) | LI-COR Biotechnology (926-68022) |
| IRDye® 800CW Donkey anti-Rabbit IgG | 1:10,000 (WB); 1:1,000 (OCW) | LI-COR Biotechnology (926-32213) |
| IRDye® 800CW Goat anti-Rat IgG | 1:10,000 (WB); 1:1,000 (OCW) | LI-COR Biotechnology (926-32219) |
| Donkey anti-Rat AlexaFluor® 594 | 1:500 (ICC) | abcam (ab150156) |

2.2 Molecular Cloning of Plasmid Constructs

2.2.1 Generation of Competent *Escherichia coli* Cells

XL1-Blue *Escherichia coli*, stored at -80°C , were thawed on ice then streaked onto sterile Luria-Bertani (LB) agar plates (1% (w/v) tryptone, 0.5% (w/v) yeast extract, 171 mM NaCl, 1.5% (w/v) bacto-agar) without selection antibiotic to obtain single colonies. Following incubation of the plate at 37°C overnight, a single colony was isolated using sterile technique and placed into a 30 mL tube containing 5 mL of sterile LB broth (1% w/v tryptone, 0.5% w/v yeast extract, 171 mM NaCl). This starter culture was incubated overnight in a shaking incubator at 200 rpm and 37°C . The starter culture was then sub-cultured into 500 mL conical flasks containing 100 mL sterile LB broth, then incubated in a shaking incubator at 200 rpm and 37°C until an optical density (OD) of 0.48 at 600 nm was obtained. Cultures were transferred to pre-chilled falcon tubes and incubated on ice for 5 minutes to slow growth, before being centrifuged for 10 minutes at 1,800 *g* at 4°C . The pellet was resuspended in 20 mL of pre-chilled solution 1 (30 mM $\text{CH}_3\text{CO}_2\text{K}$, 10 mM RbCl, 10 mM CaCl_2 , 50 mM MnCl_2 , 15% (v/v) glycerol; pH 5.8, filter sterilised) then incubated on ice for a further 5 minutes. The cells were centrifuged for 10 minutes at 1,800 *g* at 4°C and the supernatant discarded. The resulting pellet was resuspended in 2 mL of pre-chilled solution 2 (10 mM 3-(N-morpholino)propanesulfonic acid (MOPS), 75 mM CaCl_2 , 10 mM RbCl, 15% (v/v) glycerol; filter sterilised) then incubated on ice for 15 minutes. The cell suspension was aliquoted into sterile 1.5 mL tubes and stored at -80°C until use.

2.2.2 Transformation of Competent Cells by Heat-Shock Method

To transform plasmids into XL1-Blue *E. coli*, either plasmid DNA, a ligation reaction or an AQUA cloning reaction was combined with chemically competent cells (generated as per **Section 2.2.1**) and incubated on ice for 15 minutes. Cells were then heat shocked at 42°C for 45 seconds in a waterbath, then returned to ice for 2 minutes to recover. Using sterile technique, 450 μL of LB broth was added to the tube and the cells were incubated in a shaking incubator at 200 rpm and 37°C for 60 minutes. Cells were pelleted by centrifugation at 4,000 *g* for 3 minutes, then the supernatant discarded. Cells were resuspended in LB broth and

an appropriate amount spread onto LB agar plates supplemented with 100 µg/mL ampicillin. The plate was inverted and incubated at 37°C overnight.

2.2.3 Isolation of Plasmid DNA from Bacterial Cultures

To purify plasmids from bacterial cultures, either a QIAprep® Spin Miniprep or a QIAGEN® Plasmid Maxi kit (QIAGEN) was utilised depending on the DNA yield required. For the Miniprep, following the overnight culture of bacteria on LB agar plates supplemented with 100 µg/mL ampicillin, a single colony was isolated using sterile technique and inoculated into a tube containing 5 mL LB broth supplemented with 100 µg/mL ampicillin. The culture was grown overnight in a shaking incubator at 200 rpm and 37°C. Bacteria were isolated the following day by centrifugation at 3,200 g for 10 minutes at 4°C. The bacterial cells were lysed, and the plasmid DNA was isolated using the QIAprep® Spin Miniprep kit following the manufacturer's instructions. The DNA was eluted with nuclease-free dH₂O into a sterile Eppendorf tube, then the amount and purity of DNA yielded was assessed as described in **Section 2.2.3.1**.

For plasmids where a larger yield was required for downstream applications, the QIAGEN® Plasmid Maxi kit was utilised. Subsequent to overnight culture of bacteria on agar plates supplemented with 100 µg/mL ampicillin, a single colony was isolated using sterile technique and inoculated into a tube containing 5 mL LB broth and 100 µg/mL ampicillin. The culture was grown for 8 hours in a shaking incubator at 200 rpm and 37°C. This starter culture was then inoculated into a conical flask containing 100 mL LB broth and 100 µg/µL ampicillin then incubated overnight in a shaking incubator at 200 rpm and 37°C. The following day, bacterial cultures were harvested by centrifugation at 3,200 g for 15 minutes at 4°C. The bacterial cells were lysed, and the plasmid DNA isolated using the QIAGEN® Plasmid Maxi kit following the manufacturer's instructions. The resulting DNA pellet was reconstituted in nuclease-free dH₂O and transferred to a sterile Eppendorf tube. The amount and purity of the DNA yielded was assessed as described in **Section 2.2.3.1**.

2.2.3.1 Quantification of Nucleic Acid Concentration and Purity

Isolated DNA or RNA concentration and purity was assessed using an LVis Plate (BMG LabTech). An A_{260}/A_{280} absorbance ratio of 1.8 for DNA and 2.0 for RNA, and an A_{260}/A_{230} absorbance ratio of 2.0-2.2 was considered pure for nucleic acids. Once the concentration and purity of samples were recorded, DNA samples were stored at -20°C and RNA samples at -80°C until use.

2.2.4 Generation of Plasmid DNA

2.2.4.1 Polymerase Chain Reaction

Polymerase chain reaction (PCR) was performed using Herculase II fusion DNA polymerase (Agilent) in a 50 μL reaction volume. For targets between 1-10 kb, 30 ng of vector DNA template was used with 1 μL Herculase II fusion DNA polymerase, 0.25 μM of each forward and reverse oligonucleotide primers, 2% DMSO, and 250 μM of each dNTP (dATP, dCTP, dGTP and dTTP). Reaction mixtures were incubated in the thermocycler using the below cycling conditions:

Table 2.6: PCR reaction scheme.

| Segment | Number of Cycles | Temperature | Duration |
|---------------------------------------|------------------|-------------|---------------------|
| 1. Initial Denaturation | 1 | 95°C | 2 minutes |
| 2. Denaturation, Annealing, Extension | 30 | 95°C | 20 seconds |
| | | 55°C | 20 seconds |
| | | 72°C | 30 seconds per 1 kb |
| 3. Final Extension | 1 | 72°C | 3 minutes |
| 4. Inactivation | ∞ | 4°C | ∞ |

For cloning procedures where it was important to remove template plasmid DNA, methylated GATC sites were digested through treatment with 20 units of

DpnI (NEBioLabs) added to the PCR reaction and incubated at 37°C for 2 hours. To remove PCR buffers and enzymes, the QIAquick PCR Purification Kit (QIAGEN) was used according to manufacturer's instructions.

2.2.4.2 Restriction Digest

For plasmids made using restriction cloning, 1 µg of vector DNA was combined with 1X CutSmart buffer (NEBioLabs, cat no. B6004S) and 20 Units of each high-fidelity restriction enzymes (NEBioLabs) and made up to a 50 µL final volume with nuclease-free water. The same reaction was prepared for the DNA insert. The reactions was incubated at 37°C for one hour, then 1 µL of QuickCIP (NEBioLabs) was added to the vector DNA reaction and incubated at 37°C for a further 30 minutes to dephosphorylate the DNA, preventing re-ligation. Resulting DNA samples were extracted via gel purification as per **Section 2.2.4.3**.

2.2.4.3 Gel Purification

To further purify either PCR products or restriction cloning samples for use in plasmid construction reactions, DNA was gel purified. DNA samples were combined with DNA gel loading buffer (NEBioLabs) and run on a 1% (w/v) agarose gel in 1X Tris-acetate-EDTA (TAE) (40 mM Tris, 1 mM EDTA, 20 mM glacial acetic acid) containing SYBR safe gel stain (Invitrogen) at a dilution of 1:10,000. Gels were visualised using a blue light transilluminator and band size compared against a HyperLadder™ 1kb (Meridian Bioscience) DNA ladder. Then band at the expected size was excised using a single edge razor blade and the QIAquick® Gel Extraction Kit (QIAGEN) was used according to the manufacturer's instructions to purify the DNA from the gel.

To estimate the amount of DNA in the extracted sample, a sample of the purified DNA was again run on a 1% (w/v) agarose gel in 1X TAE and visualised using the Gel Doc UV transilluminator (Bio-Rad). The amount of DNA per band was estimated by comparison of band intensity to the intensity of reference bands in the HyperLadder™ 1kb.

2.2.4.4 Plasmid Construct Methods

2.2.4.4.1 T4 Ligation of Restriction Digested DNA

For ligation cloning, digested DNA insert and vector fragments cut with complementary restriction enzymes (NEBiolabs) were used. Vector fragments had been treated with QuickCIP to prevent relegation in the cloning reaction. For the ligation step, the insert and vector were combined in a molar ratio of 3:1 and incubated overnight at 15° C with 1 Unit of T4 DNA ligase (Invitrogen). Ligation reactions were then immediately transformed into XL-1 Blue *E. coli* as described in **Section 2.2.2**.

2.2.4.4.2 AQUA Cloning

For restriction site free plasmid construction, the advanced quick assembly (AQUA) cloning method, based on DNA end-homology was employed (Beyer et al., 2015). For AQUA cloning reactions, PCR was used to generate linear vector and insert DNA with 18-24 bases of overlapping end homology. Purified vector was used at 12 ng of linearised vector per 1 kb of vector size, while the insert DNA was used in a 3:1 molar ratio with the vector. DNA fragments were mixed in a total volume of 10 µL then incubated at room temperature for 1 hour before being transformed into XL-1 Blue *E. coli* (**Section 2.2.2**) to allow for end homology recombination and vector construction to occur within the *E. coli*.

2.2.4.5 Diagnostic Restriction Digest of Cloning Products

To confirm the success of plasmid constructs generated through this work, diagnostic restriction digest was carried out followed by gel electrophoresis to confirm the digest products are of the expected size. Two restriction enzymes (NEBiolabs) were selected based on the restriction sites flanking the DNA fragment of interest. Reactions were then carried out containing 1 µg of the plasmid DNA with 20 Units of each of the selected restriction enzymes (NEBioLabs). The reaction was made up in nuclease-free dH₂O and incubated at 37°C for 30 minutes, then ran on a 1% (w/v) agarose gel containing SYBR Safe DNA stain in 1X TAE. The DNA bands in the gel were visualised using the Gel

Doc UV transilluminator and compared to a Hyperladder 1kb marker to confirm that they were the intended size.

2.2.4.6 Sequencing of Plasmid DNA

To confirm the identify of plasmid DNA constructs generated through this work, samples were sequenced. DNA samples were diluted to a concentration of 50-100 ng/ μ L using nuclease-free dH₂O. Sequencing primers flanking the region of interest were selected; the forward primer targeting the CMV promoter sequence, and the reverse primer targeting the BGH-poly(A) signal were commonly used for plasmids derived from pcDNA3 or pcDNA5 backbones (Table 2.1). Primers were added to the DNA sample at a concentration of 5 μ M. Samples were sent to and processed by EuroFins Genomics (Germany) and the resulting sequence was aligned and analysed using SnapGene software (Version 5.3.2).

2.2.5 mRNA Production

For transfection of constructs into primary cortico-hippocampal neurons, mRNA was produced. The mMESSAGING mMACHINE® kit (ThermoFisher Scientific) was used to generate mRNA: 1 μ g of template DNA was combined with 1X T7 NTP/CAP, 1X reaction buffer, and 2 μ L of enzyme mix. The reaction mix was incubated at 37°C for 90 minutes. The MEGAclean™ transcription clean up kit (Invitrogen) was then utilised to separate the mRNA from unincorporated NTPs, enzymes, and buffer components. The reaction mixture was made up to 100 μ L volume with elution solution (Invitrogen) and 350 μ L of binding solution concentrate (Invitrogen) added. Finally, 250 μ L of 100% ethanol was added and the reaction mixture centrifuged through a filter cartridge at 12,400 *g* for one minute. Following washing of the mRNA twice, the mRNA was eluted in 50 μ L of elution solution through incubation at 70°C for five minutes. Eluted mRNA was recovered by centrifugation at 12,400 *g* and mRNA yield assessed as per **Section 2.2.3.1** then stored at -80°C.

2.3 Cell Culture

All cell culture steps were performed in sterile conditions in a laminar flow biosafety hood. Before use, all cell culture reagents were pre-warmed to 37°C in a waterbath.

2.3.1 Cell Line Maintenance

Parental Flp-In™ T-Rex™ 293 cells, Human Embryonic Kidney (HEK) 293A and 293T cells, and Flp-In™ T-Rex™ 293 cells stably expressing the wildtype or phospho-deficient mGlu₅ receptors were maintained in Dulbecco's Modified Eagle Media (DMEM), (Gibco; #41965-039) supplemented with 10% (v/v) fetal bovine serum, 100 Units/mL penicillin/streptomycin solution and 100 µg/mL normocin. Cells were maintained at 37°C and 5% CO₂ in a humidified atmosphere, then grown to confluence. Cell lines were tested monthly for Mycoplasma using the MycoStrip™ Mycoplasma detection kit (InvivoGen) according to manufacturer's instructions.

To passage cell lines, culture medium was aspirated from a confluent flask of cells and incubated in 1X trypsin (Sigma; T4549) for approximately 3 minutes to detach cells from the flask. Cell culture medium was added to neutralise the trypsin, and the resulting cell suspension was centrifuged at 290 g for 5 minutes. The cell pellet was resuspended in fresh cell culture medium then depending on the desired dilution of cells, the appropriate volume of cell suspension was added to a sterile flask containing fresh culture medium.

To count cells and determine viability, cells suspensions were diluted 1:1 with 0.4% trypan blue (Gibco) and counted using the Countess III cell counter (ThermoFisher).

Cells were diluted to desired concentration and seeded onto multi-well plates coated with 5 µg/mL of poly-D-lysine (Sigma) as required. Receptor expression was induced 24 hours before use by treatment with indicated concentrations of doxycycline (Sigma) diluted in assay media (glutamine free Dulbecco's Modified Eagle Media (DMEM), (Sigma; #5671) supplemented with 10% (v/v) dialysed fetal bovine serum (Gibco), 100 Units/mL penicillin/streptomycin solution) to reduce glutamate in the media.

2.3.2 Cryopreservation of Cells

For long term storage of cell lines, cells were cryopreserved and stored at -80°C or -150°C. To preserve cells, confluent flasks of cells were harvested with trypsin and pelleted as described in **Section 2.3.1**. The cell pellet was resuspended in cell culture medium containing 5% (v/v) DMSO (Fisher Scientific), then this cell suspension was stored in aliquots in cryogenic vials. The vials were placed in a Mr. Frosty™ freezing container (ThermoFisher) to allow for a slow rate of freezing in a -80°C freezer. After freezing, cells were either kept in the -80°C for short term storage or placed in a -150°C for longer term storage.

Cryopreserved cells were recovered by rapid thawing in a waterbath, addition of culture medium, then centrifugation at 290 g for 5 minutes. The medium was aspirated to remove the DMSO from the freezing medium, then the cell pellet was resuspended in fresh culture medium and placed into a culture flask and maintained at 37°C and 5% CO₂ in a humidified atmosphere until cells had grown to confluence. Cells were then maintained as described in **Section 2.3.1**.

2.3.3 Transient Transfection

2.3.3.1 DNA Transfection using Polyethylenimine

Transient transfections were carried out in a laminar flow cabinet under sterile conditions. Two reaction mixtures were produced in sterile Eppendorf tubes: one contained DNA diluted in 150 mM sodium chloride, the second contained 1 mg/mL PEI diluted in 150 mM sodium chloride. The two solutions were combined for a DNA to PEI ratio of 1:6, vortexed, then incubated at room temperature for 10 minutes. Medium was aspirated from the cells and replaced with fresh pre-warmed cell culture medium. The DNA mixture was added to the cultured cells in a dropwise manner. Cells were incubated with the transfection mixture at 37°C and 5% CO₂ for a minimum of 24 hours before use in experimental assays. To confirm successful transfection of fluorescent tagged constructs, cells were observed using the epifluorescent microscope (Nikon) equipped with a mercury lamp and eYFP filter set.

2.3.3.2 DNA Transfection using Lipofectamine™ 3000

Transient transfection using Lipofectamine™ 3000 reagent (Invitrogen) was utilised in cases where transfection via PEI yielded a low transfection efficiency, of approximately $\leq 30\%$ of the total cells. A stock of Lipofectamine™ 3000 reagent (Invitrogen) was made by diluting Lipofectamine™ 3000 reagent in serum free medium 1:30, similarly a stock of P3000 reagent was made at the same dilution. The desired amount of DNA to be transfected (1 μg /well total for 6-well plates; 100 ng/well total for 96-well plates) was combined first with the P3000 mix, then with the Lipofectamine™ 3000 mix. The solution was incubated at room temperature for 10 minutes, during which time the medium was aspirated and replenished on the cells. The DNA-lipid complexes were then added to cells in a dropwise manner. Cells were returned to the culture incubator and maintained for 24 hours before use.

2.3.3.3 mRNA Transfection using Lipofectamine MessengerMAX

To transfect mRNA into neuronal cultures, 5 μL of opti-MEM reduced serum media (Gibco) per well of a 96-well plate required for transfection was combined with 0.15 μL per well of lipofectamine MessengerMAX transfection reagent (ThermoFisher) and incubated at room temperature for 10 minutes. Simultaneously, 5 μL of opti-MEM reduced serum media (Gibco) per well of a 96-well plate required for transfection was combined with 100 ng per well total mRNA. Nanoluciferase-tagged β -arrestin 2 and mNeonGreen mRNA were used at a ratio of 1:5. The lipofectamine and mRNA solutions were combined, then incubated at room temperature for five minutes before being added to the plates.

2.3.4 Generation of Stably Transfected Flp-In™ T-Rex™ 293 Cell Lines

The Flp-In™ T-Rex™ 293 inducible expression system was used to generate cell lines expressing the below receptors, each possessing a haemagglutinin (HA) (YPYDVPDYA) epitope tag fused to the end of the C-terminus to facilitate detection:

- 1) **mGlu₅-WT**: wild type mGlu₅ receptor.
- 2) **mGlu₅-PD**: phosphodeficient mGlu₅ receptor (substitution of C-terminal serine residues to alanine).
- 3) **mGlu₅-TPD**: total phosphodeficient mGlu₅ receptor (substitution of C-terminal serine and threonine residues to alanine).

Flp-In™ T-Rex™ 293 inducible stable cell lines expressing mGlu₅ wildtype and phosphodeficient mutant receptors were generated by co-transfection of 5 µg of pOG44 recombinase expression vector and 1 µg of the mGlu₅-WT, mGlu₅-PD or mGlu₅-TPD DNA in a pcDNA5/FRT/TO plasmid into a 10 cm dish of parental Flp-In™ T-REx™ 293 cells. Transfection was carried out using PEI as per **Section 2.3.3.1**. After 48 hours, cells were then cultured in medium supplemented with 100 µg/mL hygromycin (Invivogen) and 5 µg/mL blasticidin (Invivogen). Only cells successfully incorporating the pcDNA5/FRT/TO plasmid into the Flp recombinase site in the parental host cells remain alive due to expression of the hygromycin resistance gene. Following two weeks of culture, resistant cells formed isogenetic colonies which then were pooled and maintained as the desired stable inducible cell line.

2.3.5 Primary Neuronal Cultures

Multi-well plates were coated with 40 µL per well of a 96-well plate of a solution containing 4 µg/mL poly-D-lysine (Gibco) and 7.2 µg/mL Laminin (Gibco) in DEPC-treated water, then incubated overnight at 37°C. Plates were washed three times with DEPC-treated water then left to dry for 2 hours at room temperature in a laminar flow biosafety hood.

The hippocampus and cortices from E16 mouse embryos were dissected out in a 10 cm dish containing cold Hank's Balanced Salt Solution (HBSS) (Gibco), then mechanically disrupted using a razor blade. Under sterile conditions, the tissue was washed by transferring between dishes of HBSS twice. The tissue was then placed into a falcon tube containing 3 mL of TrypLE™ express enzyme (ThermoFisher) and incubated at 37°C for 10 minutes. Neurobasal™ plus complete medium (Neurobasal plus complete medium (Gibco), 1X B-27 plus supplement (Gibco; Cat no. A3582801), 1X GlutaMAX (Gibco; Cat no. 35050061), 100 Units/mL of penicillin/streptomycin solution) was added to the cell solution to

deactivate the TrypLE , then the solution was centrifuged at 290 *g* for 5 minutes to pellet the cells. The supernatant was discarded, and cells resuspended in 10 mL of fresh neurobasal medium. Cells were counted using 0.4% trypan blue as described in **Section 2.3.1**, diluted to desired seeding density in neurobasal plus medium, then plated in the coated multi-well plates. Cells were maintained at 37°C and 5% CO₂ and were used in experiments after seven days in culture.

2.4 In-Cell and On-Cell Westerns

To measure total receptor expression, an in-cell western (ICW) was used, while cell surface expression was assessed using on-cell western (OCW). Flp-In™ T-REx™ 293 or HEK293T cells were seeded in clear 96-well plates coated with 5 µg/mL of poly-D-lysine and incubated at 37°C and 5% CO₂ until confluent in the well, then receptor expression was induced with doxycycline in assay media without glutamine and with dFBS if required. For the assay, 24 hours following addition of doxycycline cells were fixed with 10% formalin (Sigma) for 20 minutes at room temperature then washed three times with PBS. For ICW experiments, cells were permeabilised at this stage by addition of 0.1% Triton-X-100 (BioXtra) diluted in PBS for 20 minutes at room temperature with gentle agitation. This permeabilisation step was omitted for OCW experiments. To reduce antibody non-specific binding, cells were blocked with 5% BSA diluted in PBS for 2 hours at room temperature. The selected primary antibody, as listed in Table 2.4, was diluted in 5% BSA in PBS and was applied to the cells. Following agitated incubation at 4°C overnight, cells were washed three times with PBS and the corresponding secondary antibody was applied to cells, diluted in 5% BSA in PBS as listed in Table 2.5, and incubated on a shaker at room temperature in darkness for 1 hour. Cells were washed three times with PBS then proteins were visualised using LI-COR Odyssey SA scanner system with no PBS in the wells to measure the fluorophore excitation wavelength at 778 nm and emission wavelength at 795 nm. Cells were stained with CellTag™ 700 (LI-COR Biotechnology) diluted 1:500 in 5% BSA in PBS to control for cell number, including a blank control in which empty wells were incubated with CellTag™ 700. Cells were incubated in CellTag™ 700 for one hour in darkness on a shaker, then washed three times with PBS and visualised with no liquid in the wells using LI-COR Odyssey SA scanner

system, with the fluorophore excitation wavelength at 675 nm and emission wavelength at 697 nm.

2.5 Pharmacological and Functional Assays

2.5.1 BRET-Based β -Arrestin 2 Recruitment Assay

HEK293T cells were plated at a density of 40,000 cells/well in white 96-well plates coated with 40 μ L of 5 μ g/mL poly-D-lysine. Cells were transfected 24 hours after plating with 5 ng/well receptor, 2 ng/well nanoluciferase-tagged β -arrestin 2, and 48 ng/well mNeonGreen constructs (made up to 100 ng/well total DNA with pcDNA3 empty vector) using PEI (**Section 2.3.3.1**). The day after transfection, cells were washed twice with HBSS-H then incubated in 80 μ L HBSS-H (supplemented with 1-10 Units/mL glutamate-pyruvate transaminase (GPT) and 6 mM sodium pyruvate for glutamate receptor expressing cells) for 30 minutes at 37°C. NanoGlo® substrate (Promega; N1130) was added for a final dilution of 1:800, then plates were incubated a further 10 minutes in darkness. BRET measurements were taken using a PHERASStar plate reader (BMGLabTech), recording the donor emission at 475 nm and acceptor excitation at 535 nm. After five minutes, 10 μ L of either HBSS-H vehicle or agonist for a final well concentration of 100 μ M was added to the plate then continued to read the BRET measurements. A 5-point moving average curve smoothing calculation was performed and the resulting ratios were corrected for basal BRET levels in each well and corrected again to vehicle treatment.

2.5.2 NanoBiT Complementation β -Arrestin 2 Recruitment Assay

HEK293T cells were plated at a density of 40,000 cells/well in white 96-well plates coated with 40 μ L of 5 μ g/mL poly-D-lysine and transfected 24 hours later with 30 ng/well of receptor construct, 5 ng/well of SmallBiT- β -arrestin 2, and 5 ng/well of Lyn11-LargeBiT using PEI as described in **Section 2.3.3.1**. Culture medium was changed to assay medium without glutamine and with dFBS for mGlu₅ expressing cells. 24 hours following transfection, cells were washed twice

with HBSS-H then incubated with HBSS-H supplemented with 1-10 Units/mL GPT and 6 mM sodium pyruvate to reduce basal glutamate. Following a 60-minute incubation at 37°C, buffer was aspirated and replaced with fresh HBSS-H. NanoGlo® substrate (Promega; N1130) was added for a final dilution of 1:800, then plates were incubated a further 10 minutes in darkness. Luminescence measurements were then taken using a CLARIOstar plate reader (BMG Labtech) set to incubate at 37°C, recording the total light emitted at two-minute intervals. After ten minutes, vehicle or test compounds prepared at 10X the final desired concentration were added, before continuing to take measurements for an additional 60 minutes. Luminescence was recorded and a 5-point moving average curve smoothing calculation was performed. The data were corrected for basal luminescence per well prior to compound addition and expressed as the net response by subtracting the curve obtained from wells treated with vehicle. The area under the curve (AUC) was then calculated over the full 60 minutes of compound addition.

2.5.3 Receptor Internalisation Assay

To measure the receptor internalisation, an on-cell western analysis of cell surface expression following treatment with agonists was performed. mGlu₅-WT, mGlu₅-PD, mGlu₅-TPD, and FLAG epitope-tagged FFA4 expressing Flp In™ T-Rex™ 293 cells were seeded in clear 96-well plates coated with 40 µL of 5 µg/mL of poly-D-lysine and cultured at 37°C and 5% CO₂ until confluent in the well, then receptor expression was induced with 100 ng/mL of doxycycline (in culture medium for FFA4 cells, in assay medium without glutamine and with dFBS for mGlu₅ cells). The day after receptor expression was induced, mGlu₅-expressing cells were treated with 100 µM glutamate for different lengths of time to measure agonist-induced internalisation. FFA4-expressing cells were treated with 10 µM of the agonist 3-(4-((4-fluoro-49-methyl-[1,19-biphenyl]-2-yl)methoxy)phenyl)propanoic acid (TUG-891) for 30 minutes. Cells were fixed with 10% formalin (Sigma) for 20 minutes at room temperature, then washed three times with PBS and the on-cell western protocol followed as per **Section 2.4**.

2.5.4 Calcium Mobilisation Assay

Flp-In™ T-REx™ 293 cells stably expressing either mGlu₅-WT, mGlu₅-PD or mGlu₅-TPD were plated at a density of 40,000 cells/well in black clear-bottomed 96-well plates coated with 40 µL of 5 µg/mL poly-D-lysine. Cells were incubated at 37°C and 5% CO₂ for 24 hours, then receptor expression was induced with doxycycline in assay media without glutamine and with dFBS. For the assay, 24 hours following addition of doxycycline cells were incubated in darkness with 3 µM Fura-2 AM dye (Torcris) (diluted in assay media supplemented with 1-10 units/mL GPT and 6 mM sodium pyruvate to reduce the basal levels of glutamate) for 45 minutes. Cells were then washed twice with HBSS-H to remove unbound extracellular Fura-2 AM then allowed to equilibrate in HBSS-H for a further 15 minutes at 37°C. The selected agonist was diluted in HBSS-H and added to a clear 96-well plate. The agonist was applied to the cells using the FlexStation II plate-reader and the peak ratio of fluorescent emissions at 510 nm following Fura-2 AM excitation at 340 nm (Fura-2 bound to calcium ions) and 380 nm (unbound Fura-2) measured over 90 seconds as a measure of intracellular calcium concentration.

2.5.5 Measurement of Intracellular Calcium in Single Cells using Epifluorescent Microscopy

Cells were seeded onto 22 mm, zero thickness, sterile coverslips coated with poly-D-lysine, then grown to 70% confluence in a 37°C and 5% CO₂ incubator. Receptor expression was induced with 2 ng/mL doxycycline 24 hours before microscopy. On the day of the experiment, cells were loaded with 3 µM Fura-2 AM in assay medium containing 1-10 Units/mL of GPT and 6 mM sodium pyruvate to reduce basal glutamate levels, then incubated in darkness for 45 minutes at 37°C and 5% CO₂. Coverslips were then equilibrated in perfusion buffer (130 mM NaCl, 5 mM KCl, 20 mM HEPES, 10 mM glucose, 1 mM MgCl₂, 1 mM CaCl₂) for 15 minutes at room temperature then transferred to a recording chamber and mounted onto an inverted epifluorescent microscope (Nikon TE2000-E; Nikon Instruments) with a super fluor 40X oil objective. Perfusion buffer was then perfused over the cells at room temperature until the Fura-2 ratio was stable. The randomly selected cells were excited at 340 and 380 nm using a

monochromator and emission recorded at 520 nm. Agonist was perfused over the cells for the indicated time period, then switched to perfusion buffer to remove the agonist. Changes in intracellular calcium levels were presented as a ratio image of 520 emission obtained at 340/380 nm excitation using MetaFluor imaging software (Molecular Devices, Version 7.8.13.0). Calcium oscillation curves determined from the Fura-2 ratio were then plotted on GraphPad Prism software (Version 9.3.1) and expressed as a fold over basal.

2.5.6 IP₁ Accumulation Assay

To measure the Gα_q signalling pathway, the accumulation of inositol-1-phosphate (IP₁), a metabolite of IP₃, was measured using an IP₁ HTRF® assay kit (Revvity). Flp-In™ T-REx™ 293 cells stably expressing either mGlu₅-WT, mGlu₅-PD or mGlu₅-TPD, or primary neurons, were plated at a density of 40,000 cells/well in clear 96-well plates coated with 5 µg/mL of poly-D-lysine (Sigma) or 4 µg/mL poly-D-lysine (Gibco) and 7.2 µg/mL Laminin (Gibco) for primary neuronal cultures. Cells were incubated at 37°C and 5% CO₂ for 24 hours, then receptor expression was induced in Flp-In™ T-REx™ 293 cells with doxycycline in assay media without glutamine and with dFBS. For the assay, 24 hours following addition of doxycycline, cells were washed with pre-warmed 1X stimulation HBSS containing 20 mM HEPES (HBSS-H); pH 7.4), then incubated in 100 µL/well of 1X supplemented stimulation buffer (HBSS-H supplemented with 6 mM sodium pyruvate and 1-10 units/mL glutamate pyruvate transaminase (GPT) to reduce the basal levels of glutamate) for 1 hour at 37°C. The selected agonist was made up in 1X stimulation buffer containing 50 mM LiCl to prevent the metabolism of IP₁, then applied to the cells, and incubated for 60 minutes at 37°C. Cells were harvested using 40 µL lysis buffer (Revvity) and agitation on a plate shaker at 600 rpm for 10 minutes, then 14 µL of the cell suspension was added to a 384-well OptiPlate (PerkinElmer). Serial dilutions of the IP₁ standard reagent (Revvity) were made in lysis buffer and added to the OptiPlate to generate a standard curve. IP₁-d2 (Revvity) and IP₁ Tb cryptate antibody (Revvity) were diluted 1:20 in lysis buffer and 3 µL of each added to the cell lysate. The plate was incubated at room temperature for 1 hour in darkness, then the homogenous time resolved fluorescence (HTRF) emission was measured at 665 nm and 620 nm, following excitation at 337 nm, using a PHERAstar platereader (BMGLabTech). Results

were calculated from the 665/620 nm ratio. IP₁ accumulation was calculated by interpolating from the standard curve.

2.5.7 Measurement of G Protein Dissociation

To directly measure heterotrimeric G protein dissociation, a modified version of the TRUPATH biosensor system (Olsen et al. 2020) was used (NEWPATH), demonstrating greater ease of transfection and practicality compared to TRUPATH. For this, a single biosensor plasmid was used that consists of a CMV promoter driving expression of Gβ3, followed by a P2A self-cleaving peptide sequence, an mNeonGreen tagged to the N-terminal of Gγ9, an internal ribosome entry site (IRES) mammalian expression sequence, then finally Gα_q tagged to nanoluciferase 125 amino acids into the protein. This new plasmid construct was termed 'NEWPATH'.

To employ this biosensor to measure G protein dissociation, HEK293T cells were plated into 6-well plates and once confluent, were transfected with 500 ng per well of the NEWPATH plasmid alongside the indicated amount of the receptor of interest, then the total transfected DNA was made up to 1 µg using pcDNA3. The transfection was performed using PEI as described in **Section 2.3.3.1**. Cells were then cultured for 24 hours, counted as per **Section 2.3.1**, then plated into white 96-well plates coated with 5 µg/mL of poly-D-lysine at a density of 30,000 cells/well in assay medium without glutamine and with dFBS. The cells were maintained in the plate for 24 hours before proceeding with the assay.

Cells were washed twice with HBSS-H then incubated with HBSS-H supplemented with 1-10 Units/mL GPT and 6 mM sodium pyruvate for 60 minutes at 37°C to reduce basal glutamate. Buffer was then aspirated and replaced with fresh HBSS-H. NanoGlo® substrate (Promega; N1130) was added to the wells for a final dilution of 1:800 and incubated in darkness for 10 minutes. The background luminescence was recorded using a PHERAstar platereader (BMG LabTech), recording the emission at 535 nm and 475 nm. Test compounds prepared in HBSS-H at 10X the desired final concentration were added to the cells and incubated at 37°C for five minutes, then the luminescence at 535 nm and 475 nm was recorded once again. BRET was recorded as the ratio of 535 nm emission divided by 475 nm emission, followed by dividing the BRET ratio value obtained in

each well after compound addition by the BRET ratio obtained from the same well before compound addition.

2.5.8 Using BRET-based Biosensors to Measure G α -GTP

HEK293T or Flp-In™ T-Rex™ 293 cells were plated at a density of 40,000 cells/well in white 96-well plates coated with 5 μ g/mL of poly-D-lysine and transfected 24 hours later with the indicated amounts of biosensor and receptor, using PEI as described in **Section 2.3.3.1**. Cells were then cultured in assay medium without glutamine and with dFBS for a further 24 hours until the assay. Cells were washed twice with HBSS-H then incubated in HBSS-H supplemented with 1-10 Units/mL GPT and 6 mM sodium pyruvate for 60 minutes at 37°C to reduce basal glutamate. The buffer was then aspirated and replaced with fresh HBSS-H. NanoGlo® substrate (Promega; N1130) was added using an Omega POLARstar platereader (BMG LabTech) to a final dilution of 1:800. After 10 minutes, BRET measurements were then taken using a PHERAstar plate reader (BMG Labtech) set to incubate at 37°C, recording the luminescence at 475 and 535 nm at two-second intervals. After 10 seconds, either vehicle or test compounds was injected before continuing to take 0.5 second measurements at 0.5 second intervals for an additional 90 seconds. BRET was recorded as the ratio of 535 nm emission divided by 475 nm emission, and a 5-point moving average of the calculate BRET ratios was taken for curve smoothing. The data were expressed as a ratio of the basal BRET prior to compound addition before subtracting the response recorded in vehicle treated wells to obtain the net BRET above vehicle response. The area under the net BRET curve (AUC) was then calculated over the full 90 seconds of compound addition.

2.6 Western Blotting

2.6.1 Sample Preparation

2.6.1.1 Agonist Stimulation

Flp-In™ T-REx™ 293 cells were plated in 10 cm dishes and allowed to grow until confluent. Culture medium was then replaced with assay medium without glutamine and with dFBS containing 100 ng/mL of doxycycline. After a further 24 h in culture, medium was removed, and cells were serum starved for one hour at 37°C and 5% CO₂ in serum and glutamine free DMEM containing 1-10 units/mL GPT and 6 mM sodium pyruvate to reduce basal glutamate. Medium was aspirated and cells were treated with the indicated concentration of agonist or vehicle in serum free media for a further hour before cell lysates were prepared (**Section 2.6.1.2**).

2.6.1.2 Preparation of Lysates from Cells

Cells were washed twice with ice-cold PBS, then lysed with 500 µL per dish of ice-cold RIPA lysis buffer (50 mM Tris-HCl pH 7.5, 1 mM EDTA pH 8.0, 1 mM EGTA pH 8.0, 1% Triton-X-100, 0.1% β-mercaptoethanol) supplemented with cOmplete EDTA-free protease inhibitor (Roche) and phosSTOP phosphatase inhibitor (Roche) for 10 minutes on ice. Cells were harvested by scraping to ensure they were solubilised, then centrifuged at 14,000 g for 30 minutes at 4°C to remove insoluble cell debris. The supernatant was transferred to a new ice-cold tube and stored at -20°C until further use.

2.6.1.3 Protein Quantification by Bradford Assay

The Bradford assay was performed to determine the concentration of protein in cell lysates. Protein samples diluted in RIPA lysis buffer alongside bovine serum albumin (BSA) protein standards of known concentration were added to Bradford reagent (Sigma) in a clear 96-well clear plate. After 5 minutes of incubation at room temperature, the absorbance at 595 nm was recorded using an Omega POLARstar platereader (BMG LabTech). The BSA standards were fit

linear regression and used to interpolate the concentration of protein in cell lysate samples.

2.6.1.4 Immunoprecipitation

The HA-tagged receptor was immunoprecipitated from cleared lysates using anti-HA affinity matrix (Roche). Lysates were incubated with rotation overnight at 4°C with 10 µL of anti-HA affinity matrix beads. The following day, samples were centrifuged at 1,000 *g* for 30 seconds at 4°C and the supernatant discarded. As a washing step, 1 mL of RIPA buffer was added, then samples were centrifuged again at 1,000 *g* for 30 seconds at 4°C and supernatant discarded. The washing step was repeated for a total of three washes. After the final wash, samples were centrifuged again, supernatant discarded and the HA affinity matrix beads mixed with Laemmli sample buffer (4% SDS, 20% glycerol, 10% 2-mercaptoethanol, 0.004% bromophenol blue and 0.125 M Tris-HCl, pH 6.8; Sigma) for 10 minutes at 65°C to elute protein bound to the beads.

2.6.1.5 Lambda Protein Phosphatase Treatment

To dephosphorylate proteins, the Lambda protein phosphatase (λ -PP) enzyme was used. Cell lysates, washed three times in lysis buffer without phosphatase, were incubated with 10 units of λ -PP (NEBiolabs), 1X λ -PP enzyme buffer (NEBiolabs; B0761S), and 200 µM MnCl₂ for 90 min at 30°C, before washing three times with lysis buffer again.

2.6.2 SDS-PAGE

Polyacrylamide gels were cast using Bio-RAD mini-Protean equipment. Resolving gels had a typical thickness of 1.0 mm and a final acrylamide percentage of 8%, diluted in distilled water (8% acrylamide, 280 mM Tris, 0.1% (v/v) sodium dodecyl sulphate (SDS), 0.1% (v/v) ammonia persulphate (APS), 0.06% (v/v) TEMED). Once the resolving gel had set, the stacking gel (5% acrylamide, 62.5 mM Tris, 0.1% (v/v) SDS, 0.1% APS, 0.1% (v/v) TEMED) was cast above the resolving gel.

Whilst keeping the samples on ice, 2X Laemmli sample buffer was added for a final concentration of 1X to each sample then samples were heated at 65°C for 10 minutes to denature the proteins. Samples were briefly centrifuged to collect condensation from the cap, then loaded on SDS-PAGE gels, typically at 20 µg of protein per well for lysates. The samples were run in running buffer (25 mM Tris, 192 mM glycine, 0.1% SDS (w/v)) at a constant voltage of 80V through the stacking gel for approximately 20 minutes, then at 120V constantly until the dye front reached the end of the resolving gel, approximately 2 hours total.

2.6.3 Western Blot Probing and Detection

Nitrocellulose membranes (ThermoFisher), filter paper (ThermoFisher) and transfer sponges (BioRAD) were equilibrated in transfer buffer (25 mM Tris, 192 mM glycine, 20% ethanol). Gels were placed in contact with the nitrocellulose membrane and encased in filter paper and transfer sponges, then proteins were transferred to nitrocellulose membranes using wet transfer method at a constant voltage of 60V for 2 hours in pre-cooled transfer buffer. Membranes were blocked for 1 hour at room temperature in either 5% milk in TBS-T (20 mM Tris, 137 mM NaCl, 0.1% Tween-20; pH 7.6) or 5% bovine serum albumin (BSA) in TBS-T to block non-specific binding sites. Blocked membranes were incubated with primary antibody diluted 1:1,000 in 5% milk in TBS-T (Table 2.4). For phospho-site specific immunoblotting, (pS871/S872/T875, pS1018/S1020 and pS1041/S1044 antibodies) (7TM Antibodies) (Table 2.4) the antibodies were diluted in 1:1,000 in 5% BSA in TBS-T. Membranes were incubated in primary antibody at 4°C on a shaker overnight. The membranes were washed with TBS-T (three 10-minute washes) then incubated in the relevant secondary antibody conjugated with IRDye® fluorophore (LI-COR Biotechnology) (Table 2.5) diluted 1:10,000 in 5% milk or 5% BSA for 1 hour in darkness on a shaker. The membrane was washed again in TBS-T then IRDye® fluorescence was visualised using LI-COR Odyssey SA scanner system using an excitation wavelength of 778 nm and emission wavelength at 795 nm. When re-probing was necessary, the membrane was incubated in stripping buffer (ThermoScientific) for a maximum of 15 minutes then washed three times for 10 minutes each wash with TBS-T. The membrane was once again blocked in 5% milk or 5% BSA in TBS-T for one hour, then incubated

in a different primary antibody and corresponding secondary antibody for the desired protein of interest.

2.6.4 Quantification of Western Blots

Band intensity of western blots was assessed through measurement of the median pixel intensity (arbitrary units) using Image Studio Lite (Version 5.2; LI-COR Biosciences). The band intensity of the protein of interest was expressed as a ratio over the band of the housekeeping protein, commonly sodium-potassium ATPase.

2.7 Immunocytochemistry

Flp-In™ T-REx™ 293 cells were seeded onto 22 mm zero thickness sterile glass coverslips coated with poly-D-lysine. Cells were cultured for 24 hours then receptor expression induced with doxycycline in assay medium without glutamine and with dFBS, then cultured for a further 24 hours. The culture medium was aspirated, and cells were washed with PBS. The cells were then fixed with 10% formalin for 20 minutes at room temperature, then washed three times with PBS. Non-specific binding was blocked by incubation with blocking buffer (1% BSA, 0.1% Triton-X-100 in PBS) for 1 hour at room temperature. After washing three times with PBS, cells were incubated with anti-HA primary antibody (Table 2.4) at 4°C overnight. After a further three washes with PBS, the samples were incubated with donkey anti-rat AlexaFluor secondary antibody (Table 2.5) for 2 hours in darkness at room temperature. The samples were washed three times with PBS and mounted onto slides using VECTASHIELD® Hardset™ Antifade Mounting Medium with DAPI (Vector Laboratories) then left to dry overnight at 4°C. Samples were imaged using a Zeiss Aperture Correlation Vivatome Spinning Disk Microscope running Zeiss Zen software and equipped with a 63x objective. Single slice images of cells were taken that were post processed using ImageJ software.

2.8 Data Analysis

2.8.1 Analysis of Pharmacological Parameters

Data and statistical analyses were carried out using GraphPad Prism software (Version 9.3.1). Concentration response curves were fit using non-linear regression analysis to a three-parameter sigmoidal function:

$$Response (Y) = Bottom + \frac{Top - Bottom}{1 + 10^{\log EC_{50} - \log[Ligand] (X)}}$$

The top asymptote represents the maximal response (E_{MAX}) and the agonist potency can be determined using the $\log EC_{50}$. For statistical analysis and reporting, the agonist potency is described as the pEC_{50} ($-\log EC_{50}$). For vehicle points on concentration response curves, data was plotted 10-fold lower than lowest agonist concentration to fit the curve.

2.8.2 Statistical Analysis

Statistical analyses were carried out using GraphPad Prism 9 software. Data are shown as mean \pm S.E.M. and replicates are described for each experiment in the figure legends. In all cases, data was assumed to be normally distributed and compared using parametric tests, wherein a P value of <0.05 was considered statistically significant.

Typically, a two-tailed unpaired t test (for two groups), or an analysis of variance (ANOVA) (for three or more groups) was used to compare datasets. Post hoc corrections were performed where statistical tests with multiple comparisons were selected. Tukey's multiple comparisons post hoc test was used when comparing the mean of each group of data with every other mean. Šídák's correction for multiple comparisons was selected when comparing selected means, for instance comparing means to that of wildtype. For data in which normalisation to 100% or 0% had been performed, for example normalisation to wildtype or parental cells, a Kruskal-Wallis test was used, a non-parametric

analogue to one-way ANOVA. This was followed by Dunn's post hoc test for multiple comparisons.

3 Phosphorylation Controls β -Arrestin 2 Recruitment but not Internalisation of the Type 5 Metabotropic Glutamate Receptor

3.1 Introduction

The type 5 metabotropic glutamate receptor 5 (mGlu₅) plays a crucial role in regulating synaptic transmission and neuronal plasticity, making it a key target for understanding various neurological disorders. Phosphorylation, a post-translational modification, has been shown to modulate the function and signalling of mGlu₅ receptors, thereby influencing neuronal activity and synaptic plasticity (Marton et al., 2015). For dissecting the functional roles of receptor phosphorylation, investigating disease pathophysiology, and informing novel drug development, phospho-deficient (PD) mutant receptors serve as valuable tools for understanding the complex networks governing receptor signalling in health and disease. To generate PD mutants, putative phosphorylation sites are mutated to amino acid residues unable to be phosphorylated such as alanine, providing a receptor that can be pharmacologically profiled and compared to wildtype receptor to dissect out the physiological roles of direct receptor phosphorylation. This technique was utilised by Scarpa et al. (2021), discovering through use of an M1 muscarinic PD receptor that phosphorylation-dependent receptor signalling delivers neuroprotection in a mouse model of neurodegenerative disease.

Through phospho-amino acid analysis, Olsen et al., (2006) determined that the relative distribution of phosphorylated amino acids in normally growing cells was 86.4% phospho-serine, 11.8% phospho-threonine, and 1.8% phospho-tyrosine. To investigate phosphorylation of the mGlu₅ receptor, a C-terminus was synthesised in which the most abundantly phosphorylated amino acid, serine, was mutated to alanine to generate a phosphorylation deficient mutant of the mGlu₅ receptor (mGlu₅-PD). Furthermore, a 'total' phosphodeficient receptor was generated through synthesising a C-terminus where serine and threonine residues were mutated to alanine (mGlu₅-TPD). Mutation of putative phosphorylation sites in the intracellular surface of the receptor permits determination of the impact of direct receptor phosphorylation on receptor activity, cellular responses, and downstream signalling pathways through comparison of the activity to wildtype receptors. Specifically, separate serine- and serine/threonine-deficient mutants allows the distinction of the roles of the two individual amino acids in receptor phosphorylation and subsequent cellular activity.

This chapter focuses on the pharmacological characterisation of the role of direct mGlu₅ phosphorylation through the use of mGlu₅ PD mutants. Exploration into the agonist-stimulated β -arrestin 2 (β -Arr2) recruitment in cell lines expressing these phosphodeficient receptor variants (mGlu₅-PD and mGlu₅-TPD) reveals the impact of receptor phosphorylation on this process. Despite some specific locations of C-terminal phosphorylation sites of mGlu₅ being defined (Gereau IV & Heinemann, 1998; Luo et al., 2020; Uematsu et al., 2015), very little is known about the physiological and pharmacological impact of this phosphorylation. Although receptor phosphorylation and β -Arr2 recruitment has been linked, with arrestins having a higher affinity for active phosphorylated GPCRs detected by sensors within the arrestin protein (Karnam et al., 2021), the functional consequences of direct mGlu₅ phosphorylation remain incompletely understood. Here, the physiological effects of basal and agonist-induced mGlu₅ phosphorylation were evaluated in cell lines expressing wildtype mGlu₅ (mGlu₅-WT), mGlu₅-PD and mGlu₅-TPD, providing a strong foundation for understanding the link between mGlu₅ receptor phosphorylation and the downstream effects of this.

3.2 Aims

To examine the impact of C-terminal mGlu₅ phosphorylation on β -arrestin 2 recruitment and internalisation, the aims of this chapter were as follows:

- Assess the ability of wildtype and phosphodeficient mutant mGlu₅ receptors to recruit β -arrestin 2.
- Investigate the role of G protein-coupled receptor kinases on mGlu₅ receptor β -arrestin 2 recruitment.
- Validate and characterise novel mGlu₅ phospho-site specific antibodies.

3.3 Results

3.3.1 Mutation of Serine Phosphorylation Sites in the M1

Acetylcholine Receptor C-Terminus Disrupts β -Arrestin 2 Recruitment

To demonstrate the potential for using PD mutants to study the importance of phosphorylation in the recruitment of β -Arr2 to GPCRs, the murine M1 muscarinic acetylcholine receptor was used. This rhodopsin-like GPCR couples to the $G\alpha_{q/11}$ signal transduction pathway, like mGlu₅. M1 receptors are primarily found in the central nervous system (CNS), particularly in regions associated with cognition and memory (Levey et al., 1991), while mGlu₅ receptors are broadly expressed in the CNS (Shigemoto et al., 1993). Dysfunction of both receptors are implicated in neurodegenerative disorders (see Wong et al. (2023) for a review), highlighting the common localisation and role of the receptors.

Previous work has generated a phosphorylation-deficient mutant of the murine M1 receptor (M1-PD), whereby all serine residues in the C terminus and third intracellular loop were mutated to alanine (Butcher et al., 2016). It was demonstrated that this PD mutant displays reduced recruitment of β -Arr2 (Bradley et al., 2020). In order to confirm this finding, β -Arr2 recruitment to the plasma membrane in HEK293T cells expressing wildtype M1 receptor (M1-WT) or M1-PD was assessed through a bystander BRET-based system (Figure 3.1A). When plotting the muscarinic endogenous agonist acetylcholine (ACh) concentration response from cells transfected with each receptor construct (Figure 3.1B), it was apparent that while the E_{MAX} was reduced by 75.8% for M1-PD compared to M1-WT ($P=0.0309$, unpaired t-test), the potency values were unchanged. To confirm that the β -Arr2 responses observed were related to the expression of M1-WT and M1-PD, a control experiment was conducted transfecting empty vector with the bystander BRET plasmids, showing that acetylcholine (ACh) produced no recruitment of β -Arr2 to the plasma membrane (Figure 3.1C). Observing the kinetics following a 30-minute stimulation with ACh, robust, concentration dependent, β -Arr2 recruitment to the plasma membrane was recorded in cells expressing M1-WT, peaking after 4 minutes (Figure 3.1D). In cells expressing M1-PD, a peak β -Arr2 recruitment was also observed at 4 minutes, however the

magnitude of this response was reduced by 83.5% compared to wildtype ($P=0.0854$, unpaired t-test) (Figure 3.1E).

These data demonstrate that intracellular serine residues are key for β -Arr2 recruitment in cells expressing the M1 muscarinic acetylcholine receptor, as the M1-PD receptor lacking intracellular serine residues had limited capacity to recruit β -Arr2 in comparison to the wildtype receptor.

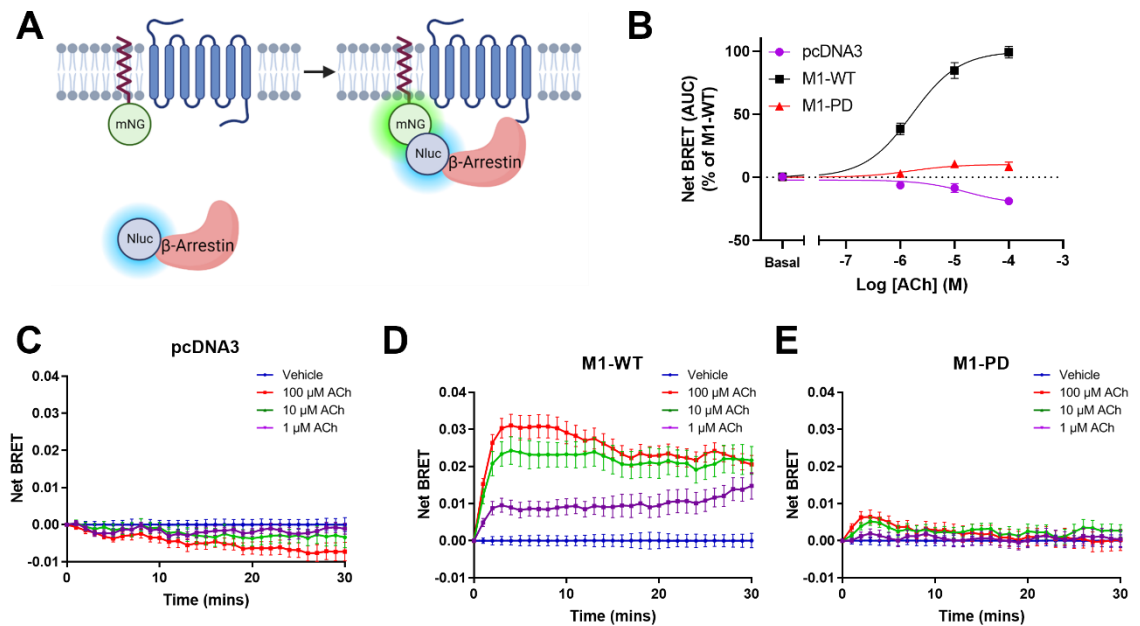


Figure 3.1: β -arrestin 2 recruitment to the murine M1 receptor is reduced but not eliminated when C-terminal serine residues are mutated to alanine. Acetylcholine (ACh)-stimulated β -arrestin 2 recruitment to the cell membrane was measured using a bystander BRET assay, as depicted in the schematic (A). The BRET donor, nanoluciferase (Nluc), is tagged to β -arrestin 2 and the BRET acceptor, mNeonGreen (mNG), is anchored at the plasma membrane via a CAAX motif. Upon β -arrestin 2 recruitment to the cell membrane by the receptor of interest, the BRET donor and acceptor proteins are brought in close proximity, producing a measurable BRET signal. The data are plotted as a concentration response curve (B) by calculating the area under curve (AUC) of the net BRET above vehicle treatment from HEK293T cells transfected with Nluc- β -arrestin 2 and mNG-CAAX as well as with (C) pcDNA3 empty vector control, (D) the wildtype murine M1 muscarinic receptor (M1-WT), or (E) the phosphodeficient mutant M1 receptor (M1-PD). Data are expressed as the means \pm S.E.M. of three independent experiments performed in quadruplicate.

To demonstrate that a phosphodeficient GPCR construct can be used to study receptor signalling in a more physiologically relevant system, I next aimed to demonstrate that M1 β -Arr2 recruitment in cortico-hippocampal neurons is also dependent on the presence of M1 phosphorylation sites. For these studies, I established neuronal cultures from both wild type C57BL/6J mice and knock-in

mice engineered to express M1-PD under the control of the murine M1 promoter, which no longer express M1-WT (Bradley et al., 2020). The same bystander BRET-based system was employed in these primary neuronal cultures to measure β -Arr2 recruitment in response to treatment with ACh. Initially, to confirm the components of the BRET system were successfully transfected into the neurons, confocal microscopy was used to look at the expression of the CAAX membrane anchored mNeonGreen (mNG) fluorescent protein (Figure 3.2A). The mNG fluorescence is visible at the cell membrane of the neuron, both in the cell body and the projections, however it was noted from the brightfield image that the transfection efficiency was low, at approximately 2%, with most neurons not expressing the fluorescent protein. To assess β -Arr2 recruitment in neurons expressing the M1-WT and M1-PD receptors, cells transfected with mNG-CAAX and Nluc- β -Arr2 were treated with 100 μ M acetylcholine and the change in BRET monitored for 30-minutes (Figure 3.2B). Looking at the kinetic traces, there is an increase in BRET over the entire time course for M1-WT, indicating recruitment of β -Arr2 to the plasma membrane of the neurons expressing M1-WT (Figure 3.2B). Mutation of intracellular serine residues of the M1 receptor decreases the magnitude of the BRET response in comparison to wildtype receptor, however there is still a BRET response which produces a second peak at the 20-minute time point; this indicates that there exists some recruitment of β -Arr2 by the M1-PD receptor, but the kinetics are differing compared to M1-WT.

Quantification of the area under curve (AUC) for the BRET responses demonstrated that there is a 66.4% decrease in BRET response to acetylcholine with removal of putative phosphorylation sites ($P=0.0735$, unpaired t test). These data corroborate the *in vitro* BRET data in that intracellular serine residues play a role in the recruitment of β -Arr2 to the M1 muscarinic acetylcholine receptor. Additionally, it was demonstrated that phosphodeficient mutants are valuable tools to study GPCR function in physiologically relevant systems and that bystander BRET β -Arr2 recruitment can be employed in primary neuronal cultures.

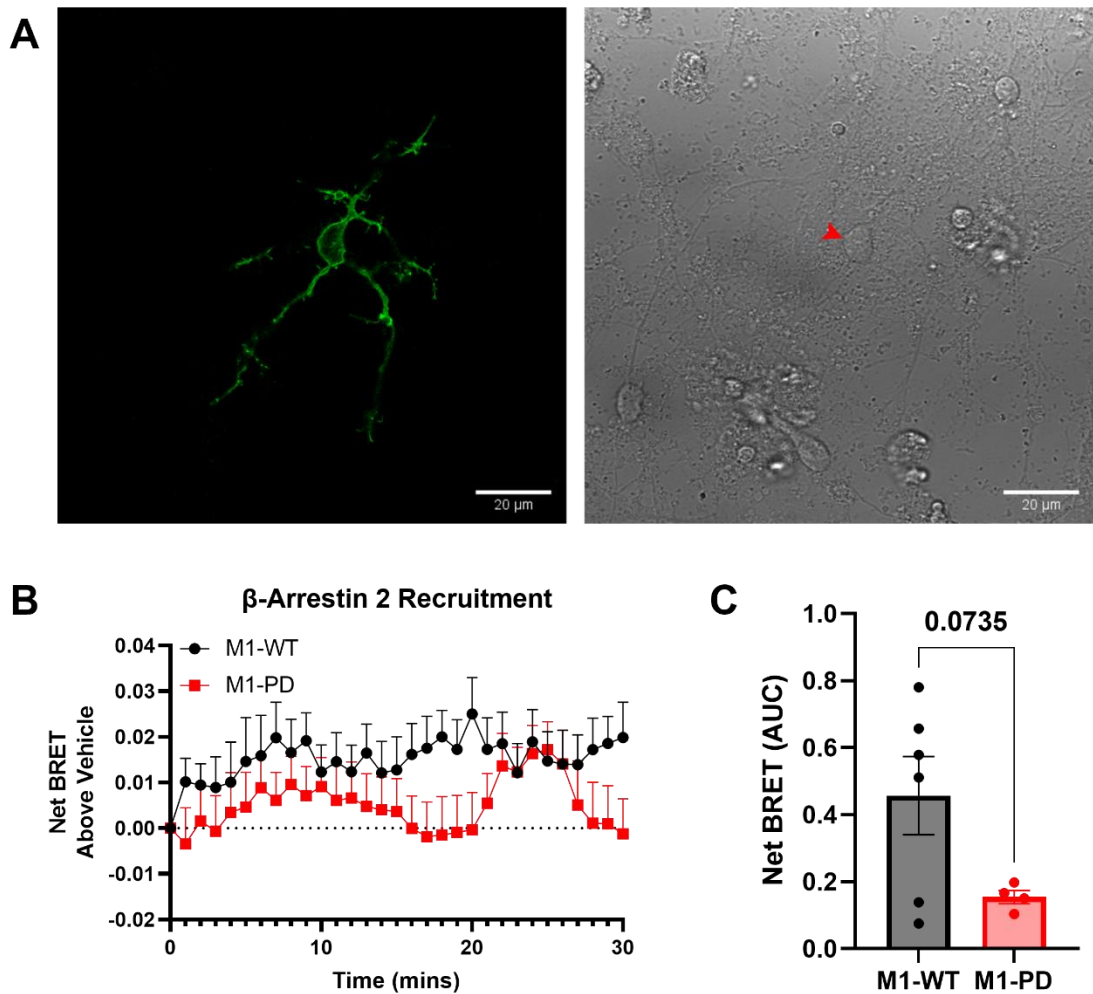


Figure 3.2: β -arrestin 2 is recruited to wild type but not phosphodeficient M1 in cultured cortico-hippocampal neurons. (A) Murine primary cortico-hippocampal neurons were transfected with nanoluciferase-tagged β -arrestin 2 and mNeonGreen fluorescent protein then visualised using a Zeiss LSM 880 inverted confocal microscope running Zeiss Zen software equipped with a 63x objective to take confocal slices of neurons to image mNeonGreen using the 488 nm excitation laser line (left) and brightfield (right). The red arrowhead indicates the cell body of the neuron. (B) The time course of β -arrestin 2 recruitment to the cell membrane in cortico-hippocampal neurons from mice expressing either wildtype (M1-WT) or phosphodeficient M1 receptor (M1-PD) was recorded following treatment with 100 μ M acetylcholine. (C) The area under the curve (AUC) for the net BRET above vehicle treatment to acetylcholine was calculated from the dataset in B. Data are expressed as means \pm S.E.M. of four and six independent experiments each performed in triplicate. Statistical analysis performed was an unpaired t-test.

3.3.2 Mutation of mGlu₅ C-Terminal Serine and Threonine Residues to Alanine Disrupts β -Arrestin 2 Recruitment

Next, I aimed to apply the concept of using GPCR PD mutants to study β -Arr2 recruitment to the mGlu₅ receptor. The M1-PD receptor consisted of mutation of serine residues alone, yet serine is not the only amino acid that can be phosphorylated. Considering this, cells expressing this M1-PD mutant receptor exhibited some residual β -Arr2 recruitment. To further these studies, two mutants of the mGlu₅ receptor were generated: the mGlu₅-PD receptor (C-terminal serine residues mutated to alanine) and the mGlu₅-TPD receptor (C-terminal serine and threonine residues mutated to alanine) (Figure 3.3), to dissect out the functions of both serine and threonine amino acid phosphorylation.

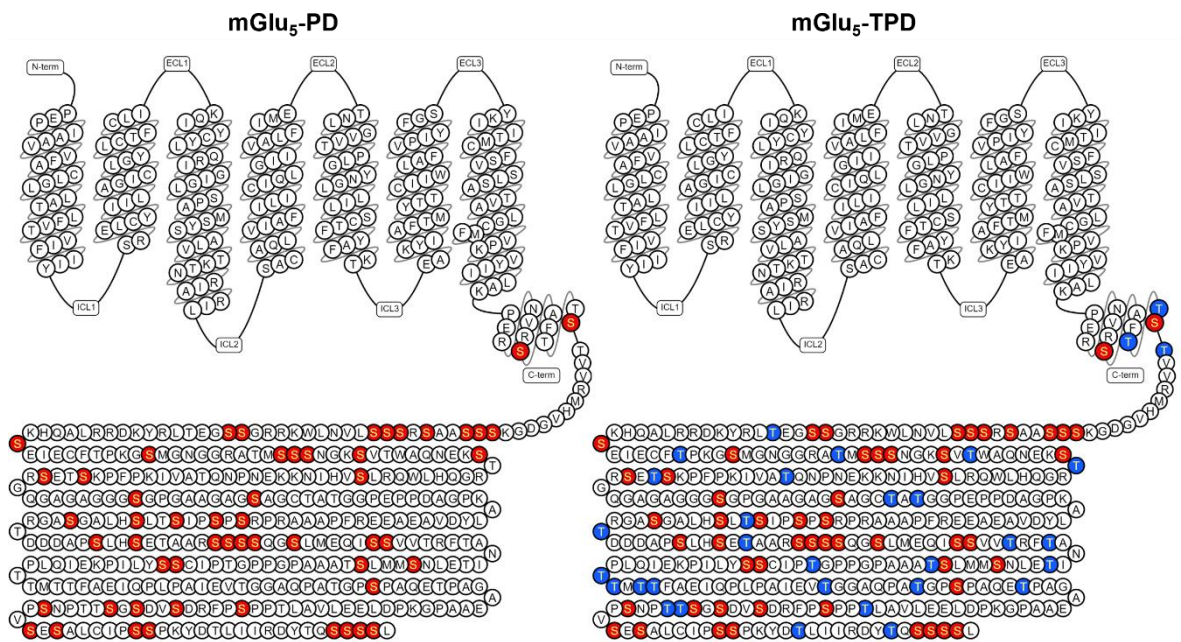


Figure 3.3: The phosphodeficient mutant receptors mGlu₅-PD and mGlu₅-TPD. mGlu₅-PD (left) consists of all C-terminal serine residues (red) mutated to alanine to prevent phosphorylation of serine residues, whereas mGlu₅-TPD (right) has the serine and threonine (blue) residues mutated to alanine. Both mutant receptors are based on the long form mGlu_{5b} isomer.

Initially the bystander BRET-based system (Figure 3.1A) was employed in HEK293T cells transiently transfected with the wildtype or PD mutant receptors to compare β -Arr2 recruitment kinetics. Preceding the assay, cells were treated with the enzyme GPT supplemented with sodium pyruvate to remove endogenous glutamate (Matthews et al., 2000), thus the β -Arr2 recruitment is stimulated by solely exogenously applied glutamate. Recording the kinetics of β -Arr2 recruitment

following stimulation with 100 μ M glutamate over the course of an hour reveals a steady increase in BRET signal in cells expressing the mGlu₅-WT receptor, demonstrating recruitment of β -Arr2 to the cell membrane (Figure 3.4A). A one-hour time course was selected for mGlu₅, as opposed to the 30-minute time period used for the M1 receptor, as the glutamate receptor family are not as robustly coupled to β -Arr2 compared to rhodopsin-like GPCRs (Abreu et al., 2021). In contrast to mGlu₅-WT, cells expressing the mGlu₅-PD receptor do not exhibit any recruitment of β -Arr2 to the cell membrane in response to 100 μ M glutamate (Figure 3.4A), however a slight increase in recruitment is observed at the 20-minute time point similar to that seen for the M1-PD expressing neurons. Interestingly, the cells expressing mGlu₅-TPD appeared to display a decrease in BRET following 100 μ M glutamate treatment (Figure 3.4A). This may be a real decrease in net BRET, or an artefact in the assay and the luminescent signal dropping. Subsequent experiments assessed the ability of multiple concentrations of glutamate to stimulate recruitment of β -Arr2 to the plasma membrane over a one-hour time period in cells expressing mGlu₅-WT, mGlu₅-PD and mGlu₅-TPD (Figure 3.4B). These data suggested a pEC₅₀ of 5.1 in cells expressing mGlu₅-WT, while again no response was observed in mGlu₅-PD and a small decrease in BRET observed in cells expressing mGlu₅-TPD.

It was also noted that expression of the different mGlu₅ mutant receptors alone, without glutamate treatment, appeared to affect the basal BRET observed between Nluc- β -Arr2 and the membrane anchored mNG (Figure 3.4C). Notably, this basal BRET was significantly elevated in cells expressing mGlu₅-WT compared to pcDNA3 transfected cells ($P < 0.0001$, one-way ANOVA), and significantly decreased in cells expressing mGlu₅-TPD ($P < 0.0001$, one-way ANOVA). There also appeared to be a clear trend toward decreasing BRET with removal of phosphorylation sites, with basal BRET significantly reduced in cells expressing mGlu₅-PD, lacking only serine sites, compared with cells expressing mGlu₅-WT ($P < 0.0001$, one-way ANOVA), and further reduced in cells expressing mGlu₅-TPD, lacking both serine and threonine sites ($P < 0.0001$, one-way ANOVA). The basal BRET ratios provide insightful information into the ligand-independent activity of the receptor and how phosphorylation impacts this. The significant increase in the basal BRET ratio in cells expressing mGlu₅-WT suggests that this receptor is highly constitutively active, and this constitutive activity increases β -

Arr2 localisation to the cell membrane, however differences in surface expression should be considered.

These data suggest that C-terminal serine residues of the mGlu₅ receptor play a substantial role in the recruitment of β -Arr2, and that threonine residues have a further function in this process. In addition to this, expression of the wildtype receptor increases the basal BRET, which could indicate an increase in constitutive activity as the BRET increases simply from expressing the wildtype receptor. The basal BRET measurement decreases back to the level observed in empty vector transfected cells upon mutation of serine residues, which also further decreases upon mutation of threonine residues, therefore it may be implied that serine and threonine residues in the C-terminus may play a role in the constitutive β -Arr2 recruitment to the mGlu₅ receptor.

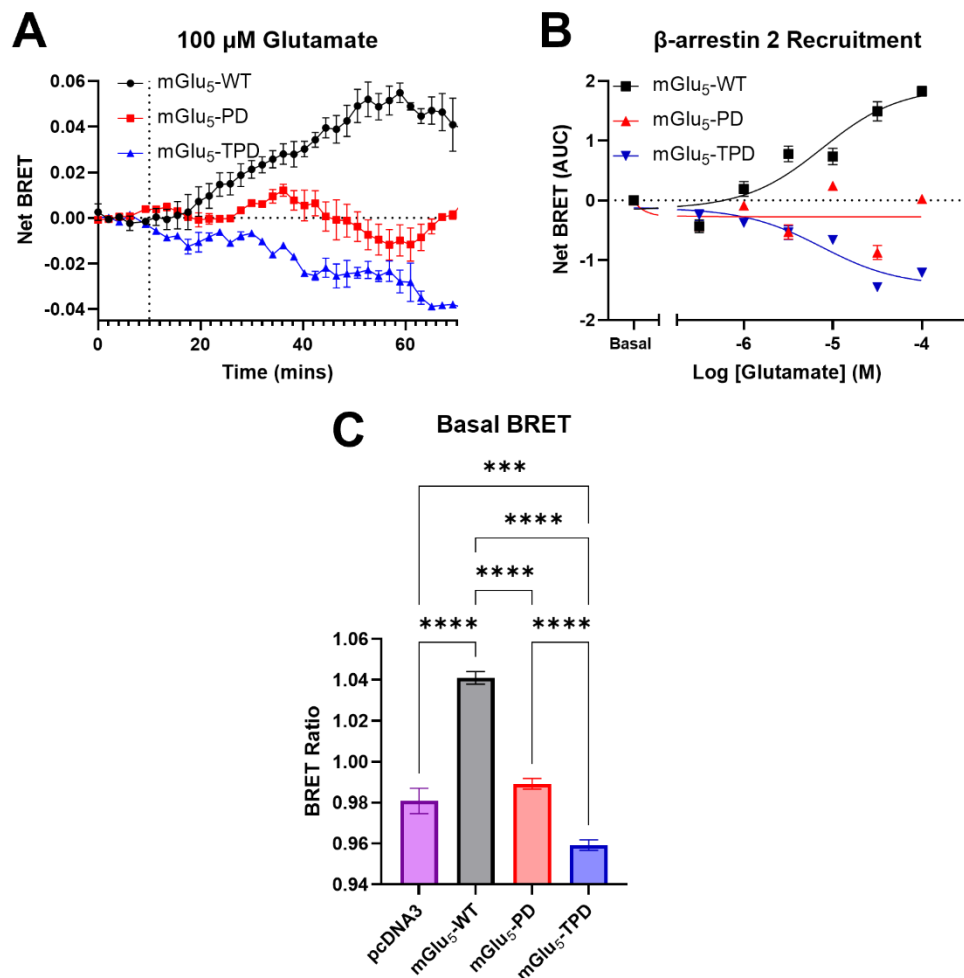


Figure 3.4: Constitutive and glutamate dependent β -arrestin 2 recruitment to mGlu₅ is reduced with removal of putative C-terminal phosphorylation sites. (A) The kinetic traces of bystander BRET β -arrestin 2 recruitment to the plasma membrane in HEK293T cells expressing wildtype mGlu₅, mGlu₅-PD and mGlu₅-TPD were measured over the course of an hour in cells treated with 100 μ M glutamate, subsequent to a 10-minute baseline read. Data are plotted as the net BRET above vehicle treatment. Data are

expressed as means \pm S.E.M. of one independent experiment performed in triplicate. (B) Concentration response curves of the agonist-stimulated β -arrestin 2 recruitment to the cell membrane were generated from net BRET above vehicle area under curve (AUC) data following stimulation with increasing concentrations of glutamate. (C) The basal BRET, measured prior to the addition of glutamate, is reported for each mGlu₅ receptor variant or pcDNA3 empty vector control. Data are expressed as means \pm S.E.M. of one independent experiment performed in triplicate. A one-way ANOVA was performed with Tukey's post-hoc multiple comparisons test. *** $P < 0.0005$, **** $P < 0.0001$.

3.3.3 Development of a NanoBiT Assay to Measure β -Arrestin 2 Recruitment to mGlu₅

To further verify the BRET-based β -Arr2 recruitment data, an alternative method to measure recruitment was pursued. For this, a bystander based NanoLuc Binary Technology (NanoBiT) luciferase complementation assay was selected (Figure 3.5A). The large BiT (LgBiT) (17.6 kDa) is anchored at the plasma membrane with a Lyn11 motif, and the small BiT (SmBiT) (11 amino acids) is tagged to β -Arr2. As the receptor recruits the tagged β -Arr2, the protein fragments come together and form an active luciferase protein, generating a bright luminescent signal. The NanoBiT technique has been validated in rhodopsin-like GPCRs to robustly measure β -Arr2 recruitment (Pedersen et al., 2021). In addition to this, the NanoBiT setup as a complementation assay has the potential to generate a larger signal window than the ratiometric BRET-based β -Arr2 recruitment technique. Therefore, I hypothesised that the NanoBiT system may be a better option for mGlu₅, as this receptor has been reported to have a poor ability to recruit β -Arr2 (Abreu et al., 2021).

To directly compare the magnitude of β -Arr2 recruitment for mGlu₅ in the NanoBiT assay with a GPCR known to strongly recruit β -Arr2, the free fatty acid receptor 4 (FFA4) was selected as a positive control. FFA4 has been shown to robustly recruit β -Arr2 in a variety of assay formats (Alvarez-Curto et al., 2016), hence is a good candidate receptor to compare to the glutamate receptor family. The mGlu₅ receptor demonstrated a much smaller signal window than the FFA4 receptor; the peak luminescent signal for the glutamate/mGlu₅-WT response was decreased by 88.1% compared to from the TUG-891/FFA4 response ($P = 0.053$, unpaired t test) (Figure 3.5B). Looking at the kinetics of the response, the use of the FFA4 agonist, TUG-891, to activate the receptor produces a robust increase in luminescence, peaking at 12-minutes post agonist addition (Figure 3.5C). In contrast, the mGlu₅-WT receptor takes a much longer time to produce a

luminescent response (Figure 3.5D), and the magnitude of luminescent response is much lower when activating mGlu₅ with glutamate than it is when activating FFA4 with TUG-891.

These data demonstrate that the NanoBiT system can be employed to measure both receptors with robust coupling to β -Arr2 recruitment and also receptors with much weaker coupling. The mGlu₅ receptor demonstrated a less robust coupling to β -Arr2 than the rhodopsin-like GPCR FFA4 and with slower kinetics, however despite this, the mGlu₅ receptor was still able to recruit β -Arr2 to the membrane.

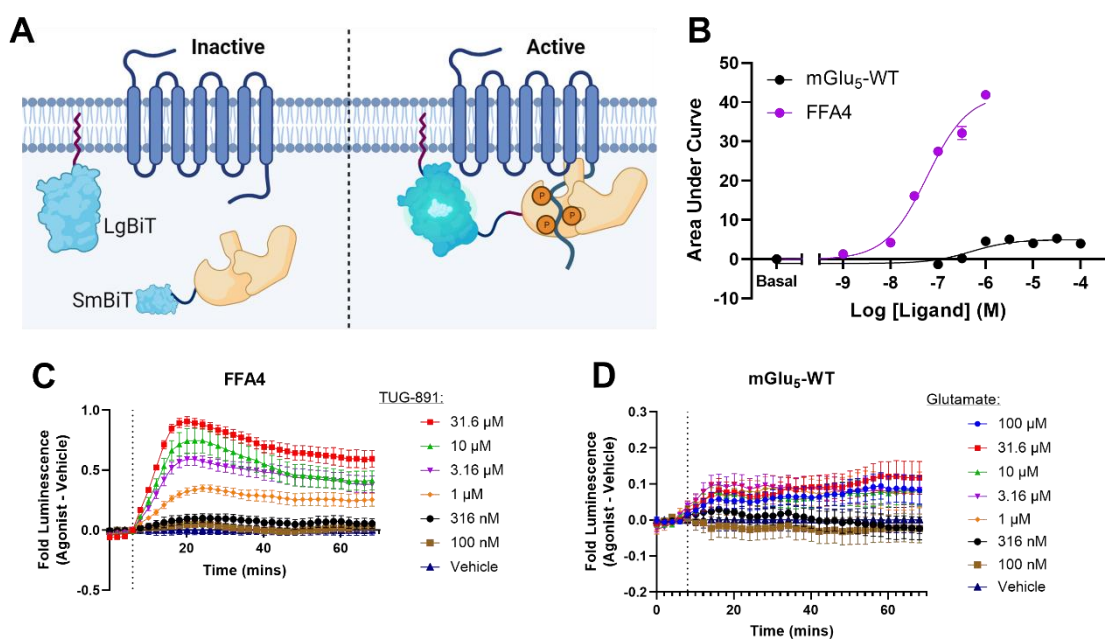


Figure 3.5: mGlu₅ demonstrates a much weaker coupling to the β -arrestin 2 pathway compared to the free fatty acid receptor 4. (A) A schematic demonstrating the NanoBiT β -arrestin 2 recruitment assay, in which the large BiT (LgBiT) fragment of the nanoluciferase protein is anchored at the plasma membrane and the β -Arrestin 2 protein is tagged with the small BiT (SmBiT). When SmBiT- β -Arrestin 2 is recruited by the receptor, the LgBiT and SmBiT fragments come together to form an active luciferase protein, producing a luminescent signal. (B) The kinetics of β -arrestin 2 recruitment were recorded subsequent to treatment with the agonists glutamate (for mGlu₅) or TUG-891 (for FFA4), then the area under the curve was plotted. The kinetics of the β -arrestin 2 recruitment in HEK293T cells expressing the FFA4 receptor (C) or the mGlu₅-WT receptor (D) was recorded over a 60-minute time course. Data are expressed as means \pm S.E.M. of three independent experiments each performed in triplicate.

The NanoBiT system was then employed in cells expressing wildtype or phosphodeficient mGlu₅ receptor constructs to see if this assay system confirmed findings on the impact of phosphorylation seen in the previous BRET-based assay. Initially, the NanoBiT assay was performed in HEK293T cells transfected with

empty vector pcDNA3 control (Figure 3.6A) (pre-treated with GPT to reduce basal glutamate) to confirm that exogenously applied glutamate did not stimulate β -Arr2 recruitment in cells that have not been transfected with an mGlu₅ receptor construct. This was then progressed into cells expressing mGlu₅-WT (also pre-treated with GPT) which were then treated with increasing concentrations of glutamate to determine if the β -Arr2 recruitment was dependent on agonist concentration. Following a 10-minute baseline recording of the luminescent signal, agonist was applied to the cells and the kinetics of the luminescent signal was recorded over a one-hour time period. The luminescent signal gradually increased in cells expressing the wildtype receptor; the magnitude of response was lower when cells were treated with 1 μ M of glutamate, but both 10 μ M and 100 μ M produced approximately equivalent magnitudes of luminescent signal (Figure 3.6B). Similarly, the mGlu₅-PD receptor demonstrated an increase in the fold luminescence in a concentration-dependent manner (Figure 3.6C). In contrast, although the cells expressing the mGlu₅-TPD receptor produced a luminescent signal at 10 μ M and 100 μ M, there was no response with 1 μ M of glutamate (Figure 3.6D). Calculating the net response from the kinetic traces reveals similar concentration response curves for both mGlu₅-WT and mGlu₅-PD, however the maximal fold luminescent value produced by mGlu₅-TPD is 46.5% lower than the maximal signal produced in cells expressing mGlu₅-WT ($P=0.1124$, unpaired t test) (Figure 3.6E).

Employing the NanoBiT system to measure β -Arr2 recruitment in cells expressing wildtype and PD mutants of mGlu₅ reveals no difference between mGlu₅-WT and mGlu₅-PD, implying that conversely to the findings from the BRET-based β -Arr2 recruitment assay, C-terminal serine residues may not play a role in glutamate stimulated recruitment of β -Arr2. However, this assay does confirm that C-terminal threonine residues do have a function in the recruitment of β -Arr2; mutating these residues to an amino acid that is unable to be phosphorylated reduces the ability of the receptor to recruit β -Arr2 to the cell membrane.

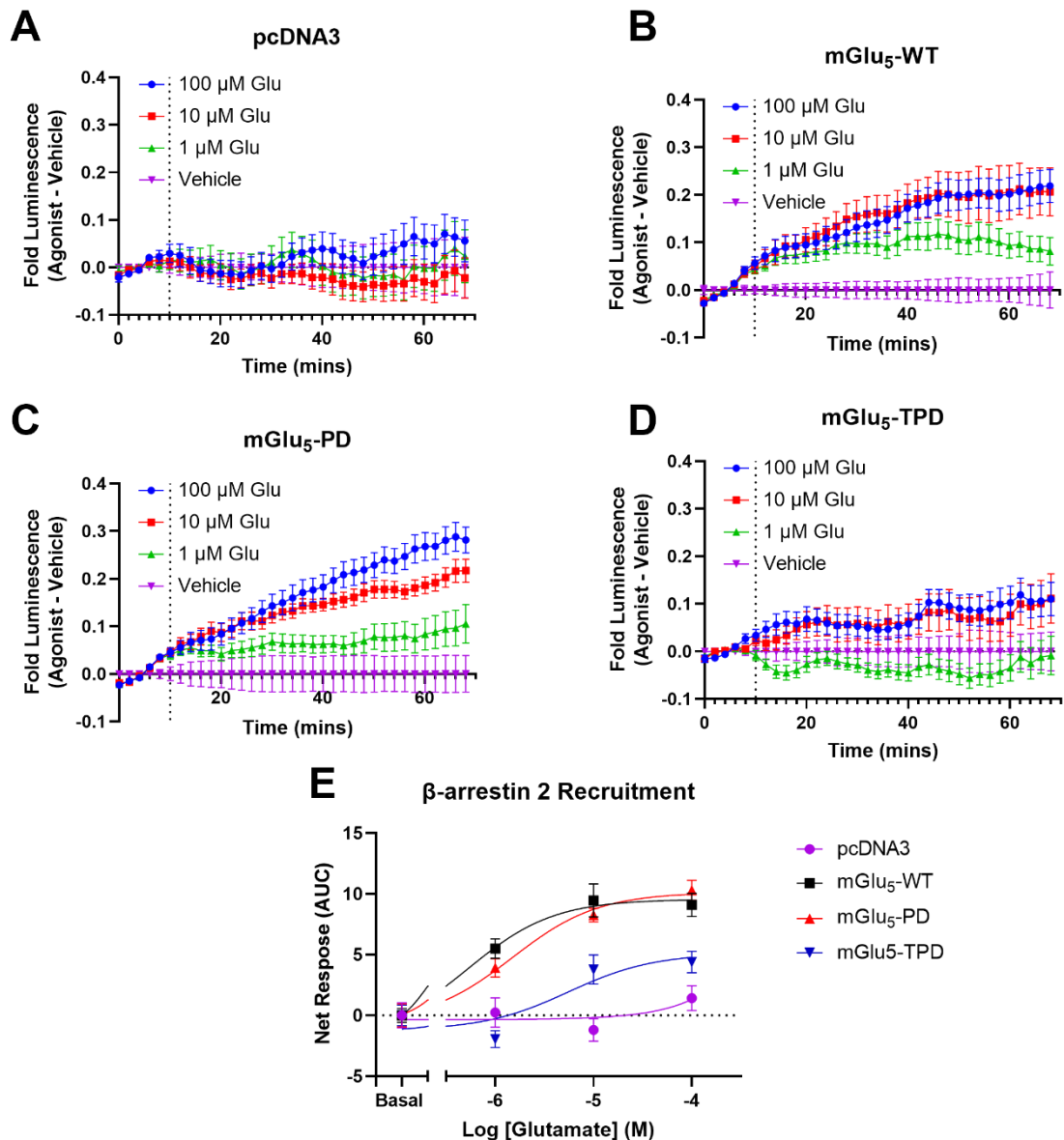


Figure 3.6: mGlu₅-TPD demonstrates reduced β -arrestin 2 recruitment compared to both mGlu₅-WT and mGlu₅-PD in the NanoBIT complementation assay. Subsequent to a ten-minute baseline read, HEK293T cells transfected with the NanoBIT β -Arr2 sensor components and either the empty vector control pcDNA3 (A), mGlu₅-WT (B), mGlu₅-PD (C), and mGlu₅-TPD (D) were treated with 1 μ M, 10 μ M or 100 μ M of the endogenous agonist glutamate (Glu) or vehicle (HBSS-H). The luminescent signal from β -arrestin 2 recruitment to the cell membrane and luciferase complementation was recorded and luminescent signal plotted as the ratio over the pre-drug addition baseline recording after subtracting the ratio obtained in vehicle treated wells. The net response was measured as the area under the curve (AUC) and plotted as a concentration response curve (E). Data are expressed as means \pm S.E.M. of three independent experiments each using six technical replicates.

Recording the basal luminescence produced by the cells in the NanoBIT complementation assay is a measure of the ligand-independent activity of the receptors. In the HEK293T cells transfected with mGlu₅-WT, the basal luminescence was significantly increased by 335.2% compared with cells

transfected with the empty vector pcDNA3 ($P < 0.0001$, two-way ANOVA) (Figure 3.7). The basal luminescence for mGlu₅-PD transfected cells, while 165.2% higher than pcDNA3 ($P < 0.0001$, one-way ANOVA), was significantly decreased by 39.1% compared to mGlu₅-WT transfected cells ($P < 0.0001$, one-way ANOVA) (Figure 3.7). Interestingly, the basal luminescence for mGlu₅-TPD was lower than that of pcDNA3, a decrease of 23.0% ($P = 0.8003$, one-way ANOVA) (Figure 3.7).

Transfecting the mGlu₅-WT receptor into HEK293T cells expressing the NanoBiT β -arrestin 2 biosensor causes an increase in ligand-independent luminescence compared to empty vector control, indicating that simply expressing the receptor causes recruitment of β -Arr2 to the cell membrane. Thus, it can be implied that mGlu₅-WT is constitutively active. Similarly, mGlu₅-PD demonstrates some constitutive activation, but this is reduced compared to mGlu₅-WT, therefore it can be inferred that C-terminal serine residues are involved in the basal recruitment of β -Arr2 to the receptor. No significant difference in basal luminescence was observed for mGlu₅-TPD compared to empty vector control, indicating both C-terminal serine and threonine residues are key for ligand-independent β -Arr2 recruitment to the plasma membrane. These data are consistent with the ligand-independent data observed in the bystander BRET-based assay; an increase in the BRET ratio pre-drug addition was observed from empty vector control to mGlu₅-WT expression, implying an increase in constitutive activity. Similar to the data from the NanoBiT assay, there was also a significant decrease in basal BRET signal with mutation of serine residues from the C-terminus, then a further decrease with the additional mutation of threonine residues. These data confirm there is an impact of C-terminal serine and threonine residues on ligand-independent mGlu₅ β -Arr2 recruitment.

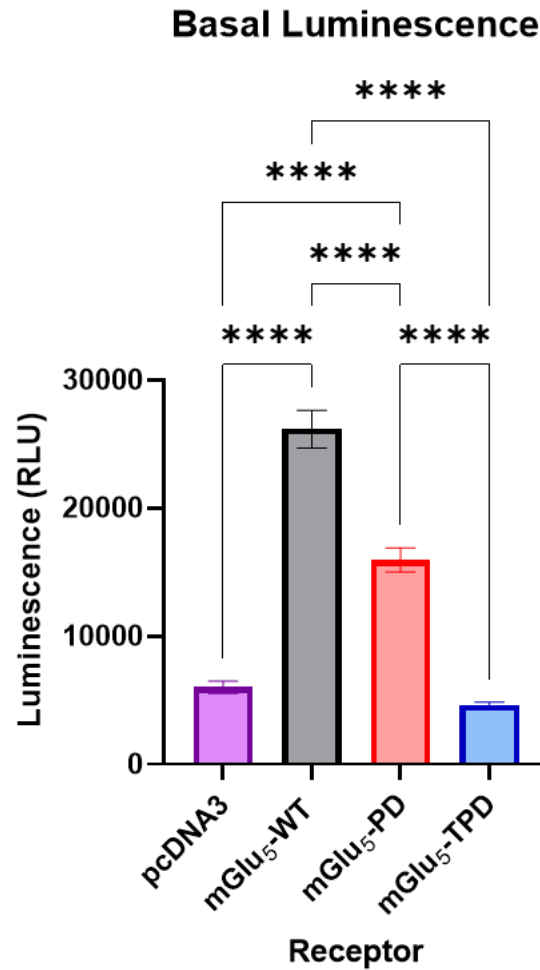


Figure 3.7: Constitutive β -arrestin 2 recruitment to mGlu₅ measured by a NanoBiT complementation assay is decreased with removal of putative C-terminal phosphorylation sites. Basal luminescence from the NanoBiT β -arrestin 2 recruitment assay for cells transfected with pcDNA3 empty vector control, mGlu₅-WT, mGlu₅-PD, and mGlu₅-TPD. Data are expressed as means \pm S.E.M. of nine independent experiments each using either three or six technical replicates. Statistical analysis was a one-way ANOVA with a Tukey post hoc test for multiple comparisons. **** P<0.0001.

3.3.4 G Protein-Coupled Receptor Kinases Play a Role in Basal and Agonist Dependent β -Arrestin 2 Recruitment to mGlu₅

G protein coupled-receptor kinases (GRKs) act as crucial mediators of GPCRs, phosphorylating active GPCRs which leads to the increased affinity for arrestins (Drube et al., 2022). Understanding how GRK activity regulates arrestin recruitment provides insights into the mechanisms of receptor desensitisation and cellular adaptation to sustained ligand stimulation. Dysregulation of GRK activity and arrestin recruitment has been implicated in various pathologies, including neurodegenerative diseases (Obrenovich et al., 2006), thus characterising the role

of GRKs in β -Arr2 recruitment permits investigation into the fundamental biology of cell signalling and the regulatory mechanisms of such. Canonically, phosphorylation of GPCRs by GRKs leads to β -Arr2 recruitment and subsequent desensitisation or internalisation, however regulation of Group I mGlu receptors by GRKs has been proposed to be phosphorylation-independent (Dhami et al., 2002). To challenge this, the phosphodeficient mutant mGlu₅ receptors were employed to explore the interplay between GRKs, phosphorylation of the mGlu₅ receptor, and β -Arr2 recruitment.

To primarily investigate the function of GRKs on mGlu₅ β -Arr2 recruitment, CRISPR/Cas9-edited HEK293 cells in which GRK2/3/5/6 were knocked out (Drube et al., 2022) were transfected with mGlu₅ receptor variants and β -Arr2 recruitment assays were performed. CRISPR/Cas9-edited HEK293 cells devoid of GRKs have previously been used to determine the roles of GRK2 and GRK3 in β -Arr2 recruitment and receptor internalisation for the rhodopsin-like μ -opioid receptor (Møller et al., 2020), demonstrating the possibility of applying this approach to mGlu₅ to reveal the role of GRKs in β -Arr2 recruitment.

The NanoBiT complementation assay was selected to measure mGlu₅ β -Arr2 recruitment. Initially, control β -Arr2 recruitment experiments were conducted in cells not transfected with mGlu₅ to provide a comparison to β -Arr2 recruitment in the GRK KO cells. This was performed in HEK293A cells, the parental cell background of the GRK KO cells. HEK293T and HEK293A cells are both derived from the human embryonic kidney (HEK) cell line, but they have a slight difference: HEK293T cells are engineered to express the SV40 large T antigen, resulting in higher transfection efficiencies and protein expression levels, whereas HEK293A cells lack this antigen. Here, parental HEK293A cells were transfected with pcDNA3 empty vector control and used in the NanoBiT complementation assay to measure any background glutamate dependant β -Arr2 recruitment in the cells (Figure 3.8A). No increase in luminescence signal was observed following treatment with glutamate, demonstrating a lack of β -Arr2 recruitment. This lack of response to glutamate in pcDNA3 transfected cells suggests that the parental cells do not express mGlu₅ (or any other glutamate family receptor) to a level where β -Arr2 recruitment is observed. Subsequently to measure the β -Arr2 recruitment to the mGlu₅ receptor, the mGlu₅-WT receptor was transfected in the parental HEK293A cells and the β -Arr2 recruitment recorded over the course of an hour.

The luminescent signal increases steadily over the time period in a concentration dependent manner (Figure 3.8B). Conversely, transfection of mGlu₅-WT in cells engineered by CRISPR to knock out expression of GRK2/3/5/6 (Drube et al., 2022), produces a kinetic profile similar to that of pcDNA3 control in response to glutamate stimulation (Figure 3.8C). Plotting these data as a concentration response curve (Figure 3.8D) demonstrate that glutamate stimulated β -Arr2 recruitment with a potency of 5.3 ± 0.10 in the parental cells, with no concentration dependent recruitment of β -Arr2 observed in the GRK2/3/5/6 KO cells. Looking at the basal luminescence, the parental cells display a 314.4% increase in basal luminescence when transfected with mGlu₅-WT compared to pcDNA3 ($P < 0.0001$, one-way ANOVA) (Figure 3.8E). It was also notable that the basal signal was substantially reduced between the parental and GRK KO cells. This was true both for cells transfected with pcDNA3, a 92.2% reduction ($P < 0.0005$, one-way ANOVA), and cells transfected with mGlu₅-WT, a 96.8% reduction ($P < 0.0001$, one-way ANOVA) (Figure 3.8E).

These data suggest that both glutamate dependent and glutamate independent β -Arr2 recruitment to the mGlu₅ receptor are dependent on GRK activity.

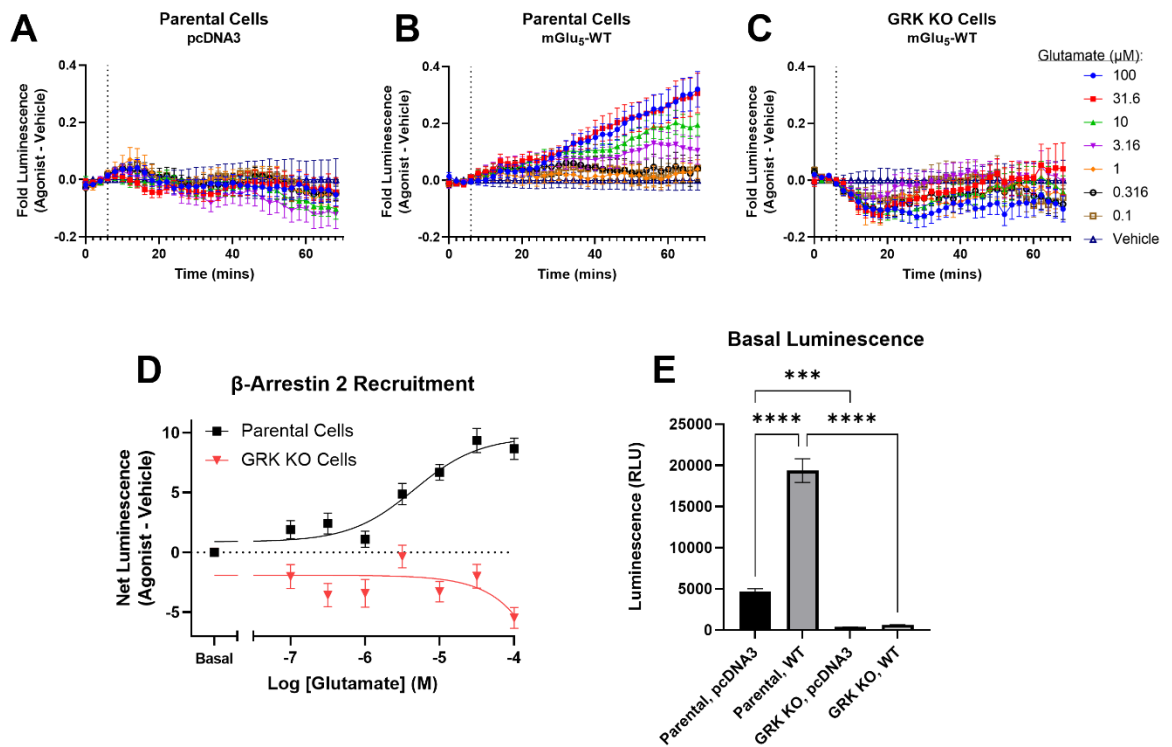


Figure 3.8: β -arrestin 2 recruitment to the mGlu₅ receptor is eliminated in GRK2/3/5/6 knockout cells. The NanoBiT bystander β -arrestin 2 recruitment assay was employed in parental HEK293A cells transfected with pcDNA3 (A) and mGlu₅-WT receptor (B); or G protein-coupled receptor kinase (GRK) 2, 3, 5, and 6 knockout (KO) cells transfected with mGlu₅-WT (C). Following a 6-minute baseline recording, the agonist glutamate was added and the kinetics of β -arrestin 2 recruitment recorded over one-hour. (D) Concentration response curve of β -arrestin 2 recruitment to both parental and GRK KO cells expressing mGlu₅-WT, calculated from the kinetic traces. (E) Basal luminescence from the NanoBiT β -arrestin 2 recruitment assay for pcDNA3 empty vector control in HEK293A and GRK KO cells, and mGlu₅-WT transfected parental and GRK KO cells. Data are expressed as means \pm S.E.M. of three independent experiments performed in triplicate. A one-way ANOVA was performed with a Tukey post-hoc test for multiple comparisons. *** $P < 0.0005$, **** $P < 0.0001$.

To validate the findings from the GRK KO model, pharmacological inhibition of GRKs was also used. Inhibitors can be employed to study the acute effects of inhibition compared with the complete genetic depletion a KO model provides. Comparing the short-term blockade with the GRK inhibitors and the chronic ablation of the KO model can outline the immediate signalling events directly regulated by GRK activity from the downstream physiological adaptations and compensatory mechanisms that may occur in response to chronic GRK deficiency. Using both approaches permits cross-validation and evaluates the robustness of the findings.

To explore the role of GRK5/6 on mGlu₅ receptor phosphorylation and subsequent β -Arr2 recruitment, a GRK5/6 inhibitor was utilised alongside mGlu₅

phosphodeficient mutants to measure β -Arr2 recruitment. Compound 19, an inhibitor of GRK5/6, was developed by Uehling et al. (2021) and here used in the NanoBiT β -Arr2 recruitment assay in the absence of agonist to measure the ligand-independent β -Arr2 recruitment to wildtype and phosphodeficient mGlu₅ receptors. Upon treatment with the vehicle (0.1% DMSO in HBSS-H), there was a decrease in basal luminescence with mutation of C-terminal serine residues and a further decrease still with mutation of C-terminal serine and threonine residues (Figure 3.9A), as seen previously (Figure 3.4C, Figure 3.7). With administration of 10 μ M of Compound 19 to inhibit GRK5/6, there was a decrease in basal luminescence for mGlu₅-WT transfected cells by 23.7% compared to vehicle treated cells ($P=0.0001$, one-way ANOVA) (Figure 3.9A). Similarly, a decrease of 29.6% was observed for mGlu₅-PD upon treatment with Compound 19 ($P=0.0004$, one-way ANOVA) (Figure 3.9A), while there was no significant effect of Compound 19 treatment in the mGlu₅-TPD basal luminescence ($P=0.2389$, one-way ANOVA) (Figure 3.9A).

Similarly, to investigate the role of GRK2/3 on mGlu₅ receptor phosphorylation and subsequent β -Arr2 recruitment, a GRK2/3 inhibitor was used in an assay measuring β -Arr2 recruitment. Compound 101 (Thal et al., 2011) was utilised to inhibit GRK2/3 and the NanoBiT assay performed to measure ligand-independent β -Arr2 recruitment to mGlu₅-WT, mGlu₅-PD and mGlu₅-TPD receptors. Once again, there was a trend of decreasing basal luminescence with mutation of C-terminal serine residues, which was reduced further upon additional mutation of threonine residues (Figure 3.9B). However, there was no significant impact of the GRK2/3 inhibitor on the basal luminescence on the β -Arr2 recruitment on any of the mGlu₅ receptors (Figure 3.9B).

Together, these data using the GRK inhibitors partially corroborate the findings from the KO studies, in that GRKs appear to play a role in the basal β -Arr2 recruitment to the mGlu₅ receptor. However, the inhibitor studies suggest that it is likely to be GRK5/6 that possesses this function. Mutation of C-terminal phosphorylation sites decreases the ligand-independent β -Arr2 recruitment, which is further reduced upon treatment with a GRK5/6 inhibitor, indicating a role for GRK5/6 in β -Arr2 recruitment.

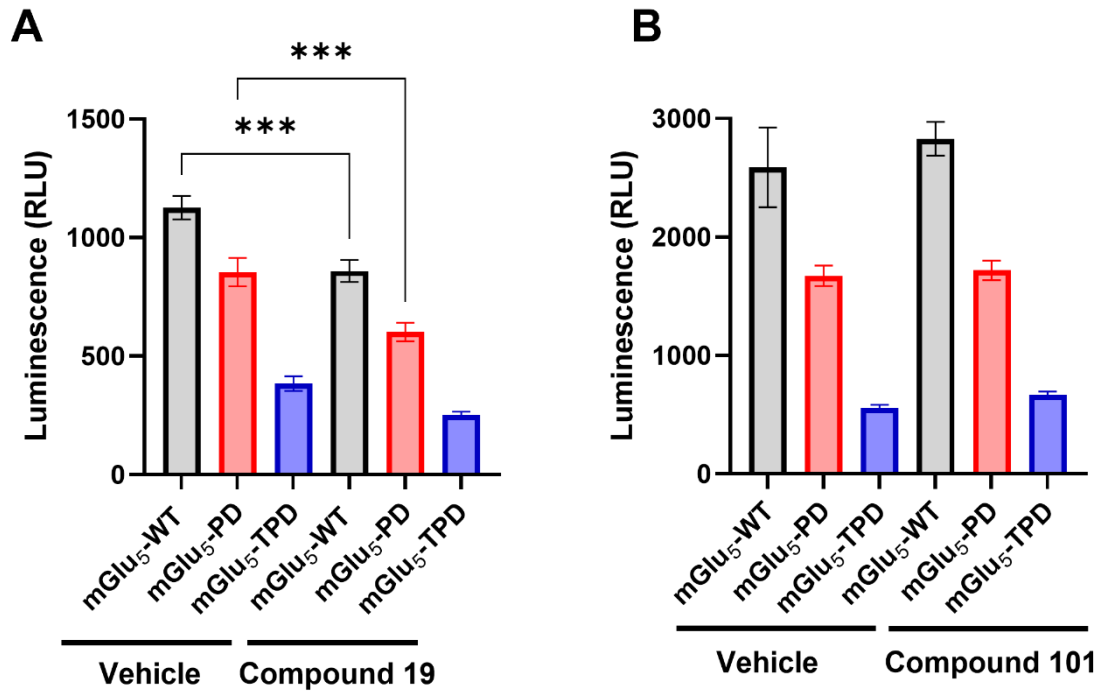


Figure 3.9: Inhibiting GRK5/6 decreases constitutive β -arrestin 2 recruitment to mGlu₅-WT and mGlu₅-PD. Basal luminescence from HEK293T cells transfected with mGlu₅-WT, mGlu₅-PD or mGlu₅-TPD in addition to the NanoBiT β -arrestin 2 complementation system. Cells were treated with 0.1% DMSO in HBSS-H (vehicle) or either 10 μ M of the GRK5/6 inhibitor Compound 19 (A), or 10 μ M of the GRK2/3 inhibitor Compound 101 (B). Data are expressed as means \pm S.E.M. of three independent experiments performed in triplicate. A one-way ANOVA was performed with a Tukey post-hoc test for multiple comparisons. *** $P < 0.0005$.

3.3.5 Mutation of mGlu₅ C-Terminal Phosphorylation Sites Does Impact Receptor Internalisation

Because I have observed that removing C-terminal phosphorylation sites reduces β -arrestin 2 recruitment, and it is known that β -arrestin 2 drives agonist dependent endocytosis of GPCRs (Ferguson et al., 1996), I aimed to determine whether agonist treatment caused endocytosis of the mGlu₅ receptor. Receptor endocytosis is a key component of GPCR desensitisation, as it removes the receptors from the cell surface thereby reducing their exposure to agonists. Additionally, internalisation of GPCRs can impact downstream signalling pathways by altering the availability of receptors at the cell surface and modulating receptor interactions with downstream effectors. Studying receptor internalisation in the context of phosphorylation provides insights into how receptor phosphorylation

contributes to the desensitisation process, shedding light on the spatial and temporal dynamics of GPCR signalling and receptor turnover.

A multitude of methods can be employed to measure receptor localisation, including biotinylation studies, radioligand binding, and fluorescence microscopy. Here, immunocytochemistry was selected to visualise the location of mGlu₅ wildtype and phosphodeficient mutant receptor constructs in the cell following administration of 100 μ M glutamate for a one-hour time period, as it was found to have recruited β -Arr2 in this time frame. The Flp-In™ T-REx™ 293 stable cell expression system was used; this option provides much more uniform expression of the receptor in the cell compared to transiently transfected cells. These cells are engineered to stably express the Flp recombinase target (FRT) site and the tetracycline repressor protein. The tetracycline repressor protein binds to tetracycline response elements present in the promoter region in the gene of interest and represses transcription in the absence of a tetracycline. To induce expression of the gene of interest at the FRT site, the cells are treated with tetracycline, or the derivative doxycycline, which binds to the tetracycline repressor protein preventing it from binding to tetracycline response elements, thereby releasing the transcriptional repression and allowing initiation of transcription of the gene of interest. This permits controlled expression of the gene; by adjusting the concentration and duration of tetracycline treatment, the expression of their gene of interest can be tightly controlled. Flp-In™ T-REx™ 293 cell lines were generated expressing mGlu₅-WT, mGlu₅-PD and mGlu₅-TPD receptor constructs, with each receptor possessing a haemagglutinin (HA) epitope tag at the C-terminus to facilitate detection.

Presently, cells were incubated overnight with 100 ng/mL of doxycycline, a concentration that produces maximal expression within the cells, to permit observation of receptor localisation within the cell. Probing the expression of the mGlu₅-WT receptor with immunocytochemical staining for the HA epitope tag indicates staining at the cell surface around the nuclei stain (DAPI) upon incubation with vehicle (HBSS-H) (Figure 3.10A). In cells stimulated with 100 μ M glutamate for one hour, the HA staining also appears to be primarily at the cell membrane (Figure 3.10A). Similarly, for both the mGlu₅-PD receptor (Figure 3.10B) and the mGlu₅-TPD receptors, the expression appears largely only at the

cell membrane (Figure 3.10C), whether treated with vehicle or endogenous agonist.

Together, this lack of change in HA staining upon agonist stimulation suggests that there is little internalisation of mGlu₅ receptor in response to agonist treatment. This is the same when looking at the phosphodeficient mutant receptors, therefore it can be inferred that phosphorylation does not impact the cellular location of the mGlu₅ receptor.

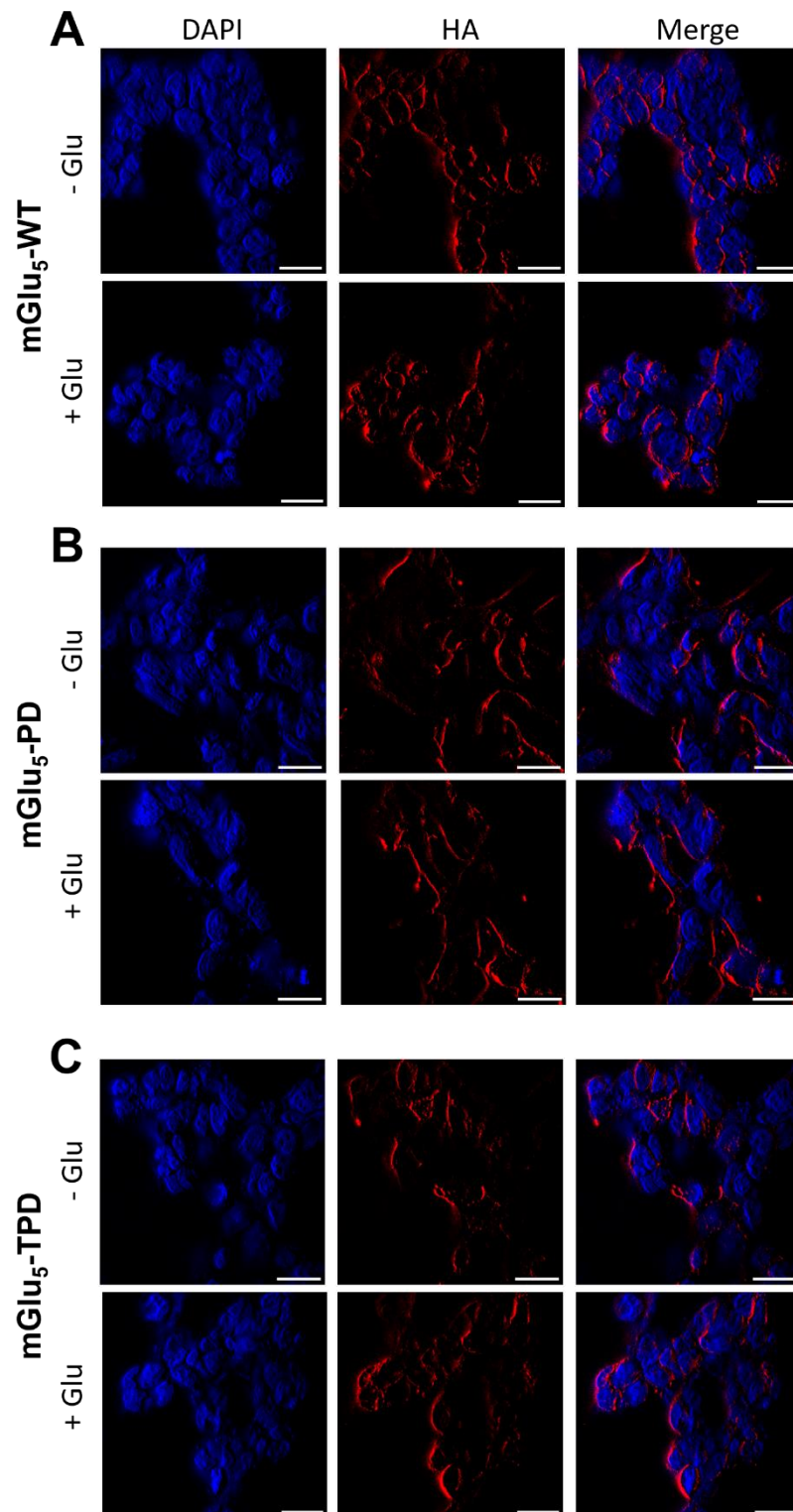


Figure 3.10: Treatment with glutamate does not alter mGlu₅ localisation. Detection of hemagglutinin (HA)-tagged mGlu₅ receptor in fixed Flp-In™ T-REx™ 293 cells treated with 100 ng/mL doxycycline overnight to induce receptor expression. Cells were treated with vehicle or 100 μM glutamate (Glu) for one hour before fixation. After fixation cells were permeabilised, nuclei were stained with DAPI (*blue*), and the receptor detected using an anti-HA antibody (*red*). Images were taken on a Zeiss Aperture Correlation Vivatome Spinning Disc Microscope with a 40X objective. The scale bar indicates 20 μm.

For a more quantitative method of measuring cell surface receptor expression, an on-cell western analysis was designed. By combining the specificity of antibody-based detection with the convenience of high-throughput analysis, it provides insights into receptor cell surface expression following agonist stimulation through detection of the receptor's N-terminal epitope tag on non-permeabilised cells.

As a positive control for this assay, FLAG-FFA4-expressing cells were treated with 10 μ M of the FFA4 agonist, TUG-891, for 30 minutes, as that is the time scale reported to cause FFA4 internalisation (Butcher et al., 2014; Hudson et al., 2013). Measuring the cell surface receptor expression via the N-terminal FLAG epitope reveals a decrease in cell surface expression of 29.3% after agonist stimulation ($P < 0.0001$, unpaired t test) (Figure 3.11A), demonstrating that this on-cell western approach is capable of measuring GPCR internalisation. The mGlu₅ expressing cell lines were treated with 100 μ M of the endogenous agonist glutamate over a time course, ranging from 0 minutes of ligand to measure constitutive internalisation, to 4 hours of ligand treatment, as it has been reported that mGlu₅ receptor recycles to the plasma membrane within 3.5 hours of internalisation (Trivedi & Bhattacharyya, 2012). The mGlu₅ receptor surface expression was then monitored using an antibody that recognises the extracellular N-terminal domain of the receptor. For the mGlu₅-WT receptor, there was the general trend of less cell surface receptor expression with agonist treatment (Figure 3.11B), however this was only significant at the 60-minute time point where the agonist stimulated cells produced an antibody signal 37.6% lower than unstimulated cells ($P = 0.0018$, mixed-model ANOVA), indicating less receptor expression at the cell surface. For the mGlu₅-PD receptor, there was no significant difference in cell surface expression between agonist stimulated and vehicle treated cell samples over the entire time course (Figure 3.11C), demonstrating a lack of receptor internalisation for this phosphodeficient mutant receptor. Similar trends were observed for the mGlu₅-TPD mutant receptor; no significant change in receptor cell surface expression was noted following agonist stimulation over the duration of the time course (Figure 3.11D).

Considering these results, these data indicate that there is little change in mGlu₅ receptor cell surface expression following agonist stimulation, corroborating the findings from the immunocytochemistry. This does not change with removal of

C-terminal phosphorylation sites, suggesting that putative C-terminal phosphorylation sites do not change internalisation.

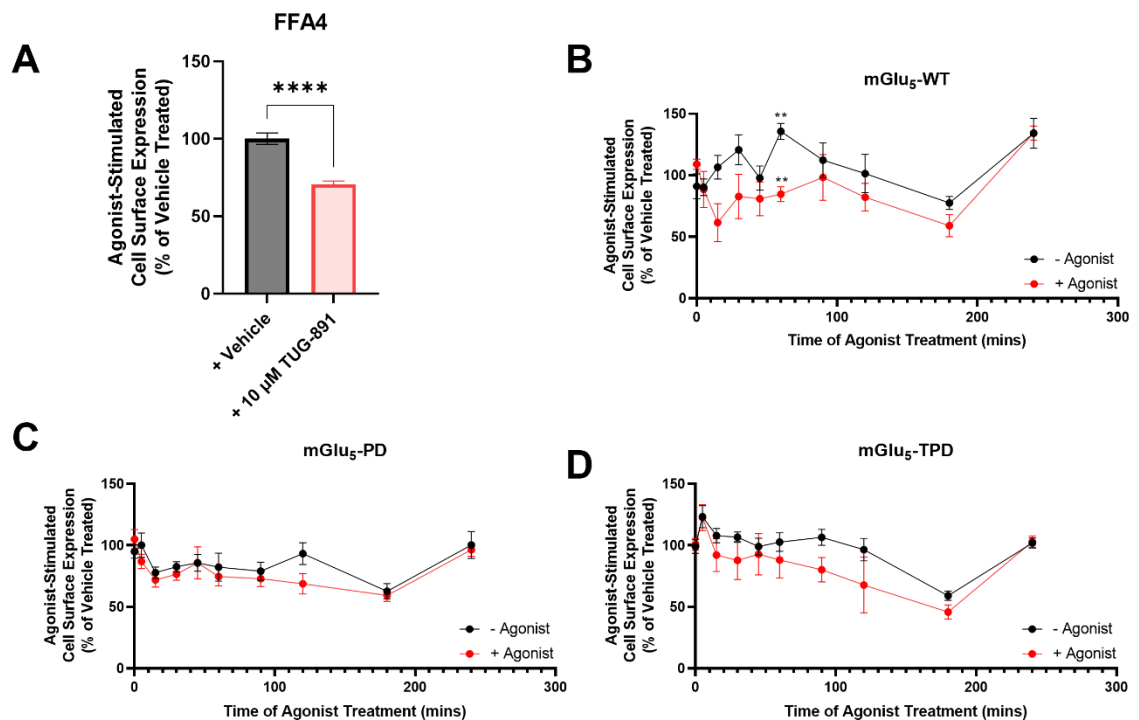


Figure 3.11: Agonist stimulation does not result in internalisation of mGlu₅-WT, mGlu₅-PD or mGlu₅-TPD. (A) Median pixel intensity quantification of on-cell western analysis using an antibody against the N-terminal FLAG epitope tag for free fatty acid receptor 4 (FFA4) to assess cell surface receptor expression following treatment with 10 μ M TUG-891 for 30 minutes. Data are expressed as the mean \pm S.E.M. of two independent experiments performed in triplicate. Statistical analysis performed was an unpaired t test. **** $P < 0.0001$. Median pixel intensity quantification of on-cell western analysis of mGlu₅-WT (B), mGlu₅-PD (C), and mGlu₅-TPD (D) using the antibody against the mGlu₅ N-terminus following treatment with either vehicle or 100 μ M glutamate. Data are expressed as the mean \pm S.E.M. of two independent experiments performed in triplicate. A mixed-model ANOVA with Šidák correction for multiple comparisons was performed. ** $P < 0.01$.

3.3.6 Validation of Novel mGlu₅ Phospho-Site Specific Antibodies

To further monitor direct mGlu₅ phosphorylation, phosphorylation site-specific antibodies were employed. This method permits investigation into the cellular conditions under which specific residues of a protein are phosphorylated, providing insight into the regulation of phosphorylation by agonist treatment. It also permits examination of specific C-terminal phosphorylation sites, as opposed to insight on global protein phosphorylation which previous methods provide, by using antibodies raised against pinpointed C-terminal putative phosphorylation sites.

To inform the generation of phosphorylation site-specific antibodies against the mGlu₅ receptor, putative phosphorylation sites were first probed. A phosphoproteomic analysis of mGlu₅ in both murine brain tissue and cells expressing wildtype mGlu₅ was performed in our laboratory, and from the LC-MS/MS analysis, a multitude of residues on the C-terminus of the mGlu₅ receptor were discovered to be phosphorylated (Table 3.1). Through collaboration with the company 7TM Antibodies (Germany), novel phosphorylation site-specific antibodies were generated based on this data from our laboratory.

Phosphorylation sites to be targeted were selected by 7TM Antibodies and novel antibodies were raised in rabbits. The resulting antibodies were against the mouse phospho-serine870/phospho-serine871/phospho-threonine874, phospho-serine1014/phospho-serine1016, and phospho-serine1037/phospho-serine1040 (Figure 3.12).

Table 3.1: Mass spectrometry and phosphoproteomics of cell and tissue samples reveals putative phosphorylation sites of the mGlu₅ C-terminus.

| SAMPLE | TREATMENT | SITE (MOUSE) |
|--|------------------|--------------|
| mGlu ₅ -WT Flp-In TM T-REx TM Cells | Vehicle | S1037 |
| mGlu ₅ -WT Flp-In TM T-REx TM Cells | Vehicle | S1173 |
| mGlu ₅ -WT Flp-In TM T-REx TM Cells | 100 μM Glutamate | S870 |
| mGlu ₅ -WT Flp-In TM T-REx TM Cells | 100 μM Glutamate | S871 |
| mGlu ₅ -WT Flp-In TM T-REx TM Cells | 100 μM Glutamate | S1014 |
| mGlu ₅ -WT Flp-In TM T-REx TM Cells | 100 μM Glutamate | S1016 |
| mGlu ₅ -WT Flp-In TM T-REx TM Cells | 100 μM Glutamate | S1037 |
| mGlu ₅ -WT Flp-In TM T-REx TM Cells | 100 μM Glutamate | S1040 |
| mGlu ₅ -WT Flp-In TM T-REx TM Cells | 100 μM Glutamate | S1173 |
| Mouse Cortex Tissue | None | S839 |
| Mouse Cortex Tissue | None | T840 |
| Mouse Cortex Tissue | None | S1014 |
| Mouse Cortex Tissue | None | S1016 |
| Mouse Cortex Tissue | None | S1037 |
| Mouse Cortex Tissue | None | S1040 |

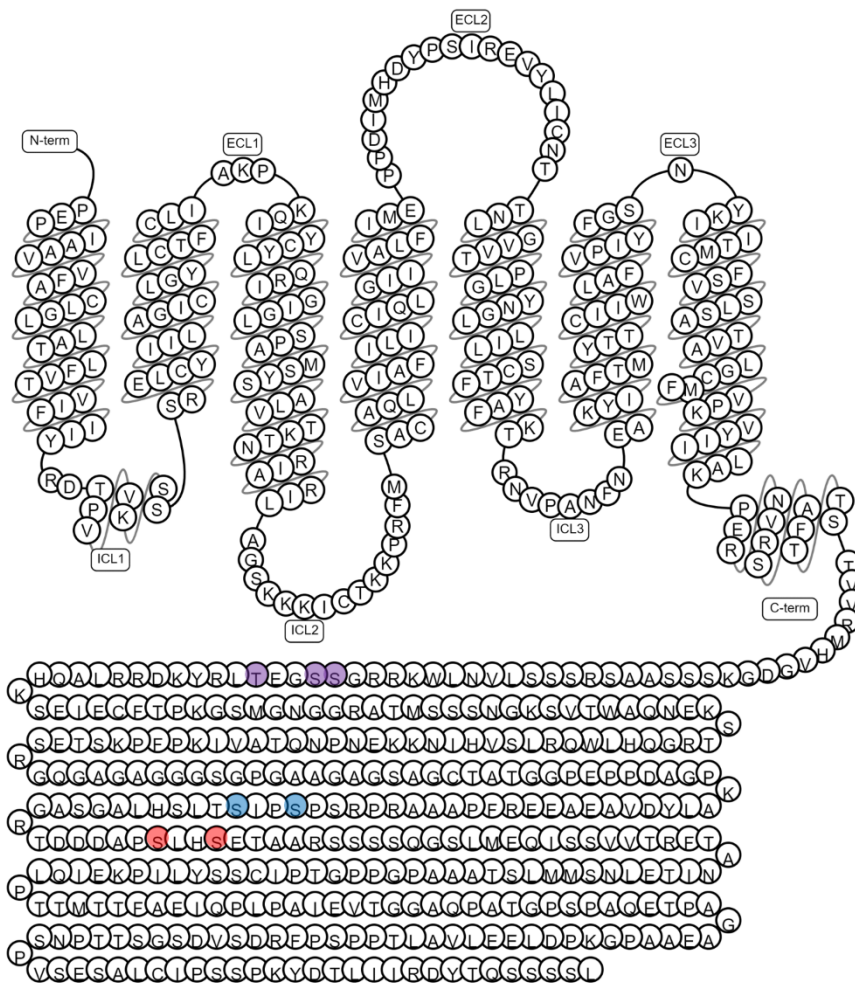


Figure 3.12: Sites in the murine mGlu₅ C-terminus used to generate novel phospho-site specific antibodies. Snake plot depicting the phospho-peptide sites identified by

mass spectrometry, then selected to be used to generate three novel antibodies against the mGlu₅ C-terminus. The antibodies were raised against phospho-serine870/phospho-serine871/phospho-threonine874 (*purple*), phospho-serine1014/phospho-serine1016 (*blue*), and phospho-serine1037/phospho-serine1040 (*red*).

In order to validate the putative phospho-site specific mGlu₅ antibodies, Flp-In™ T-REx™ 293 cells expressing murine mGlu₅-WT were utilised. A key feature of the T-REx™ system is the ability of the receptor expression to be switched on and off upon addition of doxycycline, therefore permitting measurement of phosphorylation in a variety of cellular conditions. The following cell conditions were selected to be used as samples for validating the novel antibodies: mGlu₅-WT Flp-In™ T-REx™ 293 cells where the receptor is not induced with doxycycline; cells with receptor expression maximally induced with 100 ng/mL doxycycline but treated with HBSS-H vehicle; and cells induced to express mGlu₅-WT that were treated with 100 µM of the agonist glutamate for 60 minutes.

In preliminary validation studies, the total mGlu₅ protein within as measured by SDS-PAGE and western blotting with a structural antibody targeting the C-terminus of the receptor (Figure 3.13A). No mGlu₅-WT protein expression was observed without the administration of doxycycline, while in both samples from cells treated with 100 ng/mL doxycycline overnight (one treated with vehicle and one with 100 µM glutamate), bands can be observed at ~150 kDa and at >250 kDa (Figure 3.13A). These bands are consistent with detecting the monomeric and dimeric forms of mGlu₅ respectively. The sodium-potassium ATPase protein was selected as the housekeeping protein due to its membrane localisation, similar to the receptor of interest. Bands were observed in all three samples between 75 kDa and 100 kDa, indicating there is membrane protein in all three samples.

Employing the antibody against phospho-serine870/phospho-serine871/phospho-threonine874 (pS870/S871/T874) in lysates prepared from mGlu₅-WT Flp-In™ T-REx™ 293T cells minus doxycycline, plus doxycycline treated with HBSS-H vehicle, and plus doxycycline treated with 100 µM of glutamate, a band was detected in all three samples at approximately 150 kDa (Figure 3.13B). This band, although more intense in the doxycycline treated cell samples, must be non-specific as there is no mGlu₅ expression in the minus doxycycline sample when utilising the mGlu₅ structural antibody. However, there is a band >250 kDa only in samples treated with doxycycline, consistent with the size

of band seen when using the mGlu₅ structural antibody. The intensity of this band was not affected by glutamate treatment.

Utilising the antibody against phospho-serine1014/phospho-serine1016, noted as pS1014/S1016, many bands are observed on all three samples, indicating that this antibody shows a lot of non-specific binding, and it is difficult to determine if the protein of interest is detected (Figure 3.13C).

Using an antibody against phospho-serine1037/phospho-serine1040, noted as pS1037/S1040, a band was detected at ~150 kDa in both cell samples where receptor expression was induced with doxycycline (Figure 3.13D), consistent with monomeric mGlu₅ receptor. However, the band in the vehicle treated sample had a greater intensity than the band in the agonist-stimulated sample. It could be implied that the presence of a band in both receptor induced samples indicates that mGlu₅-WT is phosphorylated at residues S1037 and S1040, with phosphorylation predominantly occurring under basal conditions. Additionally, a band was observed >250 kDa only in the doxycycline treated samples, consistent with the dimeric form of the receptor. In contrast to the ~150 kDa bands, the intensity of the >250 kDa bands are equivalent minus and plus agonist stimulation.

These validation studies are only qualitative and only from a single replicate, thus assumptions about the validity of the findings cannot be conclusive. However, in general these initial antibody validation studies indicate these antibodies may not be suitable for use on cell lysates due to the level of non-specific binding.

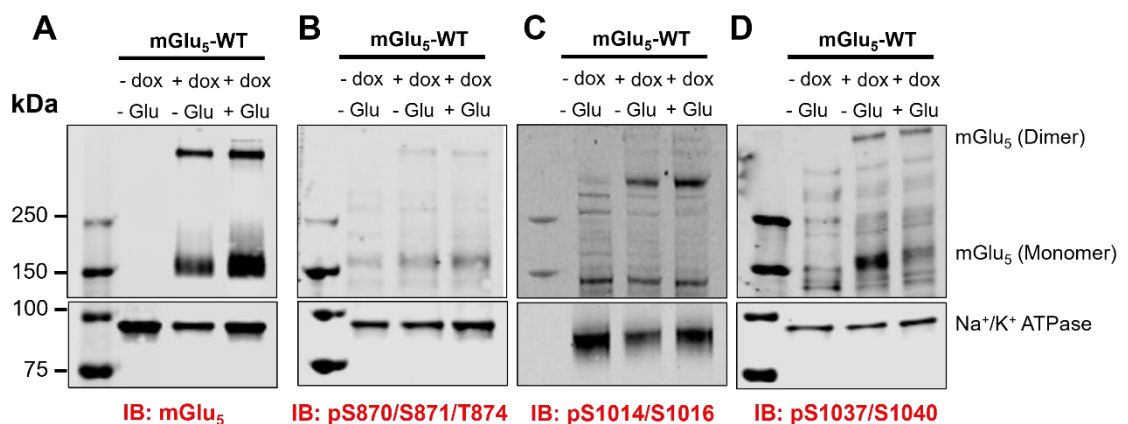


Figure 3.13: Novel phospho-site specific antibodies against mGlu₅-WT reveals basal receptor phosphorylation. Lysates were prepared from Flp-In™ T-REx™ 293T cells with and without inducible expression of mGlu₅-WT using doxycycline (dox), stimulated with either vehicle or 100 μM glutamate (Glu). These samples were probed for total mGlu₅ receptor (A), an antibody against phospho-serine871/phospho-serine872/phospho-threonine875 (B), antibody against phospho-serine1018/phospho-serine1020 (C), and an

antibody against phospho-serine1041/phospho-serine1044 (D). The sodium-potassium ATPase protein was used as the housekeeping control. Western blots shown from a preliminary study using the phospho-site specific antibodies (n=1).

Here, immunoprecipitation for the HA epitope tag was utilised in an attempt to remove the non-specific binding of the phospho-site specific antibodies seen when using cell lysates, and to further validate the novel antibodies in their ability to detect phosphorylated mGlu₅. Immunoprecipitation of the receptor to facilitate detection with phospho-site specific antisera has previously been carried out for GPR84, where cell samples were enriched via GFP-trap then SDS-PAGE western blots performed utilising phospho-site specific antisera, hereby demonstrating successful detection of bands consistent with the receptor of interest that were not detected with crude lysates (Marsango et al., 2022).

The mGlu₅ wildtype construct has a C-terminal HA epitope tag, thus to investigate the target specificity of these novel antibodies, immunoprecipitation for the HA epitope tag was performed followed by western blotting with the phospho-site specific antibodies. Lysates were prepared from samples as above, with the addition of a HBSS-H (vehicle)-treated sample and agonist (100 μ M glutamate)-treated sample with Lambda protein phosphatase (λ -PP) treatment. λ -PP was applied to the cell samples in order to remove phosphorylation on serine, threonine, and tyrosine residues within a protein, thus can be utilised to demonstrate that the antibody is specifically detecting phosphorylated receptor.

After immunoprecipitating and western blotting for the mGlu₅ receptor, the total receptor protein expression was assessed using a structural mGlu₅ antibody (Figure 3.14A). Bands were observed at ~150 kDa and >250 kDa in all samples where receptor expression was induced with doxycycline, indicating successful immunoprecipitation and detection of mGlu₅. Furthermore, no difference in band intensity is observed following treatment with λ -PP, confirming that this treatment has not led to any degradation of the mGlu₅ receptor.

Measuring phosphorylated S870/S871/T874 residues subsequent to receptor purification did not produce any protein expression bands in any of the samples evaluated (Figure 3.14B), in contrast to the results seen when employing this phospho-site specific antibody in cell lysates. This may suggest that the bands observed in the lysate experiments were non-specific and not detecting the mGlu₅ protein. Similarly, there were no bands observed when western blotting with the

pS1014/S1016 antibody after immunoprecipitation for the HA-epitope tag (Figure 3.14C). In contrast, bands were observed at molecular weights consistent with both monomeric (~150 kDa) and dimeric (>250 kDa) mGlu₅ using the pS1037/S1040 antibody (Figure 3.14D). Quantification revealed a 5.7% increase in intensity of detection of the mGlu₅ dimer compared to mGlu₅ monomer in the vehicle treated sample, and a 42.2% increase in intensity of the mGlu₅ dimer compared to mGlu₅ monomer in the glutamate treated sample. From vehicle to glutamate treated samples, there was a 71.7% increase in intensity of the monomeric form of mGlu₅ and a 131.1% increase in the dimer intensity. Critically, treatment of samples with λ-PP largely eliminated both bands corresponding to the monomer and the dimer, indicating that this antibody is indeed specific to phosphorylated residues.

The validation of these novel phosphorylation-site specific antibodies is crucial for ensuring the accuracy and reliability of utilising these tools. Here, it is highlighted through systematic investigation that several of these antibodies fail to detect specific phosphorylated residues within the mGlu₅ C-terminus; only the antibody against pS1037/S1040 appears to detect agonist mediated phosphorylation of mGlu₅.

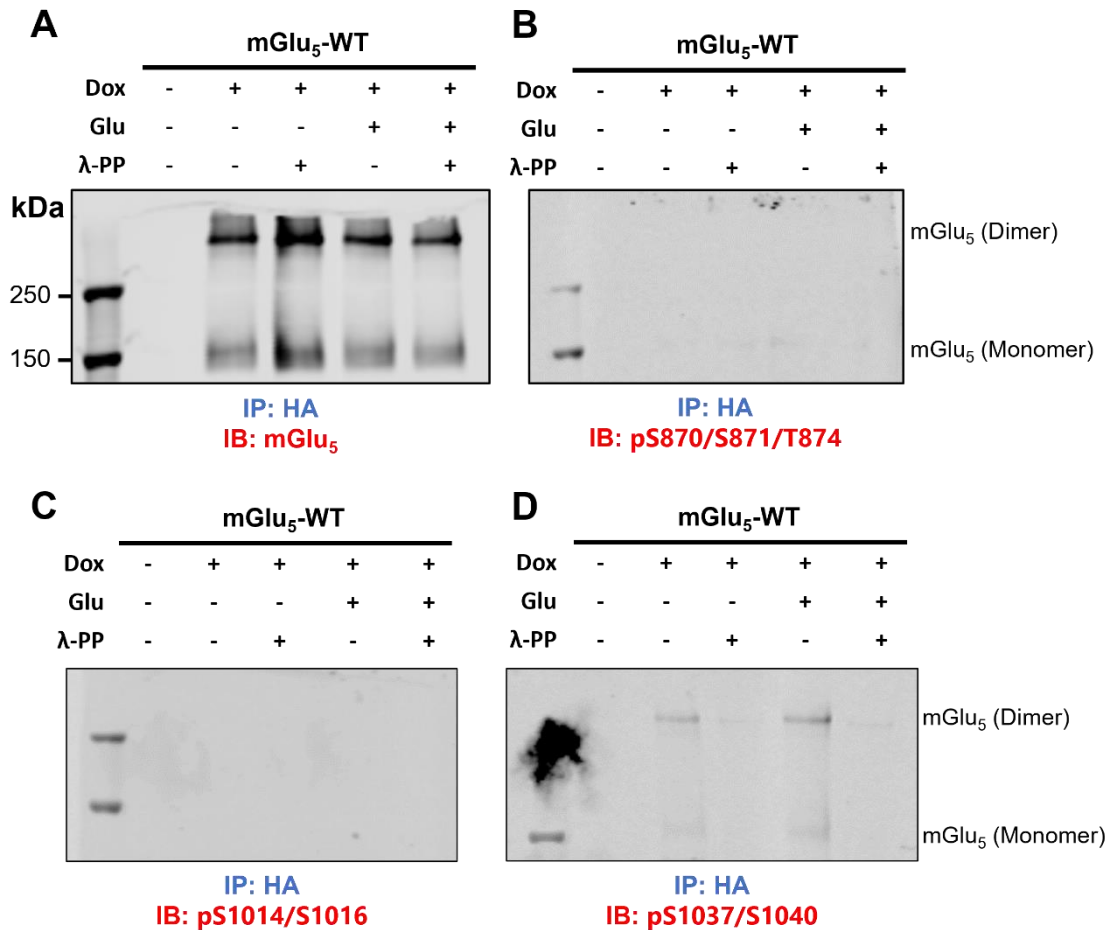


Figure 3.14: Immunoprecipitation of mGlu₅-WT receptor reveals phosphorylation of Serine1041 and Serine1044 residues. Lysates were prepared from Flp-In™ T-REx™ 293 cells with and without inducible expression of mGlu₅-WT with 100 ng/mL doxycycline (dox), treated with either vehicle or 100 μM glutamate (Glu). All the samples were immunoprecipitated with anti-HA beads, then some samples were treated with Lambda protein phosphatase (λ-PP) to remove phosphate groups. Samples were separated by SDS-PAGE then western blotting using a total mGlu₅ receptor antibody (A), an antibody against phospho-serine871/phospho-serine872/phospho-threonine875 (B), an antibody against phospho-serine1018/phospho-serine1020 (C), and an antibody against phospho-serine1041/phospho-serine1044 (D). Western blots shown from a preliminary study using the phospho-site specific antibodies (n=1).

3.4 Discussion

Here, I set out to assess the ability of wildtype and phosphodeficient mutant mGlu₅ receptors to recruit β -arrestin 2, elucidate the involvement of G protein receptor kinases in this process, and validate novel phospho-site specific antibodies in order to profile direct mGlu₅ receptor phosphorylation. Mutation of C-terminal putative phosphorylation sites of the M1 muscarinic and mGlu₅ receptor demonstrated a reduced capacity to recruit β -Arr2 in comparison to wildtype receptor. For mGlu₅, this reduction in β -Arr2 recruitment was shown to be dependent on GRKs, specifically GRK5/6. Investigations into receptor internalisation demonstrated no impact of receptor phosphorylation on the ability of the receptor to internalise. As an alternative method to measure receptor phosphorylation, phospho-site specific antibodies were validated concluding that antibodies against pS870/S871/T874 and pS1014/S1016 were not specific to phosphorylated mGlu₅, whereas an antibody against pS1037/S1040 demonstrated phospho-site specificity to mGlu₅.

A common method to investigate GPCR phosphorylation involves mutation of putative phosphorylation sites, or truncation of the C-terminus of the receptor, to generate phosphorylation-deficient mutant versions of the receptor. These constructs are then employed in pharmacological assays to determine the physiological impact of receptor phosphorylation through comparison of the physiology to wildtype receptor. Studies generating phosphorylation-deficient mutant GPCRs have been performed on, but not limited to, the M3 muscarinic receptor (Bradley et al., 2016), the FFA4 receptor (Butcher et al., 2014), and the μ -opioid receptor (Kliwer et al., 2019). Studies on the M3 receptor generating a genetically engineered mouse expressing a phosphodeficient M3 receptor assisted in teasing out the physiological impact of phosphorylation dependent pathways versus G protein dependent pathways, concluding that a ligand that shows stimulus bias towards arrestin signalling preferentially engages pathways leading to promotion of learning and memory, regulation of bronchoconstriction, and change in insulin secretion (Bradley et al., 2016). It has been well established that β -Arr2 plays an important role at the μ -opioid receptor, with genetic ablation of arrestins leading to sustained analgesic effects (Bohn et al., 1999). This has led to the development of a novel G protein-biased ligand, giving no detectable receptor internalisation, low GRK-mediated receptor phosphorylation, and low β -Arr2

recruitment demonstrating an improved therapeutic index (Chen et al., 2013). Studies by Butcher et al., (2014) noted that a C-terminal truncation of the FFA4 receptor had limited capability to recruit β -Arr2, with no impact on the G protein-coupled receptor pathway activation. Together, these works highlight the importance of studying the phosphorylation dependent versus G protein dependent transduction pathways to inform drug design and promotion of specific GPCR transduction pathways for clinical efficacy.

Initially, this chapter set out to examine the coupling of β -Arr2 to the M1 muscarinic receptor, a rhodopsin-like GPCR. The M1 receptor is a well-researched and validated target in the search for treatments for neurodegenerative diseases (Bradley et al., 2017, 2020; Conn et al., 2009; Davie et al., 2013). This provides an appropriate positive control for the mGlu₅ receptor, as both the M1 and mGlu₅ receptors are coupled to the G $\alpha_{q/11}$ protein-coupled pathway and have widespread expression in the brain with involvement in an array of neuropathologies.

Phosphorylation of the M1 receptor occurs in the third intracellular loop and in the C-terminal tail (Butcher et al., 2016). Typical of GPCRs, after phosphorylation of these sites, β -Arr2 is recruited, then mediates desensitisation by uncoupling G proteins and facilitating internalisation of the receptor. To dissect out and profile the phosphorylation dependent signal transduction pathways of the M1 receptor, a phosphorylation-deficient mutant M1 receptor (M1-PD) was genetically engineered through mutation of serine residues in the intracellular surface of the receptor. Here, previous findings on β -Arr2 recruitment to the M1-WT and M1-PD receptors (Bradley et al., 2020) were confirmed; removal of the M1 receptor intracellular serine residues reduces, but does not entirely eliminate, β -Arr2 recruitment to the receptor. This was replicated in a primary neuronal cell model from knock-in mice expressing M1-PD at the gene locus of the wildtype M1 muscarinic receptor, replicating the *in vitro* finding of reduced β -Arr2 to the M1-PD receptor. These data indicate that M1 phosphorylation is a key event in the agonist-dependent recruitment of β -Arr2 to the cell membrane, but the recruitment mechanism is not completely disrupted with the removal of intracellular serine residues. The retained β -Arr2 recruitment to the M1-PD receptor was agonist-dependent, implying the presence of further intracellular residues that may be phosphorylated.

This phosphodeficient M1 receptor consists solely of serine mutations to alanine, however alternative residues that are able to be phosphorylated (such as threonine or tyrosine residues) are still present, thus it cannot be definitely determined that phosphorylation is completely eliminated in this mutant receptor. Serine residues possess a small side chain with a hydroxyl group attached to a single carbon atom, whereas threonine has a larger side chain with a hydroxyl group attached to a secondary carbon atom. Serine residues are preferentially phosphorylated over threonine residues (Olsen et al., 2006), commonly due to bias in kinases and phosphatases which favourably phosphorylate serine residues and dephosphorylate threonine residues at a faster rate than serine residues (Pandey et al., 2023). This may be due to difference in structure, with the methyl group on the threonine residue providing additional steric hindrance. There is evidence for significant evolutionary conservation of serine and threonine residues in mammals, yet both have exhibited different rates of evolutionary change; the rates of phosphorylated serine residues have remained at a steady rate, whereas the human lineage has gained more phosphorylated threonine residues over time (Chen et al., 2010). The high frequency and lack of change in serine phosphorylation suggests a more conserved regulatory mechanism, yet conversely the historical change in threonine phosphorylation suggests a finely tuned mechanisms for regulating protein functions. This differential physiological impact between serine and threonine residue phosphorylation has recently been defined: serine phosphorylation typically induces smaller, regulatory-like changes, compared to threonine phosphorylation which promotes larger, function-like switches in proteins (Pandey et al., 2023).

Further work on the phosphodeficient M1 muscarinic receptor demonstrated that the M1 receptor exerts an inherent neuroprotective activity that is dependent on its phosphorylation status (Scarpa et al., 2021). This implies that M1 receptor-mediated adverse responses can be minimised by ensuring ligands targeting the receptor maintain phosphorylation-dependent signalling. To inform the strategy to monitor mGlu₅ receptor phosphorylation, two phosphodeficient mutants were generated: mGlu₅-PD, in which solely C-terminal serine residues were mutated to alanine, akin to the M1-PD receptor; and mGlu₅-TPD in which C-terminal serine and threonine residues were mutated to alanine. This permits the comparison of the differential downstream physiological impact of both serine and threonine phosphorylation, which was not previously studied for the M1 muscarinic receptor.

Eventually, such as with the M3 and μ -opioid receptors, dissecting out these phosphorylation dependent signal transduction pathways may inform drug development and clinical targeting of the mGlu₅ receptor.

Subsequent to generating stable cell lines expressing either the wildtype or two phosphodeficient mGlu₅ mutant receptors, β -Arr2 recruitment to the receptor was measured to explore the role of C-terminal serine and threonine residues in this process. To measure this recruitment, bystander-BRET and split luciferase assays were employed. Split luciferase assays are robust and well characterised and there exists a wide range of luciferase enzymes to select with each having a unique character, wavelength of luminescence, intensity, stability, and substrate (Hattori & Ozawa, 2014). Dixon et al. (2016) developed a novel technology using nanoluciferase, termed nanoluciferase binary technology (NanoBiT). This small but bright luciferase produces stable and sustained luminescence, advantageous for a protein complementation assay. The fragmented reporter for the complementation assay was designed to produce quantifiable signals within living cells at relevant temperatures and concentrations to replicate physiological conditions and to have marginal impact on the association kinetics of the proteins of interest (Dixon et al., 2016). NanoBiT is comprised of 18 kDa nanoluciferase fragment (LargeBiT) and a 1.3 kDa fragment (SmallBiT), optimised for high stability and expression levels to measure physiologically relevant cellular conditions, reporting efficiently even weak protein-protein interactions due to the low intrinsic affinity between the complementary fragments (Dale et al., 2019). Interaction between the tagged proteins of interest results in the assembly of the functional enzyme, leading to luminescence emission upon substrate addition.

The NanoBiT complementation system has been used to measure $G\alpha_q$ activation (Littmann et al., 2018), dimerisation (Norisada et al., 2018), and internalisation (Soave et al., 2020). The split luciferase NanoBiT system was optimised for β -Arr2 recruitment by Pedersen et al., (2021) and has since been used to study β -Arr2 recruitment to an array of rhodopsin-like GPCRs (Janetzko et al., 2022). In this thesis, the bystander NanoBiT system was employed to study β -Arr2 recruitment to the cell membrane of metabotropic glutamate receptor expressing cells. The NanoBiT β -Arr2 recruitment assay produced a small agonist-dependent signal window for the wildtype glutamate receptor in comparison to the rhodopsin-like GPCR FFA4, indicating a less robust coupling to the arrestin-

mediated signal transduction pathway. Abreu et al., (2021) reported little to no β -Arr2 recruitment by group I mGlu receptors, but here the data demonstrates mGlu₅-WT is capable of recruiting β -Arr2 to the cell surface. However, this recruitment occurs on a much longer timescale than rhodopsin-like GPCRs; receptors such as the M1 muscarinic receptor typically recruit β -Arr2 over a course of 30 minutes (Scarpa et al., 2021), however here it demonstrated mGlu₅-WT receptor recruits β -Arr2 steadily over the course of one hour. Further evidence for mGlu₅ coupling to β -Arr2-mediated signalling pathways has been reported, including evidence that genetic deletion of β -Arr2 results in deficits in neuronal plasticity by mGlu₅ receptors in CA1 pyramidal neurons (Eng et al., 2016) and that β -Arr2 mediates mGlu₅-driven synaptic protein synthesis in the hippocampus (Stoppel et al., 2017), indicating that mGlu₅ is able to functionally couple to β -Arr2.

When utilising the phosphodeficient mutant receptors in the NanoBiT β -Arr2 recruitment assay, there was a negative impact on β -Arr2 recruitment. No change from wildtype receptor to mGlu₅-PD was observed in the NanoBiT setup, yet an elimination of β -Arr2 recruitment to the mGlu₅-PD receptor was observed in the BRET-based system. Additionally, mutating both C-terminal serine and threonine residues eliminated β -Arr2 recruitment in the BRET-based assay but only reduced the maximal response in the NanoBiT complementation assay. Together, these data support the hypothesis that β -Arr2 recruitment is a process dependent on phosphorylation of C-terminal serine and threonine residues. The recruitment of β -Arr2 to the mGlu₅-PD receptor could be due to threonine residue phosphorylation, or due to phosphorylation of regions on the receptor other than the C-terminus such as the ICLs. Activating the receptor with agonist stimulation induces a conformational change, which exposes ICLs. Multiple serine and threonine residues within ICL1 (Thr606, Ser613) and ICL2 (Thr665, Thr681) of mGlu₅ have been identified as sites of phosphorylation by PKC, mediating receptor desensitisation (Gereau IV & Heinemann, 1998), thus phosphorylation of these residues may additionally play a role in β -Arr2 recruitment.

Whilst both BRET and NanoBiT have been used to study protein-protein interactions, both have distinct features. The principle of BRET relies on the transfer of energy from a bioluminescent donor molecule to a fluorescent acceptor molecule when they are in close proximity, typically 10-100 nanometres. The advantage of using BRET includes the ability to monitor protein-protein interactions in real time and high fidelity in living cells. BRET offers high sensitivity,

detecting subtle changes in protein localisation, however for mGlu₅ this signal window was not large enough. Therefore, the NanoBiT system was optimised for mGlu₅. The luciferase has a much smaller size in comparison to the donor and acceptor molecules required for BRET, decreasing the risk of steric hinderance and disruption of the proteins of interest. Although theoretically straightforward, split luciferase reporters may hinder the natural properties of the proteins they are tagged to, however this is also a consideration in the BRET assay setup. The inherent binding affinity of the luciferase fragments could bias the characteristics of the tagged protein of interest, and complementation binding could obscure the temporal dynamics of the interaction of the proteins of interest (Dixon et al., 2016). Despite this, the nanoluciferase fragments have high affinity for one another and the high sensitivity and application to live-cell assays make this system advantageous for high-throughput assays and applicable for monitoring protein-protein interactions with excellent temporal kinetics.

The difference in results seen for the phosphodeficient mutant receptors between the NanoBiT versus BRET assay setup may be explained by the sensitivity of the assays; NanoBiT assays typically offer higher sensitivity than conventional BRET. NanoBiT relies on the strong, stable signal produced by the reconstitution of the luciferase enzyme, while alternatively BRET relies on the efficiency of the resonance energy transfer. The conformation of the receptor and its interacting partners can affect the performance of both assays differently; in a BRET assay, conformational changes might disrupt the optimal distance and orientation needed for energy transfer, whilst in the NanoBiT system, these changes might still allow for reconstitution of the luciferase enzyme if the subunits are brought close enough. Here, the modifications of the receptor resulting in the mGlu₅-PD and mGlu₅-TPD receptors may be impacting the sensitivity of the BRET assay, preventing efficient resonance energy transfer thus minimal detectable BRET signal is produced with these receptors.

NanoBiT and BRET-based systems can also be utilised to look at receptor internalisation through the tagging of intracellular compartments with the detection proteins. This provides a more sensitive assay to probe receptor localisation than immunocytochemical methods, which are commonly selected to probe agonist-induced internalisation of GPCRs. Receptor phosphorylation and subsequent recruitment of β -arrestins has been shown to be key for desensitisation and internalisation of GPCRs (Dhami & Ferguson, 2006). The mGlu₁ receptor has

been shown to be internalised in a predominantly β -arrestin mediated manner (Mundell et al., 2004), however the internalisation mechanisms for mGlu₅ are conflicting; internalisation of mGlu₅ can occur in both clathrin-dependent (Bhattacharya et al., 2004) and clathrin-independent pathways (Fourgeaud et al., 2003). In ICC studies performed here, no receptor internalisation was observed for wildtype or phosphodeficient mutant mGlu₅ receptors. Despite performing on-cell western analyses of cell surface receptor expression for a more quantitative measure of internalisation, still no mGlu₅ receptor internalisation was noted.

It has been shown that mGlu₅ can internalise, with the internalisation being dependent on both conventional and novel PKC isozymes (van Senten et al., 2022) and even having pathological implications such as acting as a mediator for persistent neuropathological pain (Vincent et al., 2016). However, these studies listed here evidencing mGlu₅ internalisation have been performed on the mGlu_{5a} isoform, and the mGlu_{5b} isoform was utilised in this thesis. There is a subtle change in the receptor sequence, just a 32 amino acid insertion at the proximal end of the C-terminus just after TMD7, and although no functional differences have been reported between these two isoforms this may provide a novel explanation to the differences in internalisation observed.

The NanoBiT and BRET data demonstrate that β -Arr2 is recruited to the mGlu₅ receptor, however internalisation studies performed here do not exhibit any obvious receptor internalisation. Despite several studies showing that mGlu₅ is able to internalise (Trivedi & Bhattacharyya, 2012), the results in this work corroborate the findings from Abreu et al. (2021), where it was determined that mGlu₅ internalisation is not observed, whether that be arrestin-mediated, GRK-mediated, or constitutive. These data posit one question: if a receptor can recruit arrestins but doesn't appear to internalise, what might be happening?

Some receptors may activate downstream signalling pathways through β -arrestins without being internalised, indicating a role for β -arrestins beyond endocytosis. It has been demonstrated that there is a lack of β -arrestin signalling in the absence of active G proteins (Grundmann et al., 2018), indicating the existence of some kind of G protein/ β -arrestin complex. Sequestered β -arrestins can further recruit other proteins such as phosphatases, GTPases, and adaptor proteins, forming various signalosomes that regulate cellular activities (Jean-Charles et al., 2017). There is evidence that β -arrestin 2 mediates protein synthesis in the hippocampus and genetically reducing β -arrestin 2 corrects the

pathologies in cognition seen in FXS (Stoppel et al., 2017), thus β -arrestin 2-biased ligands acting at mGlu₅ could be promising as a therapeutic strategy for FXS. The importance of β -arrestin 2 signalling has been noted for the mGlu₁ receptor; mGlu_{1a} receptor protective signalling through MAPK and sustained phosphorylation of ERK is mediated by a G protein-independent pathway, with this sustained signalling requiring the expression of β -arrestin 2 (Emery et al., 2010). Furthermore, studies by Alvarez-Curto et al., (2016) using a phospho-deficient FFA4 receptor resulted in enhanced pERK1/2 signalling which was eliminated in β -Arr2-null cell lines. To investigate this for mGlu₅, pERK assays could be performed on the wildtype and phosphodeficient receptor mutant cell lines to determine what is happening downstream of the receptor in terms of ERK phosphorylation and the role direct receptor phosphorylation plays. Scarpa et al. (2021) performed pERK assays on the M1 wildtype and M1-PD receptors, exhibiting no significant differences between the two receptors indicating that C-terminal serine residues do not play a role in ERK phosphorylation.

Another potential explanation for the observed β -arrestin 2 recruitment to the receptor but lack of endocytosis could be due to phosphorylation barcoding. The concept of phosphorylation barcodes defines the pattern and extent of receptor phosphorylation by kinases which influence β -arrestin recruitment and subsequent receptor fate. Different phosphorylation patterns can dictate whether β -arrestin promotes receptor internalisation or remains at the plasma membrane, such as seen with the β 2-adrenergic receptor (Nobles et al., 2011), the chemokine receptor CXCR3 (Eiger et al., 2023), and the vasopressin receptor (Dwivedi-Agnihotri et al., 2020). When quantitatively mapping phosphorylation sites on the β 2-adrenergic receptor in response to stimulation with an unbiased agonist, isoproterenol, and a β -arrestin biased ligand, carvedilol, it was shown that of the 13 C-terminal sites phosphorylated in response to isoproterenol, only 2 are phosphorylated in response to carvedilol (Nobles et al., 2011), indicating that the pattern of receptor phosphorylation sites establishes a barcode that determines the conformation of β -Arr2 and subsequently its functional outcomes. To examine this for the mGlu₅ receptor, site-directed mutagenesis could be performed then the constructs used in functional β -arrestin recruitment studies to examine the impact of different combinations of phosphorylation of residues impacts the recruitment of arrestins.

Finally, β -arrestin 2 may be acting as a scaffold to facilitate interactions between the GPCR and other proteins. A receptor might recruit β -arrestin but remain at the cell surface due to interactions with anchors, docking proteins and adaptors that stabilises the receptor at the plasma membrane. Homer proteins are known to secure mGlu₅ at the cell surface, counteracting the internalisation process promoted by β -arrestins. It has been shown that cooperation between Homer1b and Shank scaffolding proteins leads to accumulation of mGlu₅ in synapses (Roche et al., 1999; Tu et al., 1999). This is a key interaction, as the disruption of mGlu receptor and Homer complexes has been implicated in Fragile X syndrome (Giuffrida et al., 2005), addiction (Szumlinski et al., 2004), and schizophrenia (Spellmann et al., 2011). Additionally, it has been shown that α -Actin-1, a major cross-linking protein, interacts with mGlu_{5b}; the levels of mGlu_{5b} receptor present at the cell surface is increased 4-fold when co-expressed with α -Actin-1 in HEK293 cells and also in cultured neurons of the rat striatum (Cabello et al., 2007). Here, the mGlu_{5b} isoform is used, thus it could be being held at the plasma membrane by this α -Actin-1 protein, preventing internalisation. To examine this scaffolding of the mGlu₅ receptor, co-immunoprecipitation experiments could be performed to examine the scaffolding proteins that form complexes with the receptor and this implication for interactions with β -arrestin proteins.

High constitutive activity was demonstrated in the exploration into the roles of GRKs in mGlu₅ signalling. The basal β -Arr2 recruitment in the parental HEK293A cells increases after overexpression of the mGlu₅-WT receptor, whereas there is a decrease seen in the GRK KO cells overexpressing the wildtype receptor. This implies that GRKs are required for mGlu₅-mediated β -Arr2 recruitment, but it cannot be determined if GRKs are required for constitutive activity of the receptor. Even the pcDNA3 transfected cells demonstrated a decrease in β -Arr2 recruitment when comparing parental HEK293A cells to the GRK KO cells, potentially explained by constitutive β -Arr2 recruitment by endogenous GPCRs within the cells (see (Attwood & Findlay, 1994) for a list of endogenously expressed GPCRs). It is known that Homer proteins can control the constitutive activity of mGlu receptors through scaffolding to IP₃ receptors on the endoplasmic reticulum (Fagni et al., 2003), which may be occurring here. Additionally, previous studies have shown that mutation of specific residues in the allosteric binding domain of mGlu receptors results in conformational changes and

modulates the constitutive activity of the receptor (Yanagawa et al., 2009), providing a 'switch' for constitutive activity.

Antibodies specific to phosphorylated GPCRs have historically been used to further dissect the conditions under which receptor phosphorylation occurs. Here, phospho-site specific antibodies against the mGlu₅ C-terminus were validated. The phospho-specificity and agonist dependence for three novel phospho-site specific antibodies was examined through western blotting of both total cell lysate and immunoprecipitated cell samples. In order to validate these phosphorylation site specific antibodies, several questions need to be addressed: Is the antibody specific to the receptor? Is the antibody phosphorylation site-specific? Is the phosphorylated receptor detected because it is constantly phosphorylated, or constitutively active and therefore phosphorylated?

The first of these questions was addressed here: the antibodies were first tested in lysates from cells expressing the mGlu₅ receptor to see if they can detect protein, then in immunoprecipitated samples to see if the protein the antibodies detect is the protein of interest. It was found that antibodies against pS870/S871/S874 and pS1014/S1016 did not detect any protein following immunoprecipitation for the mGlu₅ receptor, however the antibody against pS1037/1040 detected protein consistent with the mGlu₅ monomer and dimer subsequent to immunoprecipitation.

To address the second unknown question on phospho-specificity, samples were treated with λ -PP to remove phosphorylation on amino acid residues. If the antibody is phosphorylation site specific, it is predicted that there will be no bands observed in samples treated with λ -PP. This was undetermined for antibodies against pS870/S871/S874 and pS1014/S1016, however it was concluded that the antibody against pS1037/1040 was specific to phosphorylated residues as bands did not appear on the western blot upon sample treatment with λ -PP.

To answer the third of these unknowns, cells were treated with the enzyme GPT supplemented with sodium pyruvate to remove endogenous glutamate, then incubated in exogenously applied glutamate or vehicle for one hour to measure agonist-induced phosphorylation. Previous mass spectrometry data revealed that S870 and S871 in the C-terminus of murine mGlu₅ were phosphorylated following agonist stimulation, however the antibody is specific to not only pS870/S871 but also T874. The addition of a phosphate group to an amino acid adds additional

negative charge, creating a difficult environment to add another negatively charged phosphate group on a residue next to the first; this raises the question of how likely the double or triple phosphorylation events are to occur *in vivo*, and if detected on a western blot, how physiologically relevant and biologically realistic this occurrence is. However, the antibody targeting this site did not show clear differences between basal and agonist stimulated phosphorylation. Similarly, the pS1014/S1016 site was previously found through mass spectrometry to be phosphorylated following agonist stimulation, but again the antibody targeting this site did not show clear differences between basal and agonist stimulated phosphorylation. S1037 was found in mass spectrometry to be phosphorylated in basal conditions, which the pS1037/S1040 antibody western blot supports; phosphorylated protein is detected in the vehicle treated sample.

To further validate and characterise these novel phospho-site specific antibodies, the studies presented here should be extended using the mGlu₅-PD and mGlu₅-TPD mutants to explore the specificity of the antibodies to phosphorylated mGlu₅; testing the phosphoserine- or phosphothreonine-specific antibodies using a cell line expressing a receptor mutant unable to be phosphorylated on serine and threonine residues should reveal if the antibodies truly are specific to the noted phosphorylated amino acid residues within the mGlu₅ C-terminus. As a next step for testing these novel antibodies, an mGlu₅ immunoprecipitation experiment should be performed on murine cortex tissue and utilise the novel phospho-site specific antibodies to detect mGlu₅ phosphorylation, as observed in the previous phosphoproteomic study. Additionally, the phospho-site specific antibodies should be utilised to measure mGlu₅ phosphorylation *in situ* in immunocytochemical and immunohistochemical studies. This would permit mapping of the receptor localisation, providing visualisation of receptor location within the different cell compartments and the impact of agonist treatment on this. However, this may be challenging due to the lack of specificity of the antibodies as demonstrated by the western blots. Future studies could include generation of an mGlu₅ receptor mutant in which serine, threonine and tyrosine residues within the C-terminus are mutated to alanine, as tyrosine is also a residue that becomes phosphorylated at a rate of abundance of 1.8% alongside serine and threonine residues (Olsen et al., 2006). Furthermore, receptor phosphorylation outwith the C-terminus could be studied; sites within the first and second intracellular loop are known to be phosphorylated by protein kinase C (Thr606, Ser613, Thr665,

Thr681) and these residues have been shown to be key for mGlu₅ receptor activity, as mutating Thr681 to alanine, removing the potential for amino acid phosphorylation, is a loss-of-function mutation (Gereau IV & Heinemann, 1998).

Previous work validating phosphorylation-site specific antibodies for GPCRs has proved successful in terms of antibody specificity to the receptor and in utilising the resulting antibody as a biosensor to monitor GPCR localisation and activity following agonist stimulation. Marsango et al. (2022) employed phospho-site-targeted antisera against pS221/pS224 and pT263/pT264 in the ICL3 of GPR84, determining through immunoprecipitation for the receptor via GFP-trap and treatment with λ-PP that the antisera were specific to phosphorylated receptor. Furthermore, through immunocytochemical studies utilising the phosphorylation site specific antibodies, it was demonstrated that Thr263 and Thr264 are required for agonist-induced internalisation of GPR84, also proving these antibodies can measure GPCR phosphorylation *in situ* (Marsango et al., 2022). Similarly, Barki et al., (2023) discovered that phosphorylation site specific antibodies could act as sensitive biomarkers for constitutive and agonist-mediated phosphorylation for the free fatty acid receptor 2 (FFA2). FFA2 signalling exhibited tissue-specific signalling; GPCR phosphorylation, measured by phosphorylation site specific antisera, was different in different tissues with the same agonist-receptor pairing, supporting the 'phosphorylation barcode' hypothesis, a concept centred around the possibility of different agonists to promote certain phosphorylation patterns on the receptor (Barki et al., 2023; Tobin et al., 2008).

Whilst there is no literature on the phosphorylation sites that the novel antibodies validated in this thesis target, other C-terminal mGlu₅ sites have been studied using phosphorylation site specific antibodies. Ser1126 in the mGlu₅ C-terminus has been identified as a site of phosphorylation in the mGlu₅ C-terminus. Hu et al. (2012) used a Group I mGlu receptor anti-phosphoserine antibody to demonstrate that serine phosphorylation is mediated by kinases such as Cyclin-dependent kinase 5 (CDK5) and ERK and that this phosphorylation increases Homer-mGlu₅ coimmunoprecipitation, a process dependent on Preso1. This work was supported by Luo et al., (2020), who determined using an antibody specific to phosphorylated Ser1126 in mGlu₅ that phosphorylation of this residue increases mGlu₅-Homer interaction in complete Freund's adjuvant-induced inflammatory pain, with mutation of this serine residue to an amino acid unable to be phosphorylated relieving the pain. Additionally, acute administration of cocaine

was found to enhance phosphorylation of mGlu₅ at Ser1126 in the mouse striatum, with cocaine-induced behaviour being markedly reduced in mice possessing an mGlu₅ mutant receptor in which Ser1126 cannot be phosphorylated (Park et al., 2013). Together, this demonstrates the importance of phosphorylation specific antibodies targeting exact phosphorylation sites; development of antibodies against precise residues permits investigation into mGlu₅ phosphorylation and leads to discoveries aiding clinical therapies for disorders such as chronic inflammatory pain or cocaine use disorder.

The apparent constitutive phosphorylation of mGlu₅ observed on the phospho-blots supports the constitutive activity seen in the β -arrestin 2 recruitment assays: if the receptor is constitutively phosphorylated, it is highly likely that this leads to agonist-independent β -arrestin 2 recruitment to the cell surface. To examine the role of these specific sites that the novel antibodies target, found to be phosphorylated both following agonist-stimulation and under basal conditions, site-specific mutagenesis could be performed on these sites and use these novel constructs in *in vitro* β -arrestin 2 recruitment assays. This would reveal the functional outcome of phosphorylation of these specific residues and would permit cross-validation of the phospho-site specific antibodies tested here with the β -arrestin 2 recruitment assays.

3.5 Conclusion

In conclusion, the *in vitro* data presented in this chapter imply that mutation of serine and threonine residues from the C-terminus of mGlu₅ functionally impact the receptor's ability to recruit β -arrestin 2, a process mediated by GRKs. It has been found that phosphorylation of mGlu₅ C-terminal serine and threonine residues can dynamically regulate the constitutive activity, localisation, and interaction with other proteins. The investigation into the precise functional consequences of direct receptor phosphorylation ultimately informs novel drug discovery mechanisms for the treatment of neurological and psychological disorders through exploring the beneficial pathways to promote and avoiding clinically adverse receptor signal transduction pathways.

The next chapter of this thesis sets out to investigate the impact of mGlu₅ receptor phosphorylation on the G protein-coupled transduction pathway and how this may be useful for understanding the fundamental biology of the type 5 metabotropic glutamate receptor.

4 The Impact of Phosphorylation of the Type 5 Metabotropic Glutamate Receptor on G Protein Signalling

4.1 Introduction

Understanding the impact of GPCR phosphorylation on G protein-dependent signalling is important for providing insight into the mechanisms and pathways that are impacted by this post translational modification. GPCRs are common drug targets, hence measuring how GPCR phosphorylation modulates G protein signalling may inform the design of drugs that can either promote or inhibit specific receptor states, potentially leading to more precise therapeutic strategies and potential minimising of off-target effects. An example of a ligand with such capacity is carvedilol, a biased agonist at the β 1-adrenergic receptor. It preferentially stabilises a conformation that activates β -arrestin-mediated signalling pathways, which can have cardioprotective effects, without activating G protein-mediated pathways that increase heart rate (Abiko et al., 2024). Exploring the specific signalling pathways downstream of the mGlu₅ receptor may in the future distinguish clinically beneficial pathways to potentiate, such as with the β 1-adrenergic receptor, and as phosphorylation is a key event in GPCR signalling, the interplay of phosphorylation in this process should be considered.

4.1.1 The Impact of Phosphorylation on G Protein-Dependent Signalling

How phosphorylation-induced structural changes in GPCRs translate to altered G protein activation is not fully resolved. Whilst Chapter 3 demonstrated that phosphorylation plays a critical role in the regulation of β -arrestin 2 recruitment to mGlu₅, the role of this post-translational modification in the activation of G proteins is not fully defined. In addition, the role of phosphorylation in G protein activation may vary between different cell types and tissues; these context-dependent effects are not yet fully mapped out.

To explore the role of phosphorylation on G protein coupling for the mGlu₅ receptor, the calcium mobilisation, IP₁ production, and heterotrimeric G protein dissociation can be measured in the context of phosphorylation. This has previously been explored for the M1 muscarinic receptor, in which no difference was found between a phosphodeficient mutant and wildtype receptor in the IP₁ assay, yet the potency was shifted with the phosphodeficient mutant in the G

protein dissociation assay (Scarpa et al., 2021). For FFA4, no difference was observed between the wildtype and a version of the receptor where the C-terminus was truncated in the calcium mobilisation assay (Butcher et al., 2014), yet differing kinetics of calcium signalling was observed between wildtype and phosphodeficient FFA4 receptors in another study (Alvarez-Curto et al., 2016). This has yet to be explored for the mGlu₅ receptor; thus, to address the question of whether phosphorylation of mGlu₅ impacts G protein signalling, the mGlu₅ phosphodeficient mutants described in Chapter 3 of this thesis were employed in G protein signalling assays.

4.1.2 Using the Flp-In™ T-REx™ System to Measure Glutamate Receptor Signalling

In this chapter, the expression and functionality of cell lines expressing wildtype and phosphodeficient mutant mGlu₅ receptors was assessed. The Flp-In™ T-REx™ 293 expression system was selected (Ward et al., 2011). These cells are typically maintained without expression of the gene of interest, then on requirement, cells are treated with a tetracycline derivative to induce expression of the receptor. Controlling gene expression is helpful when investigating the glutamate receptor family, a group of receptors known to be highly constitutively active due in part to high cellular production of glutamate (Young et al., 2013). Additionally, selecting the Flp-In™ T-REx™ 293 system over transiently transfected cells eliminates the cell-to-cell variability in expression levels observed when using transiently transfected cells. The use of Flp-In™ T-REx™ 293 cells allows for selection of the optimum amount of inducible receptor expression, preventing over-activation of the receptor by controlling the amount of tetracycline derivative used to induce expression.

4.1.3 Strategies to Measure G Protein-Dependent Signalling

Throughout history, there have been many techniques available to measure this rapid and transient calcium ion flux in cells. Some methods involve genetically

encoded calcium biosensors, which give off a fluorescent or luminescent signal upon binding to calcium (GCaMP, cameleon, aequorin), or calcium microscopy imaging. The latter methodology can be combined with fluorescent calcium indicators to allow high resolution imaging of dynamic calcium oscillations with spatial and temporal information. Some calcium indicators are single wavelength (BAPTA, Fluo-3, Fluo-4, Rho-2), giving an increase in fluorescent intensity upon binding to calcium, yet some are dual wavelength (Fura-2, Indo-1), giving a ratiometric measurement of calcium release. This ratiometric approach compensates for variables such as dye concentration, cell number, cell thickness, and photobleaching. These indicators are also commonly used in plate-based assays to allow high throughput calcium screening; both the FlexStation and Fluorescence Imaging Plate Reader (FLIPR) automated systems are designed for calcium mobilisation experiments and are commonly used in GPCR signalling research due to the wide availability and ease of use (Price & Lummis, 2005; Woszczek et al., 2021).

For calcium mobilisation experiments performed in this chapter, the calcium sensitive dye fura-2 acetoxymethyl ester (AM) was selected. This calcium indicator changes its excitation wavelengths depending on whether calcium is bound to the dye or not (Grynkiewicz et al., 1985). Fura-2 AM is a lipophilic form of fura-2, permitting the dye to permeate through cell membranes; upon entry into the cell, cytoplasmic esterases cleave the ester bond, converting the dye into its hydrophilic active form (fura-2) which is trapped inside the cell (Oakes et al., 1988). When bound to calcium ions, the fluorescent emission changes; fura-2 can be excited at two different wavelengths, typically at 340 nm with calcium ions bound and 380 nm when calcium ions are not bound. In both cases, the dye emits light at 510 nm. The ratio of 510 nm emission obtained with excitation at each of these two wavelengths is used to determine the concentration of calcium within the cell (Figure 4.1).

An alternative measure of the $G\alpha_q$ coupled pathway activation is the inositol-1-phosphate (IP_1) assay (Garbison et al., 2012). This is a more proximal measure of $G\alpha_q$ protein-coupled receptor activation than measuring the second messenger calcium ions. GPCRs coupled to this $G\alpha_q$ protein stimulate the generation of IP_3 and subsequent increase in intracellular calcium ions (Figure 4.1). IP_3 production is rapid and transient before it is metabolised, leading to formation of IP_2 and furthermore IP_1 , which is then degraded by inositol

monophosphatase (IMPase) into myo-inositol (Hughes & Putney, 1990). This short half-life makes assessing IP₃ production challenging. Lithium chloride acts as an inhibitor of IMPase (Berridge et al., 1989) (Figure 4.1), thus when stimulating Gα_q coupled-GPCRs, pre-treatment of cells with high concentrations of lithium chloride allows accumulation of IP₁ as a surrogate measure of IP₃ production.

Like with calcium mobilisation, there are many options when it comes to selecting techniques to measure IP₃ (or IP₁) generation. A classic measurement is the radiolabelled inositol assay: cells are labelled with [³H]-inositol which gets incorporated into phosphoinositides, then extracted and separated using ion-exchange chromatography following cell stimulation then quantified using a scintillation counter (Wreggett et al., 1990). Whilst this technique is highly sensitive and has been optimised for ease of practice (Brandish et al., 2003), the time-consuming and technically demanding protocol means alternative methods have been developed. Other techniques such as an ELISA (Barodia et al., 2022), or fluorescent sensors of IP₃ (Oh & Ahn, 2008) exist, however the most accessible and commonly selected method to measure accumulation of inositol phosphates is a time resolved fluorescent resonance energy transfer (TR-FRET)-based system (Liu et al., 2008). TR-FRET consist of a donor and acceptor fluorophore that change relative fluorescent intensity upon binding to IP₁; if the donor fluorophore is excited by a light source, it can transfer energy non-radiatively to the acceptor fluorophore, leading to the emission of fluorescence from the acceptor. The principle of this competitive immunoassay involves anti-IP₁ terbium (Tb) cryptate, which binds to the free IP₁ produced by cells after receptor activation and then competes with IP₁-d2 (Figure 4.1). This results in TR-FRET signal that is inversely proportional to the concentration of IP₁ in the cell lysate. Using a standard with a known concentration of IP₁ permits conversion of this TR-FRET signal to a nanomolar concentration of IP₁.

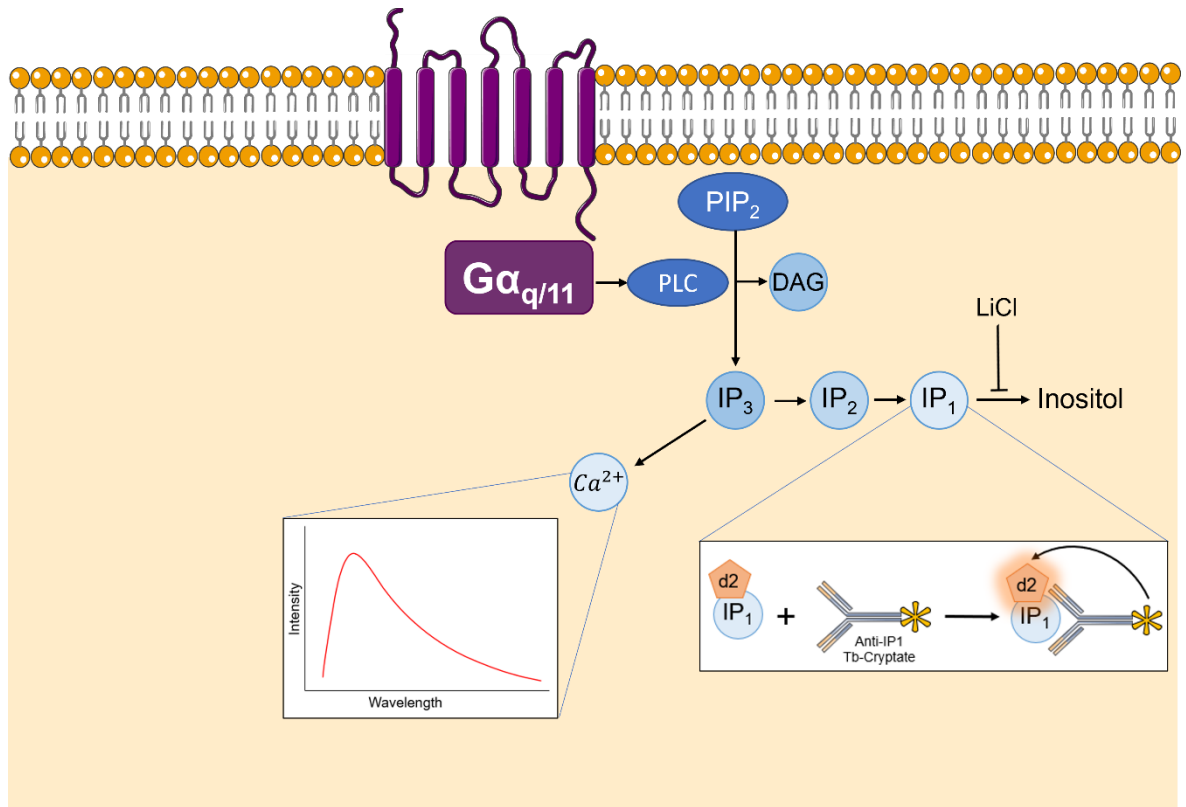


Figure 4.1: Measurement of the $G\alpha_{q/11}$ protein-coupled receptor activation. Activation of the $G\alpha_{q/11}$ protein stimulates production of IP_3 and release of calcium ions from the endoplasmic reticulum. Free calcium ions in the cytosol and IP_1 , a metabolite of IP_3 , can be measured as an indicator of $G\alpha_{q/11}$ protein pathway activation.

Furthermore, to measure GPCR receptor activation even more proximal to the receptor than IP_1 accumulation or calcium flux, the dissociation of the G protein heterotrimer can be measured. Again, a multitude of methodologies exist for measuring this, each with their own advantages and limitations. Firstly, the $[^{35}S]GTP\gamma S$ binding assay can be utilised; this assay measures the activation of G proteins through assessment of the binding of the non-hydrolysable, radiolabelled GTP analogue, $[^{35}S]GTP\gamma S$ (Mistry et al., 2011). Responses of $[^{35}S]GTP\gamma S$ binding assays for $G\alpha_q$ protein-coupled receptors can be achieved (Harrison & Traynor, 2003), but are often very disappointing. This seems to be due to the decreased rate of guanine nucleotide exchange at $G\alpha_q$, combined with relatively low levels of expression of this G protein (Strange, 2010). This assay provides direct measurement of G protein activation with high sensitivity, however, use with $G\alpha_q$ requires enrichment and radioactive protocols are not always accessible, therefore researchers may seek out other assays.

Another option to measure G protein activation is a BRET or FRET-based assay, in which the GPCR and interacting proteins are tagged with RET donor and

acceptor proteins permitting measurement of an energy transfer signal once the GPCR and tagged proteins interact. This measures real-time recordings in live cells with high spatial resolution, however an even more direct version of this assay involves tagging the G proteins themselves with the RET donor and acceptor to directly measure activation. One such assay to measure this heterotrimeric G protein dissociation is the TRUPATH system, a suite of BRET-based biosensors generated by Olsen et al. (2020), specific to 16 G α proteins and combined with 4 major G β subunits and 12 G γ subunits. The G α protein is tagged with the luciferase donor RLuc8, with G γ tagged with GFP2 fluorescent protein and the G β left untagged. In resting state, there is high BRET signal as the heterotrimeric complex is assembled at the cell membrane. Upon receptor activation and guanine nucleotide exchange, the G protein subunits dissociate, leading to a decrease in BRET signal. This provides a direct measure of G protein activation.

4.2 Aims

With the previous chapter concluding that phosphorylation impacts β -arrestin 2 recruitment, this was progressed into studies examining the G protein dependent signal transduction pathway. The aims of this chapter were as follows:

- Characterise the expression of wildtype and phosphodeficient mutant mGlu₅ receptors in Flp-In™ T-REx™ 293 cell lines.
- Assess the impact of phosphorylation on the G protein signalling through measurement of the following stages of the G α_q transduction pathway:
 - Calcium mobilisation
 - IP₁ accumulation
 - Heterotrimeric G protein dissociation

4.3 Results

4.3.1 Expression of Wildtype and Phospho-Deficient mGlu₅ Receptors in Flp-InTM T-RExTM 293 Cells

To explore G protein-dependent signal transduction of mGlu₅ and the impact of phosphorylation on this, Flp-InTM T-RExTM 293 cell lines were used. The Flp-InTM system facilitates integration of a gene of interest into the genome of a mammalian host cells. Initially, a Flp-InTM host cell line is generated by integration of the vector pFRT/lacZeo encoding for a lacZ-Zeocin gene, with expression controlled by the SV40 promoter, and the integrated Flp recombination target (FRT) located downstream of the ATG initiation codon (Craig, 1988; Sauer, 1994). The host cells also constitutively express a tetracycline repressor to inhibit transcription from the cytomegalovirus (CMV) promoter. Zeocin resistant cells are selected to generate the parental host cell line.

Parental Flp-InTM T-RExTM 293 cells (Invitrogen) were co-transfected with two plasmids: one containing the gene of interest in a pcDNA5/FRT/TO (Invitrogen), and the pOG44 plasmid which expresses Flp recombinase. When these plasmids are co-transfected, the Flp recombinase catalyses homologous recombination between FRT sites in host cell genome the pcDNA5/FRT/TO plasmid, permitting integration of the gene of interest into the genome of the parental cells whilst also integrating a hygromycin resistance gene (O'Gorman et al., 1991). Plasmids encoding the mGlu₅-WT, mGlu₅-PD and mGlu₅-TPD receptors in a pcDNA5/FRT/TO plasmid were used to generate isogenetic cell lines inducibly expressing wildtype or phosphodeficient mGlu₅. Upon treatment of the cell lines with doxycycline, a derivative of tetracycline, the tetracycline repressor protein unbinds from the tetracycline response elements upstream of the receptor coding sequence, thereby permitting transcription.

To confirm successful integration of the genes of interest in the parental cells, after overnight incubation with doxycycline immunocytochemical analysis was performed to visualise expression of the receptors. This method allows for the visualisation of protein expression in individual cells and can provide insights into protein localisation within the cell. Cells were incubated overnight with 100 ng/mL of doxycycline, a concentration that canonically produces maximal expression within the cells (Zhou et al., 2006). The receptor constructs possess a C-terminal

HA epitope tag to aid post-hoc visualisation, thus immunostaining for the HA tag was performed on permeabilised cell lines with and without doxycycline treatment (Figure 4.2).

The mGlu₅-WT cell line lacking doxycycline treatment does not exhibit any HA staining despite the 4',6-diamidino-2-phenylindole (DAPI) nuclei stain revealing cells are present in the sample (Figure 4.2A). However, upon addition of 100 ng/mL doxycycline to the cell culture medium the day before imaging, HA staining is observed at the membranes of the cells, indicating expression of the mGlu₅-WT receptor at the cell surface (Figure 4.2A). Similarly, there is no HA staining visible for the mGlu₅-PD (Figure 4.2B) and mGlu₅-TPD (Figure 4.2C) cell lines in the absence of doxycycline, yet there is cell membrane-localised HA staining for each of these cell lines upon addition of 100 ng/mL doxycycline to the culture medium.

Together, this lack of HA staining in the absence of doxycycline indicates that there is no detectable transcription of the HA tagged mGlu₅ receptor when no doxycycline is present. This result is the same when looking at the phosphodeficient mutant receptors, therefore it can be inferred that the Flp-In™ T-REx™ 293 cell lines are functioning correctly and expressing the receptor of interest in a controlled manner.

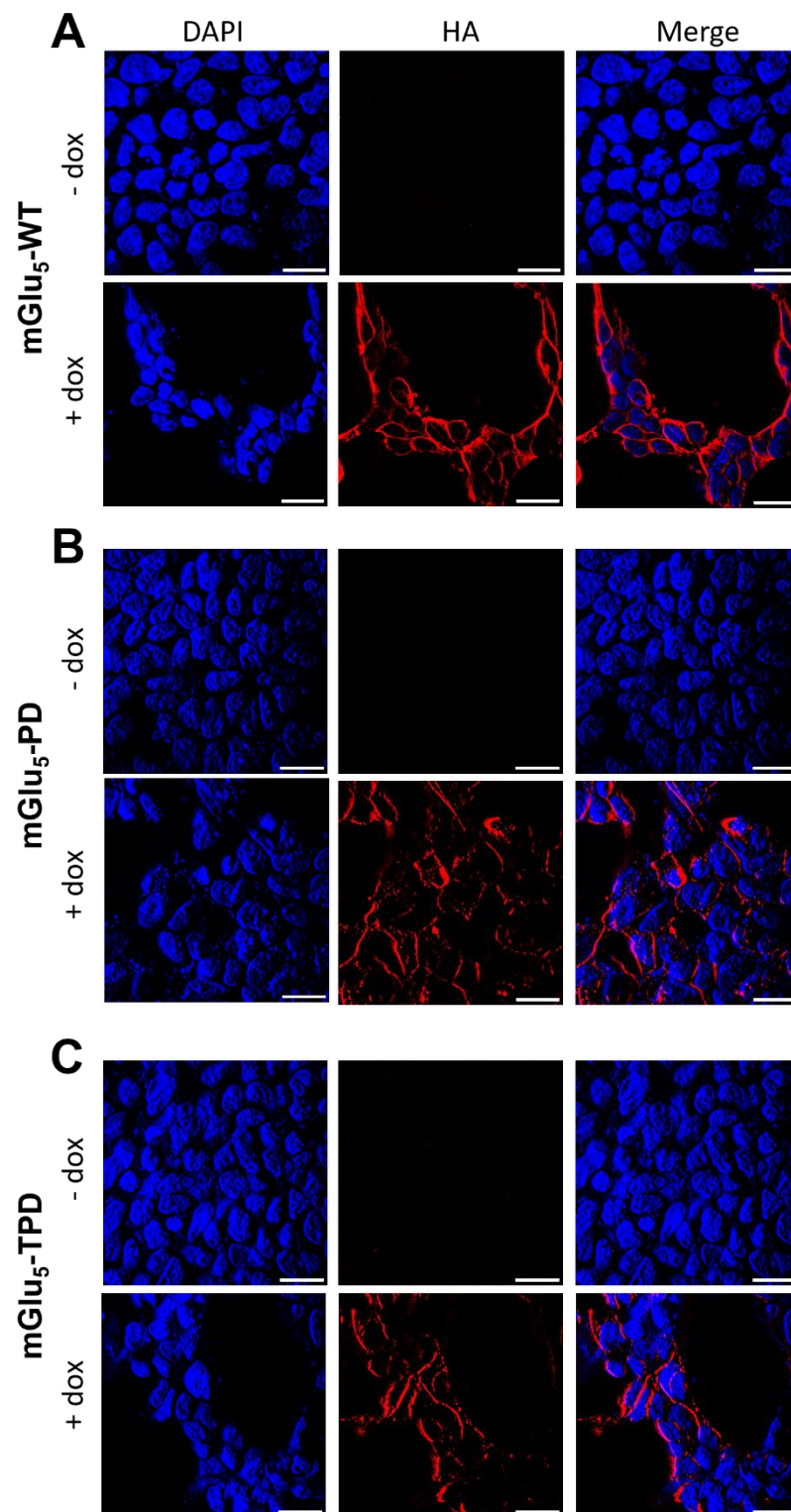


Figure 4.2: Doxycycline induction of F1p-In™ T-REx™ 293 cell lines leads to expression of mGlu5-HA constructs. Immunocytochemistry detection of hemagglutinin (HA)-tagged mGlu5-WT (A), mGlu5-PD (B) and mGlu5-TPD (C) receptors in formalin-fixed F1p-In™ T-REx™ 293 cells, treated with 100 ng/mL doxycycline (dox) overnight to induce receptor expression. The cell nuclei were stained with DAPI (blue), then the receptor detected using an anti-HA antibody (red). Single slice images were taken on a Zeiss Aperture Correlation Vivatome Spinning Disc Microscope. The scale bar indicates 20 μm.

An alternative way to confirm the functionality of the Flp-In™ T-REx™ 293 cell lines and to validate the immunocytochemical studies is through western blotting for the receptor construct. Initially, an mGlu₅ structural antibody binding to the C-terminus of the receptor was selected to detect the receptor within the cell lines (Kim et al., 2009). In the 24 hours before cell lysates were generated, cells were either treated with culture medium containing 100 ng/mL of doxycycline, or culture medium in the absence of doxycycline, to compare receptor expression between cells in the presence or absence of a tetracycline. This concentration of doxycycline is expected to produce maximal receptor expression in Flp-In™ T-REx™ 293 cells, which should be ideal for western blotting where receptor overexpression is beneficial to observe protein levels in samples. Untransfected parental Flp-In™ T-REx™ 293 cell lysates were utilised to compare to the samples from cells in the absence of doxycycline. No bands were observed on the western blot in the parental cell sample or in cell samples without doxycycline addition, yet there was membrane protein present within the sample as confirmed by detection of sodium-potassium ATPase, a membrane-localised protein (Figure 4.3A). Upon addition of doxycycline to the medium, bands can be observed on the blot at ~150 kDa and >250 kDa, consistent with monomeric and dimeric mGlu₅ receptor. There was a trend of decreasing expression of the monomeric form of the receptor with mutation of C-terminal serine residues, with a further reduction upon additional mutation of C-terminal threonine residues: there was a 4.8% decrease in receptor expression from mGlu₅-WT to mGlu₅-PD ($P > 0.9999$, Kruskal-Wallis test with Dunn's post hoc test), and a decrease of 33.7% in receptor expression from mGlu₅-WT to mGlu₅-TPD ($P = 0.4868$, Kruskal-Wallis test with Dunn's post hoc test) (Figure 4.3B). This trend was also observed for the dimeric form of the receptor: there was a 37.1% decrease in expression from mGlu₅-WT to mGlu₅-PD ($P > 0.9999$, Kruskal-Wallis test with Dunn's post hoc test), and a decrease of 73.4% in expression from mGlu₅-WT to mGlu₅-TPD ($P = 0.0930$, Kruskal-Wallis test with Dunn's post hoc test) (Figure 4.3C).

Because the mGlu₅ structural antibody binds to the C terminal of the receptor, the same region where the phosphodeficient mutations are present, this western blot analysis was repeated using an HA-specific antibody. Again, no bands were observed on the western blot in the parental cell sample or in cell samples without doxycycline addition, yet there was protein present within the sample as confirmed by the sodium-potassium ATPase housekeeping protein

(Figure 4.3D). Upon addition of doxycycline in the medium, bands can be observed on the blot at ~150 kDa and >250 kDa, consistent with monomeric and dimeric mGlu₅ receptor. There was a 4.4% decrease in receptor monomer expression from mGlu₅-WT to mGlu₅-PD ($P>0.9999$, Kruskal-Wallis test with Dunn's post hoc test), and a decrease of 14.0% in receptor monomer expression from mGlu₅-WT to mGlu₅-TPD ($P=0.5172$, Kruskal-Wallis test with Dunn's post hoc test) (Figure 4.3E). As was observed with the structural mGlu₅ antibody, a stronger trend was also observed for the dimeric form of the receptor: there was an 8.3% decrease in dimer expression from mGlu₅-WT to mGlu₅-PD ($P>0.9999$, Kruskal-Wallis test with Dunn's post hoc test), and a decrease of 72.6% in expression from mGlu₅-WT to mGlu₅-TPD ($P=0.6991$, Kruskal-Wallis test with Dunn's post hoc test) (Figure 4.3F).

Together, this western blot analysis demonstrates that there is no receptor expression detected with either an antibody to the mGlu₅ C-terminus or against the HA epitope tag in samples in which no doxycycline is present. Upon treatment of cells with doxycycline, a band consistent with the expected size of the mGlu₅ monomer and dimer is detected in both the wildtype and phosphodeficient cell lines.

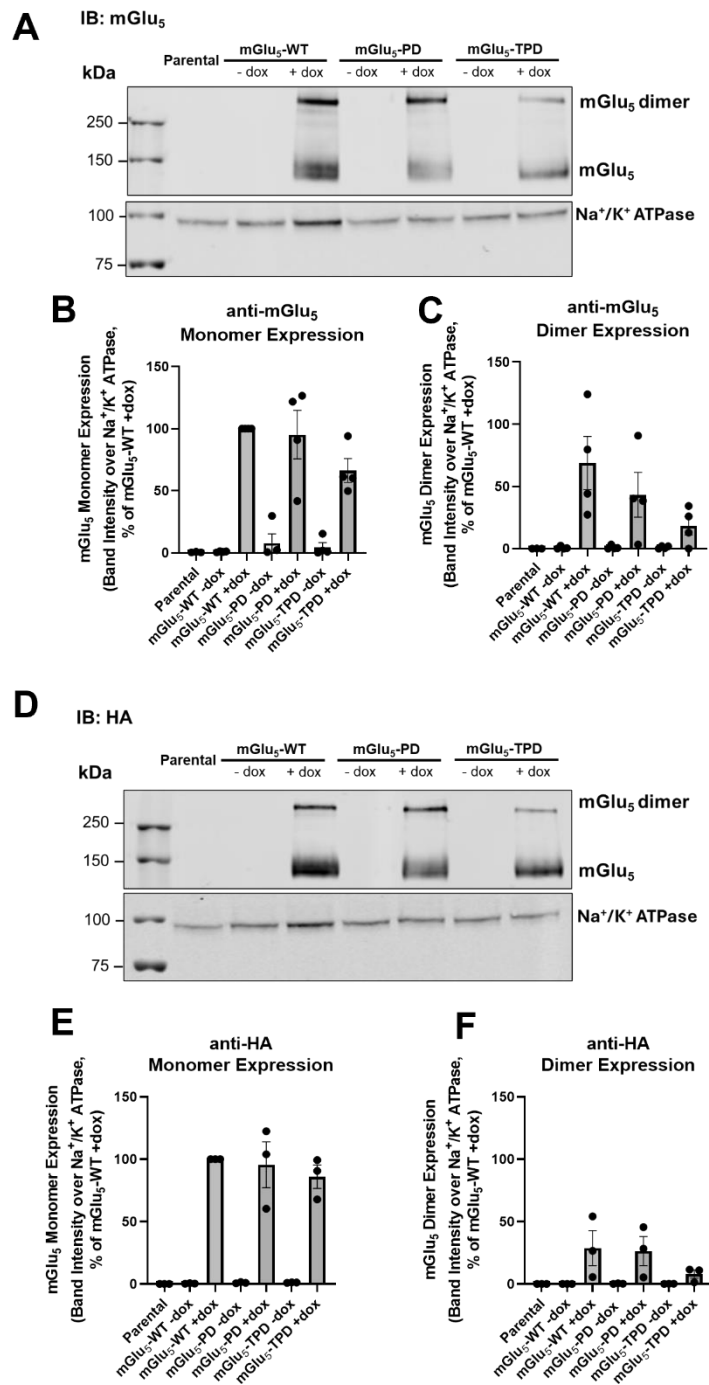


Figure 4.3: Western blots to quantify inducible mGlu₅ receptor expression.

Expression in lysates prepared from mGlu₅-WT, mGlu₅-PD and mGlu₅-TPD stable cell lines was assessed by SDS-page followed by western blotting with an antibody to the mGlu₅ C-terminus (A-C) or the HA epitope tag (D-F). Sodium-potassium ATPase was used as a loading control. Blots were quantified and expressed as median pixel intensity for the indicated band, divided by median pixel intensity for the sodium-potassium ATPase loading control. Expression of the monomeric receptor (B, E) and dimeric receptor (C, F) was quantified. Representative blots are shown from 3-4 independent experiments. Statistical analysis performed was a Kruskal-Wallis test with Dunn's multiple comparison correction on +dox samples only.

4.3.2 Quantitative Assessment of mGlu₅ Total and Surface Expression

To fully characterise the expression of mGlu₅, it is essential to quantitatively assess both its total and surface expression levels within cells. Utilising an N-terminal binding antibody offers a targeted approach to measure mGlu₅ expression via its extracellular domain, providing valuable insights into the receptor's distribution in both western blot and on-cell western contexts.

Once again, 24 hours preceding generation of cell lysates, cells were either treated with medium containing 100 ng/mL of doxycycline, or medium in the absence of doxycycline. Western blotting using the antibody against the mGlu₅ C-terminus revealed no significant difference in protein expression between the parental cell sample or in cell samples without doxycycline addition (Figure 4.4A). Upon addition of doxycycline in the medium overnight preceding generation of cell lysates, bands can be observed on the blot at ~150 kDa and >250 kDa, consistent with monomeric and dimeric mGlu₅ receptor. No significant difference in monomeric expression was observed between mGlu₅-WT and mGlu₅-PD ($P > 0.9999$, Kruskal-Wallis test with Dunn's post hoc test) or mGlu₅-WT and mGlu₅-TPD ($P > 0.9999$, Kruskal-Wallis test with Dunn's post hoc test) in samples treated with doxycycline (Figure 4.4B). Similarly, no significant difference in dimeric expression was observed between mGlu₅-WT and mGlu₅-PD ($P > 0.9999$, Kruskal-Wallis test with Dunn's post hoc test) or mGlu₅-WT and mGlu₅-TPD ($P = 0.5443$, Kruskal-Wallis test with Dunn's post hoc test) samples treated with doxycycline, despite there being a 56.1% reduction in expression from mGlu₅-WT to mGlu₅-TPD (Figure 4.4C).

Western blotting using the antibody against the mGlu₅ N-terminus revealed a lot of non-specific binding, making it difficult to determine which bands indicated monomeric mGlu₅ receptor. However, bands consistent with the dimeric form of the receptor were detected at >250 kDa. A reduction in dimeric receptor expression was observed between mGlu₅-WT and mGlu₅-PD ($P = 0.5391$, Kruskal-Wallis test with Dunn's post hoc test) and mGlu₅-WT and mGlu₅-TPD ($P = 0.0219$, Kruskal-Wallis test with Dunn's post hoc test) in samples treated with doxycycline (Figure 4.4D).

Together, this demonstrates that both the monomeric and dimeric forms of mGlu₅ is detected in cell lines expressing wildtype and phosphodeficient mutants

of mGlu₅ using the antibody against the C-terminus, however this is much more challenging using the antibody to the N-terminus. Despite this, a significant decrease in dimeric receptor expression was observed with mutation of C-terminal serine residues, with a further reduction in expression when threonine residues are additionally mutated.

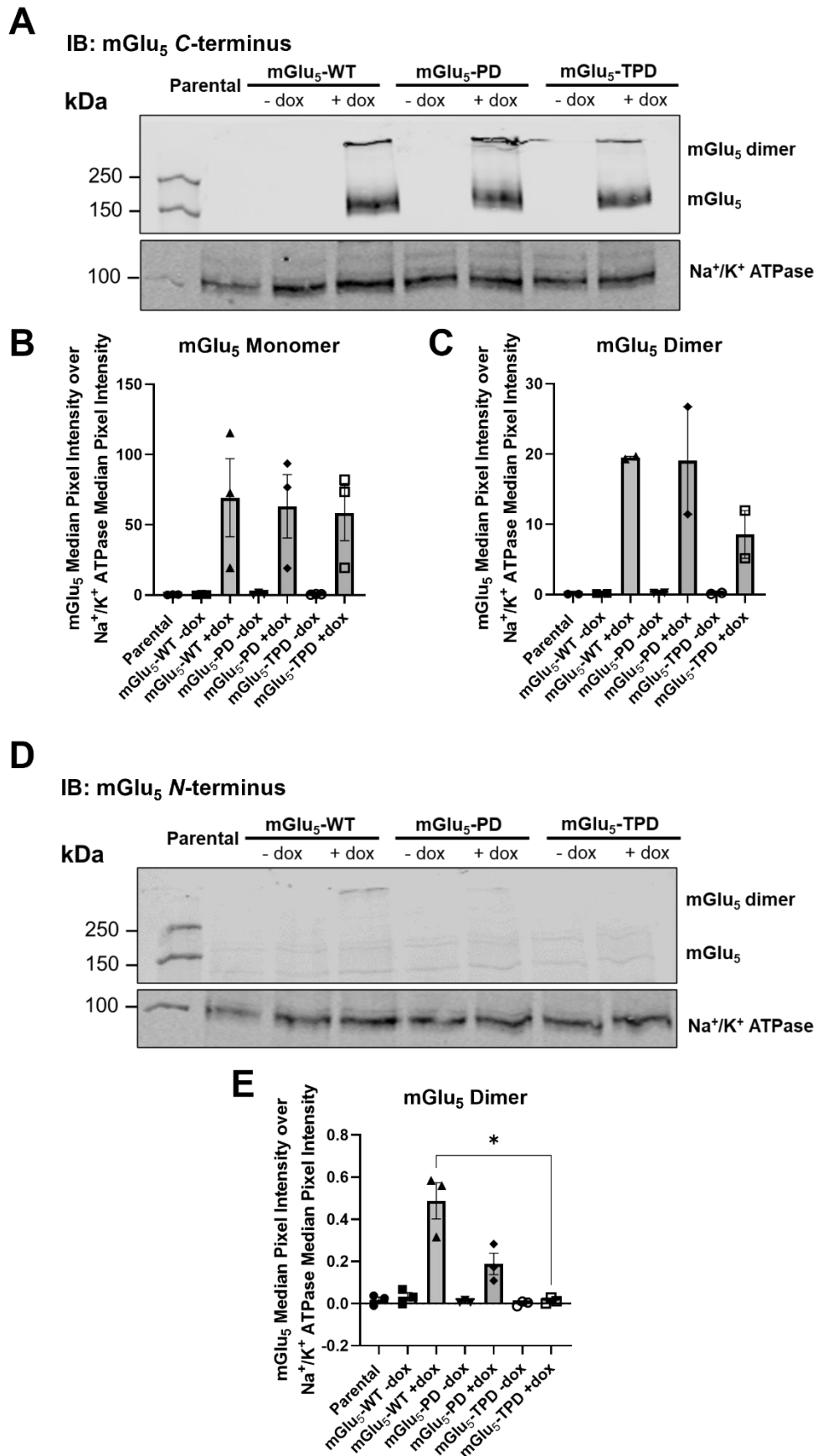


Figure 4.4: Western blot analysis of the structure of mGlu₅. Receptor expression in lysates prepared from mGlu₅-WT, mGlu₅-PD and mGlu₅-TPD stable cell lines was assessed by SDS-page followed by western blotting with an antibody to the mGlu₅ C-terminus (A-C) or N-terminus (D-E). Sodium-potassium ATPase was used as a loading

control. Blots were quantified and expressed as median pixel intensity for the indicated band, divided by median pixel intensity for the sodium-potassium ATPase loading control. Expression of the monomeric receptor (B) and dimeric receptor (C, E) was quantified. Representative blots are shown from three independent experiments. Statistical analysis performed was a Kruskal-Wallis test with Dunn's post hoc test on +dox samples only. * $P \leq 0.05$.

In order to further quantify both total and cell surface expression of the mGlu₅ receptors in the Flp-In™ T-REx™ 293 cell lines, in-cell western (ICW) and on-cell western (OCW) analysis was performed. These techniques involve antibody incubation on fixed cells seeded in 96-well plates, permitting more rapid, high throughput and quantitative examination of protein expression than traditional western blots (Pal et al., 2022). The ICW and OCW techniques differ in that the cells are permeabilised for the ICW, whilst left intact for the OCW. Therefore, if using an antibody that binds to an extracellular epitope, an OCW can be used to quantify cell surface expression of the receptor, whereas the ICW can be used with an antibody recognising either an extracellular or intracellular epitope to measure total expression.

To investigate the expression of mGlu₅ wildtype receptor, an OCW and ICW analysis was performed utilising the N-terminal binding mGlu₅ antibody alongside the C-terminal binding mGlu₅ antibody. Cells were either left intact or treated with Triton-X-100 to permeabilise the cells. To control for background signal produced by the secondary antibody, there was a condition in which receptor expression was induced with 100 ng/mL doxycycline, but not incubated with primary antibody. Conversely, to control for the background signal produced by the secondary antibody, a minus primary antibody control sample was prepared. To measure any potential background signal in the cells not related to the receptor construct, a cell samples both in the absence of doxycycline and with parental Flp-In™ T-REx™ 293 cells were used. Finally, control wells containing phospho-buffered saline (PBS) with no cells, but with both primary and secondary antibodies were included to show background fluorescence of the assay plate.

In the OCW treated with the N-terminal mGlu₅ antibody, no signal is observed when there is no primary antibody or no secondary antibody (Figure 4.5A). There is also no signal detected in the absence of doxycycline, while a clear signal is apparent in cells treated with 100 ng/mL doxycycline. Little signal was also observed in the parental Flp-In™ T-REx™ 293 cells, however upon quantification, it was clear that a slightly higher background was observed in these

cells than in the cells not treated with doxycycline ($P > 0.9999$, Kruskal-Wallis test with Dunn's post hoc test) (Figure 4.5B). With permeabilisation, the ICW showed the amount of non-specific binding from the N-terminal antibody appeared to increase, apparent by the relatively higher signal in both the cells not treated with doxycycline and the parental cells (Figure 4.5C), which translated to smaller quantified differences between these conditions and the doxycycline treated condition (Figure 4.5D). Despite this, there is still an increase of antibody labelling comparing the minus to plus doxycycline ($P = 0.0688$, Kruskal-Wallis test with Dunn's post hoc test) (Figure 4.5D).

Using the C-terminal mGlu₅ antibody in an OCW is predicted to detect no signal, due to the antibody binding to the intracellular surface of the receptor and the cells are not permeabilised in this condition. There is no signal observed for cells minus doxycycline and parental cells, yet there did appear to be some staining present in the plus doxycycline condition (Figure 4.5E). When permeabilised, the signal with the C-terminal antibody increases and is observed almost entirely in only the plus doxycycline condition (Figure 4.5G). Quantification of this ICW using the C-terminal antibody demonstrated that the signal was increased in the plus doxycycline condition compared both to the parental cells ($P = 0.5172$, Kruskal-Wallis test with Dunn's post hoc test), and to cells in the absence of doxycycline ($P = 0.0190$, Kruskal-Wallis test with Dunn's post hoc test) (Figure 4.5H).

These OCW and ICW analyses indicate that the N-terminal binding antibody has some non-specific binding, as was also seen in the traditional western blots, as signal is detected in the minus doxycycline and parental cell samples following cell permeabilisation. Despite this, there is still specific detection of the receptor without cell permeabilisation, indicating that this antibody can be used to measure cell surface expression of mGlu₅. In contrast, the C-terminal mGlu₅ antibody is very specific to its target; there is little to no background signal from the minus doxycycline and parental cells, and the receptor is detected in the doxycycline-treated cell. It is surprising that some staining was observed for the C-terminal antibody in the non-permeabilised cells, but this is likely due to breakage of the cells in the fixation process.

Taken together, these OCW and ICW analyses provide a good method to quantify total and cell surface mGlu₅ expression within cells. The use of an N-terminal binding antibody to measure mGlu₅ receptor total and surface expression

provided a useful tool for measuring total and surface mGlu₅ expression. By specifically targeting the N-terminal region, this approach allows for accurate quantification of both the overall and cell surface populations of the receptor.

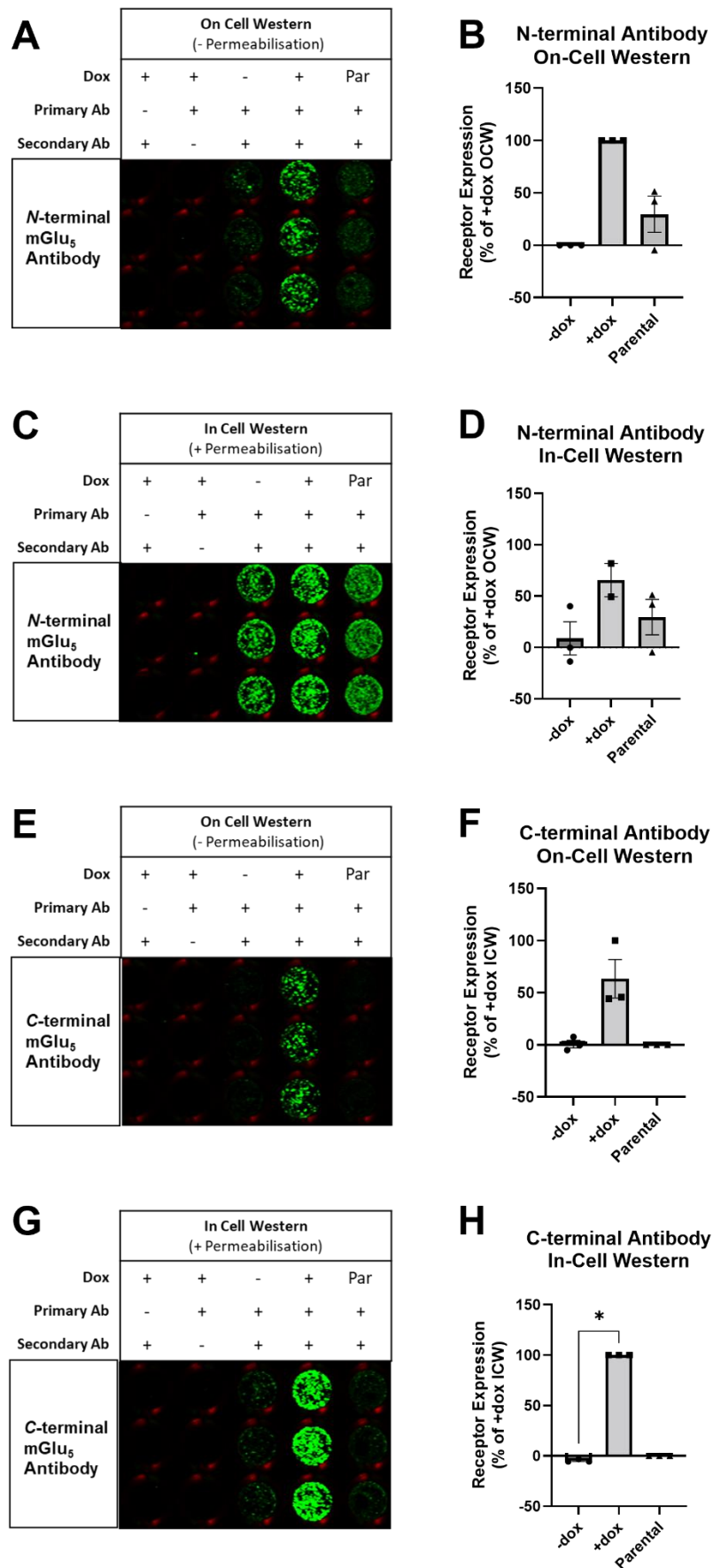


Figure 4.5: On-cell and in-cell western analysis can be used to quantify mGlu₅ surface and total expression. A representative on-cell western (OCW) (A, E) or in-cell western (ICW) (C, G) analysis of mGlu₅-WT expression. Cells were treated with 100

ng/mL of doxycycline and compared to control parental cells (Par) that do not express mGlu₅. N-terminal antibody quantification (B, D) and C-terminal antibody quantification (F, H) is from three biological replicates each performed in quadruplicate. Data are corrected to parental cell background signal and expressed over Hoechst staining measurements to correct for cell number. Data are normalised to show the percent signal relative to doxycycline treated cells based on the OCW for the N-terminal antibody, and the ICW for the C-terminal antibody. Data plotted are the means \pm S.E.M. of three individual experiments each performed in triplicate. Statistical analysis performed was a Kruskal-Wallis test with Dunn's post hoc test to control for multiple comparisons. * $P \leq 0.05$.

4.3.3 The Impact of Doxycycline Concentration on Receptor Expression in Flp-In™ T-REx™ 293 Cells

One advantage of using the Flp-In™ T-REx™ system is that receptor expression can be fine-tuned and manipulated by the concentration of doxycycline applied to the cells. In order to optimise the conditions of gene induction, doxycycline titration experiments were performed to compare the expression levels of receptor within mGlu₅-WT, mGlu₅-PD and mGlu₅-TPD cell lines across the differing levels of doxycycline treatment.

To examine the level of receptor expression with increasing doxycycline concentration, mGlu₅-WT, mGlu₅-PD and mGlu₅-TPD Flp-In™ T-REx™ 293 cells were treated with a range of doxycycline concentrations overnight, then expression assessed using western blot analysis (Figure 4.6). First examining the mGlu₅-WT cell line, there is an increase in band intensity when doxycycline concentration increases, detected using the C-terminal binding mGlu₅ structural antibody (Figure 4.6A). No protein is detected in the parental cells or with 0 ng/mL doxycycline, despite the housekeeping protein (sodium-potassium ATPase) indicating protein is present in the sample. Treating the cell samples with 10 ng/mL and above produced maximal expression of the monomer (Figure 4.6B) and dimer (Figure 4.6C). Previous unpublished data from our laboratory has suggested that specifically for the mGlu₅ expressing Flp-In™ T-REx™ 293 cell lines, treatment with 2 ng/mL of doxycycline produces the best signal window in functional assays. Here, to corroborate this, the 2 ng/mL concentration of doxycycline was compared to the canonical 100 ng/mL concentration that is typically used for GPCRs in Flp-In™ T-REx™ 293 cell lines (Zhou et al., 2006). When the mGlu₅-WT cell line was treated with a low concentration of doxycycline (2 ng/mL), the band consistent with the mGlu₅ monomer produces a lower level of expression than at 100 ng/mL (peak band intensity of 16.7 ± 3.90 % of the 100 ng/ml band, ($P > 0.9999$, Kruskal-Wallis

test with Dunn's post hoc test) (Table 4.1). The dimeric form of mGlu₅ also demonstrated a significantly lower level of expression (peak band intensity of 24.0 ± 4.90 % of the 100 ng/ml doxycycline band ($P=0.9999$, Kruskal-Wallis test with Dunn's post hoc test) (Table 4.1).

Next, looking at the mGlu₅-PD cell line, a similar trend is seen to that observed for the wildtype receptor. No protein band is seen on the western blot in the absence of doxycycline, or in the parental cells without expression of the mGlu₅-PD construct (Figure 4.6D). Once again, treating the cell samples with 10 ng/mL and above produced maximal expression of the monomer (Figure 4.6E) and dimer (Figure 4.6F). When the mGlu₅-PD cell line was treated with a low concentration of doxycycline (2 ng/mL), the band consistent with the mGlu₅ monomer produces a lower level of expression than at 100 ng/mL for both the monomeric and dimeric form of the receptor, however this is not significant ($P>0.9999$, Kruskal-Wallis test with Dunn's post hoc test) (Table 4.1).

Looking at the mGlu₅-TPD cell line, a similar trend is seen to that observed for the wildtype and mGlu₅-PD receptor, but with somewhat lower overall expression. No band is seen on the western blot in the absence of doxycycline or in the parental cells without expression of the gene of interest (Figure 4.5G). Again, treating the cell samples with 10 ng/mL and above produced maximal expression of both the monomer (Figure 4.6H) and dimer (Figure 4.6I). However, none of the concentrations of doxycycline produced significantly different band intensities for both the monomer and dimer expression (Figure 4.6H, Figure 4.6I). When the mGlu₅-TPD cell line was treated with 2 ng/mL, the band consistent with the mGlu₅ monomer produces a lower level of expression, however again this is not significant ($P>0.9999$, Kruskal-Wallis test with Dunn's post hoc test) (Table 4.1).

Comparing the level of expression between the three cell lines reveals no significant differences in expression of either the monomer or dimer at 2 ng/mL doxycycline concentration (Table 4.2). However, comparing the level of expression at 100 ng/mL doxycycline concentration reveals significant differences in expression (Table 4.2). There is no significant difference in expression of monomeric mGlu₅-WT and mGlu₅-PD at 100 ng/mL doxycycline ($P>0.9999$, Kruskal-Wallis test with Dunn's post hoc test) (Table 4.2), and additionally there is lower expression of monomeric mGlu₅-TPD observed compared to both mGlu₅-WT ($P=0.2065$, Kruskal-Wallis test with Dunn's post hoc test) and mGlu₅-PD

($P=0.0688$, Kruskal-Wallis test with Dunn's post hoc test). Looking at the dimer expression following induction with 100 ng/mL doxycycline, there are significant difference in expression of the receptor among the three cell lines (Table 4.2). The peak intensity for mGlu₅-PD is increased compared to mGlu₅-WT ($P=0.5172$, Kruskal-Wallis test with Dunn's post hoc test), however mGlu₅-TPD demonstrated a significant decrease in dimer expression compared to mGlu₅-PD ($P=0.0190$, Kruskal-Wallis test with Dunn's post hoc test).

Together, these data reveal that all three mGlu₅ receptor cell lines demonstrate the same trend of increasing receptor expression with increasing doxycycline concentration. However, for mGlu₅-TPD, the receptor expression was generally lower compared to mGlu₅-WT and mGlu₅-PD, but this is consistent with my initial characterisation of these cells, finding mGlu₅-TPD expression, in particular the dimer, to be significantly lower than wildtype (Figure 4.3C, Figure 4.4E). Comparing the expression between the three cell lines reveals significantly different levels of expression of the receptor at 100 ng/mL doxycycline, however at 2 ng/mL, the differences in expression level were not as drastic. This data, combined with the previous data from our laboratory demonstrating 2 ng/mL gives the best functional response for these mGlu₅ cell lines, provided evidence that this concentration should be utilised to induce receptor expression in further experiments.

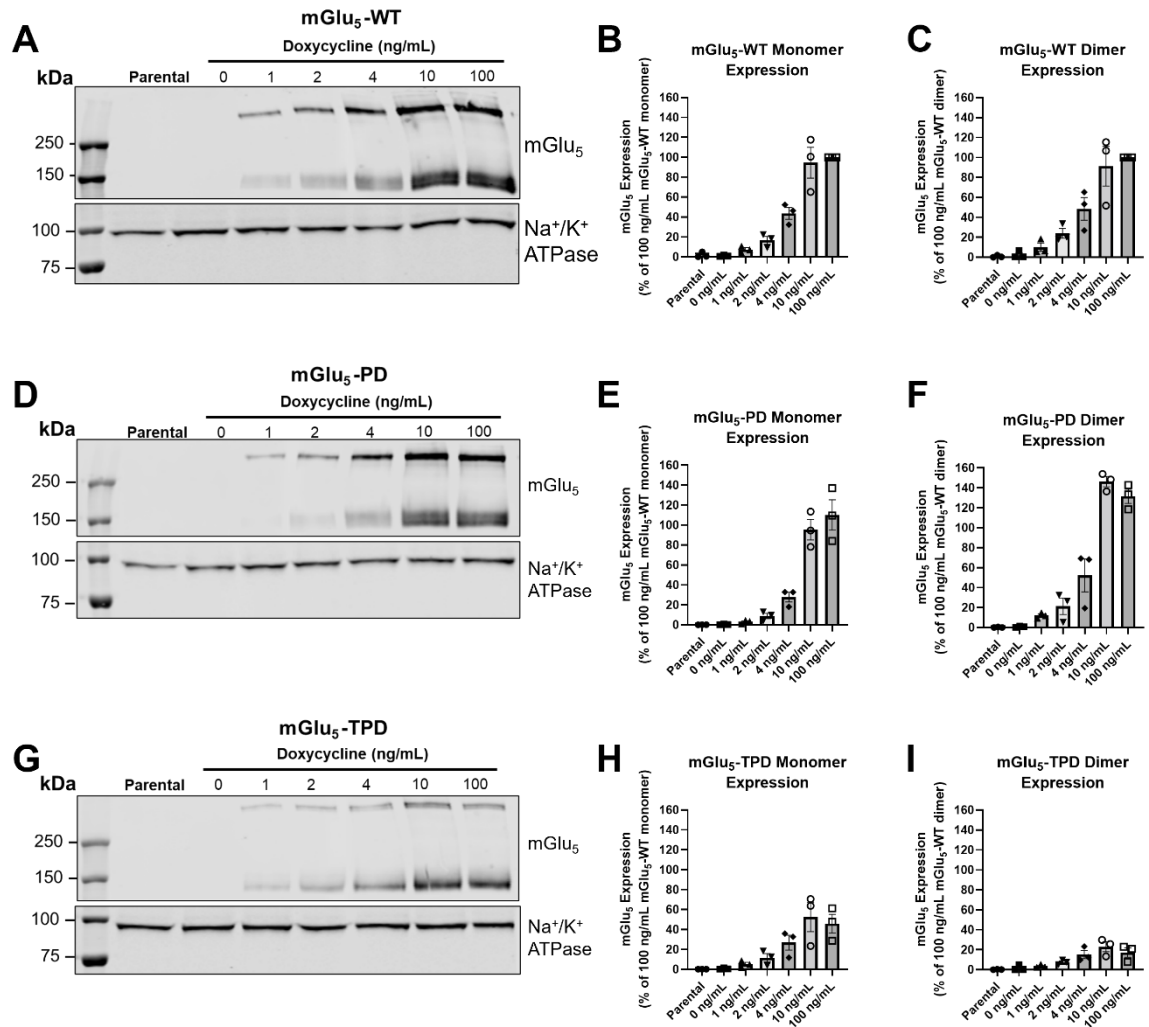


Figure 4.6: Expression of mGlu₅-WT, mGlu₅-PD and mGlu₅-TPD increases with doxycycline concentration. Expression of mGlu₅ constructs in lysates generated from Flp-In™ T-REx™ 293 cell lines expressing mGlu₅-WT (A-C), mGlu₅-PD (D-F) and mGlu₅-TPD (G-I) and treated with increasing concentrations of doxycycline was assessed by SDS-PAGE and western blot. Blots were probed with an antibody directed against the mGlu₅ C-terminus, while a sodium-potassium ATPase antibody was used as a loading control. Representative blots are shown from three independent experiments. Quantification of blots is normalised to the signal obtained with 100 ng/mL doxycycline in the mGlu₅-WT cell line.

Table 4.1: Peak band intensity, normalised as a percentage to wildtype receptor, of western blots following treatment with 2 ng/mL is significantly lower than treatment with 100 ng/mL doxycycline.

| Receptor | | Doxycycline | Peak Intensity | <i>P</i> |
|------------------------|---------|-------------|----------------|----------|
| mGlu ₅ -WT | Monomer | 2 ng/mL | 16.7 ± 3.90 | >0.9999 |
| | | 100 ng/mL | 100.0 ± 0.00 | |
| | Dimer | 2 ng/mL | 24.0 ± 4.89 | >0.9999 |
| | | 100 ng/mL | 100.0 ± 0.00 | |
| mGlu ₅ -PD | Monomer | 2 ng/mL | 8.9 ± 2.65 | >0.9999 |
| | | 100 ng/mL | 110.2 ± 15.27 | |
| | Dimer | 2 ng/mL | 21.4 ± 8.26 | >0.9999 |
| | | 100 ng/mL | 131.6 ± 7.09 | |
| mGlu ₅ -TPD | Monomer | 2 ng/mL | 11.6 ± 4.19 | >0.9999 |
| | | 100 ng/mL | 45.9 ± 9.43 | |
| | Dimer | 2 ng/mL | 7.4 ± 1.35 | >0.9999 |
| | | 100 ng/mL | 17.3 ± 4.73 | |

Table 4.2: Western blots from mGlu₅-WT, mGlu₅-PD and mGlu₅-TPD cell lysates demonstrate no significant differences in expression when induced with 2 ng/mL doxycycline.

| Condition | Receptor | Peak Intensity (Mean Difference) | <i>P</i> |
|-----------------------------------|---|----------------------------------|----------|
| Monomer, 2 ng/mL doxycycline | mGlu ₅ -WT vs mGlu ₅ -PD | 7.8 | 0.6991 |
| | mGlu ₅ -WT vs mGlu ₅ -TPD | 5.1 | 0.8902 |
| | mGlu ₅ -PD vs mGlu ₅ -TPD | -2.7 | >0.9999 |
| Dimer, 2 ng/mL doxycycline | mGlu ₅ -WT vs mGlu ₅ -PD | 2.6 | >0.9999 |
| | mGlu ₅ -WT vs mGlu ₅ -TPD | 16.6 | 0.2209 |
| | mGlu ₅ -PD vs mGlu ₅ -TPD | 14.0 | 0.5391 |
| Monomer, 100 ng/mL doxycycline | mGlu ₅ -WT vs mGlu ₅ -PD | -10.2 | >0.9999 |
| | mGlu ₅ -WT vs mGlu ₅ -TPD | 54.1 | 0.2065 |
| | mGlu ₅ -PD vs mGlu ₅ -TPD | 64.3 | 0.0688 |
| Dimer, 100 ng/mL doxycycline | mGlu ₅ -WT vs mGlu ₅ -PD | -31.6 | 0.5172 |
| | mGlu ₅ -WT vs mGlu ₅ -TPD | 82.8 | 0.5172 |
| | mGlu ₅ -PD vs mGlu ₅ -TPD | 114.4 | 0.0190 * |

In addition to measuring the doxycycline dependent induction of expression in these cell lines by western blot, cell surface and total expression of the receptor constructs were also measured using OCWs and ICWs. To examine the impact of

doxycycline concentration on cell surface expression, an OCW using the antibody targeted to the N-terminal of mGlu₅ and an ICW using the C-terminal antibody were first performed on cells from the mGlu₅-WT cell line treated with a range of doxycycline concentrations. There is no visible signal on either the OCW or ICW in the absence of primary antibody or the secondary antibody (Figure 4.7A). However, when incubating cells expressing the mGlu₅-WT receptor with the N-terminal binding antibody, this OCW showed a visual trend of increasing intensity as the concentration of doxycycline increases (Figure 4.7A). Similarly, with the C-terminal binding antibody, the ICW showed a trend of increasing signal with increased concentration of doxycycline (Figure 4.7A). For the mGlu₅-PD receptor, a similar trend of increasing intensity was observed with increasing concentrations of doxycycline for both the OCW and ICW, with highest antibody intensity at 10 ng/mL and 100 ng/mL (Figure 4.7B). Likewise, for the mGlu₅-TPD receptor both the OCW and ICW intensity increases across the increasing concentration of doxycycline tested, with maximal intensity at 10 ng/mL and 100 ng/mL doxycycline (Figure 4.7C).

Quantification of these ICWs and OCWs (Figure 4.8) indicates that no measurable expression was produced by the treatment of mGlu₅-WT expressing cells with no treatment with doxycycline. For the mGlu₅-WT OCW, 1 ng/mL doxycycline resulted in an expression level 11.0% of the maximal expression produced by 100 ng/mL, rising to 22.0% with 2 ng/mL doxycycline and 53.1% with 10 ng/mL doxycycline (Figure 4.8A). For the ICW, expression was detected as the lowest concentrations of doxycycline, with 0.5 ng/mL producing 26.6% of the maximal expression obtained with 100 ng/mL doxycycline (Figure 4.8B). The total expression of the mGlu₅-WT receptor as detected by the ICW steadily increased as the doxycycline concentration was increased. For the mGlu₅-PD receptor, surface expression as detected by OCW, showed measurable expression at 1 ng/mL doxycycline of 8.3% of the 100 ng/mL doxycycline maximal expression level (Figure 4.8C). Surface expression then increased with increasing doxycycline concentration. Similar to that seen with the wildtype receptor, signal was detected for the mGlu₅-PD receptor in the ICW at low concentrations of doxycycline, with a value of 14.3% of the 100 ng/mL maximal expression produced by 0.5 ng/mL doxycycline (Figure 4.8D). The expression of the mGlu₅-TPD receptor in the OCW was more variable, with expression of the receptor at 10 ng/mL doxycycline 126.8% of the 100 ng/mL expression (Figure 4.8E). However, the ICW produced a

more consistent and steady increase in expression with increasing doxycycline, with 10 ng/mL producing a similar level of signal to 100 ng/mL (Figure 4.8F).

Together, these ICW and OCW studies reveal that cell membrane expression of mGlu₅-WT, mGlu₅-PD, and mGlu₅-TPD can be assessed with this assay setup, and that both cell surface and total expression of the mGlu₅ constructs are controlled by doxycycline concentration.

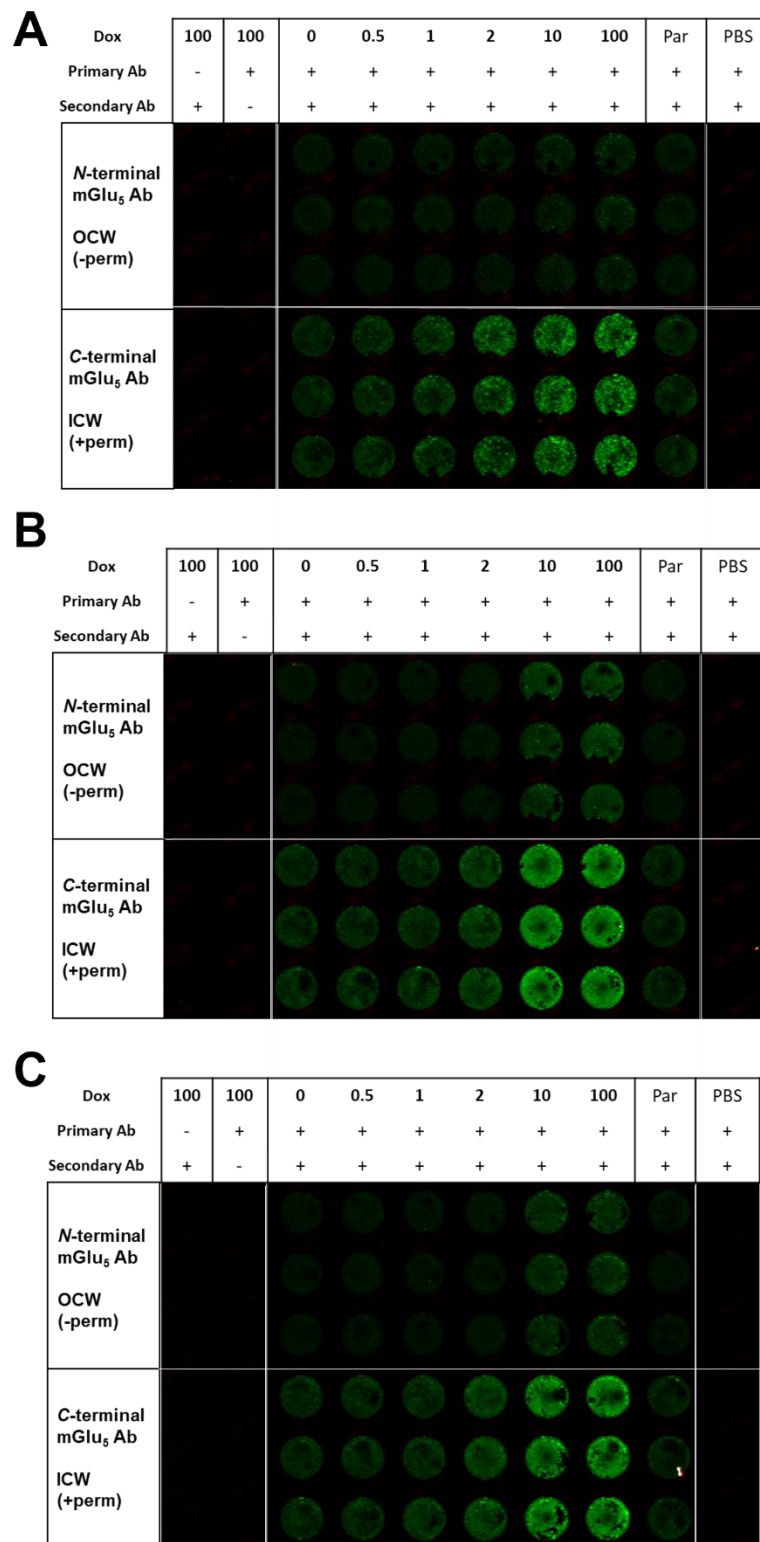


Figure 4.7: Cell membrane expression of the mGlu₅-WT, mGlu₅-PD, and mGlu₅-TPD receptors increases with increasing concentration of doxycycline. An in- and on-cell western analysis of mGlu₅-WT (A), mGlu₅-PD (B) and mGlu₅-TPD (C) cell surface expression upon overnight treatment with increasing concentrations of doxycycline (dox; ng/mL) compared to parental cells (Par). Representative images shown from three biological replicates each performed in triplicate.

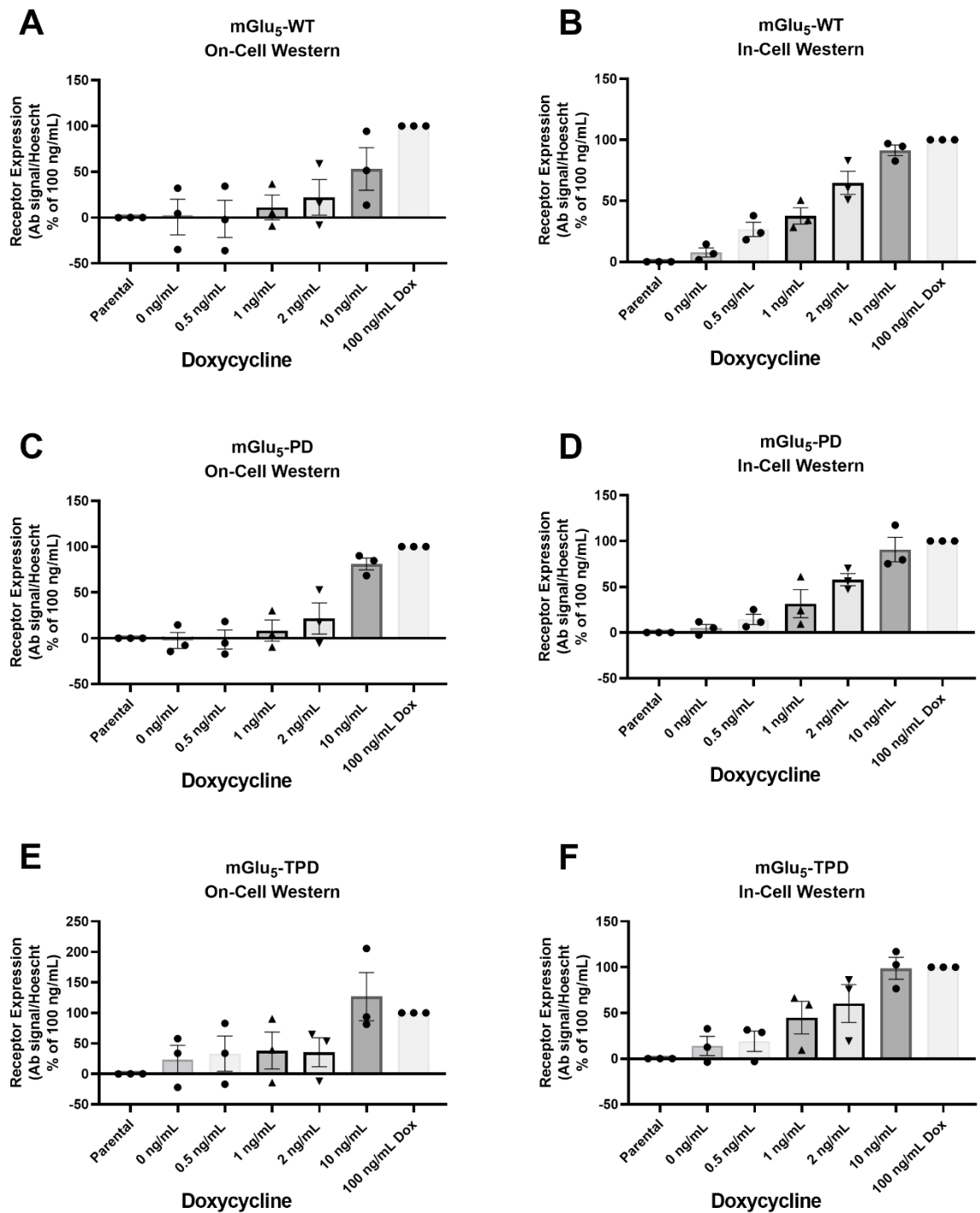


Figure 4.8: Quantification of in- and on-cell western analyses of mGlu₅ receptor expression reveals an increase in membrane expression with increasing concentrations of doxycycline. Quantification of median pixel intensity of on-cell western analyses (A, C, E) and in-cell western analyses (B, D, F) of expression of the mGlu₅-WT receptor (A, B), the mGlu₅-PD receptor (C, D) and the mGlu₅-TPD receptor (E, F). Data shown is mean \pm S.E.M. of three biological replicates each performed in triplicate. Median pixel intensity data is corrected to antibody background signal and expressed over Hoechst-stained cells to correct for cell number. Data is further normalised to percent of 100 ng/mL doxycycline treated cells.

4.3.4 Removal of C-terminal Phosphorylation Sites of the mGlu₅ Receptor Impacts Intracellular Calcium Mobilisation

Measuring the calcium mobilisation in the cell is a key feature when looking at G α_q protein signalling. In the context of phosphodeficient receptors, measuring calcium flux allows exploration into how the direct receptor phosphorylation impacts the mobilisation and oscillation of calcium ion release.

To investigate how mGlu₅ C-terminal phosphorylation affect G α_q signalling, calcium mobilisation experiments were performed using the wildtype and phosphodeficient mutant mGlu₅ receptor cell lines with the endogenous agonist glutamate and the group I mGlu receptor specific agonist (S)-3,5-dihydroxyphenylglycine (DHPG). To first confirm that the Flp-In™ T-REx™ 293 cell line does not express any endogenous glutamate receptors leading to calcium responses, experiments were first carried out on parental cells demonstrating that glutamate treatment resulted in no increase in intracellular calcium ion levels in these cells (Figure 4.8A). In contrast, in cells expressing mGlu₅-WT receptor, a clear concentration dependant increase in calcium mobilisation was observed following glutamate treatment, with pEC₅₀ of 6.0 ± 0.12 (Figure 4.8A). Concentration responses with similar potency to glutamate were observed in the mGlu₅-PD (6.1 ± 0.25) and mGlu₅-TPD (6.3 ± 0.16) expressing cells (Figure 4.8A). The E_{MAX} of mGlu₅-WT and mGlu₅-PD responses were comparable, while the E_{MAX} for the mGlu₅-TPD appeared somewhat greater, although this was not statistically significant (P=0.3672, one-way ANOVA) compared to wildtype.

The same trends were observed when using the agonist DHPG (Figure 4.8B). The pEC₅₀ value for mGlu₅-WT of 5.6 ± 0.05 was not significantly different to the value of 5.3 ± 0.06 for mGlu₅-PD (P=0.0518, one-way ANOVA) (Figure 4.8B). Additionally, there was no significant difference between the pEC₅₀ of wildtype receptor and mGlu₅-TPD (pEC₅₀ of 5.6 ± 0.10 , P=0.8364, one-way ANOVA) or between the mGlu₅-PD receptor and mGlu₅-TPD (P=0.1257, one-way ANOVA). The E_{MAX} for mGlu₅-TPD once again trended to be higher than the wildtype receptor and serine-only mutant, but this was not significant (P=0.2696 compared to wildtype, one-way ANOVA; P=0.2608 compared to mGlu₅-PD, one-way ANOVA) (Figure 4.8B).

To summarise, following treatment with glutamate there was no significant differences in the pEC₅₀ or E_{MAX} of response between wildtype receptor and

phosphodeficient mutants in the calcium mobilisation assay, although mGlu₅-TPD trended to have a higher maximal peak fura-2 ratio. These same trends were observed with treatment with the group I mGlu receptor-specific agonist DHPG.

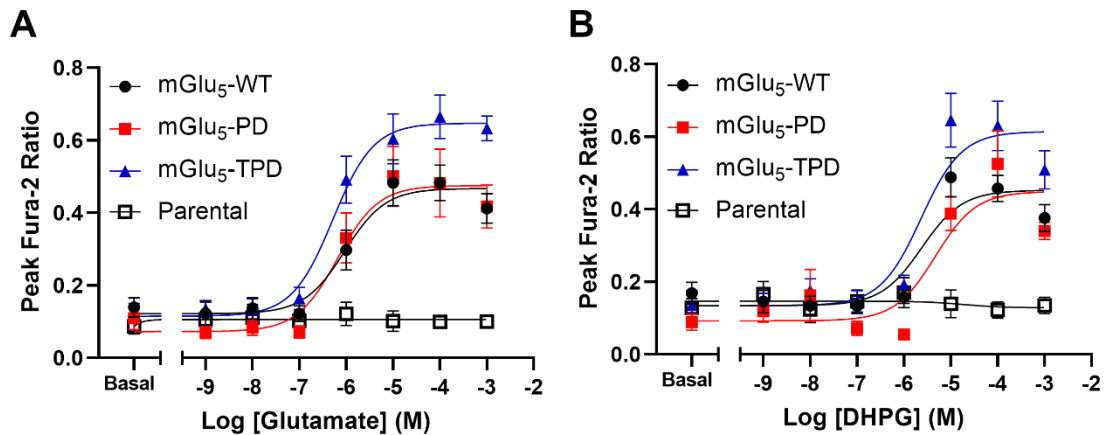


Figure 4.9: mGlu₅-TPD produces a higher peak Fura-2 ratio in the calcium mobilisation assay than mGlu₅-WT and mGlu₅-PD. Glutamate- (A) or DHPG- (B) induced calcium mobilisation was measured in parental Flp-In™ T-REx™ 293 cells or cells induced with 2 ng/mL doxycycline to express mGlu₅-WT, mGlu₅-PD and mGlu₅-TPD receptors, using Fura-2 AM dye. Data are expressed as means ± S.E.M of three independent experiments performed in triplicate.

To provide an understanding of the impact of mGlu₅ C-terminal phosphorylation sites on calcium signalling kinetics, single cell calcium analysis was performed. Whilst plate-based calcium experiments are efficient and can provide information on calcium mobilisation in whole cell populations, single cell calcium analyses provides information on the kinetics of the calcium release within each cell, thus insight into the temporal dynamics of the oscillations (Kawabata et al., 1996).

Looking at the mGlu₅-WT receptor subsequent to loading the stably expressing cells with fura-2 AM dye, there is a calcium response following treatment with 100 μM glutamate (Figure 4.9A). Similarly, there is an agonist-stimulated calcium response in the mGlu₅-PD (Figure 4.9B) and mGlu₅-TPD (Figure 4.9C) cell lines, consistent with the calcium mobilisation concentration response curves that were able to be produced previously (Figure 4.8). Quantifying the kinetics of this calcium flux for the mGlu₅-WT cell line reveals an initial large peak in the fura-2 ratio, followed by two smaller oscillations over the three-minute time period recorded (Figure 4.9D). Conversely, for the mGlu₅-PD

cell line (Figure 4.9E) and mGlu₅-TPD cell line (Figure 4.9F) there is one large initial peak followed by only one subsequent peak.

This difference in number of calcium oscillations compared to wildtype infers that there is an impact of C-terminal phosphorylation on the calcium mobilisation, with this effect being down to the serine residues. This can be assumed as mGlu₅-PD, in which C-terminal serine residues are mutated to alanine, exhibits this difference in number of oscillations compared to wildtype and there is no observable difference between mGlu₅-PD and mGlu₅-TPD.

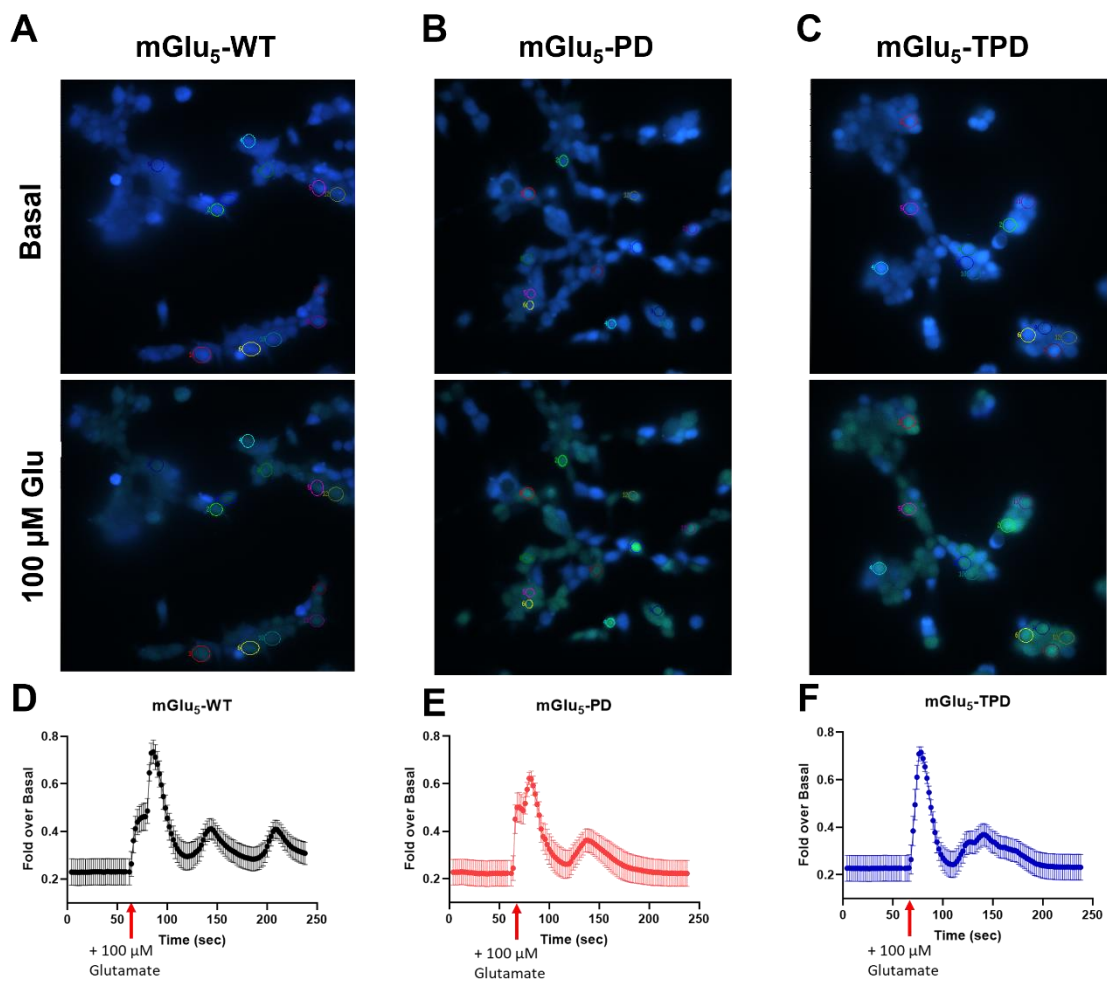


Figure 4.10: Removal of mGlu₅ C-terminal phosphorylation sites alters calcium oscillations. Single cell calcium analysis was performed in mGlu₅-WT (A), mGlu₅-PD (B) and mGlu₅-TPD (C) stable cell lines. Images represent cells at stable baseline and peak calcium mobilisation following stimulation with 100 μM glutamate (Glu). Images are representative of three independent experiments. (D-F) Quantification of single cell calcium imaging subsequent to stimulation with 100 μM glutamate for 60 seconds at the timepoint indicated by the red arrow. Data shown is the means ± S.E.M. of three independent experiments, where within each experiment 12 cells were selected for measurements as indicated by the circles in the representative images. Fluorescent images are 167 μm wide.

4.3.5 Removal of C-terminal Phosphorylation Sites of the mGlu₅ Receptor Reduces Ligand-Independent IP₁ Accumulation

In addition to calcium mobilisation experiments, inositol monophosphate (IP₁) accumulation assays were performed to provide a comprehensive analysis of the Gα_q protein-coupled signalling pathway and the impact of C-terminal receptor phosphorylation on said pathway. Both calcium ions and IP₁ are released upon activation of a Gα_q protein-coupled GPCR, but at different stages of the transduction pathway; IP₁ is a stable downstream product of PIP₂ hydrolysis, providing a measurement early on in the signalling process. This can be useful for studying the impact of phosphorylation, permitting observation of the stage of the G protein-dependent signalling cascade at which phosphorylation may have an impact. Measurement of IP₁ accumulation also permits measurement of constitutive activity, a measure that the calcium mobilisation experiments do not provide (Garbison et al., 2012). Performing both IP₁ accumulation and calcium mobilisation assays permits the teasing out of the specific stages of signal transduction affected by phosphorylation, in addition to cross validating findings from each assay format.

Initially, the cell number per well of the 96-well plate was optimised for the IP₁ accumulation assay. This assay measures total IP₁ accumulation in one hour, so it is expected that the number of cells in a well would affect the readout of IP₁ concentration. Too few cells may produce a low signal not strong enough to be detected over background readings, but too many cells may lead to over saturation and affect cell viability. Here, mGlu₅-WT cells were utilised and seeded at a variety of densities to examine the impact of increasing cell number on IP₁ accumulation. All cell numbers tested produced a concentration response curve following stimulation with the endogenous agonist glutamate (Figure 4.10A), indicating that cell viability was not impacted at high cell densities. There were no significant differences observed in the pEC₅₀ values (Figure 4.10B), however there was a trend of decreasing potency of glutamate with increasing cell number. A steady increase in the maximum amount of IP₁ produced was observed when increasing the cell seeding densities (Figure 4.10C), from 179.0 ± 15.47 nM produced by cells seeded at a density of 20,000 cells per well to 2137.0 ± 66.78 nM from cells plated at 160,000 cells per well (P<0.0001, one-way ANOVA). This

is to be expected; more cells in the well should in theory produce more IP₁, leading to an increasing readout of IP₁ concentration. An increase in the signal window span is also observed (Figure 4.10D); as the seeding density increases, the window of signal readout increases by 1023.7%, from a mean IP₁ concentration of 130.2 ± 18.48 nM produced by cells at a density of 20,000 cells per well to 1463.0 ± 74.89 nM produced by cells at a density of 160,000 cells per well ($P < 0.0001$, one-way ANOVA). However, this is relative to the increase in the basal amount of IP₁ produced; when the cell seeding density increased, basal IP₁ accumulation also increased (Figure 4.10E). As the number of cells per well increased, the concentration of IP₁ increased, from an IP₁ concentration of 47.6 ± 14.38 nM for 20,000 cells per well and 733.3 ± 47.37 nM for 160,000 cells per well ($P < 0.0001$, one-way ANOVA).

A Z' calculation was performed to further analyse the cell seeding density optimisation for the IP₁ accumulation assay. The Z' equation considers four assay parameters: the means (μ) of the maximum and minimum signal, and the standard deviations (σ) of these values. A Z' score of less than zero indicates too much overlap between the signal and noise to be a valid assay, 0-0.5 indicates an acceptable assay, and a score between 0.5 and 1.0 indicates an excellent assay (Zhang et al., 1999). When seeding 20,000 cells per well in a 96-well plate, a Z' score of -0.14 was achieved, indicating that this density is too low to detect IP₁ signal over the background (Table 4.3). A density of 40,000 cells per well produced an acceptable score of 0.42, however this was improved on when increasing the density; all densities tested from 60,000 to 160,000 cells per well produced a Z' factor indicating an excellent assay (Table 4.3).

Considering this, a mid-range cell seeding density of 80,000 cells per well was chosen as there was no significant difference in the pEC₅₀, a maximal response that was in range of the testing kit sensitivity, a sufficient Z' score, and a comparatively low ligand-independent activity compared to higher cell densities.

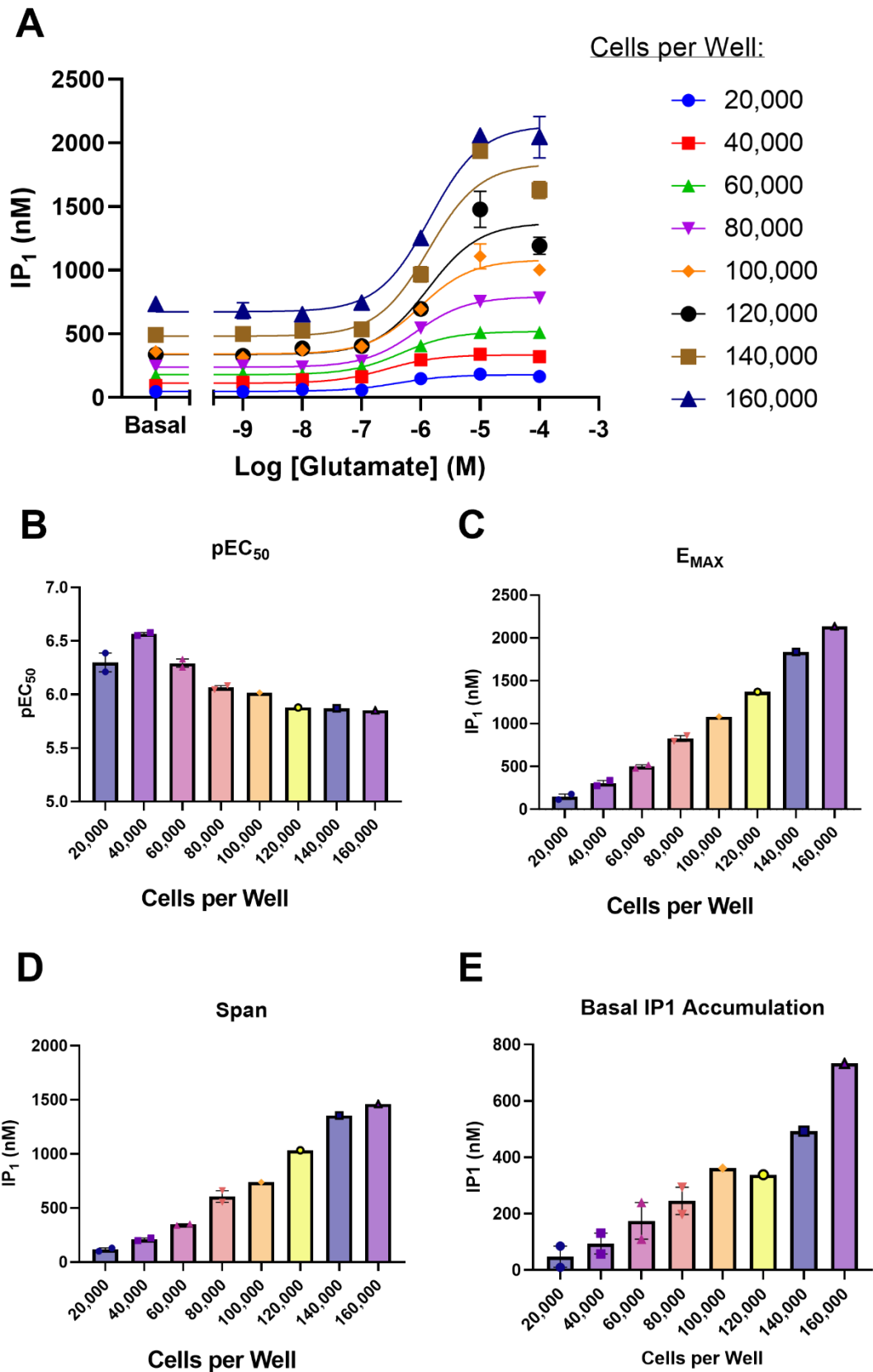


Figure 4.11: Optimisation of cell number in the IP₁ accumulation assay. (A) Concentration response curves for IP₁ accumulation in mGlu₅-WT cells following agonist stimulation. The potency (B), maximal response (C) and signal window span (D) were recorded to observe changes due to increasing cell number. Data are expressed as means \pm S.E.M. of one to two independent experiments performed in quadruplicate.

Table 4.3: The Z' score for IP₁ accumulation curves at increasing cell seeding densities.

| Cell Number | Z' Score |
|-------------|----------|
| 20,000 | -0.14 |
| 40,000 | 0.42 |
| 60,000 | 0.77 |
| 80,000 | 0.66 |
| 100,000 | 0.85 |
| 120,000 | 0.66 |
| 140,000 | 0.75 |
| 160,000 | 0.52 |

To determine the ideal concentration of doxycycline to use in functional assays, a doxycycline titration was performed in the IP₁ accumulation assay. All concentrations tested, including 0 ng/mL doxycycline, produced a concentration response curve subsequent to stimulation with the endogenous agonist glutamate (Figure 4.11A). The pEC₅₀ is not significantly different among the concentrations of doxycycline tested (Figure 4.11B), indicating no change in the potency of glutamate. Conversely, there are significant differences in the signal window span (Figure 4.11C) and the E_{MAX} (Figure 4.11D) with change in the doxycycline concentration. Utilising 2 ng/mL of doxycycline produced the greatest signal window span of response, 211.6% greater than 0 ng/mL doxycycline (P=0.0001, mixed effects analysis with Tukey's multiple comparisons test), and an E_{MAX} 162.1% greater than the cells without doxycycline treatment (P=0.0009, mixed effects analysis with Tukey's multiple comparisons test). However, upon increasing the doxycycline concentration, the basal level of IP₁ produced also increases (Figure 4.11E). From 0 ng/mL doxycycline to 100 ng/mL doxycycline, the ligand-independent concentration of IP₁ increases by 121.3% (P=0.0002, one-way ANOVA).

Altogether, the amount of doxycycline decided to be used for future functional assays was 2 ng/mL, as at this concentration a large signal window was achieved with a high maximal response (corroborating previous data from our laboratory), whilst the potency does not change and the basal IP₁ concentration is not too high.

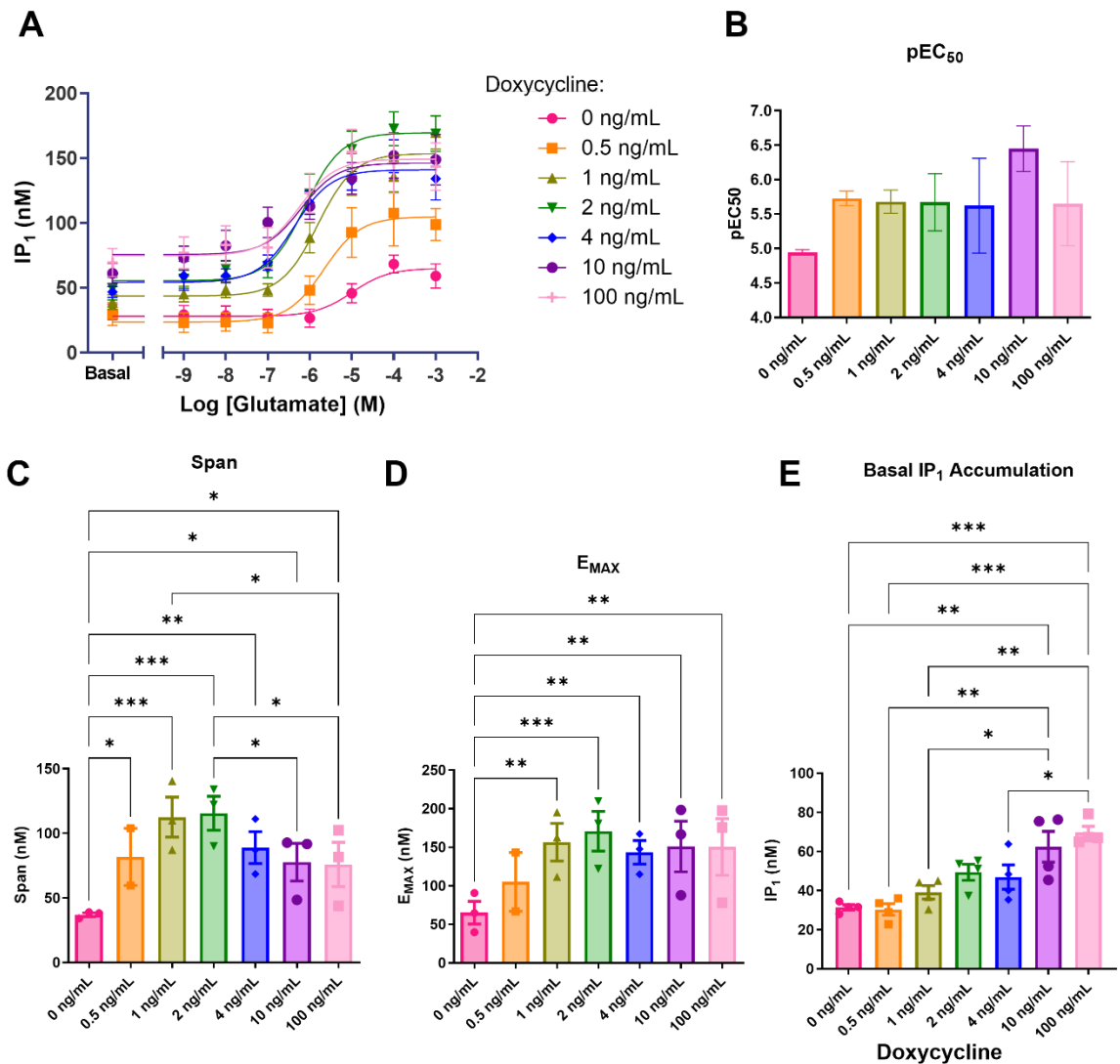


Figure 4.12: Generation of IP₁ increases with increasing concentration of doxycycline. (A) Concentration response curves showing IP₁ accumulation in mGlu₅-WT cells subsequent to 24 hr induction with increasing concentrations of doxycycline. The potency (B), signal window span of response (C), and maximal response (D) were noted from the concentration response curves for each doxycycline concentration. The ligand-independent IP₁ accumulation over the course of one hour was recorded as a measure of the constitutive activity (E). Data are expressed as means \pm S.E.M. of three independent experiments performed in quadruplicate. Statistical analysis performed was a mixed effects analysis with Tukey's multiple comparisons test (C,D) or a one-way ANOVA with Tukey's multiple comparisons test (E). * $P \leq 0.05$, ** $P \leq 0.01$, *** $P \leq 0.001$.

Once the appropriate concentration of doxycycline was determined, the assay was performed on cell lines induced with 2 ng/mL doxycycline to investigate how C-terminal receptor phosphorylation impacts the G α_q protein-coupled signal transduction. Utilising the endogenous agonist glutamate with these cell lines produced concentration response curves for all three receptors, yet no response was produced in the untransfected parental cells showing the response is specific to the receptors (Figure 4.12A). Similarly, when using the group I mGlu receptor specific agonist DHPG, there was IP₁ produced for all three receptors but not for

the parental cells (Figure 4.12B). When looking at the potency of glutamate in the IP₁ assay between the wildtype and phosphodeficient mutant receptors, there was a significant rightward shift and reduction in potency with removal of putative C-terminal phosphorylation sites; there was no significant difference in potency of glutamate at the wildtype receptor versus a C-terminal serine-deficient receptor ($P=0.9523$, one-way ANOVA), yet a significant decrease in potency was noted between mGlu₅-PD and mGlu₅-TPD ($P=0.0461$, one-way ANOVA) (Figure 4.12C), likely to be due to differing expression levels. Despite this, there was no significant difference in the E_{MAX} (Figure 4.12D) or signal window span of response to glutamate (Figure 4.12E). When treated with DHPG, the potency of the agonist trended to decrease with removal of C-terminal serine residues: a pEC₅₀ of 5.1 ± 0.26 was produced for the wildtype receptor, 4.7 ± 0.07 for the mGlu₅-PD receptor, and 4.4 ± 0.24 for mGlu₅-TPD (Figure 4.12F). Similar to that observed for the glutamate-treated cells, there was no significant change in E_{MAX} (Figure 4.12G) or signal window span of response to agonist (Figure 4.12H) when treated with DHPG.

When plotting the ligand-independent IP₁ produced by the receptors, there was a trend of decreased basal IP₁ with removal of putative phosphorylation sites in the mGlu₅ C-terminus. With the mGlu₅-PD receptor, the ligand-independent concentration of IP₁ produced was 22.1% lower than that produced by the wildtype receptor ($P=0.3794$, one-way ANOVA) (Figure 4.12I). Removing the C-terminal threonine residues, in addition to the serine residues, there was a decrease in ligand-independent IP₁ of 84.0% compared to that produced by the wildtype receptor ($P<0.0001$, one-way ANOVA) (Figure 4.12I).

In summary, there was no change in Gα_q protein-dependent signal transduction pathway between the wildtype and phosphodeficient mutant receptors in terms of the efficacy or signal window, however there was a trend of decreasing potency of both glutamate and DHPG agonists with removal of serine residues then furthermore with removal of serine and threonine residues. This difference is likely to be due to differences in the expression levels of the receptors in the cell line. Additionally, there was a decrease in the ligand-independent IP₁ produced from the wildtype receptor to the serine-deficient, and serine- and threonine-deficient receptors.

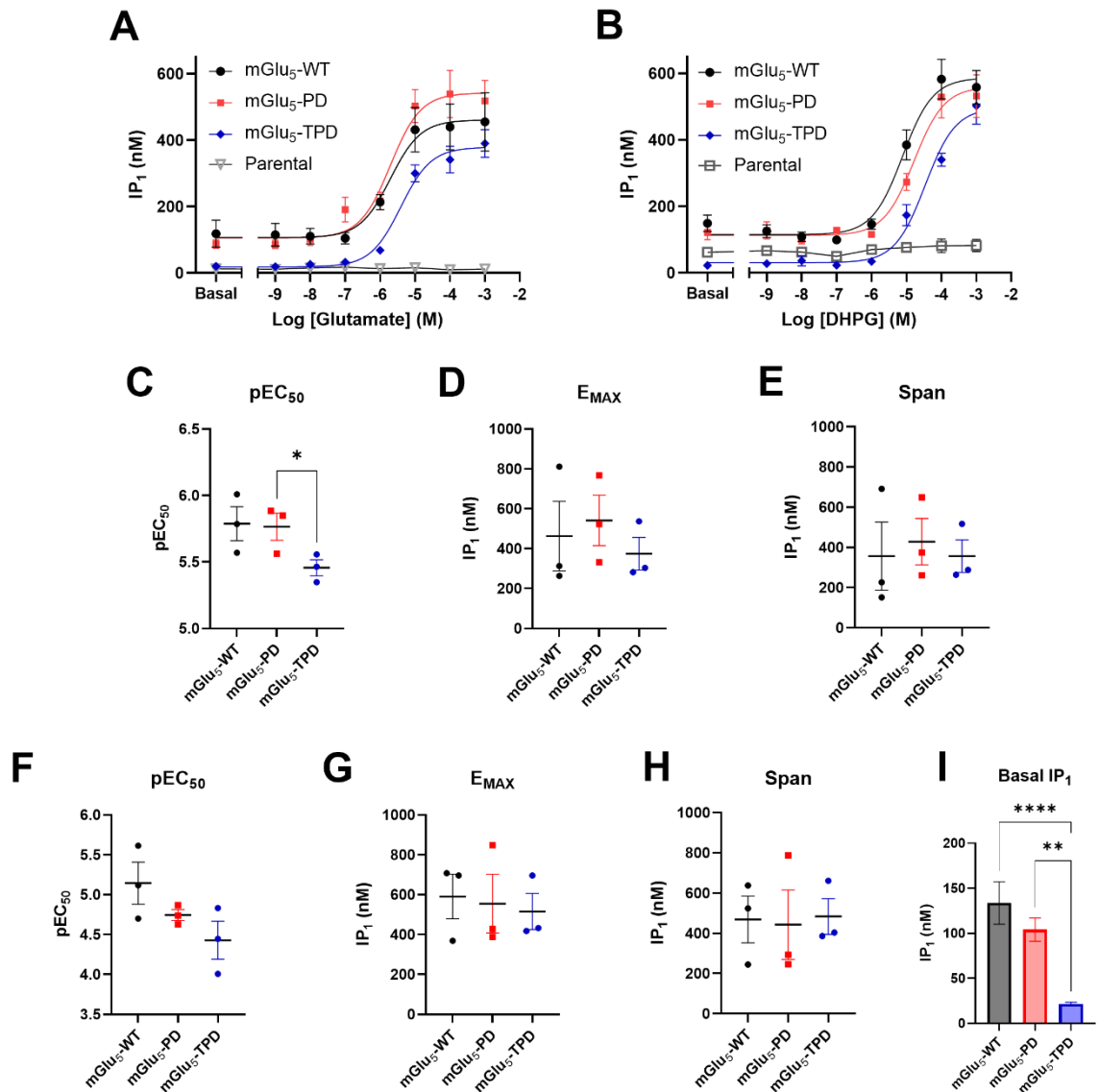


Figure 4.13: Mutation of mGlu₅ C-terminal serine and threonine residues decreases basal IP₁ release. Expression of mGlu₅-WT, mGlu₅-PD and mGlu₅-TPD receptors was induced 24-hours before the assay with 2 ng/mL of doxycycline, then the IP₁ accumulation was recorded after a 1-hour stimulation with glutamate (A) or DHPG (B). The pEC₅₀, E_{MAX}, and signal window span were recorded following the IP₁ accumulation after treatment with glutamate (C-E) or DHPG (F-H). (I) The ligand-independent basal levels of IP₁ produced by mGlu₅-WT, mGlu₅-PD and mGlu₅-TPD. Data are expressed as means ± S.E.M. of three independent experiments performed in quadruplicate. Statistical analysis performed was a one-way ANOVA with a Tukey post hoc test. * P ≤ 0.05, ** P ≤ 0.01, **** P ≤ 0.0001.

4.3.6 Removal of C-terminal Phosphorylation Sites of the mGlu₅ Receptor Reduces Constitutive Heterotrimeric G Protein Dissociation

To investigate the impact of receptor phosphorylation at a stage in the signalling pathway more proximal to the receptor than IP₁ or calcium mobilisation, an assay measuring heterotrimeric G protein dissociation was selected. This system, named TRUPATH, was developed by Olsen et al., (2020) to generate a suite of 14 BRET-based biosensors to measure heterotrimeric G protein dissociation with single pathway resolution. The G α protein is tagged with a luciferase, and the G γ is tagged with a fluorescent protein. These components are transiently transfected into HEK293T cells, with the receptor of interest and G β also being co-transfected. In resting state, the G protein heterotrimer is assembled and produces a high BRET signal, however upon receptor activation and G protein dissociation, there is a decrease in BRET recorded and the G proteins dissociate to activate further effector proteins (Figure 4.13A). Typically, this system involves transfecting multiple constructs: the receptor, G α -luciferase, G β , and G γ -fluorescent protein, all at a 1:1:1:1 ratio. Our laboratory has developed a novel version of this system termed 'NEWPATH', in which all three G protein components are expressed in one construct. There exists 16 different G α subunits, 4 major G β subunits and 12 G γ subunits, thus the appropriate combination of these proteins was selected for use with the mGlu₅ receptor, as advised by Olsen et al., (2020). The NEWPATH construct consists of the untagged G β 3 protein; the P2A sequence, which sits in between two genes of interest, causing ribosomal 'skipping' during translation to effectively separate the two genes of interest that flank it; G γ 9 tagged to mNeonGreen; the pIRES mammalian expression sequence which allows high level of expression of two genes of interest from the same mRNA transcript; and the G α_q protein tagged to nanoluciferase (Figure 4.13B).

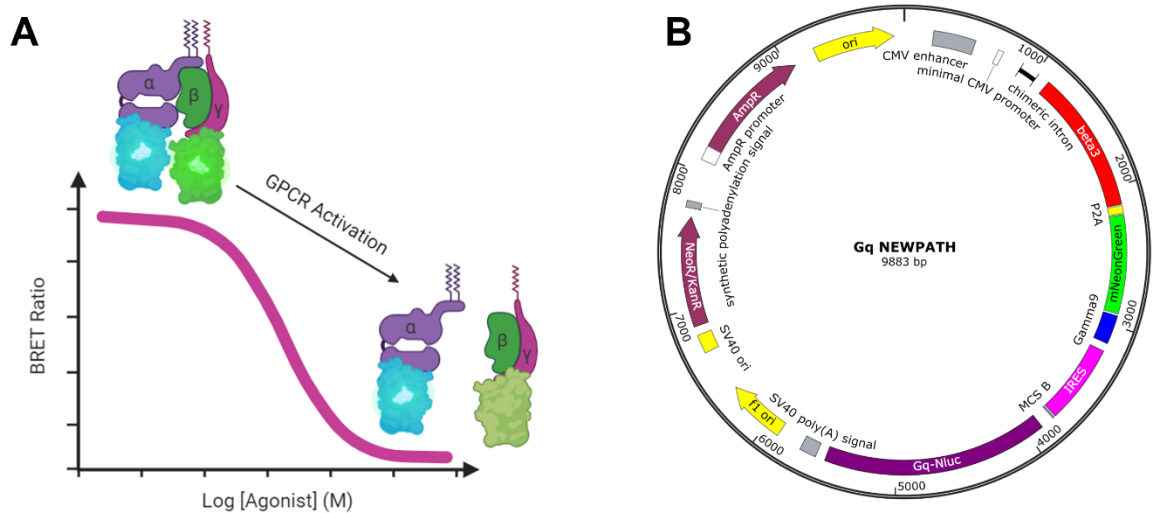


Figure 4.14: The TRUPATH paradigm can be encoded into a single plasmid, called 'NEWPATH'. (A) A schematic illustrating the effect of agonist-stimulated GPCR activation and G protein dissociation on the measurable BRET ratio. (B) A plasmid map depicting the components of the single $G\alpha_q$ -specific NEWPATH construct. A combination of $G\beta_3$ and $G\gamma_9$ was selected to pair with the $G\alpha_q$ protein.

To measure the G protein activation, increasing amounts of the receptor of interest were transiently transfected into HEK293T cells with the NEWPATH plasmid. The M1 muscarinic receptor, a receptor shown to robustly couple to the $G\alpha_q$ protein-coupled signal transduction pathway, was selected as a positive control. When using the mGlu5-WT receptor with the $G\alpha_q$ NEWPATH biosensor, no clear concentration response curves were observed in response to stimulation with glutamate, however a concentration response curve was successfully achieved with the M1 positive control (Figure 4.14A). This indicates a lack of glutamate-stimulated $G\alpha_q$ protein dissociation at the mGlu5-WT receptor. A similar effect was observed for both the mGlu5-PD (Figure 4.14B) and mGlu5-TPD (Figure 4.14C) receptors. Whilst the agonist-stimulated activation of the M1 receptor indicates that the NEWPATH biosensor is successful at measuring $G\alpha_q$ protein dissociation from $G\gamma_9$ in response to agonist treatment, there is no clear heterotrimeric G protein activation stimulated by agonist treated wildtype or phosphodeficient receptor mutants. However, looking at just the ligand-independent heterotrimeric G protein dissociation reveals that there is significant G protein dissociation compared to the pcDNA3 empty vector control: with the mGlu5-WT receptor, there is a significant trend of lower BRET ratio as the amount of receptor increases (Figure 4.14D). Transiently transfecting in 250 ng of wildtype receptor per well of a 6-well plate gives a 48.9% decrease in BRET from pcDNA3 ($P < 0.0001$, one-way ANOVA), indicating high constitutive activity over the basal G protein activation in the cells.

There is no significant difference between the lowest amount of wildtype receptor transfected and pcDNA3 control, a decrease of 4.5% ($P=0.2186$, one-way ANOVA). Similarly, a significant trend of increasing basal G protein activation with increasing amounts of receptor is observed for the C-terminal serine-deficient mutant mGlu₅ receptor. The decrease in basal BRET ratio from pcDNA3 to that produced by transfecting 250 ng of mGlu₅-PD is 29.5% ($P<0.0001$, one-way ANOVA). The difference in the decrease between pcDNA3 and wildtype and between pcDNA3 and mGlu₅-PD is 19.4%. Furthermore, there are no significant differences observed in the basal BRET ratio in the NEWPATH assay between any of the receptor amounts transfected for the mGlu₅-TPD receptor. There is a difference of only 4.8% between 250 ng mGlu₅-TPD and pcDNA3 ($P=0.8907$, one-way ANOVA), and there was a slight increase of 7.7% between 1 ng of receptor and pcDNA3 ($P=0.4133$, one-way ANOVA).

When comparing the ligand independent heterotrimeric G protein dissociation between the wildtype and phosphodeficient mutant mGlu₅ receptors at the highest amount of receptor transfected, there is a significant difference. Firstly, there is no significant difference in the basal BRET between the M1 receptor and pcDNA3 empty vector control ($P=0.3632$, one-way ANOVA), demonstrating that the M1 receptor exhibits little to no constitutive activity (Figure 4.15). The wildtype mGlu₅ receptor exhibits high constitutive activity, revealed by the low basal BRET ratio, 51.1% of pcDNA3 BRET ratio, meaning high levels of G protein dissociation (Figure 4.15). The mGlu₅-PD receptor also exhibits high constitutive activity compared to the M1 receptor, a decrease in the BRET ratio of 41.2% ($P<0.0001$, one-way ANOVA) (Figure 4.15). However, this observed constitutive activity is significantly reduced compared to wildtype, giving a basal BRET ratio with an increase of 15.0% compared to wildtype ($P=0.0288$, one-way ANOVA) (Figure 4.15). Further still, the mGlu₅-TPD receptor demonstrates less basal activity than the mGlu₅-PD receptor, increasing from a mean of 60.22% of pcDNA3 BRET ratio for mGlu₅-PD to 76.79% of pcDNA3 for mGlu₅-TPD ($P<0.0001$, one-way ANOVA) (Figure 4.15). Despite this trend of decreasing constitutive activity with removal of C-terminal phosphorylation sites, the mGlu₅-TPD receptor still exhibits significantly different basal BRET ratio to pcDNA3 (a decrease of 30.2%, $P<0.0001$, one-way ANOVA), indicating that whilst constitutive activity at the mGlu₅-TPD receptor is reduced compared to that of wildtype, the receptor still shows constitutive activity over empty vector control.

It is clear that the wildtype and phosphodeficient mutant receptors couple to the $G\alpha_q$ protein-coupled pathway because although the signal windows were small, IP_1 and calcium responses were still recorded for each receptor. Taken together, these data from the NEWPATH BRET system indicate that phosphorylation of C-terminal serine and threonine residues play a role in the basal activity of the mGlu₅ receptor, as the basal G protein heterotrimer dissociation was high for wildtype receptor but trended to be not as high when C-terminal serine residues were mutated, then further reduced when additionally removing C-terminal threonine residues.

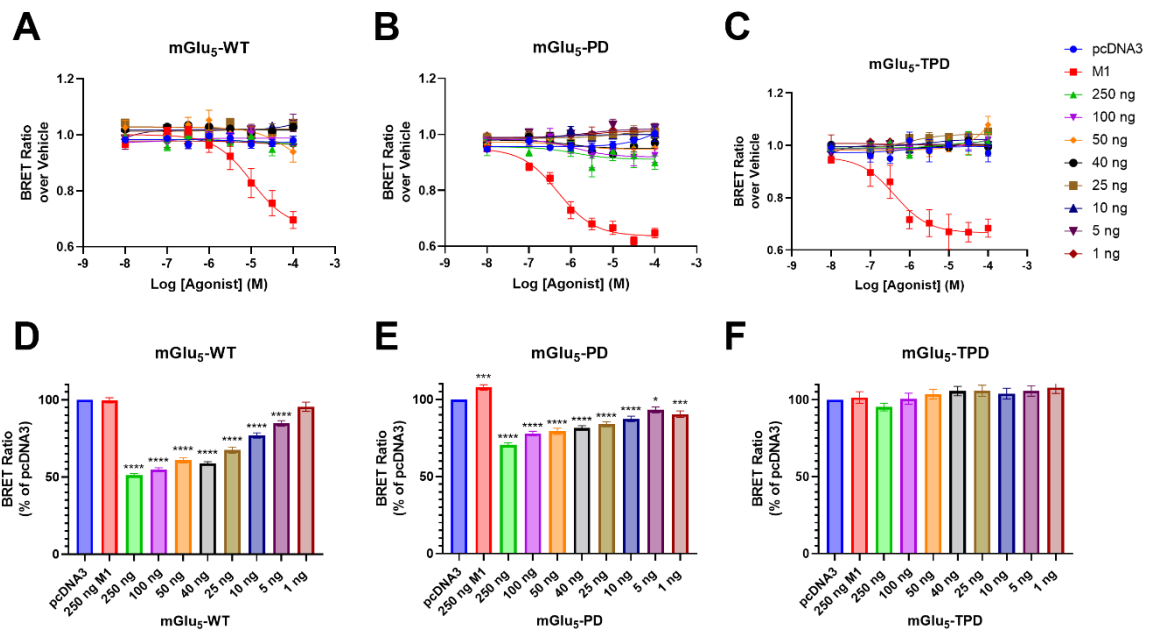


Figure 4.15: Mutation of mGlu₅ C-terminal phosphorylation sites reduces $G\alpha_q$ constitutive activation. Titration of the mGlu₅-WT (A), mGlu₅-PD (B), and mGlu₅-TPD (C) in the NEWPATH heterotrimeric G protein dissociation assay in response to stimulation with the agonist glutamate, increasing the amount of DNA of the receptor of interest per well of a 6-well plate. The basal G protein dissociation was measured as an indicator of constitutive activity for the mGlu₅-WT (D), mGlu₅-PD (E) and mGlu₅-TPD (F) receptors. Statistical analysis performed was a one-way ANOVA compared to pcDNA3, with Tukey post hoc test to control for multiple comparisons. * $P \leq 0.05$, *** $P \leq 0.001$, **** $P \leq 0.0001$.

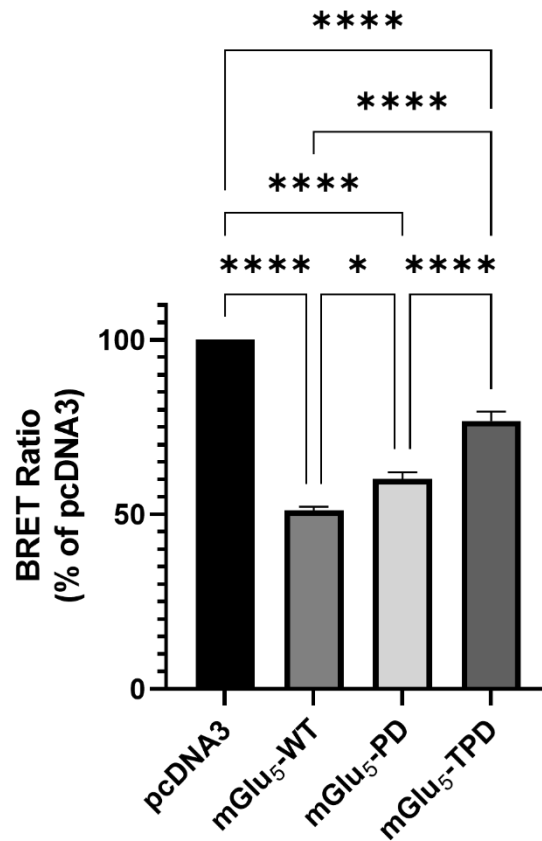


Figure 4.16: Basal BRET ratio from the NEWPATH assay, a measure of constitutive activity, is significantly different with removal of putative C-terminal mGlu₅ phosphorylation sites. The basal G protein dissociation was measured following transfection of 250 ng of receptor in a 6-well plate as an indicator of constitutive activity for the mGlu₅-WT, mGlu₅-PD and mGlu₅-TPD receptors compared to pcDNA3 empty vector control and the M1 muscarinic receptor positive control. Statistical analysis performed was a Kruskal-Wallis test, with Dunn's post hoc test to control for multiple comparisons. * $P \leq 0.05$, **** $P \leq 0.0001$.

4.4 Discussion

In this chapter, following generation of Flp-In™ T-REx™ 293 cell lines and demonstration of robust receptor expression in said cell lines, the signalling profiles of mGlu₅-PD and mGlu₅-TPD were assessed using *in vitro* pharmacological assays and compared to that of mGlu₅-WT to provide information on the mechanisms underlying phosphorylation-dependent signal transduction. Differences in calcium oscillations, basal IP₁ signalling, and constitutive Gα_q protein activation were noted between the wildtype and phosphodeficient mGlu₅ receptors. The differences in calcium oscillations were found to be attributed to C-terminal serine residues, whilst the decrease in ligand-independent IP₁ concentration and Gα_q protein activation was seen following mutation of both serine and threonine residues.

The Flp-In™ T-REx™ 293 inducible receptor expression system, developed by Invitrogen Life Technologies, has been widely used due to its many advantages over transiently transfected cells (Ward et al., 2011). This cell model permits integration of a gene of interest into a defined location in the genome, which allows for stable expression following treatment with a tetracycline, providing precise temporal control of gene expression. This inducible expression also permits finely tuned modulation of receptor expression and thus assessment of how the receptor expression level affects signalling. However, there are also complications of the Flp-In™ T-REx™ system, most notably that it can sometimes be 'leaky' and exhibit expression of the gene of interest without tetracycline treatment. This brings about issues particularly when relying on uninduced cells as a control group. In this work, the leakiness of this system presented itself in the IP₁ accumulation assay, where cell lines were treated with a range of doxycycline concentrations to induce mGlu₅ expression and yet the cells in the absence of doxycycline still produced an effective response to glutamate. This contrasts to the parental cells, in which no IP₁ is generated following agonist stimulation, indicating that these cell lines are indeed expressing the mGlu₅ receptor constructs independent of doxycycline treatment. The lack of response in the parental cells is also consistent with microarray analysis performed by Atwood et al., (2011) showing that HEK293 cells do not endogenously express mGlu₅. The western blot analysis of expression does not detect any protein consistent with the mGlu₅

receptor in the absence of doxycycline, yet here in the IP₁ assay there is Gα_q protein-coupled pathway activation recorded. Western blots may not detect proteins expressed at low levels whereas *in vitro* signalling assays may be more sensitive (Ghosh et al., 2014), hence the IP₁ assay here may be recording true mGlu₅ expression that was not revealed in the western blot.

The Flp-In™ T-REx™ 293 cell lines demonstrated robust receptor construct expression, providing a suitable tool to permit measurement of the pharmacological output of the receptor. Controlling the amount of receptor expression induced is advantageous specifically for the glutamate receptors, as it helps overcome issues relating to basal glutamate release: the metabolism of glutamine in the cell culture media to glutamate, in addition to cells releasing glutamate into the medium, contributes to constitutive signalling by mGlu receptors (Desai et al., 1995). Hence, it is useful to have an expression system in which the glutamate receptor is not persistently expressed to reduce the impact of this constitutive signalling.

Ward et al. (2011) showed that when using the Flp-In™ T-REx™ 293 cell line to control expression of the ghrelin receptor, turning on expression of the receptor of interest causes rounding of cells and poor viability. This was proposed to be due to the ghrelin receptor being a highly constitutively active Gα_q protein-coupled receptor, as cells appeared healthier when a ghrelin receptor specific inverse agonist or an inhibitor of Gα_q proteins was applied (Ward et al., 2011). This phenomenon was observed in this work when observing routinely cultured mGlu₅ cell lines; upon treatment with doxycycline and induction of receptor expression, the cells tended to have a rounder physiology and became clumped together, most notably for the wildtype receptor. As with the features observed with the ghrelin receptor, this change in cell morphology could be due to the wildtype mGlu₅ receptor's high basal signalling. Considering this, it confirms that the Flp-In™ T-REx™ inducible expression system was a good choice of *in vitro* receptor expression model, due to the ability to 'switch on' the expression of the receptor providing the ability to maintain mGlu₅ expression at very low levels during growth, circumventing issues with constitutive activity and cell viability during cell line maintenance.

When looking at the detection of mGlu₅ expression using the C-terminus in western blot analyses, there is a trend of decreasing expression of the dimer with removal of phosphorylation sites; this could be a true trend in expression, or it

could be the fact that the antibody binds to the C-terminus of the receptor and the C-terminus has been altered in the phosphodeficient mutant receptors, hence this may affect the binding of the antibody. Measuring the dimeric mGlu₅ receptor expression using an N-terminal binding antibody (to circumvent the issue of using an antibody that recognising the mutated region of the receptor) also demonstrates a trend of decreasing dimer expression with mutation of C-terminal putative phosphorylation sites. The C-terminal mutation of the receptor is not expected to directly affect dimer formation, as the mGlu₅ dimer is linked via an intermolecular disulphide bridge at Cys140 in the extracellular N-terminal domain, 17 kDa from the distal end of the N-terminus (Kunishima et al., 2000; Romano et al., 1996). Clearly, mutating C-terminal serine and threonine residues has an impact on expression of the dimer, yet the mechanism for such phenomenon is unclear. The alteration of C-terminal serine and threonine residues to alanine may impact the structure of the receptor or ability to be trafficked from the endoplasmic reticulum, where the dimer forms (Robbins et al., 1999), to the membrane, indicated by the reduction in dimer expression in whole cell lysates.

In the on-cell western analysis utilising the N-terminal binding antibody, signal is obtained from solely the plus doxycycline sample condition, indicating receptor can be detected by this antibody and better than in the traditional western blot. Permeabilising these cells and applying the N-terminal antibody results in more non-specific binding, as the antibody has access to more intracellular proteins to non-specifically bind to. Unexpectedly, there is slight signal obtained from using the C-terminal binding antibody on cells that were not permeabilised. In hindsight, this could be due to the fixation process: commercially available formalin used for fixing cells contains methanol at a concentration of ≤ 1 to $< 3\%$ to generate hemiacetal/acetal compounds which prevent the precipitation of the formaldehyde (Alonso-Buenaposada et al., 2016). Methanol dissolves the membranes of cells, providing a potential explanation for why signal is detected from the C-terminal antibody in non-permeabilised cells.

In the calcium mobilisation assay, a similar maximum response is generated for wildtype and mGlu₅-PD, equivalent trends to that found by Butcher et al., (2014) for the FFA4 receptor, using a C-terminal truncated receptor as a phosphodeficient receptor, finding no difference in E_{MAX} between wildtype and the truncated receptor. The increase in E_{MAX} from mGlu₅-TPD cells compared to

wildtype could be explained by the lack of phosphorylation sites preventing receptor desensitisation and internalisation, meaning more cell surface receptor expression leading to a higher calcium response. To address this, cells could be pre-treated with an mGlu₅ antagonist or negative allosteric modulator to reduce the basal level of glutamate receptor activation, wash the drug off, then perform the agonist-stimulated calcium assay to see if the increased E_{MAX} as seen for the mGlu₅-TPD receptor is seen for the wildtype receptor. In addition, the constitutive signalling of the receptor may explain why the observed peak calcium ratio is relatively low compared to that seen for other Gα_q coupled-GPCRs (Bradley et al., 2020; Liu et al., 2008); the ligand independent receptor activity or basal glutamate released by the cells raises the baseline Gα_{q/11} activation, therefore the agonist can only further increase the response a limited amount from this point. Abreu et al., (2021) found that mGlu₅ calcium transients were reduced with GRK2 expression, indicating a role for phosphorylation in calcium response. This is consistent with these studies; removal of a receptor's ability to be phosphorylated (mGlu₅-TPD) increases calcium response compared to wildtype.

It is well established that phosphorylation of mGlu₅ induces calcium oscillations, caused by rapid dynamic cycles of phosphorylation and dephosphorylation (Bradley & Challiss, 2011; Kawabata et al., 1996; Nakahara et al., 1997). When observing the single cell calcium oscillations here, there was a difference between phosphodeficient mutant receptor and wildtype, with no difference in the oscillations produced by mGlu₅-PD and mGlu₅-TPD, indicating that the change in calcium oscillations is due to C-terminal serine residues not threonine residues. This is consistent with the literature: it was previously thought that phosphorylation of threonine at position 840 by protein kinase C was responsible for the observed calcium oscillations (Kawabata et al., 1996), however subsequent studies examining this have determined that this threonine plays a permissive role, and it is in fact serine at position 839 that controls the oscillations (Kim et al., 2005). This group also demonstrated that mutation of Thr840 to alanine, thus preventing phosphorylation of this residue, has no observable impact on calcium oscillations further supporting the view that the calcium oscillations are due to phosphorylation of Ser839. This is consistent with the results demonstrated here: there was a difference in number of calcium oscillations compared to wildtype with the receptor containing mutated serine residues, but there was no change between the serine mutant and the threonine and serine mutant. Despite

Butcher et al., (2014) finding no difference in the calcium response between the FFA4 receptor and a C-terminal truncated receptor, Alvarez-Curto et al. (2016) discovered that the kinetics of the calcium response differed between the FFA4 receptor and a phosphodeficient mutant FFA4 receptor. Here, there was no difference between wildtype and mGlu₅-PD in the plate-based calcium mobilisation assay, but the single cell calcium analysis revealed differing kinetics of release.

In the IP₁ accumulation assay, there was a trend of decreasing potency of the agonists DHPG and glutamate with mutation of C-terminal serine residues, with a further decrease in potency with additional mutation of threonine residues. This may be attributed to the observed lower expression levels of mGlu₅-PD and mGlu₅-TPD compared to wildtype receptor. The most plausible explanation relates to a change in receptor efficacy, meaning a larger pool of cell surface receptors need to be active to achieve the same response. This change in potency with mutation of the receptor's C-terminus was observed by Butcher et al. (2014) in their FFA4 construct with a C-terminal truncation; a decrease in agonist potency was observed in the TUG-891 stimulated β -arrestin 2 recruitment and is proposed to be due to the GPCR and arrestin protein forming a high-affinity, agonist-bound complex. Conversely, there was no significant change in the E_{MAX} or signal window span between mGlu₅-WT and mGlu₅-PD, an equivalent trend to that previously seen for the M1-PD receptor (Scarpa et al., 2021).

There was a significant decrease in the basal IP₁ produced with mutation of both serine and threonine residues in the mGlu₅ C-terminus. This indicates that in this context removing C-terminal serine and threonine residues affects G protein-dependent signalling but removing serine residues alone does not. The western blot data revealed that there were no issues in the structure and expression of the receptor, thus it cannot be attributed to issues in the formation and translocation of the receptor. Additionally, it is well established that receptors in the glutamate family need to be in a dimeric conformation to transduce extracellular stimuli to intracellular signals (Bai, 2004; Kunishima et al., 2000; Romano et al., 1996, 2001). Glutamate binds in the VFT, triggering conformational changes that are transmitted through the cysteine-rich domain, to the conserved 7TMDs which establish an asymmetric TMD6-TMD6 interface, promoting conformational change of the intracellular surface of one protomer, which couples to the intracellular G protein (Koehl et al., 2019; Seven et al., 2021). These hydrophilic interactions

between intracellular loop 1 and the intracellular side of TMD6 have to be disrupted to reach a theoretically active-like conformation (Lans et al., 2020). The phosphodeficient mutant receptor mGlu₅-TPD has less dimeric formation and expression than wildtype receptor as shown by the western blot analysis, indicating that the C-terminal serine and threonine residues somehow play a role in formation and expression of the dimeric receptor. The observed effect on G protein-dependent basal signalling could be due to the receptor needing to be in a dimeric conformation to elicit a signalling response (Romano et al., 1996), and the lower dimer expression level seen with the mGlu₅-TPD mutant in the western blot analysis reflects as the reduced amount of basal IP₁ produced. I have demonstrated that following mutation of C-terminal serine residues of the mGlu₅ receptor to alanine residues, the resulting phosphodeficient receptor retains the ability to couple to the G α_q signalling pathway, with the demonstration of altered calcium oscillations. Mutation of C-terminal serine and threonine residues demonstrated a significantly reduced level of basal IP₁ compared to solely serine residue mutation. This may be due to either signalling from a constitutively active receptor, or due to constitutive glutamate release activating the receptor.

IP₁ accumulation assays and calcium mobilisation assays are both used to study GPCR signalling pathways, but they measure different downstream events and have distinct methodologies and applications. The two key advantages of the IP₁ assay over measuring calcium mobilisation is the ability to measure slow-acting compounds, and the ability to characterise inverse agonists (Trinquet et al., 2011). The main advantage in this case is that the constitutive activity of the receptor can be better measured in an IP₁ assay than in the calcium mobilisation assay. The calcium mobilisation assay is transient, recording the release of calcium ions over the course of 90 seconds, compared to the IP₁ accumulation assay in which the sum of the IP₁ produced over the course of 60 minutes is measured. The advantage of measuring the IP₁ accumulation is that it is more proximal to the GPCR and more stable and less prone to transient fluctuations compared to calcium signalling. The IP₁ assay is dependent on cell number, whilst calcium ion mobilisation assay is a true ratiometric measure and not conceptually dependent on cell number at all. The calcium assay provides an immediate readout of receptor activity with high temporal resolution, capturing real-time monitoring of cellular response and rapid changes in calcium ion release.

In summary, IP₁ accumulation and calcium mobilisation assays are complementary techniques used to study Gα_q receptor signalling. IP₁ assays offer stability and suitability for long-term and high-throughput studies, providing an indirect but sustained measure of activation. In contrast, calcium mobilisation assays offer real-time insights into rapid signalling events with high temporal resolution, directly reflecting intracellular calcium ion changes.

When using the NEWPATH system to measure heterotrimeric G protein dissociation, it is unclear why this assay shows no Gα_q activation in response to agonist stimulation for mGlu₅-WT, mGlu₅-PD and mGlu₅-TPD, even though Gα_q protein-coupled pathway activation was measured through IP₁ accumulation and calcium mobilisation assays. This lack of response could be the receptor not responding to glutamate in this assay, or the agonist potency is shifted, and the correct concentrations of the agonist were not tested, or it could be an error in removing the endogenous glutamate in the cells leading to high basal activity. The basal BRET ratio in the NEWPATH assay, a measure of basal activation, indicates that phosphorylation of serine and threonine residues plays a role in the basal heterotrimeric G protein dissociation. The wildtype receptor exhibited high levels of basal activity, indicated by the significantly lower basal BRET ratio compared to pcDNA3 empty vector control, meaning high levels of G protein dissociation in the absence of glutamate treatment. This trend was present, but less pronounced, with the mGlu₅-PD receptor, and further reduced to a level where there was no significant difference between pcDNA3 and the mGlu₅-TPD receptor. This impact of phosphorylation on basal activity was also observed in the IP₁ assay, where removal of putative C-terminal phosphorylation sites reduced the basal IP₁ accumulation. Despite the calcium assay not permitting measurement of constitutive activity, the bigger signal window observed for mGlu₅-TPD in this assay could be due to the reduced constitutive activity reducing the basal signalling, permitting a larger signal window. Constitutive activity of the mGlu₅ receptor has influence on synaptic modulation, neuroprotection, and excitotoxicity (Niswender & Conn, 2010), all three of which are implicated in a multitude of neuropathologies including Fragile X syndrome, schizophrenia and anxiety, thus constitutive activity has pharmacological considerations for drug development. Inverse agonists that stabilise the inactive receptor conformation reduces the

constitutive activity, which may be useful in disorders in which mGlu₅ activity contributes to pathological states.

4.5 Conclusion

In conclusion, the *in vitro* data presented in this chapter imply that mutation of serine and threonine residues from the C-terminus of mGlu₅ present no significant differences in the impact on the glutamate-stimulated G protein-coupled transduction pathway, but instead impacts the basal ligand-independent G protein activation in the cells. This begins to define a function of direct mGlu₅ phosphorylation in the G protein-coupled transduction pathway.

To further explore the impact of phosphorylation on the G protein-coupled transduction pathway, Chapter 5 generates and optimises a genetically encoded biosensor to explore the activation of Gα_q protein-coupled pathway activation.

5 Developing a Genetically Encoded Biosensor to Directly Measure mGlu₅ Gα_q Protein Activation

5.1 Introduction

In recent years, the use and development of biosensors to deconvolute the complex pharmacology of GPCRs has increased (Olsen & English, 2023). These systems provide resources to measure response to stimuli on a microscopic level, to measuring global cellular changes on a macro level. Generating a biosensor to examine mGlu₅ G protein activation in the context of phosphorylation can provide several significant advantages for understanding receptor signalling and developing therapeutic interventions. The limitations of biosensors previously used in this work, *i.e.* NEWPATH and NanoBiT, include limited dynamic range and the requirement to overexpress G proteins tagged with BRET donors and acceptors in optimal proportions in limited cell lines (DiBerto et al., 2022; Janicot et al., 2024). To bypass these issues, an alternative biosensor system should be selected in which the receptor is not interfered with, the appropriate BRET donor and acceptor pairing is selected, and there is the opportunity for high dynamic range.

A biosensor permits real-time monitoring of mGlu₅ receptor G protein activation. This is crucial for understanding the dynamics of G protein activation and how it is influenced by phosphorylation. Additionally, biosensors can be applied in more relevant cell models such as primary cell lines, permitting the study of endogenous receptor function providing a more comprehensive understanding of the role of the receptor. A sensor that can measure endogenous G α_q activation at the cell membrane, which can also be applied to study endogenous receptors, is advantageous predominantly due to the physiological relevance. Overexpression of receptors can lead to artificial signalling responses that do not reflect normal cellular behaviour, hence measuring GPCR activity in their native environment leads to more reliable insights (Janicot et al., 2024). Ability of a biosensor to measure native GPCRs allows the study of receptor function in a range of cell types, broadening the scope of research and accommodating tissue-specific receptor bias.

5.1.1 BRET-Based Biosensors

An array of biosensors exists for monitoring G protein activation, each with their advantages, disadvantages, and limitations. Genetically encoded resonance energy transfer (RET) biosensors can be intermolecular, tagging two separate

proteins, or intramolecular, tagging a protein in a single construct (Hudson, 2016). These biosensors can directly measure G protein activation in real time in living cells to understand the basic biology of GPCR activation, the pharmacology of novel drugs, or explore pathophysiology. Typical GPCR second messenger assays as a measure of G protein activation are compromised by signal amplification and pathway crosstalk (Maziarz et al., 2020), whereas utilising BRET-based biosensors provide a sensitive measure of G protein activation, with high temporal and spatial resolution, and precise direct measurement of G protein activity (Lohse et al., 2012).

BRET highly relies on the conformation of the receptor and location of the donor and acceptor molecules. BRET-based sensors have some limitations: early BRET-based biosensors could only measure heterotrimeric G protein subunit dissociation, but not $G\alpha$ -GTP formation which would be the most direct readout of GPCR-mediated activation. Maziarz et al. (2020) generated a novel biosensor and is the first described biosensor able to detect $G\alpha$ -GTP formation in fully native conditions with endogenous GPCRs without compromising downstream signalling.

5.1.1.1 BERKY Biosensors

BRET biosensors with a glutamic acid, arginine, and lysine (ER/K) linker with yellow fluorescent protein (YFP) (BERKY) are a suite of biosensors employed to measure endogenous G protein activation through detection of $G\alpha$ -GTP, the most defining event in G protein activation. The BERKY-style biosensors are structured as follows: the unimolecular biosensor is anchored at the lipid membrane via an 11-amino acid long lipid anchor sequence. Functioning as a separator between the BRET donor and acceptor modules (nanoluciferase and YFP respectively), the ER/K linker is comprised of glutamic acid (E), arginine (R), and lysine (K) residues generating a single alpha-helix with a length of approximately 10 nm, to minimize BRET under resting conditions (Sivaramakrishnan and Spudich, 2011; Maziarz et al., 2020). A biosensor detection module should fit the following three requirements for high specificity, sensitivity and fidelity: the detector should bind to $G\alpha$ -GTP but not $G\alpha$ -GDP, should bind reversibly but with high affinity for the target, and should not affect the activity of the target G protein (Maziarz et al., 2020). For a $G\alpha_q$ -specific biosensor,

the detector module used was the regulator of G protein Signalling (RGS) homology (RH) domain of GRK2 (GRK2RH). This domain binds with reversible high specificity and affinity to $G\alpha_{q/11}$ bound to GTP without disturbing the fundamental function (Carman et al., 1999).

This biosensor style is similar to the systematic protein affinity strength modulation (SPASM) style biosensors which typically involve fusion of a biosensor at the C-terminus of the $G\alpha$ protein to the intact GPCR (Malik et al., 2013). With these biosensors, it was found that the ER/K linker length tunes the GPCR-G protein interaction and consequently the second messenger signalling. Advantage of SPASM sensors is that they have the purpose of detecting agonist-induced changes in G protein activation, and links this to signalling pathways further downstream (Malik et al., 2017). Whilst SPASM biosensors are designed to measure GPCR activity in artificial systems, BERKY biosensors have been optimised to measure endogenous GPCR activation.

The BERKY-SPASM style biosensor was selected here for optimisation for monitoring mGlu₅ G protein activation due to the unimolecular structure permitting use in live cells, enabling non-invasive measurements of receptor activity without perturbing cellular function, which is particularly important for studying the physiological relevance of receptor signalling in its native cellular environment. Additionally, because these biosensors are genetically encoded, they can minimise disturbance of native cellular systems. The biosensors allow for real-time monitoring of receptor activation and signalling events. This is crucial for capturing the dynamic processes involved in GPCR signalling and how these processes are modulated by phosphorylation events. These biosensors provide high sensitivity and specificity in detecting conformational changes and interactions within the receptor or between the receptor and its signalling partners. These biosensors can also provide quantitative data on the extent of receptor activation and the kinetics of signalling events.

5.2 Aims

With the previous chapter concluding that phosphorylation impacts basal G protein activation, there is a requirement for a tool to look at this physiologically. The aims here were as follows:

- Develop a BERKY-SPASM style biosensor as a tool to measure $G\alpha_q$ -specific activation with high affinity for the G protein, high sensitivity, and high fidelity.
- Employ the biosensor to measure how G protein-coupled pathway activation changes with removal of putative phosphorylation sites in the mGlu₅ C-terminus.
- Measure endogenously expressed glutamate receptor activation in primary neuronal cultures.

5.3 Results

5.3.1 Generation and Optimisation of a $G\alpha_q$ -Specific Biosensor

To generate a biosensor to detect mGlu₅ G protein activation, the ideal detector module should bind to $G\alpha_q$ -GTP not $G\alpha_q$ -GDP and have no effect on activity of the $G\alpha_q$ protein (Maziarz et al., 2020). An existing biosensor designed to measure $G\alpha_q$ protein activation, Lyn11-SpNG-GRK2, was utilised here to generate a biosensor optimised to measure endogenous $G\alpha_q$ activation through a BRET-based system. This Lyn11-SpNG-GRK2 biosensor possesses a Lyn11 membrane anchor to insert the biosensor into the membrane, followed by the fluorescent BRET acceptor mNeonGreen, an ER/K α -helical linker to provide flexibility and to separate the BRET pair by ~ 10 nm, the nanoluciferase BRET donor, and the regulator of G protein signalling (RGS) homology domain of GRK2 serving as the detector module for GTP-bound $G\alpha_q$ by increasing GTP hydrolysis (Figure 5.1A). This results in a genetically encoded unimolecular biosensor serving as a detector for active GTP-bound $G\alpha_q$. To optimise this biosensor and to make it more like the previously published BERKY-style biosensor (Maziarz et al., 2020), the orientation of the BRET acceptor and donor was inverted to generate a biosensor called Lyn11-iSpNG-GRK2 (Figure 5.1B).

Upon receptor activation, a conformational change occurs in the receptor stimulating exchange of GDP to GTP on the $G\alpha_q$ protein, triggering dissociation of the heterotrimeric $G\alpha\beta\gamma$ complex. This change is registered by the RH domain of GRK2, the detector module on the biosensor, binding in an activation-dependent manner (Carman et al., 1999), forming a well-established complex with the $G\alpha_q$ protein (Day et al., 2004; Sterne-Marr et al., 2003; Tesmer et al., 2005). This results in the BRET donor and acceptor being brought in close proximity due to the flexible α -helical linker, permitting resonance energy transfer producing a quantifiable BRET signal (Figure 5.1C).

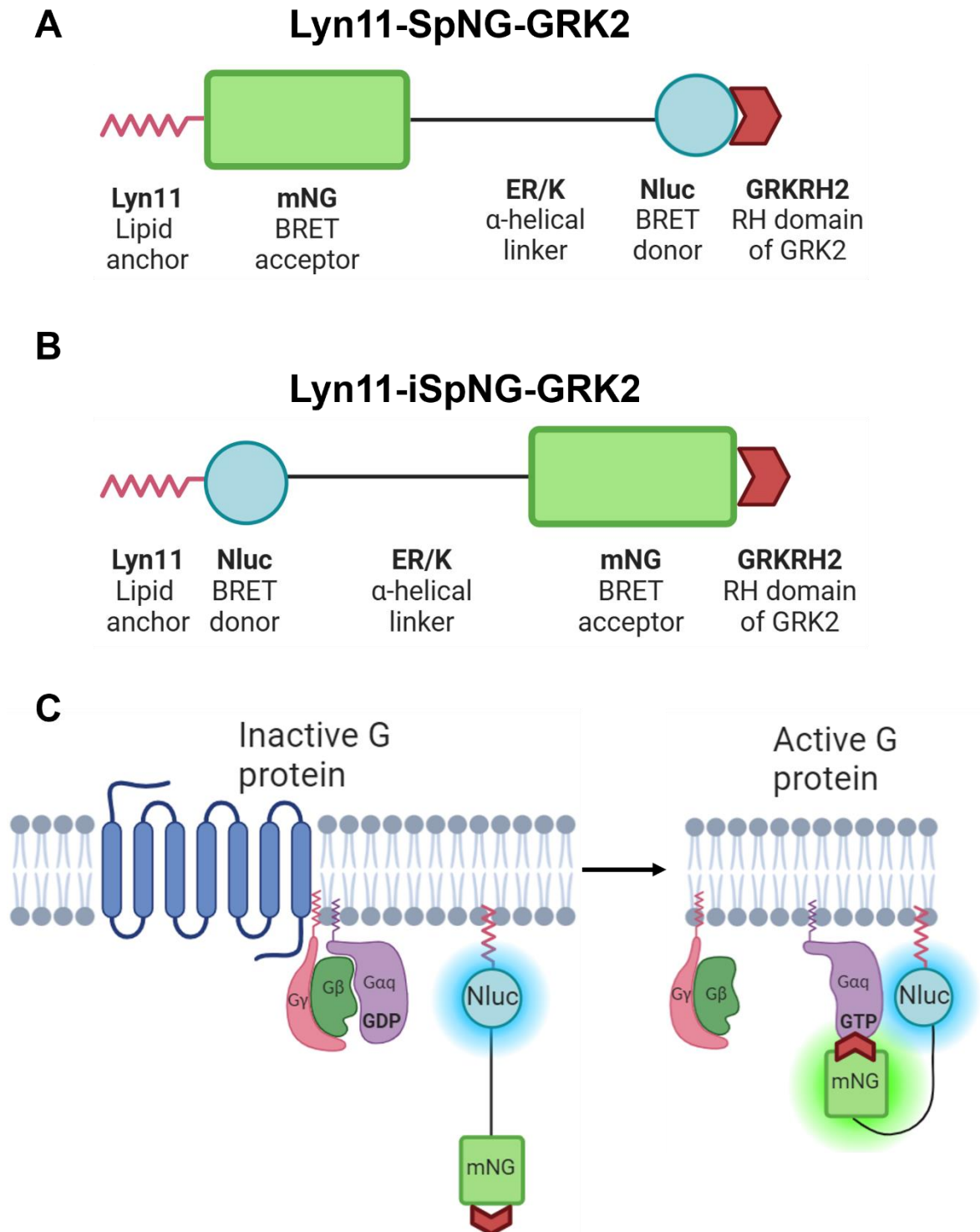


Figure 5.1: The structure of the novel unimolecular biosensors. The schematic design of the Lyn11-SpNG-GRK2 biosensor (A) and the inverted Lyn11-iSpNG-GRK2 biosensor (B). (C) The mechanism of action of the BERKY style biosensors, detecting active GTP-bound G α_q protein. The diagram depicts the inverted iSpNG-GRK2 sensor design. Figure created using BioRender.

To evidence that this novel biosensor can be transfected into cells and expressed, western blots were performed. Cell lysates were made from mGlu₅-WT Flp-InTM T-RExTM 293 cells transfected with or without the Lyn11-iSpNG-GRK2 (iSpNG) biosensor, then cells were with induced or not to express mGlu₅-WT by treating with doxycycline. In the western blot, bands consistent with the expected size of the biosensor (75 kDa) are observed only in the samples in which the biosensor is transfected into the cells, as detected by the nanoluciferase antibody (Figure 5.2A). In the samples in which there was no biosensor transfected, there was no band detected yet there was still membrane protein present in the sample, as confirmed using a sodium-potassium ATPase antibody (Figure 5.2A). The expression of the biosensor was not significantly different in the minus doxycycline versus the plus doxycycline conditions when not transfected with the biosensor ($P > 0.9999$, Kruskal-Wallis test with Dunn's post hoc test), but significantly different minus and plus doxycycline when the biosensor is expressed ($P = 0.0351$, Kruskal-Wallis test with Dunn's post hoc test).

Together, these data indicate that the novel iSpNG biosensor can be genetically expressed in Flp-InTM T-RExTM 293 cells independently of whether mGlu₅-WT receptor expression is induced with doxycycline.

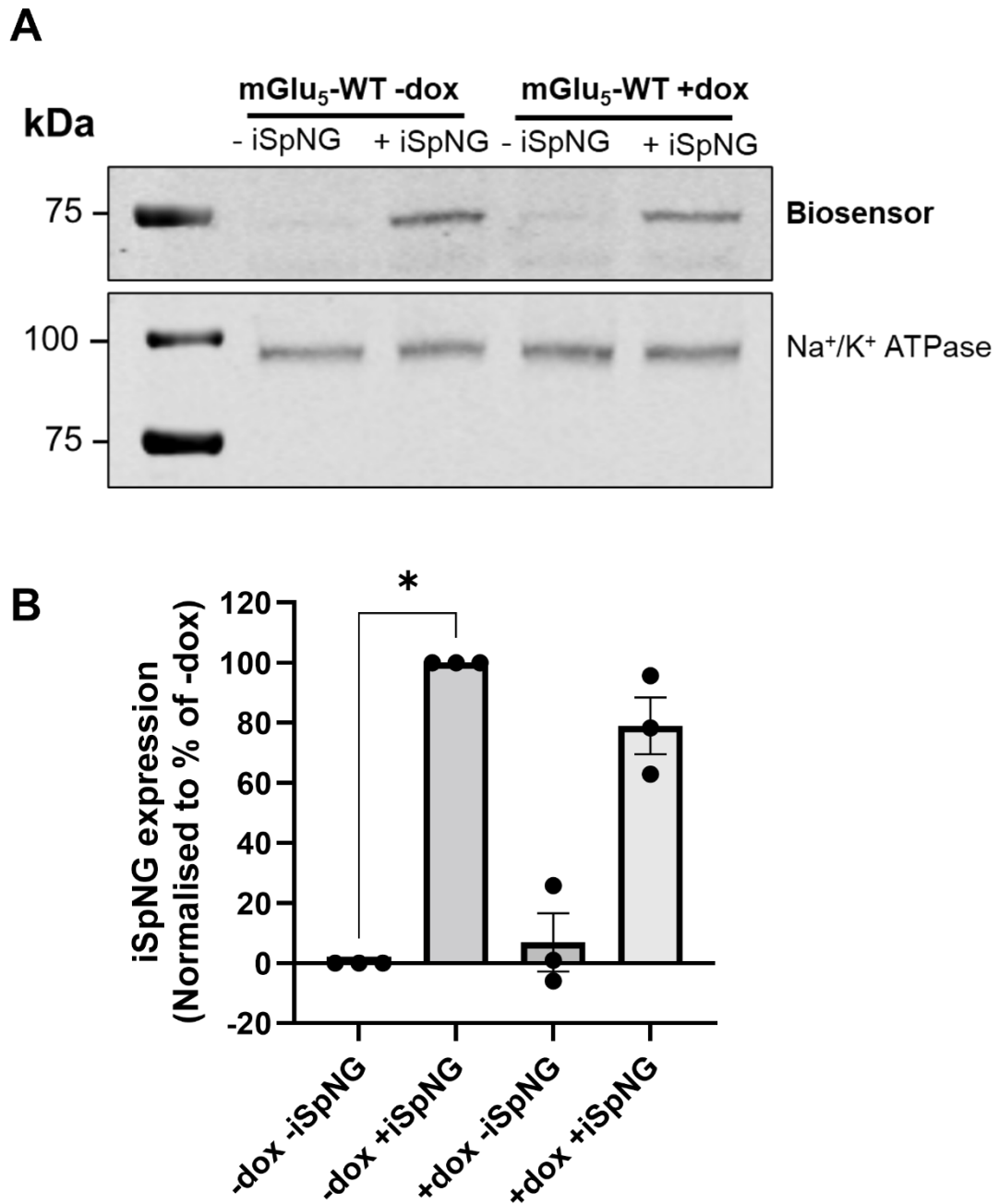


Figure 5.2: A protein of the expected molecular weight for the iSpNG biosensor is detected by western blotting following transfection into cells. Biosensor expression was assessed by SDS-PAGE using 20 μ g of lysates prepared from mGlu₅-WT stable cell lines transfected with 5 μ g per 10 cm dish of iSpNG biosensor. The biosensor expression was assessed by western blotting with an antibody to nanoluciferase. Representative blots are shown from three independent experiments. Median pixel intensity data are expressed as means \pm S.E.M. normalised to sodium-potassium ATPase loading control, then further normalised to the expression of mGlu₅-WT without doxycycline treatment. Statistical analysis performed was Kruskal-Wallis test with Dunn's post hoc test. * $P \leq 0.05$.

After confirming the iSpNG biosensor can be expressed in the mGlu₅ cell line, the ideal amount of biosensor to be transfected was optimised. This stage is critical to ensure there is functional expression levels. Additionally, optimising the

amount of biosensor transfected may improve the signal-to-noise ratio, ensuring that the signal is strong enough to be detected without excessive background noise. Here, transfection of the Lyn11-SpNG-GRK2 (SpNG) biosensor was compared to the inverted iSpNG biosensor to examine differences in fluorescent intensity and transfection. Increasing amounts of biosensor were transfected per well of a 96-well plate and imaged. From these experiments, a visual increase in mNeonGreen fluorescence was noticeable for both the SpNG and iSpNG biosensors upon increasing amounts of biosensor transfected (Figure 5.3A). Quantification of this fluorescence demonstrated a clear trend of increasing expression with increasing amount of sensor transfected (Figure 5.3B). At the highest amount of biosensor transfected (100 ng/well of a 96-well plate), the iSpNG biosensor demonstrated 43.8% higher fluorescent intensity compared to the SpNG biosensor ($P=0.0182$, two-way ANOVA). Looking at how the amount of biosensor transfected affects the ability of the sensor to measure G protein activation, the kinetics of G protein activation by mGlu₅ receptor following stimulation with 100 μ M glutamate were recorded. For the SpNG biosensor, all four amounts of biosensor transfected produced a net BRET signal above vehicle, suggesting the sensors can record G protein activation (Figure 5.3C). Similarly for the inverted iSpNG biosensor, each amount of biosensor transfected produced a BRET signal (Figure 5.3D). The largest BRET response was observed at 100 ng of biosensor transfected, thus broadly there is a trend of increasing BRET response with higher expression of the biosensor.

It is difficult to predict the expression rates of a biosensor and correlate the expression level to the BRET response, hence experiments examining the expression level of the biosensor should be performed. Here, it was shown that higher levels of biosensor transfected into the cells produced higher BRET responses. From this dataset, it was decided to progress with 100 ng/well of biosensor, as this produced a good level of fluorescence over the background and the maximum net BRET area under curve above vehicle in the kinetic traces.

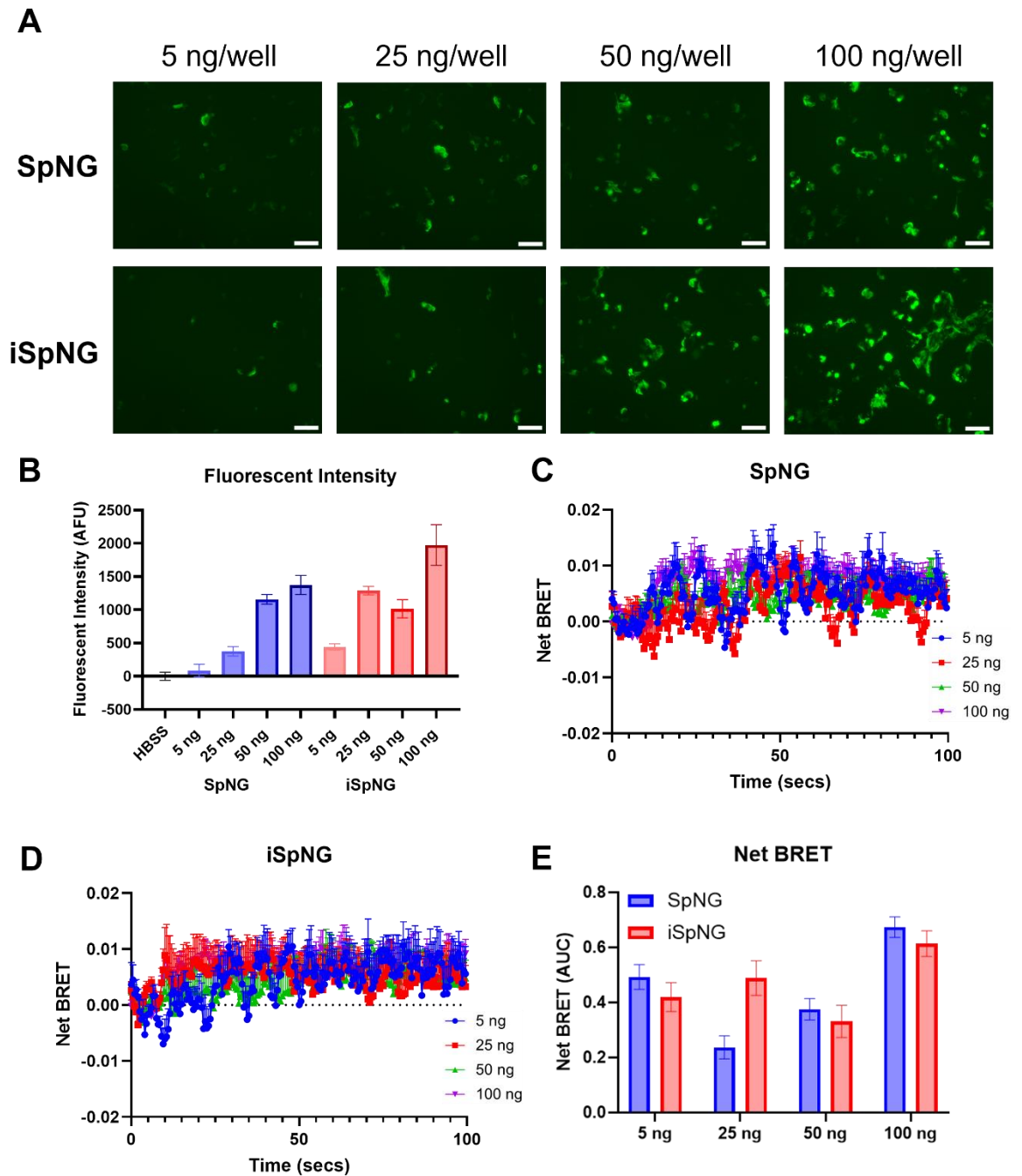


Figure 5.3: Increasing the amount of biosensor transfected results in an increase in sensor expression. (A) Representative images of transfection of increasing amounts of SpNG or iSpNG biosensors in transiently transfected HEK293T cells in one well of a 96-well plate. (B) Fluorescent intensity of cells was measured and compared to HBSS-H only background control. The kinetic traces for SpNG biosensor (C) and iSpNG biosensor (D) are plotted and the net BRET above vehicle data was recorded for each amount of biosensor (E). Data are expressed as means \pm S.E.M. of three independent experiments performed in triplicate. Scale bar indicates 50 μ m.

To further optimise the biosensor transfection, not only should the amount of biosensor be considered but also the amount of receptor. In endogenous cells, the expression of the receptor cannot be controlled, thus to determine at which amounts of receptor expression the biosensor is able to function at, multiple receptor levels should be tested.

The ratio of receptor expression to biosensor expression is important to monitor, as overexpression of either component may skew recordings. Here, utilising mGlu₅-WT Flp-In™ T-REx™ 293 cells permit control of receptor expression through administering differing concentrations of doxycycline. To optimise the amount of receptor to use with the biosensor, a doxycycline titration was performed. As per the previous experiment, 100 ng/well of biosensor was transfected per well of a 96-well plate, then a range of doxycycline concentrations used to titrate the expression of the mGlu₅ receptor within the cell line. The fluorescent intensity of the SpNG biosensor showed a trend of increasing fluorescence with increasing amounts of receptor induced (Figure 5.4A). This trend was unexpected, as the biosensor is transfected independently and other than both being driven by a form of the CMV promotor there should be no relationship between the two. Conversely, the fluorescent intensity of the iSpNG biosensor, therefore the expression, did not change with increasing amounts of mGlu₅ receptor (Figure 5.4A), consistent with the previous western blot data (Figure 5.2). Looking at the kinetics of the SpNG biosensor in its ability to measure G α_q activation of the mGlu₅ receptor, there was no obvious net BRET above vehicle for 2 ng/mL and 10 ng/mL doxycycline, yet there was a response to the alternative concentrations of doxycycline tested, including the 0 ng/mL doxycycline condition (Figure 5.4B). This is not entirely surprising, as previous cells without doxycycline treatment demonstrated an IP₁ accumulation response. Opposingly, the kinetic traces of G protein activation for the iSpNG biosensor demonstrated a net BRET above vehicle for all concentrations of doxycycline tested, most notably for 0.5 ng/mL and 10 ng/mL doxycycline. When the area under curve of the kinetic traces were quantified, it revealed significant differences between the two biosensors. For each 0, 0.5, 2, and 10 ng/mL doxycycline, the iSpNG biosensor produced a significantly greater area under curve net BRET measurement than the SpNG biosensor ($P < 0.0001$, two-way ANOVA).

These data demonstrated that the biosensor can measure G protein activation at a broad range of receptor expression levels, indicating that the biosensor is likely to be able to record and detect endogenous receptor activation where expression is unpredictable and potentially varied.

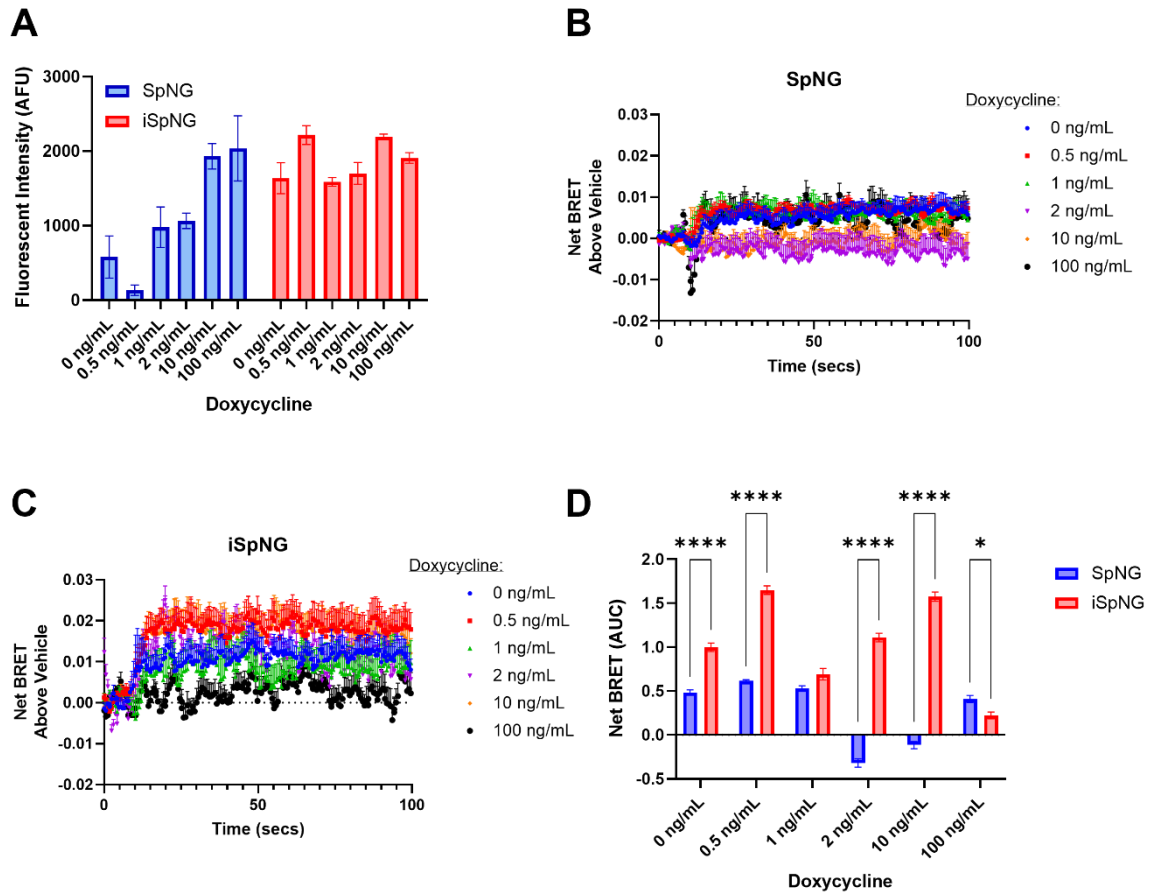


Figure 5.4: Varying receptor expression with doxycycline impacts the signal produced by the biosensor. (A) The fluorescent intensity of mGlu5-WT stable cell lines treated with different concentrations of doxycycline and transfected with 1 μ g per well of a 6-well plate of each biosensor, corrected to background fluorescence. The kinetic traces of G protein activation, subsequent to stimulation with 100 μ M glutamate, measured by SpNG (B) and iSpNG (C) biosensors in mGlu₅-WT cells treated with various doxycycline concentrations. (D) The net BRET above vehicle area under curve data was calculated from the kinetic traces for both SpNG and iSpNG biosensors for each concentration of doxycycline. Data are expressed as means \pm S.E.M. of two independent experiments performed in triplicate. Statistical analysis performed was a two-way ANOVA with a Šídák's multiple comparisons post hoc test. * $P < 0.05$, **** $P < 0.0001$.

To further improve the biosensor assay, the platereader protocol used to measure the kinetics of G protein activation was optimised. Typically, the platereader records the background BRET ratio for 10 seconds, then agonist is injected at 220 μ L/s, then 1.5 seconds later the platereader shakes at 200 rpm to mix the solutions in the well. However, a dip in the raw BRET ratio was observed at the 10 second timepoint (Figure 5.5A). Despite this dip in BRET, after correcting

for vehicle treatment, the net BRET above vehicle still has a clear signal window (Figure 5.5B). To explore whether this dip in the signal was triggered by the plate shaking step, the protocol was performed with the shaking stage removed (Figure 5.5C, D). Looking at the BRET ratio upon removal of the shaking step, a dip in the signal is still observed (Figure 5.5C), but despite this the net BRET above vehicle still has a clear signal window (Figure 5.5D). This protocol without the shaking step demonstrates a slower response compared to the typical protocol. To separate out the drug addition and the plate shake to determine which of these is the cause of the dip in the signal, the two were separated by a 10 second time frame as opposed to the standard 1.5 second gap (Figure 5.5E, F). Here, a dip in the BRET ratio is observed upon drug addition and at the shake stage (Figure 5.5E), yet despite this the net BRET above vehicle is broadly similar to the previous conditions. To further alter the speed of the drug addition, the injection pump speed was reduced to 100 $\mu\text{L/s}$ with the injection and shake step separated by 1.5 seconds (Figure 5.5G, H). In this setup, the dip in the BRET ratio was still observed and the net BRET above vehicle was reduced compared to the original protocol. This was proposed to be due to the agonist not reaching and activating the receptors as fast as in the previously tested protocol setups, thus to balance this out, the low pump speed was utilised but with a faster shake speed of 700 rpm. The artefact in the BRET ratio is larger than the previous protocols (Figure 5.5G) and the net BRET above vehicle displays a similar signal window to the other protocol with low pump speed, yet a faster response (Figure 5.5H). This difference caused by the change in pump speed from 220 $\mu\text{L/s}$ to 100 $\mu\text{L/s}$ may be due to improper drug injection, and the increase in response time correlates with the increasing shaking speed.

In summary, to achieve the greatest signal window whilst compromising on the injection of and mixing of the agonist, the original protocol of a 200 rpm shake 1.5 seconds after drug addition with 220 $\mu\text{L/s}$ pump speed was selected for further kinetic reads.

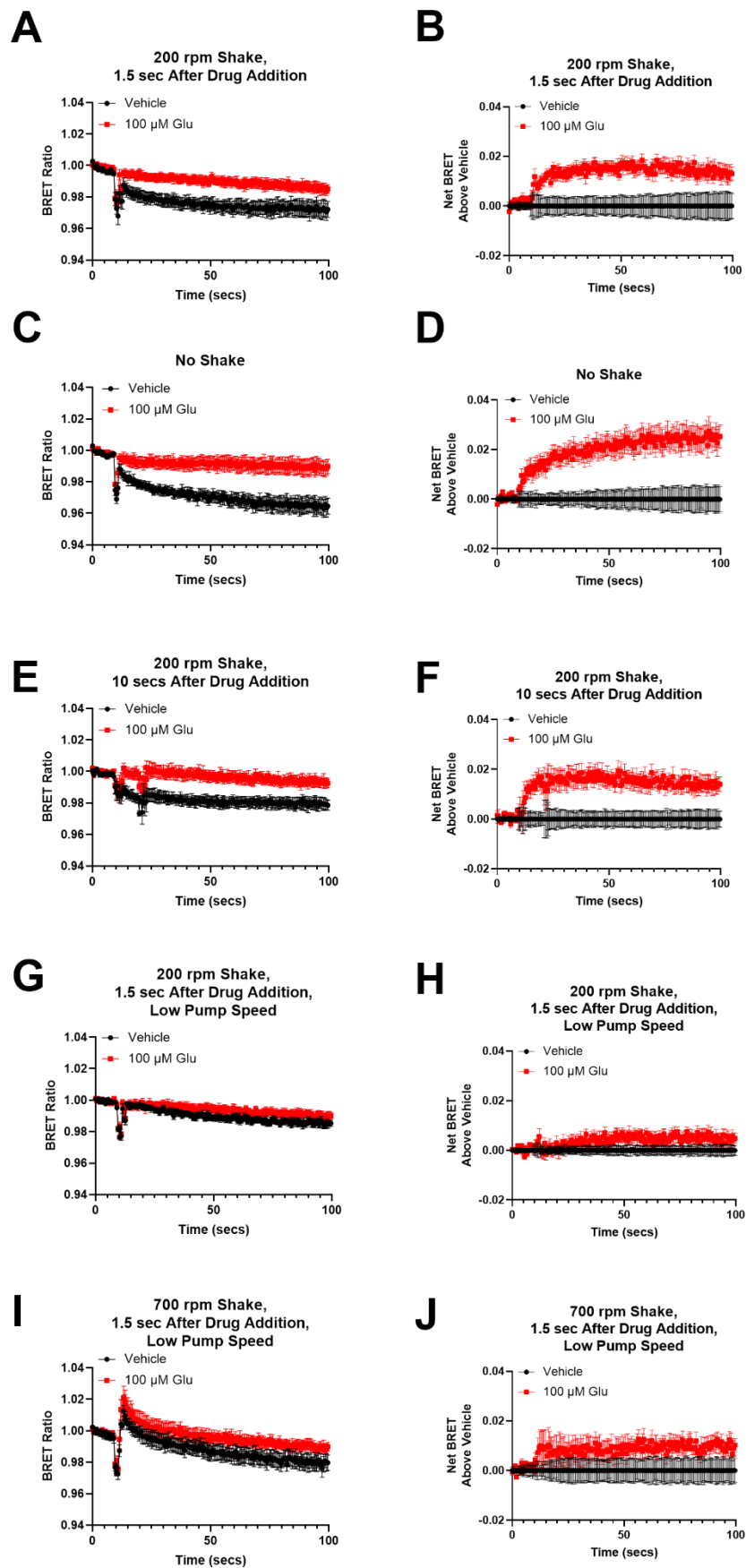


Figure 5.5: Protocol optimisation for biosensor BRET kinetic reads. Cells expressing the mGlu₅-WT receptor after treatment with 2 ng/mL doxycycline were transfected with 5 μg per 10 cm dish of iSpNG biosensor. (A) 100 μM of the agonist glutamate was added after 10 seconds, then biosensor kinetic measurements of G protein activation were

recorded. The BRET ratio (A, C, E, G, I) and net BRET above vehicle treatment (B, D, F, H, J) are shown. (A, B) Addition of the agonist without a shaking step was recorded to observe the impact of the drug addition on the BRET recordings. (C, D) 1.5 seconds after the agonist is added, the platereader shakes the plate at 200 rpm to mix the solutions in the well. (E, F) To separate out the drug addition and the shake to observe the impact on the BRET signal, a 10 second time period separated the drug addition and plate shake. (G, H) The drug pump injection speed was decreased, and the shake maintained at 200 rpm 1.5 seconds after the drug addition, and finally 700 rpm shake speed was tested (I, J) to mix the slowly added drug. Data are expressed as means \pm S.E.M. of two independent experiments performed in triplicate.

5.3.2 Validating the Biosensors with $G\alpha_q$ Protein-Coupled Receptors

To further validate the biosensor in its ability to measure $G\alpha_q$ protein-coupled pathway activation, the SpNG and iSpNG biosensors were tested with several additional $G\alpha_q$ protein-coupled receptors. Testing the biosensors with multiple GPCRs confirms the specificity of the biosensor, ensuring it can detect $G\alpha_q$ activation. The selected GPCRs to test the ability of the biosensor to measure G protein activation were the M1 muscarinic receptor and FFA1 free fatty acid receptor. Cells were transfected with pcDNA3 to demonstrate if the agonists had an effect in cells without receptor expressed, then this was compared to agonist-stimulated $G\alpha_q$ protein activation.

Utilising the SpNG biosensor in cells transfected with pcDNA3 and treated with acetylcholine (ACh), there is no net BRET above vehicle, whilst the ACh stimulated net BRET above vehicle in cells transfected with the M1 receptor produced a higher peak response (Figure 5.6A). Comparing this response to the iSpNG biosensor, the agonist-stimulated BRET is greater than that produced by the SpNG biosensor (Figure 5.6B). When utilising the SpNG biosensor and treating pcDNA3 transfected cells with the FFA1 specific full agonist T-3601386 (Ueno et al., 2019), there is a high BRET response (Figure 4.6C), suggesting that the cells may be endogenously expressing the FFA1 receptor. The iSpNG biosensor produced an agonist-stimulated net BRET above vehicle greater than the pcDNA3 net BRET above vehicle, indicating a signal more specific to the receptor than that produced by the SpNG biosensor (Figure 5.6D). The SpNG biosensor with the mGlu₅ receptor did not produce an agonist-stimulated response

greater than the background noise (Figure 5.6E), however the iSpNG biosensor managed to produce a specific net BRET above vehicle greater than the noise (Figure 5.6F). The net BRET area under curve data revealed that the net BRET area under curve for the iSpNG biosensor was consistently greater compared to the SpNG biosensor (Figure 5.6G).

To summarise, these data indicate that the iSpNG biosensor is better equipped than the SpNG biosensor to measure $G\alpha_q$ protein activation.

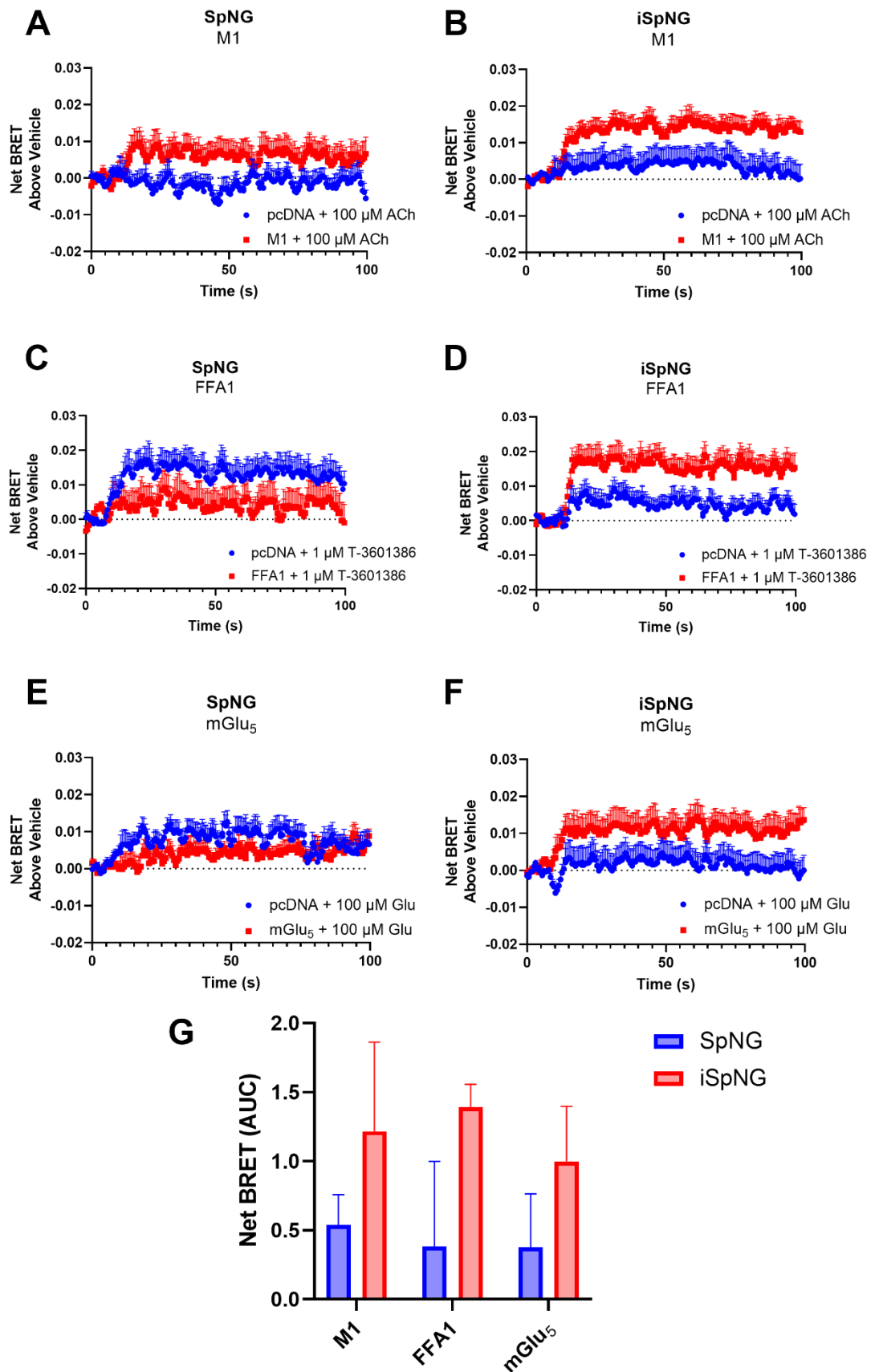


Figure 5.6: The SpNG and iSpNG biosensors can detect G_{α_q} at the M1, FFA1 and mGlu₅ receptors. HEK293T cells were transiently transfected with 10 ng of receptor and 90 ng of biosensor per well of a 96-well plate. The SpNG biosensor (A, C, E) in comparison with the iSpNG biosensor (B, D, F) in the ability to detect active G_{α_q} protein following stimulation of the M1 muscarinic receptor with 100 μ M of acetylcholine (A, B),

the FFA1 receptor with 1 μ M T-3601386 (C, D), and the mGlu₅ receptor with 100 μ M glutamate (E, F). (G) The net BRET above vehicle area under curve data derived from the kinetic reads is shown. Data are expressed as means \pm S.E.M. of three independent experiments performed in triplicate.

5.3.3 Employing a G α_q -Specific Biosensor to Investigate the Effect of Phosphorylation of the mGlu₅ Receptor

To investigate how mGlu₅ mediated G protein activation is influenced by receptor phosphorylation, the SpNG and iSpNG biosensors were utilised alongside the mGlu₅ phosphodeficient mutant receptors. Employing the SpNG biosensor to measure G α_q activation produces a lot of noise, and no clear agonist stimulated response was observed for either the wildtype, mGlu₅-PD, or mGlu₅-TPD versions of the mGlu₅ receptor (Figure 5.7A). However, when utilising the iSpNG biosensor, a clear BRET response was observed for the wildtype receptor (Figure 5.7B). In contrast, there was no visible response for either the mGlu₅-PD or mGlu₅-TPD receptors with the iSpNG biosensor (Figure 5.7B). When quantifying the net BRET responses, it confirms no G protein activation was measured by the SpNG biosensor for the mGlu₅-WT receptor, yet with the iSpNG biosensor an area under curve value greater than that produced by the SpNG biosensor was produced (Figure 5.7C). No meaningful responses were recorded for the mGlu₅-PD and mGlu₅-TPD receptors with either the SpNG or the iSpNG biosensor (Figure 5.7C).

As a measure of constitutive G α_q protein activation, the basal BRET ratio produced by the biosensor before the addition of any agonists was also recorded. When using the SpNG biosensor, there was a high basal BRET ratio in cells transfected with the wildtype mGlu₅ receptor, yet this was significantly decreased by 17.2% when measuring G protein activation in cells transfected with the mGlu₅-PD receptor ($P=0.0004$, two-way ANOVA) (Figure 5.7D). Cells transfected with the mGlu₅-TPD receptor produced a low level of basal BRET, indicating diminished G protein activation. This basal BRET for the mGlu₅-TPD receptor mutant was 66.6% lower than that produced by the wildtype receptor ($P<0.0001$, two-way ANOVA) (Figure 5.7D). Similarly, with the iSpNG biosensor, there was a decrease in the basal BRET ratio observed in cells expressing the mGlu₅-TPD receptor: 47.7% lower than that in cells expressing the mGlu₅-WT receptor ($P<0.0001$, two-way

ANOVA) (Figure 5.7D). However, unlike the SpNG biosensor, there was no difference in the basal BRET ratio observed in cells expressing mGlu₅-WT and mGlu₅-PD with the iSpNG biosensors ($P=0.8970$, two-way ANOVA).

Whilst the net BRET area under curve data for the phosphodeficient mutant receptors did not demonstrate an increase in BRET, the basal BRET ratio data corroborated the finding that there is less G protein activation with mutation of mGlu₅ C-terminal serine residues and a further reduction when both C-terminal serine and threonine residues are mutated.

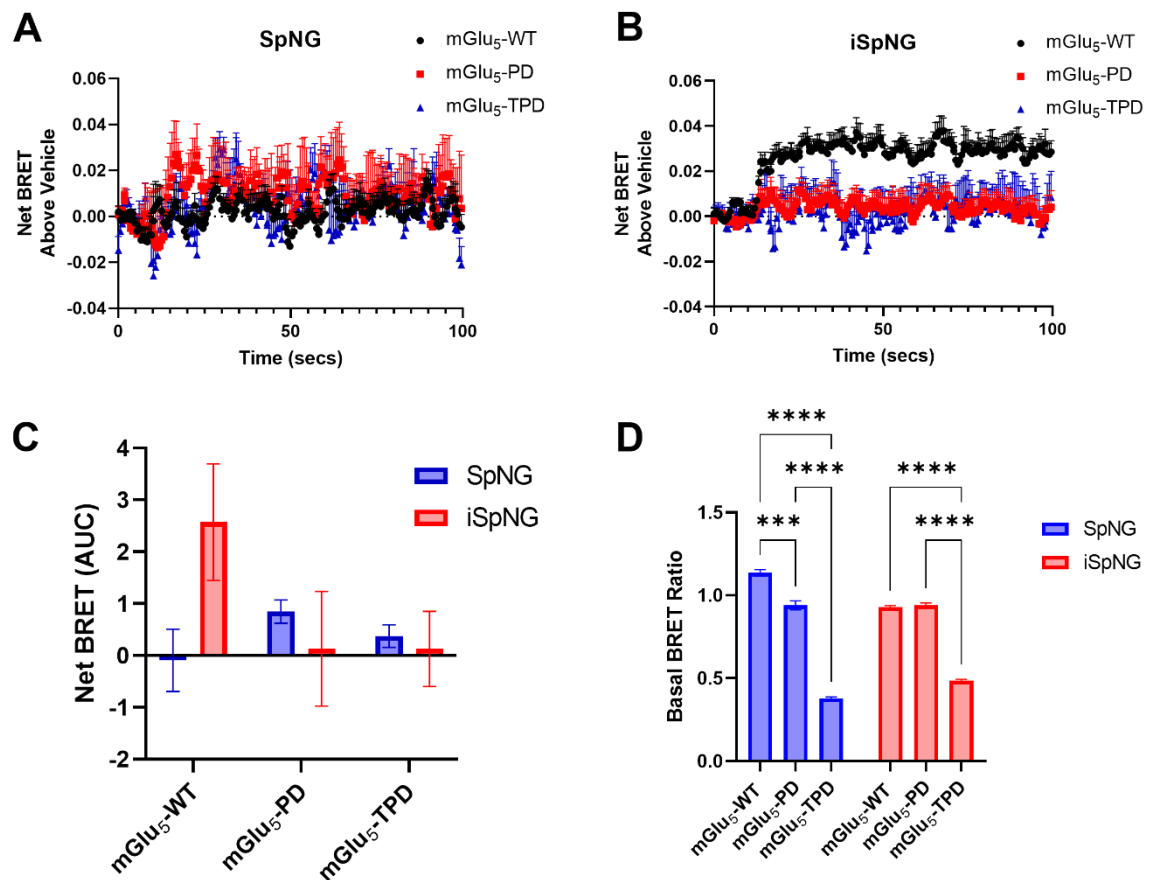


Figure 5.7: Measuring the impact of mGlu₅ potential phosphorylation sites on G α_q activation using a genetically encoded biosensor. HEK293T cells were transiently transfected with 10 ng of receptor and 90 ng of biosensor per well of a 96-well plate. (A) The SpNG biosensor in comparison with the iSpNG biosensor (B) in their ability to detect active G α_q protein following stimulation of the mGlu₅-WT, mGlu₅-PD and mGlu₅-TPD receptors with glutamate. (C) The net BRET above vehicle area under curve data derived from the kinetic reads for the SpNG sensor and iSpNG sensor. (D) Basal BRET ratios detected by the biosensors at each of the mGlu₅ receptors are reported. Data are expressed as means \pm S.E.M. of three independent experiments performed in triplicate. *** $P < 0.001$, **** $P < 0.0001$.

5.3.4 Employing a $G\alpha_q$ Biosensor to Measure Endogenous Glutamate Receptor Mediated G Protein Activation

Utilising biosensors in primary cell models permits real time measurement of endogenous GPCR signalling, providing dynamic insights into signalling pathways. The mGlu₅ receptor is expressed notably in the cortex, on post-synaptic excitatory neurons (Shigemoto et al., 1993). Initially to demonstrate expression of mGlu₅ in the CNS, western blot analysis was carried out on lysates from murine cortices obtained from wildtype, mGlu₅ knockout, and mGlu₅ heterozygous mice. Probing with an antibody against the C-terminus of mGlu₅ resulted in bands consistent with the mGlu₅ monomer and dimer observed in the wildtype sample, yet no bands were detected in the knockout sample (Figure 5.8A). It was also notable that in the heterozygous sample, while bands were observed consistent with both the monomer and dimer, were less intense than in the wildtype sample. Membrane protein was also confirmed to be present and comparable across all three samples through western blotting for sodium-potassium ATPase (Figure 5.8A).

As mGlu₅ was shown to be expressed in the cortex, and it is well established that the receptor is expressed on neurons, primary cortico-hippocampal neurons were selected as a physiologically relevant model for endogenous mGlu₅ expression. A western blot using an mGlu₅ C-terminal specific antibody was carried out in lysates generated from these primary neuronal cultures to confirm receptor expression and compared to mGlu₅ expression in the Flp-In™ T-REx™ 293 cells as a positive control (Figure 5.8B). Bands consistent with the mGlu₅ monomer and dimer are observed in the neuronal cell, and these bands were comparable in size to those observed in the Flp-In™ T-REx™ 293 treated with doxycycline to induce expression of mGlu₅ (Figure 5.8B). To demonstrate that endogenous mGlu₅ receptor is functional in the neuronal cultures, an IP₁ accumulation assay was performed. This assay measures $G\alpha_q$ protein-coupled receptor activation, thus as a positive control ACh was used, as cortico-hippocampal neurons are known to endogenously express the M1 muscarinic acetylcholine receptor (Levey et al., 1991). The neurons treated with ACh produced a concentration dependent increase in IP₁ (Figure 5.8C), indicating IP₁ can be used to measure $G\alpha_q$ GPCR signalling in the neuron cultures. When using glutamate to stimulate endogenous mGlu receptors in these neuronal

cultures, a clear concentration dependent increase in IP₁, with a pEC₅₀ of 5.1 ± 0.74 , was observed (Figure 5.8C). Whilst it is expected that only group I mGlu receptors will produce an IP₁ response as this group is the only group in the metabotropic glutamate receptor family that couple to G α_q , the group I mGlu receptor specific agonist DHPG was used in the IP₁ assay to confirm it was indeed this receptor group responding to glutamate in the neurons. Stimulation with DHPG also produced a concentration dependent increase in IP₁ with a pEC₅₀ of 6.0 ± 0.51 (Figure 5.8C), indicating that the mGlu receptors responding in this assay were likely to be either mGlu₅ or mGlu₁.

Taken together, these data demonstrate that mGlu₅ is present in both the murine cortex and murine cortico-hippocampal primary neuronal cultures, and a functional response from the endogenously expressed group I mGlu receptors is present in these primary cultures.

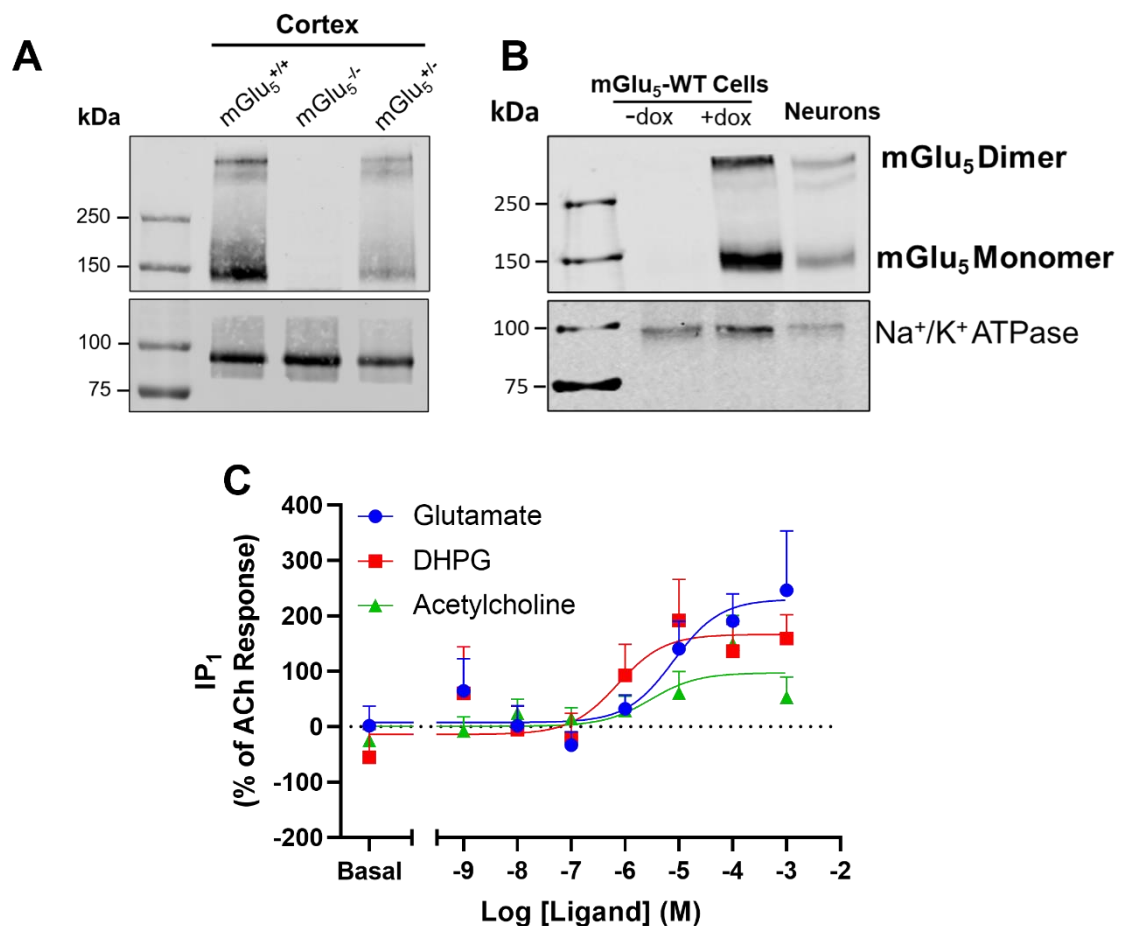


Figure 5.8: The mGlu₅ receptor is endogenously expressed in cortico-hippocampal neurons and produces a functional IP₁ response. (A) Detection of mGlu₅ in lysate samples prepared from mGlu₅ homozygous, knockout, and heterozygous mouse cortex tissues. SDS-PAGE was carried out on 20 μ g of protein on an 8% polyacrylamide gel. Western blotting was then carried out using mGlu₅ and sodium-potassium ATPase specific antibodies. The blot shown is representative of two independent experiments. (B)

Detection of mGlu₅ in lysate samples prepared from mGlu₅-WT cells without receptor expression induced with doxycycline and with receptor induced using 2 ng/mL doxycycline. Lysates were also generated from primary murine cortico-hippocampal neurons, then 5.5 µg of these samples was loaded onto an 8% polyacrylamide gel. Western blotting was then carried out using mGlu₅ and sodium-potassium ATPase specific antibodies. The data shown are representative of two independent experiments. (C) Concentration response curves showing the agonist-stimulated IP₁ accumulation over an hour in primary murine cortico-hippocampal neurons. Data shown are means ± S.E.M. of three independent experiments, performed in triplicate or quadruplicate.

To finally achieve the aim of directly measuring endogenous mGlu₅ mediated Gα_q activation, the SpNG and iSpNG biosensors were transfected into primary cortico-hippocampal neuronal cultures. Using the SpNG biosensor in the neuronal cultures did not appear to generate a BRET response (Figure 5.9A). However, when using the optimised iSpNG biosensor, a trend towards increasing BRET with the higher concentrations of glutamate tested was apparent (Figure 5.9B). The kinetic traces appear to show oscillations, likely cycles of GTP/GDP conversion. When quantifying the net BRET area under curve data from the kinetic traces, the SpNG biosensor did not produce a clear response, while iSpNG biosensor did result in a clear concentration dependent response to glutamate (pEC₅₀ of 5.5 ± 0.28) (Figure 5.9C). Notably, this potency compares favourably to the potency I observed in these cells when measuring glutamate stimulated IP₁.

Altogether, these data demonstrate that the iSpNG biosensor was successful in recording the dynamic endogenous Gα_q activation stimulated by glutamate in neuronal cultures.

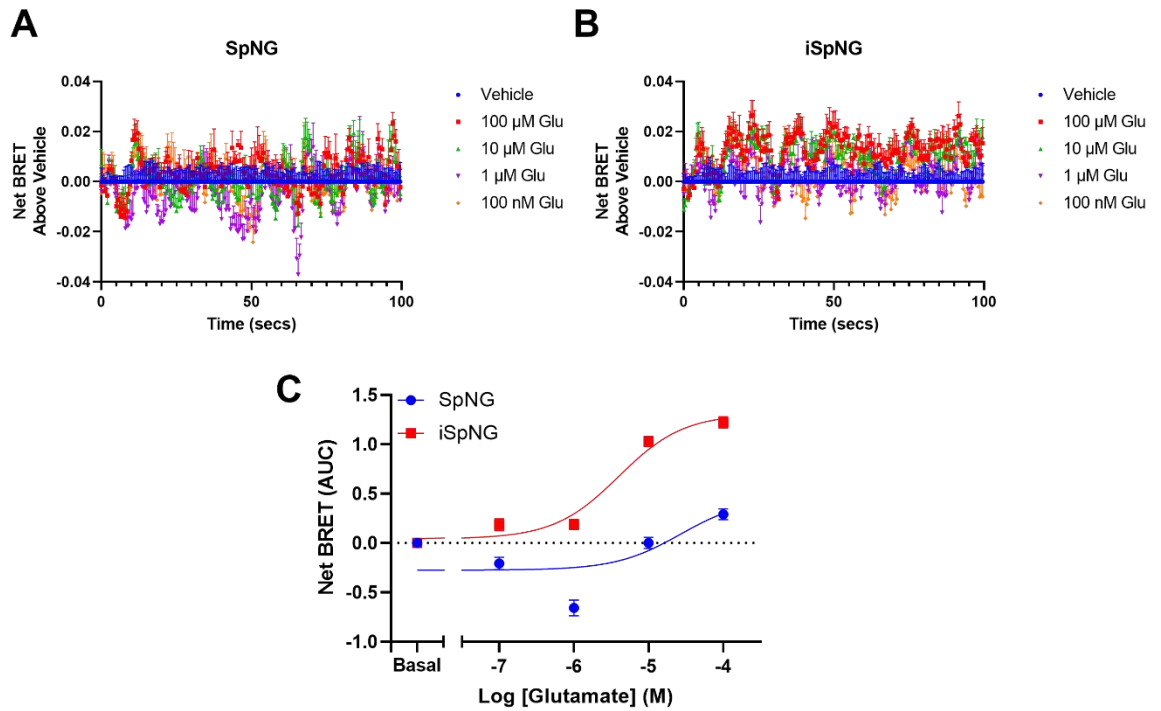


Figure 5.9: Glutamate stimulated endogenous $G\alpha_q$ protein activation in neurons can be measured with the iSpNG biosensor. Net BRET above vehicle endogenous $G\alpha_q$ protein activation in neurons as measured by the SpNG biosensor (A) or iSpNG biosensor (B) in response to glutamate stimulation. (C) Concentration response curves from the area under curve of the data in (A) and (B). Data are expressed as means \pm S.E.M. of two independent experiments performed in triplicate.

5.4 Discussion

In this chapter, following demonstration of expression of a genetically encoded $G\alpha_q$ -GTP biosensor in cells, the ability of the biosensor to measure $G\alpha_q$ protein activation was assessed. The optimised novel inverted biosensor was demonstrated to have a greater signal window than its original counterpart and demonstrated that it can measure G protein activation at a broad range of receptor expression levels, indicating it may be suitable for measuring G protein activation at endogenously expressed receptors. Evidence was given that the biosensor had the capability to measure $G\alpha_q$ -GTP at multiple receptors that couple to this G protein. This biosensor was then employed to compare phosphodeficient mGlu₅ receptor signalling, with the basal BRET ratio data supporting the finding that there is less G protein activation with mutation of mGlu₅ C-terminal serine residues and a further reduction when both C-terminal serine and threonine residues are mutated, indicating that direct receptor phosphorylation plays a role in the G protein activation of the mGlu₅ receptor. Finally, the optimised biosensor was then successfully used to measure endogenous mGlu₅ receptor activation into primary neuron cultures.

A multitude of fluorescent proteins are available for use in BRET assays; the most traditionally selected fluorophores are variants of green fluorescent protein (GFP), initially generated as a marker for gene expression (Chalfie et al., 1993). GFP was first isolated from the *Aequorea Victoria* jellyfish (Shimomura et al., 1962). Since then, there have been many developments in the options available for fluorophores, broadening the available pool of acceptor molecules for selection in BRET assays. In this work, the mNeonGreen fluorescent protein was selected over the YFP originally utilised in the BERKY-style biosensors, as mNeonGreen is considered to be the brightest monomeric green or yellow fluorescent protein (Shaner et al., 2013), providing the opportunity for a brighter BRET signal. Additionally, there has been development of brighter luciferases for optimised BRET systems. The development of the novel luciferase nanoluciferase (Nluc) offers enhanced stability, smaller size (19 kDa compared to 37 kDa of Rluc), and a 150-fold increase in luminescence in comparison to *Renilla* derived luciferases (England et al., 2016; Hall et al., 2012), ideal as a pairing with mNeonGreen. Nanoluciferase is best for overall brightness and mNeonGreen has

strong spectral overlap, high quantum yield and good brightness as a fluorophore and therefore is likely to facilitate efficient energy transfer and strong BRET acceptor emission.

Here, to measure the expression of the iSpNG biosensor within the cell lines, western blots were performed utilising the nanoluciferase antibody. There were bands detected consistent with the expected size of the biosensor, indicating that the unimolecular genetically encoded biosensor was expressed in the mGlu₅-WT cells lines. There was no significant difference in biosensor expression whether the receptor was expressed or not, as expected; it is not thought that the induction of a gene of interest in stable Flp-In™ T-REx™ 293 cell lines would impact the expression of a transiently transfected plasmid construct, however this is dependent on the promotor driving expression of the plasmid.

Measuring expression of biosensors through western blotting with an antibody to nanoluciferase has previously been reported for one vector G protein optical (ONE-GO) biosensor constructs (Janicot et al., 2024). To further evidence that expression of the ONE-GO biosensor did not impact endogenous GPCR signalling, this group performed cyclic adenosine monophosphate (cAMP) experiments with and without co-transfection of the biosensor. This could be replicated in this piece of work, performing either calcium mobilisation or IP₁ accumulation assays with and without co-expression of the iSpNG biosensor to provide evidence that the introduction of the biosensor into the cell does not impact the function of the G α_q protein. Other groups have demonstrated expression of their biosensors through western blotting for other biosensor components such as G proteins (Maziarz et al., 2020), an option that could be considered in this scenario. Western blotting for the fluorescent protein could be performed, as GFP antibodies that will detect mNeonGreen exist. This would aid the validation of the expression of the biosensor, as multiple components of the biosensor can be looked at and confirmed to be expressed.

To further study the expression of the biosensor, it is useful to consider looking at where the sensor is being expressed within the cell. For this biosensor to work, it conceptually should be on the plasma membrane. The microscopy performed here demonstrates that the biosensor is expressed in the cell, but the magnification and resolution are not sufficient to observe where exactly in the cell

it is. To improve on this, confocal microscopy on transfected cells will provide higher resolution and permit determination of the localisation of the biosensor.

Biosensors designed to detect $G\alpha_q$ protein-coupled receptor activity can provide valuable insights into cellular signalling mechanisms, thus should be tested with multiple $G\alpha_q$ protein-coupled receptors in order to validate the robustness of the biosensor. In the current study, a biosensor setup was engineered to detect active $G\alpha_q$, then tested against the M1 muscarinic receptor, the FFA1 free fatty acid receptor, and the mGlu₅ receptor. The biosensor demonstrated a robust and specific response following stimulation with each receptor's respective agonist, indicating detection of G protein activation at each receptor. This validation process, utilising a biosensor with multiple GPCRs, was reported in a study by Janicot et al. (2024), in which their generated ONE-GO biosensor was examined across 72 GPCRs as a proof of concept, observing distinct BRET profiles for each receptor confirming the functional integrity of the biosensor system providing comprehensive insights into receptor-specific signalling pathways. Alternatively, split luciferase assays have been developed and optimised for measuring $G\alpha_q$ protein activation, assessing the interaction between the G protein and its effector phospholipase C- β 3 (PLC- β 3) (Littmann et al., 2018). This luciferase complementation assay permits analysis of untagged GPCRs, similar to the iSpNG biosensor used here. This is advantageous when designing biosensors for measuring activation of endogenous GPCRs, as if a biosensor can detect G protein activation *in vitro* without modification of the receptor, it is more likely to work in measuring endogenous G protein activation.

In this study, one aim was to probe the impact of direct mGlu₅ phosphorylation through use of the G protein activation biosensor with phosphorylation-deficient mGlu₅ mutant receptors. The biosensor, able to be expressed in Flp-In™ T-REx™ 293 cell lines and to detect active $G\alpha$ -GTP, demonstrated a reduction in BRET signal with the mutant receptors with C-terminal serine and threonine residues mutated to alanine, indicating a decrease in G protein activation. There was also a significant decrease in the BRET recorded for the ligand-independent G protein activation. The use of a G protein-sensitive biosensor in the current study provided real-time, high-resolution data on G protein activation, revealing that phosphorylation of C-terminal serine and threonine residues of mGlu₅ plays a role in both basal and agonist-stimulated G protein

activation. This method has not previously been employed to examine how mGlu₅ phosphorylation impacts G protein activation. These data corroborate the data from Chapter 4; calcium mobilisation, IP₁ accumulation, and NEWPATH assays all demonstrated an impact of mGlu₅ C-terminal phosphorylation on the G protein dependent transduction pathway, particularly in the ligand-independent activity.

Using a biosensor to measure mGlu₅ G protein activation in neurons presents a powerful approach to dissecting the complex signalling mechanisms of this receptor in a highly relevant physiological context. Metabotropic glutamate receptors play a pivotal role in synaptic plasticity, learning, memory, and various neuropsychiatric disorders; thus, it is key to learn the biology and signal transduction of this receptor. Traditional biochemical methods often fail to capture the dynamics of endogenous GPCR signalling in living neurons. Employing a biosensor, first optimised in heterologous cell systems, to measure endogenous receptor activation reveals the precise temporal dynamics of G protein activation. The integration of such biosensors into experimental neuroscience represents a significant advancement, allowing for more precise manipulation and observation of mGlu₅ signalling pathways in their native cellular environments.

To confirm the specificity of the mGlu receptor response to glutamate, firstly the group I mGlu receptor specific agonist DHPG could be used. This would confirm if the receptor responding to glutamate in the biosensor assay was a group I mGlu receptor. Furthermore, mGlu₅-specific negative allosteric modulators could be utilised to dampen the response and examine whether it is the type 5 metabotropic glutamate receptor responding to this agonist-stimulated G protein activation through manipulation of receptor's active conformation. Finally, the key experiment would be to perform these experiments in primary neuronal cultures generated from mGlu₅ heterozygous or knockout mice, demonstrating through comparison to wildtype that the response is specific to the mGlu₅ receptor

Gα_q inhibitors or mutations in Gα_q can be used alongside this Gα_q-specific activation biosensor to investigate the dynamic regulation of Gα_q signalling. By introducing pharmacological inhibitors of Gα_q, such as FR900359, or employing loss-of-function mutations in Gα_q, the specificity and magnitude of biosensor responses can be assessed, confirming that observed signals are directly attributable to Gα_q activity. Conversely, constitutively active Gα_q mutants can be used to validate biosensor sensitivity and probe downstream signalling

mechanisms. This approach is valuable for dissecting the molecular determinants of $G\alpha_q$ -mediated signalling and for screening potential modulators of Gq activity in physiological and pathological contexts.

One further possible area of optimisation could be increasing the number of fluorescent proteins within the biosensor. Within the piece of work describing the original BERKY-style biosensor, constructs possessing either one, two, or three YFP proteins were compared to investigate whether increasing the ratio of the BRET donor and acceptor molecules improved the signal window range of the biosensor, revealing that three YFP proteins within one biosensor produced the most robust window (Maziarz et al., 2020). In addition to the number of fluorescent proteins, the length of the α -helical linker could be increased. This amino acid sequence is used to regulate the interaction between the two BRET donor and acceptor proteins by controlling the length of the helix, thus the distance between the two proteins. The concept of SPASM sensors is that if the length is correct, the effective concentration will be in line with the K_D of the detector for whatever it binds to (in this case $G\alpha_q$ -GTP). Changing the length of the linker changes this effective concentration and therefore if the affinity of the detector for $G\alpha_q$ is too high or too low, changing the length of this linker may have an effect (Sivaramakrishnan & Spudich, 2011).

Furthermore, the biosensor should be employed in alternative formats such as BRET microscopy (Coulon et al., 2008; Namkung et al., 2016). This technique allows for the real-time visualisation and quantification of molecular interactions in live cells. The largest issue when utilising the BRET-based biosensors in primary cell models is the poor transfection. Examining a biosensor using BRET microscopy offers several distinct advantages, particularly as it allows selection and measurement from the few cells that actually express the biosensor.

5.5 Conclusions

In summary, here it was demonstrated that a biosensor can be designed to measure $G\alpha$ -GTP, the most proximal measure of G protein activation, and optimised to reduce background and increase the signal window of detection. This biosensor was employed in studies measuring mGlu₅ receptor activation then continued into studies on how mGlu₅ receptor phosphorylation impacts G protein activation, revealing a decrease in G protein activation with removal of C-terminal serine and threonine residues. The biosensor was then successfully progressed into neuronal cultures to measure endogenous G protein activation by glutamate receptors, indicating that the generated unimolecular, genetically encoded biosensor is capable of measuring endogenous glutamate receptor activation.

6 Final Discussion

As with the other members of the GPCR superfamily, the mGlu₅ receptor couples to two fundamental pathways: the phosphorylation/ β -arrestin 2-mediated pathway, and the G protein-dependent pathway. Hence, to explore the impact of direct receptor phosphorylation on said pathways *in vitro*, two phosphorylation-deficient mutants of the mGlu₅ receptor were generated. One consisted of all C-terminal serine residues being removed through mutation to alanine residues (mGlu₅-PD), and another whereby both C-terminal serine and threonine residues were removed (mGlu₅-TPD).

Studies performed in Chapter 3 established that whilst removal of C-terminal phosphorylation sites of mGlu₅ reduces β -arrestin 2 recruitment to the receptor, receptor internalisation is unaffected, however internalisation was not observed for the wildtype receptor. This was contrary to other studies, in which either β -arrestin 2 recruitment to mGlu₅ was not demonstrated (Abreu et al., 2021), or internalisation of the receptor was observed (Ribeiro et al., 2009; Trivedi & Bhattacharyya, 2012; van Senten et al., 2022). One drawback of the current study is that mGlu₅ signalling has broadly been investigated in artificial overexpressing HEK293 cell lines; whilst the simplicity of these *in vitro* models permit measurement of basic GPCR signalling, the complexities of receptor signalling that occurs *in vivo* are not recapitulated and are not representative of the signalling network in the central nervous system. The signal transduction pathways of mGlu₅ could be explored in primary cortico-hippocampal neurons, an example of a cell type that endogenously expresses the receptor. On the whole, data from Chapter 3 indicates that phosphorylation-dependent signal transduction from the mGlu₅-PD and mGlu₅-TPD receptors is impaired, drawing the conclusion that C-terminal phosphorylation of serine and threonine residues plays a key role in β -arrestin 2 recruitment.

Further studies in this work on the impact of phosphorylation on the G protein-dependent signal transduction pathway (Chapter 4) imply that mutation of serine and threonine residues from the C-terminus of mGlu₅ present no significant differences in the impact on agonist activated G protein transduction but impacts the agonist-independent G protein activation in the cells. Subsequent to the establishment of expression of the mGlu₅ receptor and its phosphorylation-

deficient mutants in stable cell lines, *in vitro* G protein-dependent signal transduction assays were performed to examine the impact of phosphorylation on this transduction pathway.

Throughout this piece of work, the mGlu₅ receptor has consistently exhibited high constitutive activity in a variety of assay formats. The constitutive activity of mGlu₅ represents a critical aspect of its function, with significant implications for both normal physiology and disease pathology. The findings from this study, in conjunction with existing literature, underscore the importance of this receptor's basal activity in modulating intracellular signalling pathways and influencing cellular behaviour. This study observed that phosphorylation is important to the constitutive activity of mGlu₅. Using biosensors to measure both G protein activation and β -arrestin 2 recruitment, alongside *in vitro* assays measuring other G protein dependent downstream signalling factors, constitutive activity was detected. The question remains as to whether this is due to constitutive direct phosphorylation, or constitutive phosphorylation due to constitutive glutamate release within the cell. The constitutive activity of mGlu₅ has been well-documented in the literature (Ango et al., 2001; Young et al., 2008, 2013b), finding that constitutive activity plays a key role in neuronal plasticity. Pathologically, constitutive activity has been implicated in disorders such as Fragile X Syndrome and schizophrenia. Several studies have explored the molecular mechanisms underlying the constitutive activity of mGlu₅: it has been suggested that specific regions within the receptor's structure, such as the cross-linking of cysteine-rich domains, contribute to its basal activity by stabilising an active conformation (Huang et al., 2011). It was found that the TMDs of mGlu₅ can spontaneously activate G α_q proteins in the absence of the Venus fly trap domains (Goudett et al., 2004), indicating that the constitutive activity arises from the TMDs. This was corroborated by a later study, in which it was found that mutating Ser613 (located at the base of TMD2) to lysine resulted in higher levels of constitutive activity caused by charge repulsion with Lys665 (TMD3) (Doré et al., 2014).

The experiments performed here indicate that the responses are specific to the mGlu₅ receptor, demonstrated by comparison to pcDNA3 transfected cells, cells without doxycycline treatment, and parental cells throughout the study. However, to further confirm that the basal level of signalling is specific to the mGlu₅ receptor, a negative allosteric modulator such as 2-methyl-6-(phenylethynyl)pyridine (MPEP) or VU0424238 (Felts et al., 2017) could be utilised

to dampen down the signal. Pharmacological modulation of the constitutive activity of mGlu₅ has therapeutic potential: negative allosteric modulators such as MPEP and CTEP have been shown to reduce excessive mGlu₅ signalling, providing symptomatic relief in preclinical models of neuropsychiatric disorders (Milanese et al., 2021; Yan et al., 2005). The development of selective inverse agonists and negative allosteric modulators that impact the constitutive activity of a GPCR holds promise for treating disorders associated with excessive receptor activity. Furthermore, whilst cells were treated with GPT preceding assays to reduce basal glutamate levels, different concentrations or durations of administration were not investigated. Alternatively, the receptor could be co-expressed with an excitatory amino acid transporter (as employed in studies by Koehl et al. (2019) and van Senten et al. (2022)), as a substitute measure for removal of glutamate from the cell. To confirm the glutamate levels in the assay buffer have been reduced, the levels of glutamate in the medium or assay buffer could be measured through colorimetric spectrophotometry, a fluorometric assay, or a Glutamate-Glo™ assay to ensure glutamate levels are consistently reduced between experiments.

An impact of phosphorylation was observed on both agonist dependent and agonist independent receptor activity within Chapter 3, however an impact on solely agonist independent receptor activity was observed in Chapter 4. A decrease in receptor activity was seen with removal of C-terminal phosphorylation sites for arrestin recruitment, G protein dissociation, and G protein dependent second messenger production, indicating there may be some common feature within all of these receptor-dependent events that is reliant on C-terminal phosphorylation. Phosphorylation of the C-terminal tail may be having an effect on the receptor's ability to elicit a conformational change, preventing movement of the receptor thus hindering G protein activation or recruitment of arrestins, however this would not explain the differences seen between ligand dependent and ligand independent activity.

Within Chapter 5, a genetically encoded unimolecular biosensor was generated and optimised to measure Gα_q activation. This was utilised to measure G protein activation in cells expressing Gα_q protein-coupled receptor activation, and then phospho-deficient mGlu₅ mutant receptor signalling, revealing that C-terminal phosphorylation of the receptor negatively impacts G protein activation. This contradicts data presented in Chapter 4, in which only agonist independent G protein activation was affected by phosphorylation, yet here agonist dependent G

protein activation was reduced by removal of C-terminal sites of phosphorylation. One explanation for this finding could be that the generated and optimised biosensor is more sensitive at measuring G protein activation than the assays employed in Chapter 4; the assays in the latter chapter measure downstream signalling factors and G protein dissociation, whilst Chapter 5 measures receptor activation at a stage far more proximal to the receptor. Additionally, the NEWPATH assay utilised in Chapter 4 requires exogenous G proteins whereas the novel iSpNG biosensor measures receptor activity through endogenous G proteins.

Furthermore, the biosensor was used in primary neuronal cultures to measure endogenous G protein activation after stimulation with the agonist glutamate, demonstrating that endogenous $G\alpha_q$ protein-coupled receptor activation can be detected with this novel biosensor. Previously, biosensors have been employed to measure endogenous GPCR signalling in primary neuronal cultures, detecting $G\alpha_{i/o}$ protein-coupled receptor activation. This study revealed that the $GABA_B$, α_2 adrenergic receptor, and the cannabinoid CB1 receptors produced different pharmacological activity in primary neurons versus heterologous cells (Xu et al., 2024), highlighting the key use of biosensors for evaluating endogenous GPCRs and the considerations of this differencing behaviour when translating research studies. However, this study noted low neuron transfection efficiency (at around 2%), as noted here in this piece of work. Considering this, the study by Xu et al. (2024) performed neuronal transfection via lipofectamine, similar to my work here, whereas previous neuronal biosensor transfections have used viral vectors (Maziarz et al., 2020) to improve this transfection efficiency.

A glutamate-specific biosensor was previously generated and optimised, designed to measure in real-time the metabolism of glutamate in living cells, tissues, or intact organisms. These glutamate-sensitive fluorescent reporters (iGluSnFR) have been used to detect glutamate in *Caenorhabditis elegans*, zebrafish, mice and ferrets, then in pyramidal neurons in acute brain slices, showing that iGluSnFR responds robustly and specifically *in situ* to glutamate release (Marvin et al., 2013). This iGluSnFR reporter has been optimised to generate functionally brighter reporters permitting *in vivo* imaging where previous sensors were too dim, detecting sub-micromolar to millimolar glutamate levels, and having yellow, cyan, green, or blue emission profiles (Marvin et al., 2018). Recently, the glutamate reporters have been further optimised to possess greater dynamic range, expression and photostability reporting rapid activation kinetics

and measurement of synaptic glutamate release in cultured neurons (Aggarwal et al., 2023). Finally, faster versions of iGluSnFR have been evolved to measure individual glutamate release events in rat hippocampal slices with improved signal-to-noise ratios and kinetics (Helassa et al., 2018). These studies demonstrate the availability of biosensors to measure with high precision the endogenous glutamate release in the nervous system, despite requiring years of optimisation. Such sensors could be employed in the mGlu₅ Flp-In™ T-REx™ model generated in this work to determine if endogenous glutamate is present at a level that would activate the receptor and induce signalling, aiding in answering the question as to whether the basal activity is ligand dependent or otherwise.

To translate the studies on mGlu₅ C-terminal phosphorylation to an *in vivo* setting, phospho-deficient mutant mice can be generated. Utilising a mouse model in which mGlu₅ C-terminal phosphorylation sites have been mutated would permit further study on the impact of phosphorylation on physiology. If phosphorylation regulates constitutive activity, a phosphodeficient mutant receptor will exhibit changes in basal receptor activity, which in turn should impact downstream signalling and receptor-mediated physiological or behavioural functions. Constitutive activity is often linked to specific physiological functions of mGlu₅ receptors, such as synaptic plasticity, anxiety, or learning and memory. By comparing wildtype, knockout, and phosphodeficient mutant mice, it can be demonstrated as to whether constitutive activity contributes to these functions.

To assess these functions, behavioural tests can be performed such as fear conditioning or spatial memory tasks (for learning and memory) or elevated plus maze and open field tests (for anxiety-like behaviour). Synaptic function can be monitored *ex vivo* through electrophysiological recordings in, for example, cortico-hippocampal slices to evaluate the impact of the phosphodeficient mutation on synaptic plasticity. These anxiety-like behavioural tests have been performed for the M1 receptor, comparing the wildtype receptor to a knockout and phosphodeficient M1 receptor mutant (M1-PD), demonstrating that M1-PD mice show fewer entries to open elevated plus maze arms thus are more anxious, indicating phosphorylation regulates anxiety (Bradley et al., 2020). In addition, M1-PD mice were hypoactive in the open field test; in contrast to the anxiolytic responses, regulation of locomotor behaviour is not dependent on receptor phosphorylation but potentially regulated in a G protein-dependent manner.

As an intermediate to animal studies, wildtype mGlu₅ expressing neurons could be treated with kinase inhibitors to mimic a phosphodeficient state, then employed in assays utilised in the studies performed here throughout these chapters such as β -arrestin 2 recruitment, downstream second messenger assays, and a G protein activation biosensor assay to see the impact of phosphorylation on the activity of the endogenous mGlu₅ receptor. This links to true *in vivo* readouts through measurement of the endogenous receptor *in situ*. Translating the pharmacology from artificial *in vitro* experiments to these endogenous receptor experiments provides greater clinical significance and more relevance to drug discovery.

GPCRs are excellent drug targets for a multitude of pathologies, but it is important to understand the pharmacological profile of the receptors to inform drug development. There is the need to dissect the signalling pathways these receptors engage with to identify clinically beneficial transduction pathways versus pathways that may bring about adverse effects. There are multiple mGlu₅-targeting drugs that have entered clinical trials (dipraglurant, completed Phase II for Parkinson's Disease; basimglurant, completed Phase II for Fragile X Syndrome; AZD2516, completed Phase I for neuropathic pain), however many drugs have been discontinued in clinical trials (raseglurant, terminated Phase II for migraine; AZD2066, terminated Phase II for major depressive disorder; mavoglurant, discontinued in Phase III for Fragile X Syndrome) (see Budgett et al., (2022) for a review). Further investigation into the mGlu₅ transduction pathways and the role of direct receptor phosphorylation will aid in the understanding of the clinical potential of this receptor.

This failure of mGlu₅-targeting drugs in the clinical setting could also be impacted by the difficulty in translating preclinical results into clinical trials. Basimglurant, an mGlu₅ NAM, has shown promising results in an APP^{swe}/PS1 Δ E9 Alzheimer's mouse model (Hamilton et al., 2016). However, this same drug failed to demonstrate efficacy over placebo in clinical trials for depression or FXS (Quiroz et al., 2016; Youssef et al., 2017). Similarly, mavoglurant (developed predominantly for FXS) failed to show improvements over placebo in the clinical setting, and this was proposed to be attributed to FXS potentially manifesting itself differently in humans compared to rodent models (Berry-Kravis et al., 2016). Additionally, the complex nature of mGlu₅ signalling

and widespread expression in the brain gives rise to significant side effects when targeting this receptor. For instance, fenobam, an mGlu₅ NAM, despite showing efficacy for anxiety (Pecknold et al., 1982), with an early study finding no clinically significant adverse effects (Berry-Kravis et al., 2009), was later removed from clinical trials due to association with impairment in learning and other cognitive disturbances (Jacob et al., 2009). Finally, many mGlu₅-targeting drugs fail due to the heterogeneity of the disorders that are targeted, hence mGlu₅ modulation may not be effective for every patient. All things considered, further basic research on the precise signalling mechanisms of mGlu₅ and the interplay with receptor phosphorylation is required to find a way to precisely target and modulate this receptor.

In conclusion, the data presented here indicate that direct phosphorylation of the mGlu₅ C-terminal serine and threonine residues not only impacts β -arrestin 2 signalling, but also G protein-dependent signalling. These findings are important as they highlight that the requirement for understanding the basic signalling profiles of receptors in order to deconvolute the complicated signal transduction. Moreover, the data presented in this thesis highlights the importance of elucidating the mechanisms by which phosphorylation modulates mGlu₅ activity, through which we gain critical insights into the dynamic regulation of synaptic transmission and plasticity, fundamental processes underlying learning, memory, and overall brain function.

7 References

- Abd-Elrahman, K. S., Albaker, A., de Souza, J. M., Ribeiro, F. M., Schlossmacher, M. G., Tiberi, M., Hamilton, A., & Ferguson, S. S. G. (2020). A β oligomers induce pathophysiological mGluR5 signaling in Alzheimer's disease model mice in a sex-selective manner. *Science Signaling*, 13(662). <https://doi.org/10.1126/scisignal.abd2494>
- Abd-Elrahman, K. S., Hamilton, A., Albaker, A., & Ferguson, S. S. G. (2023). mGluR5 Contribution to Neuropathology in Alzheimer Mice Is Disease Stage-Dependent. *Cite This: ACS Pharmacol. Transl. Sci*, 2020, 4. <https://doi.org/10.1021/acsptsci.0c00013>
- Abd-Elrahman, K. S., Hamilton, A., Vasefi, M., & Ferguson, S. S. G. (2018). Autophagy is increased following either pharmacological or genetic silencing of mGluR5 signaling in Alzheimer's disease mouse models. *Molecular Brain*, 11(1). <https://doi.org/10.1186/s13041-018-0364-9>
- Abe, T., Sugiharas, H., Nawasq, H., Shigemotoy, R., Mizunoll, N., & Nakanishis, S. (1992). Molecular Characterization of a Novel Metabotropic Glutamate Receptor mGluR5 Coupled to Inositol Phosphate/Ca²⁺ Signal Transduction*. In *THE JOURNAL OF BIOLOGICAL CHEMISTRY* (Vol. 267, Issue 0).
- Abiko, L. A., Petrovic, I., Tatli, M., Desai, S., Stahlberg, H., Spang, A., Grzesiek, S., & Abiko, L. (2024). Biased agonism of carvedilol in the β 1-adrenergic receptor is governed by conformational exclusion. *BioRxiv*. <https://doi.org/10.1101/2024.07.19.604263>
- Abreu, N., Acosta-Ruiz, A., Xiang, G., & Levitz, J. (2021). Mechanisms of differential desensitization of metabotropic glutamate receptors. *Cell Reports*, 35(4), 109050. <https://doi.org/10.1016/j.celrep.2021.109050>
- Aggarwal, A., Liu, R., Chen, Y., Ralowicz, A. J., Bergerson, S. J., Tomaska, F., Mohar, B., Hanson, T. L., Hasseman, J. P., Reep, D., Tsegaye, G., Yao, P., Ji, X., Kloos, M., Walpita, D., Patel, R., Mohr, M. A., Tillberg, P. W., GENIE Project Team, T., ... Podgorski, K. (2023). Glutamate indicators with improved activation kinetics and localization for imaging synaptic transmission. *Nature Methods* |, 20, 925–934. <https://doi.org/10.1038/s41592-023-01863-6>
- Aguirre, V., Werner, E. D., Giraud, J., Lee, Y. H., Shoelson, S. E., & White, M. F. (2002). Phosphorylation of Ser307 in insulin receptor substrate-1 blocks interactions with the insulin receptor and inhibits insulin action. *The Journal of Biological Chemistry*, 277(2), 1531–1537. <https://doi.org/10.1074/JBC.M101521200>
- Alexander, S. P. H., Christopoulos, A., Davenport, A. P., Kelly, E., Mathie, A., Peters, J. A., Veale, E. L., Armstrong, J. F., Faccenda, E., Harding, S. D., Pawson, A. J., Southan, C., Davies, J. A., Abbracchio, M. P., Alexander, W., Al-hosaini, K., Bäck, M., Barnes, N. M., Bathgate, R., ... Ye, R. D. (2021). THE CONCISE GUIDE TO PHARMACOLOGY 2021/22: G protein-coupled receptors. *British Journal of Pharmacology*, 178(S1), S27–S156. <https://doi.org/10.1111/bph.15538>
- Alonso-Buenaposada, I. D., Rey-Raap, N., Calvo, E. G., Menéndez, J. A., & Arenillas, A. (2016). Effect of methanol content in commercial formaldehyde solutions on the porosity of RF carbon xerogels. <https://doi.org/10.1016/J.JNONCRY SOL.2015.06.017>
- Alvarez-Curto, E., Inoue, A., Jenkins, L., Raihan, S. Z., Prihandoko, R., Tobin, A. B., & Milligan, G. (2016). Targeted elimination of G proteins and arrestins

- defines their specific contributions to both intensity and duration of G protein-coupled receptor signaling. *Journal of Biological Chemistry*, 291(53), 27147–27159. <https://doi.org/10.1074/jbc.M116.754887>
- Ango, F., Prézeau, L., Muller, T., Tu, J. C., Xiao, B., Worley, P. F., Pin, J. P., Bockaert, J., & Fagni, L. (2001). Agonist-independent activation of metabotropic glutamate receptors by the intracellular protein Homer. *Nature*, 411(6840), 962–965. <https://doi.org/10.1038/35082096>
- Attwood, T. K., & Findlay, J. B. C. (1994). Fingerprinting G-protein-coupled receptors. In *Protein Engineering* (Vol. 7, Issue 2). <https://academic.oup.com/peds/article/7/2/195/1515951>
- Atwood, B. K., Lopez, J., Wager-Miller, J., Mackie, K., & Straiker, A. (2011). Expression of G protein-coupled receptors and related proteins in HEK293, AtT20, BV2, and N18 cell lines as revealed by microarray analysis. *BMC Genomics*, 12, 14. <https://doi.org/10.1186/1471-2164-12-14>
- Ayala, J. E., Chen, Y., Banko, J. L., Sheffler, D. J., Williams, R., Telk, A. N., Watson, N. L., Xiang, Z., Zhang, Y., Jones, P. J., Lindsley, C. W., Olive, M. F., & Conn, P. J. (2009). mGluR5 Positive Allosteric Modulators Facilitate both Hippocampal LTP and LTD and Enhance Spatial Learning. *Neuropsychopharmacology*, 34(9), 2057–2071. <https://doi.org/10.1038/npp.2009.30>
- Bäckström, P., & Hyytiä, P. (2005). *Ionotropic and Metabotropic Glutamate Receptor Antagonism Attenuates Cue-Induced Cocaine Seeking*. <https://doi.org/10.1038/sj.npp.1300845>
- Bagur, R., & Hajnóczky, G. (2017). Intracellular Ca²⁺ sensing: role in calcium homeostasis and signaling. *Molecular Cell*, 66(6), 780. <https://doi.org/10.1016/J.MOLCEL.2017.05.028>
- Bai, M. (2004). Dimerization of G-protein-coupled receptors: Roles in signal transduction. *Cellular Signalling*, 16(2), 175–186. [https://doi.org/10.1016/S0898-6568\(03\)00128-1](https://doi.org/10.1016/S0898-6568(03)00128-1)
- Balázs, R., Miller, S., Romano, C., De Vries, A., Chun, Y., & Cotman, C. W. (1997). Metabotropic glutamate receptor mGluR5 in astrocytes: pharmacological properties and agonist regulation. *Journal of Neurochemistry*, 69(1), 151–163. <https://doi.org/10.1046/J.1471-4159.1997.69010151.X>
- Barki, N., Jenkins, L., Marsango, S., Dedeo, D., Bolognini, D., Dwomoh, L., Abdelmalik, A. M., Nilsen, M., Stoffels, M., Nagel, F., Schulz, S., Tobin, A. B., & Milligan, G. (2023). Phosphorylation bar-coding of Free Fatty Acid receptor 2 is generated in a tissue-specific manner. *ELife*. <https://doi.org/10.1101/2023.09.01.555873>
- Barodia, S. K., Sophronea, T., & Luthra, P. M. (2022). A2A R mediated modulation in IP3 levels altering the [Ca²⁺]_i through cAMP-dependent PKA signalling pathway. *Biochimica et Biophysica Acta (BBA) - General Subjects*, 1866(12), 130242. <https://doi.org/10.1016/J.BBAGEN.2022.130242>
- Bartas, K., Hui, M., Zhao, W., Macchia, D., Nie, Q., & Beier, K. T. (2024). Analysis of changes in inter-cellular communications during Alzheimer's Disease pathogenesis 1 reveals conserved changes in glutamatergic transmission in mice and humans. *BioRxiv*. <https://doi.org/10.1101/2024.04.30.591802>
- Bear, M. F., Huber, K. M., & Warren, S. T. (2004). The mGluR theory of fragile X mental retardation. *Trends in Neurosciences*, 27(7), 370–377. <https://doi.org/10.1016/j.tins.2004.04.009>
- Bellozi, P. M. Q., Gomes, G. F., da Silva, M. C. M., Lima, I. V. de A., Batista, C. R. Á., Carneiro Junior, W. de O., Dória, J. G., Vieira, É. L. M., Vieira, R. P., de

- Freitas, R. P., Ferreira, C. N., Candelario-Jalil, E., Wyss-Coray, T., Ribeiro, F. M., & de Oliveira, A. C. P. (2019). A positive allosteric modulator of mGluR5 promotes neuroprotective effects in mouse models of Alzheimer's disease. *Neuropharmacology*, *160*. <https://doi.org/10.1016/j.neuropharm.2019.107785>
- Benquet, P., Gee, C. E., & Gerber, U. (2002). *Two Distinct Signaling Pathways Upregulate NMDA Receptor Responses via Two Distinct Metabotropic Glutamate Receptor Subtypes*.
- Berridge, M. J., Downes, C. P., & Hanley, M. R. (1989). Neural and developmental actions of lithium: A unifying hypothesis. *Cell*, *59*(3), 411–419. [https://doi.org/10.1016/0092-8674\(89\)90026-3](https://doi.org/10.1016/0092-8674(89)90026-3)
- Berry-Kravis, E., Des Portes, V., Hagerman, R., Jacquemont, S., Charles, P., Visootsak, J., Brinkman, M., Rerat, K., Koumaras, B., Zhu, L., Barth, G. M., Jaecklin, T., Apostol, G., & Von Raison, F. (2016). Mavoglurant in fragile X syndrome: Results of two randomized, double-blind, placebo-controlled trials. *Science Translational Medicine*, *8*(321). https://doi.org/10.1126/SCITRANSLMED.AAB4109/SUPPL_FILE/8-321RA5_SM.PDF
- Berry-Kravis, E., Hessel, D., Coffey, S., Hervey, C., Schneider, A., Yuhas, J., Hutchison, J., Snape, M., Tranfaglia, M., Nguyen, D. V., & Hagerman, R. (2009). A pilot open label, single dose trial of fenobam in adults with fragile X syndrome. *J Med Genet*, *46*, 266–271. <https://doi.org/10.1136/jmg.2008.063701>
- Bessis, A.-S., Rondard, P., Gaven, F., Brabet, I., Triballeau, N., Pré Zeau †, L., Acher, F., & Pin, J.-P. (2002). Closure of the Venus flytrap module of mGlu8 receptor and the activation process: Insights from mutations converting antagonists into agonists. *PNAS*, *99*(17), 11097–11102. <https://www.pnas.org>
- Beyer, H. M., Gonschorek, P., Samodelov, S. L., Meier, M., Weber, W., & Zurbriggen, M. D. (2015). AQUA cloning: A versatile and simple enzyme-free cloning approach. *PLoS ONE*, *10*(9). <https://doi.org/10.1371/journal.pone.0137652>
- Bhattacharya, M., Babwah, A. V., Godin, C., Anborgh, P. H., Dale, L. B., Poulter, M. O., & Ferguson, S. S. G. (2004). Ral and phospholipase D2-dependent pathway for constitutive metabotropic glutamate receptor endocytosis. *Journal of Neuroscience*, *24*(40), 8752–8761. <https://doi.org/10.1523/JNEUROSCI.3155-04.2004>
- Black, J. W., & Leff, P. (1983). Operational Models of Pharmacological Agonism. In *Proc. R. Soc. Lond. B* (Vol. 220). <https://royalsocietypublishing.org/>
- Bohn, L. M., Lefkowitz, R. J., Gainetdinov, R. R., Peppel, K., Caron, M. G., & Lin, F. T. (1999). Enhanced morphine analgesia in mice lacking beta-arrestin 2. *Science (New York, N.Y.)*, *286*(5449), 2495–2498. <https://doi.org/10.1126/SCIENCE.286.5449.2495>
- Boudin, H., Doan, A., Xia, J., Shigemoto, R., Huganir, R. L., Worley, P., & Craig, A. M. (2000). Presynaptic clustering of mGluR7a requires the PICK1 PDZ domain binding site. *Neuron*, *28*(2), 485–497. [https://doi.org/10.1016/S0896-6273\(00\)00127-6](https://doi.org/10.1016/S0896-6273(00)00127-6)
- Bradley, S. J., Bourgognon, J. M., Sanger, H. E., Verity, N., Mogg, A. J., White, D. J., Butcher, A. J., Moreno, J. A., Molloy, C., Macedo-Hatch, T., Edwards, J. M., Wess, J., Pawlak, R., Read, D. J., Sexton, P. M., Broad, L. M., Steinert, J. R., Mallucci, G. R., Christopoulos, A., ... Tobin, A. B. (2017). M1 muscarinic allosteric modulators slow prion neurodegeneration and restore memory loss. *Journal of Clinical Investigation*, *127*(2), 487–499. <https://doi.org/10.1172/JCI87526>

- Bradley, S. J., & Challiss, R. (2011). Defining protein kinase/phosphatase isoenzymic regulation of mGlu 5 receptor-stimulated phospholipase C and Ca²⁺ responses in astrocytes. *British Journal of Pharmacology*, *164*(2 B), 755–771. <https://doi.org/10.1111/j.1476-5381.2011.01421.x>
- Bradley, S. J., & Challiss, R. A. J. (2012). G protein-coupled receptor signalling in astrocytes in health and disease: A focus on metabotropic glutamate receptors. *Biochemical Pharmacology*, *84*(3), 249–259. <https://doi.org/10.1016/j.bcp.2012.04.009>
- Bradley, S. J., Molloy, C., Valuskova, P., Dwomoh, L., Scarpa, M., Rossi, M., Finlayson, L., Svensson, K. A., Chernet, E., Barth, V. N., Gherbi, K., Sykes, D. A., Wilson, C. A., Mistry, R., Sexton, P. M., Christopoulos, A., Mogg, A. J., Rosethorne, E. M., Sakata, S., ... Tobin, A. B. (2020). Biased M1-muscarinic-receptor-mutant mice inform the design of next-generation drugs. *Nature Chemical Biology*, *16*(3), 240–249. <https://doi.org/10.1038/s41589-019-0453-9>
- Bradley, S. J., Wiegman, C. H., Iglesias, M. M., Kong, K. C., Butcher, A. J., Plouffe, B., Goupil, E., Bourgoignon, J. M., Macedo-Hatch, T., Legouill, C., Russell, K., Laporte, S. A., König, G. M., Kostenis, E., Bouvier, M., Chung, K. F., Amrani, Y., & Tobin, A. B. (2016). Mapping physiological G protein-coupled receptor signaling pathways reveals a role for receptor phosphorylation in airway contraction. *Proceedings of the National Academy of Sciences of the United States of America*, *113*(16), 4524–4529. <https://doi.org/10.1073/pnas.1521706113>
- Bradley, S. R., Rees, H. D., Yi, H., Levey, A. I., & Conn, P. J. (1998). Distribution and developmental regulation of metabotropic glutamate receptor 7a in rat brain. *Journal of Neurochemistry*, *71*(2), 636–645. <https://doi.org/10.1046/J.1471-4159.1998.71020636.X>
- Brandish, P. E., Hill, L. A., Zheng, W., & Scolnick, E. M. (2003). Scintillation proximity assay of inositol phosphates in cell extracts: High-throughput measurement of G-protein-coupled receptor activation. *Analytical Biochemistry*, *313*(2), 311–318. [https://doi.org/10.1016/S0003-2697\(02\)00630-9](https://doi.org/10.1016/S0003-2697(02)00630-9)
- Brašić, J. R., Nandi, A., Russell, D. S., Jennings, D., Barret, O., Martin, S. D., Slifer, K., Sedlak, T., Seibyl, J. P., Wong, D. F., & Budimirovic, D. B. (2021). Cerebral expression of metabotropic glutamate receptor subtype 5 in idiopathic autism spectrum disorder and fragile x syndrome: A pilot study. *International Journal of Molecular Sciences*, *22*(6), 1–16. <https://doi.org/10.3390/ijms22062863>
- Brown, J., Grayson, B., Neill, J. C., Harte, M., Wall, M. J., & Ngomba, R. T. (2023). Oscillatory Deficits in the Sub-Chronic PCP Rat Model for Schizophrenia Are Reversed by mGlu5 Receptor-Positive Allosteric Modulators VU0409551 and VU0360172. *Cells*, *12*(6), 919. <https://doi.org/10.3390/CELLS12060919/S1>
- Bruno, V., Copani, A., Knopfel, T., Kuhn, R., Casabona, G., Dell Albani, P., Condorelli, D. F., & Nicoletti, F. (1995). Activation of Metabotropic Glutamate Receptors Coupled to Inositol Phospholipid Hydrolysis Amplifies NMDA-induced Neuronal Degeneration in Cultured Cortical Cells. *34*(95), 1089–1098.
- Budgett, R. F., Bakker, G., Sergeev, E., Bennett, K. A., & Bradley, S. J. (2022). Targeting the Type 5 Metabotropic Glutamate Receptor: A Potential Therapeutic Strategy for Neurodegenerative Diseases? *Frontiers in Pharmacology*, *13*. <https://doi.org/10.3389/fphar.2022.893422>

- Burnett, G., & Kennedy, E. P. (1954). The Enzymatic Phosphorylation of Proteins. *Journal of Biological Chemistry*, 211(2), 969–980. [https://doi.org/10.1016/S0021-9258\(18\)71184-8](https://doi.org/10.1016/S0021-9258(18)71184-8)
- Butcher, A. J., Bradley, S. J., Prihandoko, R., Brooke, S. M., Mogg, A., Bourgognon, J.-M., Macedo-Hatch, T., Edwards, J. M., Bottrill, A. R., Challiss, R. A. J., Broad, L. M., Felder, C. C., & Tobin, A. B. (2016). An Antibody Biosensor Establishes the Activation of the M1 Muscarinic Acetylcholine Receptor during Learning and Memory. *The Journal of Biological Chemistry*, 291(17), 8862–8875. <https://doi.org/10.1074/jbc.M115.681726>
- Butcher, A. J., Hudson, B. D., Shimpukade, B., Alvarez-Curto, E., Prihandoko, R., Ulven, T., Milligan, G., & Tobin, A. B. (2014). Concomitant action of structural elements and receptor phosphorylation determines arrestin-3 interaction with the free fatty acid receptor FFA4. *Journal of Biological Chemistry*, 289(26), 18451–18465. <https://doi.org/10.1074/jbc.M114.568816>
- Cabello, N., Remelli, R., Canela, L., Soriguera, A., Mallol, J., Canela, E. I., Robbins, M. J., Lluís, C., Franco, R., McIlhinney, R. A. J., & Ciruela, F. (2007). Actin-binding Protein α -Actinin-1 Interacts with the Metabotropic Glutamate Receptor Type 5b and Modulates the Cell Surface Expression and Function of the Receptor*. *Journal of Biological Chemistry*, 282(16), 12143–12153. <https://doi.org/10.1074/jbc.M608880200>
- Campbell, R. R., Domingo, R. D., Williams, A. R., Wroten, M. G., McGregor, H. A., Waltermire, R. S., Greentree, D. I., Goulding, S. P., Thompson, A. B., Lee, K. M., Quadir, S. G., Chavez, C. L. J., Coelho, M. A., Gould, A. T., Von Jonquieres, G., Klugmann, M., Worley, P. F., Kippin, T. E., & Szumlanski, K. K. (2019). Increased Alcohol-Drinking Induced by Manipulations of mGlu5 Phosphorylation within the Bed Nucleus of the Stria Terminalis. *The Journal of Neuroscience : The Official Journal of the Society for Neuroscience*, 39(14), 2745–2761. <https://doi.org/10.1523/JNEUROSCI.1909-18.2018>
- Cao, Y., Namkung, Y., & Laporte, S. A. (2019). Methods to Monitor the Trafficking of β -Arrestin/G Protein-Coupled Receptor Complexes Using Enhanced Bystander BRET. *Methods in Molecular Biology*, 1957, 59–68. https://doi.org/10.1007/978-1-4939-9158-7_3
- Carman, C. V., & Benovic, J. L. (1998). G-protein-coupled receptors: Turn-ons and turn-offs. *Current Opinion in Neurobiology*, 8(3), 335–344. [https://doi.org/10.1016/S0959-4388\(98\)80058-5](https://doi.org/10.1016/S0959-4388(98)80058-5)
- Carman, C. V., Parent, J. L., Day, P. W., Pronin, A. N., Sternweis, P. M., Wedegaertner, P. B., Gilman, A. G., Benovic, J. L., & Kozasa, T. (1999a). Selective Regulation of G α q/11 by an RGS Domain in the G Protein-coupled Receptor Kinase, GRK2. *Journal of Biological Chemistry*, 274(48), 34483–34492. <https://doi.org/10.1074/JBC.274.48.34483>
- Carman, C. V., Parent, J. L., Day, P. W., Pronin, A. N., Sternweis, P. M., Wedegaertner, P. B., Gilman, A. G., Benovic, J. L., & Kozasa, T. (1999b). Selective Regulation of G α q/11 by an RGS Domain in the G Protein-coupled Receptor Kinase, GRK2. *Journal of Biological Chemistry*, 274(48), 34483–34492. <https://doi.org/10.1074/JBC.274.48.34483>
- Cerione, R. A., Benovic, J. L., Lefkowitz, R. J., Caron, M. G., Codina, J., & Birnbaumer, L. (1984). The mammalian beta 2-adrenergic receptor: reconstitution of functional interactions between pure receptor and pure stimulatory nucleotide binding protein of the adenylate cyclase system. *Biochemistry*, 23(20), 4519–4525. <https://doi.org/10.1021/BI00315A003>

- Chalfie, M., Tu, Y., Ward, W., & Prasher, D. (1993). Green Fluorescent Protein as a Marker for Gene Expression. In *Sov. Phys. Usp* (Vol. 286). Digital Instruments, Inc. <http://science.sciencemag.org/>
- Chang, K., & Roche, K. W. (2017). Structural and molecular determinants regulating mGluR5 surface expression. *Neuropharmacology*, *115*, 10–19. <https://doi.org/10.1016/j.neuropharm.2016.04.037>
- Chen, S. C. C., Chen, F. C., & Li, W. H. (2010). Phosphorylated and Nonphosphorylated Serine and Threonine Residues Evolve at Different Rates in Mammals. *Molecular Biology and Evolution*, *27*(11), 2548–2554. <https://doi.org/10.1093/MOLBEV/MSQ142>
- Chen, X. T., Pitis, P., Liu, G., Yuan, C., Gotchev, D., Cowan, C. L., Rominger, D. H., Koblisch, M., Dewire, S. M., Crombie, A. L., Violin, J. D., & Yamashita, D. S. (2013). Structure-activity relationships and discovery of a G protein biased μ opioid receptor ligand, [(3-methoxythiophen-2-yl)methyl]({2-[(9R)-9-(pyridin-2-yl)-6-oxaspiro-[4.5]decan-9-yl]ethyl})amine (TRV130), for the treatment of acute severe pain. *Journal of Medicinal Chemistry*, *56*(20), 8019–8031. https://doi.org/10.1021/JM4010829/SUPPL_FILE/JM4010829_SI_001.PDF
- Chen, Z., & Cole, P. A. (2015). Synthetic approaches to protein phosphorylation. *Current Opinion in Chemical Biology*, *28*, 115–122. <https://doi.org/10.1016/J.CBPA.2015.07.001>
- Chiamulera, C., Epping-Jordan, M. P., Zocchi, A., Marcon, C., Cottiny, C., Tacconi, S., Corsi, M., Orzi, F., & Conquet, F. (2001). Reinforcing and locomotor stimulant effects of cocaine are absent in mGluR5 null mutant mice. *Nature Neuroscience* *2001* *4*:9, *4*(9), 873–874. <https://doi.org/10.1038/nn0901-873>
- Chul, H. K., Lee, J., Lee, J. Y., & Roche, K. W. (2008). Metabotropic glutamate receptors: Phosphorylation and receptor signaling. In *Journal of Neuroscience Research* (Vol. 86, Issue 1, pp. 1–10). <https://doi.org/10.1002/jnr.21437>
- Ciruela, F., & McIlhinney, R. A. J. (1997). Differential internalisation of mGluR1 splice variants in response to agonist and phorbol esters in permanently transfected BHK cells. *FEBS Letters*, *418*(1–2), 83–86. [https://doi.org/10.1016/S0014-5793\(97\)01353-7](https://doi.org/10.1016/S0014-5793(97)01353-7)
- Conde-Ceide, S., Martínez-Vituro, C. M., Alcázar, J., García-Barrantes, P. M., Lavreysen, H., Mackie, C., Vinson, P. N., Rook, J. M., Bridges, T. M., Daniels, J. S., Megens, A., Langlois, X., Drinkenburg, W. H., Ahnaou, A., Niswender, C. M., Jones, C. K., Macdonald, G. J., Steckler, T., Conn, P. J., ... Lindsley, C. W. (2015). Discovery of VU0409551/JNJ-46778212: An mGlu5 Positive Allosteric Modulator Clinical Candidate Targeting Schizophrenia. *ACS Medicinal Chemistry Letters*, *6*(6), 716–720. <https://doi.org/10.1021/acsmedchemlett.5b00181>
- Conn, P. J., Jones, C. K., & Lindsley, C. W. (2009). Subtype-selective allosteric modulators of muscarinic receptors for the treatment of CNS disorders. *Trends in Pharmacological Sciences*, *30*(3), 148–155. <https://doi.org/10.1016/j.tips.2008.12.002>
- Correddu, D., Sharma, N., Kaur, S., Varnava, K. G., Mbenza, N. M., Sarojini, V., & Leung, I. K. H. (2020). An investigation into the effect of ribosomal protein S15 phosphorylation on its intermolecular interactions by using phosphomimetic mutant. *Chemical Communications*, *56*(57), 7857–7860. <https://doi.org/10.1039/D0CC01618G>
- Corti, C., Restituito, S., Rimland, J. M., Brabet, I., Corsi, M., Pin, J. P., & Ferraguti, F. (1998). Cloning and characterization of alternative mRNA forms for the rat metabotropic glutamate receptors mGluR7 and mGluR8. *European Journal of*

- Neuroscience*, 10, 3629–3641. <https://doi.org/10.1046/j.1460-9568.1998.00371.x>
- Coulon, V., Audet, M., Homburger, V., Bockaert, J., Fagni, L., Bouvier, M., & Perroy, J. (2008). Subcellular Imaging of Dynamic Protein Interactions by Bioluminescence Resonance Energy Transfer. *Biophysical Journal*, 94(3), 1001–1009. <https://doi.org/10.1529/BIOPHYSJ.107.117275>
- Coyle, J. T. (1996). The glutamatergic dysfunction hypothesis for schizophrenia. *Harvard Review of Psychiatry*, 3(5), 241–253. <https://doi.org/10.3109/10673229609017192>
- Coyle, J. T. (2006). Glutamate and Schizophrenia: Beyond the Dopamine Hypothesis. *Cellular and Molecular Neurobiology*, 26, 4–6. <https://doi.org/10.1007/s10571-006-9062-8>
- Craig, N. L. (1988). *THE MECHANISM OF CONSERVATIVE SITE-SPECIFIC RECOMBINATION*. www.annualreviews.org
- Craig Venter, J., Adams, M. D., Myers, E. W., Li, P. W., Mural, R. J., Sutton, G. G., Smith, H. O., Yandell, M., Evans, C. A., Holt, R. A., Gocayne, J. D., Amanatides, P., Ballew, R. M., Huson, D. H., Wortman, J. R., Zhang, Q., Kodira, C. D., Zheng, X. H., Chen, L., ... Zhu, X. (2001). The sequence of the human genome. *Science*, 291(5507), 1304–1351. <https://doi.org/10.1126/science.1058040>
- Crasto, C. J. (2010). Hydrophobicity profiles in G protein-coupled receptor transmembrane helical domains. *Journal of Receptor, Ligand and Channel Research*, 2010, 3–123. <https://doi.org/10.2147/JRLCR.S14437>
- Curtis, D. R., & Watkins, J. C. (1960). THE EXCITATION AND DEPRESSION OF SPINAL NEURONES BY STRUCTURALLY RELATED AMINO ACIDS. *Journal of Neurochemistry*, 6(2), 117–141. <https://doi.org/10.1111/j.1471-4159.1960.tb13458.x>
- Czernik, A. J., Girault, J.-A., Nairn, A. C., Chen, J., Snyder, G., Kebejian, J., & Greengard, P. (1991). Production of Phosphorylation State-Specific Antibodies. *Methods in Enzymology*, 201.
- Daaka, Y., Luttrell, L. M., & Lefkowitz, R. J. (1997). Switching of the coupling of the β 2-adrenergic receptor to different g proteins by protein kinase A. *Nature*, 390(6655), 88–91. <https://doi.org/10.1038/36362>
- Dale, N. C., Johnstone, E. K. M., White, C. W., & Pflieger, K. D. G. (2019). NanoBRET: The bright future of proximity-based assays. *Frontiers in Bioengineering and Biotechnology*, 7(MAR), 1–13. <https://doi.org/10.3389/fbioe.2019.00056>
- Davie, B. J., Christopoulos, A., & Scammells, P. J. (2013). Development of M1 mAChR allosteric and bitopic ligands: Prospective therapeutics for the treatment of cognitive deficits. *ACS Chemical Neuroscience*, 4(7), 1026–1048. https://doi.org/10.1021/CN400086M/ASSET/IMAGES/LARGE/CN-2013-00086M_0033.JPEG
- Day, P. W., Tesmer, J. J. G., Sterne-Marr, R., Freeman, L. C., Benovic, J. L., & Wedegaertner, P. B. (2004). Characterization of the GRK2 Binding Site of G α q. *Journal of Biological Chemistry*, 279(51), 53643–53652. <https://doi.org/10.1074/JBC.M401438200>
- Delahaye, L., Mothe-Satney, I., Myers, M. G., White, M. F., & Van Obberghen, E. (1998). Interaction of Insulin Receptor Substrate-1 (IRS-1) with Phosphatidylinositol 3-Kinase: Effect of Substitution of Serine for Alanine in Potential IRS-1 Serine Phosphorylation Sites. *Endocrinology*, 139(12), 4911–4919. <https://doi.org/10.1210/ENDO.139.12.6379>

- Desai, M. A., Burnett, J. P., Mayne, N. G., & Schoepp, D. D. (1995). Cloning and expression of a human metabotropic glutamate receptor 1 alpha: enhanced coupling on co-transfection with a glutamate transporter. *Molecular Pharmacology*, 48(4).
- Desai, M. A., Burnett, J. P., Mayne, N. G., & Schoepp, D. D. (1996). Pharmacological characterization of desensitization in a human mGlu1 α -expressing non-neuronal cell line co-transfected with a glutamate transporter. *British Journal of Pharmacology*, 118(6), 1558–1564. <https://doi.org/10.1111/J.1476-5381.1996.TB15574.X>
- Dev, K. K., Nakanishi, S., & Henley, J. M. (2001). Regulation of mglu(7) receptors by proteins that interact with the intracellular C-terminus. *Trends in Pharmacological Sciences*, 22(7), 355–361. [https://doi.org/10.1016/S0165-6147\(00\)01684-9](https://doi.org/10.1016/S0165-6147(00)01684-9)
- Dhami, G. K., Anborgh, P. H., Dale, L. B., Sterne-Marr, R., & Ferguson, S. S. G. (2002). Phosphorylation-independent regulation of metabotropic glutamate receptor signaling by G protein-coupled receptor kinase 2. *Journal of Biological Chemistry*, 277(28), 25266–25272. <https://doi.org/10.1074/jbc.M203593200>
- Di Marco, B., Dell'Albani, P., D'Antoni, S., Spatuzza, M., Bonaccorso, C. M., Musumeci, S. A., Drago, F., Bardoni, B., & Catania, M. V. (2021). Fragile X mental retardation protein (FMRP) and metabotropic glutamate receptor subtype 5 (mGlu5) control stress granule formation in astrocytes. *Neurobiology of Disease*, 154, 105338. <https://doi.org/10.1016/j.nbd.2021.105338>
- DiBerto, J. F., Smart, K., Olsen, R. H. J., & Roth, B. L. (2022). Agonist and antagonist TRUPATH assays for G protein-coupled receptors. *STAR Protocols*, 3(2). <https://doi.org/10.1016/j.xpro.2022.101259>
- Dingledine, R., Borges, K., Bowie, D., & Traynelis, S. F. (1999). The glutamate receptor ion channels. In *Pharmacological Reviews* (Vol. 51, Issue 1, pp. 7–61). <http://www.pharmrev.org>
- DiPilato, L. M., Cheng, X., & Zhang, J. (2004). Fluorescent indicators of cAMP and Epac activation reveal differential dynamics of cAMP signaling within discrete subcellular compartments. *Proceedings of the National Academy of Sciences of the United States of America*, 101(47), 16513–16518. <https://doi.org/10.1073/PNAS.0405973101>
- Dixon, A. S., Schwinn, M. K., Hall, M. P., Zimmerman, K., Otto, P., Lubben, T. H., Butler, B. L., Binkowski, B. F., Machleidt, T., Kirkland, T. A., Wood, M. G., Eggers, C. T., Encell, L. P., & Wood, K. V. (2016). NanoLuc Complementation Reporter Optimized for Accurate Measurement of Protein Interactions in Cells. *ACS Chem. Biol*, 11, 35. <https://doi.org/10.1021/acscchembio.5b00753>
- Dölen, G., Osterweil, E., Rao, B. S. S., Smith, G. B., Auerbach, B. D., Chattarji, S., & Bear, M. F. (2007). Correction of Fragile X Syndrome in Mice. *Neuron*, 56(6), 955–962. <https://doi.org/10.1016/j.neuron.2007.12.001>
- Doré, A. S., Okrasa, K., Patel, J. C., Serrano-Vega, M., Bennett, K., Cooke, R. M., Errey, J. C., Jazayeri, A., Khan, S., Tehan, B., Weir, M., Wiggin, G. R., & Marshall, F. H. (2014). Structure of class C GPCR metabotropic glutamate receptor 5 transmembrane domain. *Nature* 2014 511:7511, 511(7511), 557–562. <https://doi.org/10.1038/nature13396>
- Doumazane, E., Scholler, P., Zwier, J. M., Trinquet, E., Rondard, P., & Pin, J. (2011). A new approach to analyze cell surface protein complexes reveals specific heterodimeric metabotropic glutamate receptors. *The FASEB Journal*, 25(1), 66–77. <https://doi.org/10.1096/fj.10-163147>

- Drube, J., Haider, R. S., Matthees, E. S. F., Reichel, M., Zeiner, J., Fritzwanker, S., Ziegler, C., Barz, S., Klement, L., Filor, J., Weitzel, V., Kliewer, A., Miess-Tanneberg, E., Kostenis, E., Schulz, S., & Hoffmann, C. (2022). GPCR kinase knockout cells reveal the impact of individual GRKs on arrestin binding and GPCR regulation. *Nature Communications*, *13*(1). <https://doi.org/10.1038/s41467-022-28152-8>
- Dwivedi-Agnihotri, H., Chaturvedi, M., Baidya, M., Stepniwski, T. M., Pandey, S., Maharana, J., Srivastava, A., Caengprasath, N., Hanyaloglu, A. C., Selent, J., & Shukla, A. K. (2020). Distinct phosphorylation sites in a prototypical GPCR differently orchestrate β -arrestin interaction, trafficking, and signaling. *Science Advances*, *6*(37). <https://doi.org/10.1126/SCIADV.ABB8368>
- Eiger, D. S., Smith, J. S., Shi, T., Stepniwski, T. M., Tsai, C. F., Honeycutt, C., Boldizsar, N., Gardner, J., Nicora, C. D., Moghieb, A. M., Kawakami, K., Choi, I., Hicks, C., Zheng, K., Warman, A., Alagesan, P., Knape, N. M., Huang, O., Silverman, J. D., ... Rajagopal, S. (2023). Phosphorylation barcodes direct biased chemokine signaling at CXCR3. *Cell Chemical Biology*, *30*(4), 362. <https://doi.org/10.1016/J.CHEMBIOL.2023.03.006>
- El Far, O., Airas, J., Wischmeyer, E., Nehring, R. B., Karschin, A., & Betz, H. (2000). Interaction of the C-terminal tail region of the metabotropic glutamate receptor 7 with the protein kinase C substrate PICK1. *The European Journal of Neuroscience*, *12*(12), 4215–4221. <https://doi.org/10.1046/J.1460-9568.2000.01309.X>
- El Moustaine, D., Granier, S., Doumazane, E., Scholler, P., Rahmeh, R., Bron, P., Mouillac, B., Banères, J. L., Rondard, P., & Pin, J. P. (2012). Distinct roles of metabotropic glutamate receptor dimerization in agonist activation and G-protein coupling. *Proceedings of the National Academy of Sciences of the United States of America*, *109*(40), 16342–16347. <https://doi.org/10.1073/pnas.1205838109>
- Emery, A. C., Pshenichkin, S., Rodrigue Takoudjou, G., Grajkowska, E., Wolfe, B. B., & Wroblewski, J. T. (2010). The Protective Signaling of Metabotropic Glutamate Receptor 1 Is Mediated by Sustained, Beta-Arrestin-1-dependent ERK Phosphorylation. *Journal of Biological Chemistry*, *285*, 26041–26048. <https://doi.org/10.1074/jbc.M110.139899>
- Eng, A. G., Kolver, D. A., Hedrick, T. P., & Swanson, G. T. (2016). Transduction of group I mGluR-mediated synaptic plasticity by β -arrestin2 signalling. *Nature Communications*, *7*, 1–14. <https://doi.org/10.1038/ncomms13571>
- England, Christopher G., Ehlerding, E. B., & Cai, W. (2016). NanoLuc: A Small Luciferase is Brightening up the Field of Bioluminescence. *Bioconjug Chem.*, *27*(5), 1175–1187. <https://doi.org/10.1021/acs.bioconjchem.6b00112>
- Enz, R. (2012). Structure of metabotropic glutamate receptor C-terminal domains in contact with interacting proteins. *Frontiers in Molecular Neuroscience*, *5*(APRIL). <https://doi.org/10.3389/FNMOL.2012.00052>
- Fabian, C. B., Jordan, N. D., Cole, R. H., Carley, L. G., Thompson, S. M., Seney, M. L., Joffe, M. E., & Professor, A. (2024). Parvalbumin interneuron mGlu5 receptors govern sex differences in prefrontal cortex physiology and binge drinking. *BioRxiv*, 2023.11.20.567903. <https://doi.org/10.1101/2023.11.20.567903>
- Fagni, L., Ango, F., Perroy, J., & Bockaert, J. (2004). Identification and functional roles of metabotropic glutamate receptor-interacting proteins. *Seminars in Cell and Developmental Biology*, *15*(3), 289–298. <https://doi.org/10.1016/j.semcd.2003.12.018>

- Fagni, L., Ango, F., Prezeau, L., Worley, P. F., Pin, J. P., & Bockaert, J. (2003). Control of constitutive activity of metabotropic glutamate receptors by Homer proteins. *International Congress Series, 1249(C)*, 245–251. [https://doi.org/10.1016/S0531-5131\(03\)00600-9](https://doi.org/10.1016/S0531-5131(03)00600-9)
- Fazakerley, D. J., van Gerwen, J., Cooke, K. C., Duan, X., Needham, E. J., Díaz-Vegas, A., Madsen, S., Norris, D. M., Shun-Shion, A. S., Krycer, J. R., Burchfield, J. G., Yang, P., Wade, M. R., Brozinick, J. T., James, D. E., & Humphrey, S. J. (2023). Phosphoproteomics reveals rewiring of the insulin signaling network and multi-nodal defects in insulin resistance. *Nature Communications, 14*(1). <https://doi.org/10.1038/S41467-023-36549-2>
- Felts, A. S., Rodriguez, A. L., Blobaum, A. L., Morrison, R. D., Bates, B. S., Thompson Gray, A., Rook, J. M., Tantawy, M. N., Byers, F. W., Chang, S., Venable, D. F., Luscombe, V. B., Tamagnan, G. D., Niswender, C. M., Daniels, J. S., Jones, C. K., Conn, P. J., Lindsley, C. W., & Emmitte, K. A. (2017). Discovery of N-(5-Fluoropyridin-2-yl)-6-methyl-4-(pyrimidin-5-yloxy)picolinamide (VU0424238): A Novel Negative Allosteric Modulator of Metabotropic Glutamate Receptor Subtype 5 Selected for Clinical Evaluation. *Journal of Medicinal Chemistry, 60*(12), 5072–5085. <https://doi.org/10.1021/acs.jmedchem.7b00410>
- Ferguson, S. S. G., Downey, W. E., Colapietro, A. M., Barak, L. S., Ménard, L., & Caron, M. G. (1996). Role of β -arrestin in mediating agonist-promoted G protein-coupled receptor internalization. *Science, 271*(5247), 363–366. <https://doi.org/10.1126/SCIENCE.271.5247.363>
- Ferré, S., Karcz-Kubicha, M., Hope, B. T., Popoli, P., Burgueño, J., Gutiérrez, M. A., Casadó, V., Fuxe, K., Goldberg, S. R., Lluís, C., Franco, R., & Ciruela, F. (2002). Synergistic interaction between adenosine A2A and glutamate mGlu5 receptors: Implications for striatal neuronal function. *Proceedings of the National Academy of Sciences of the United States of America, 99*(18), 11940–11945. <https://doi.org/10.1073/PNAS.172393799/ASSET/3F708159-C02B-4F87-8E4B-487B3B8A4C55/ASSETS/GRAPHIC/PQ1723937004.JPEG>
- Flajolet, M., Rakhilin, S., Wang, H., Starkova, N., Nuangchamngong, N., Nairn, A. C., & Greengard, P. (2003). *Protein phosphatase 2C binds selectively to and dephosphorylates metabotropic glutamate receptor 3*. *100*(26). www.pnas.org/cgi/doi/10.1073/pnas.2136600100
- Flor, P. J., Lukic, S., Rüegg, D., Leonhardt, T., Knöpfel, T., & Kühn, R. (1995). Molecular cloning, functional expression and pharmacological characterization of the human metabotropic glutamate receptor type 4. *Neuropharmacology, 34*(2), 149–155. [https://doi.org/10.1016/0028-3908\(94\)00149-M](https://doi.org/10.1016/0028-3908(94)00149-M)
- Förster, Th. (1960). Transfer Mechanisms of Electronic Excitation Energy. *Radiation Research Supplement, 2*, 326–339.
- Fourgeaud, L., Bessis, A. S., Rossignol, F., Pin, J. P., Olivo-Marin, J. C., & Hémar, A. (2003). The metabotropic glutamate receptor mGluR5 is endocytosed by a clathrin-independent pathway. *Journal of Biological Chemistry, 278*(14), 12222–12230. <https://doi.org/10.1074/jbc.M205663200>
- Fowler, M. A., Varnell, A. L., & Cooper, D. C. (2011). mGluR5 knockout mice exhibit normal conditioned place-preference to cocaine. *Nature Precedings 2011*, 1–1. <https://doi.org/10.1038/npre.2011.6180.2>
- Fredriksson, R., Lagerström, M. C., Lundin, L. G., & Schiöth, H. B. (2003). The G-protein-coupled receptors in the human genome form five main families. Phylogenetic analysis, paralogon groups, and fingerprints. *Molecular Pharmacology, 63*(6), 1256–1272. <https://doi.org/10.1124/mol.63.6.1256>

- Fukata, Y., & Fukata, M. (2010). Protein palmitoylation in neuronal development and synaptic plasticity. *Nature Reviews Neuroscience* 2010 11:3, 11(3), 161–175. <https://doi.org/10.1038/nrn2788>
- Garbison, K. E., Heinz, B. A., & Lajiness, M. E. (2012). IP-3/IP-1 Assays. *Assay Guidance Manual*. <https://www.ncbi.nlm.nih.gov/books/NBK92004/>
- Gass, J. T., & Olive, M. F. (2009). Positive allosteric modulation of mGluR5 receptors facilitates extinction of a cocaine contextual memory. *Biological Psychiatry*, 65(8), 717–720. <https://doi.org/10.1016/J.BIOPSYCH.2008.11.001>
- Gereau IV, R. W., & Heinemann, S. F. (1998). Role of protein kinase C phosphorylation in rapid desensitization of metabotropic glutamate receptor 5. *Neuron*, 20(1), 143–151. [https://doi.org/10.1016/S0896-6273\(00\)80442-0](https://doi.org/10.1016/S0896-6273(00)80442-0)
- Ghosh, R., Gilda, J. E., & Gomes, A. V. (2014). The necessity of and strategies for improving confidence in the accuracy of western blots. *Expert Review of Proteomics*, 11(5), 549. <https://doi.org/10.1586/14789450.2014.939635>
- Giuffrida, R., Musumeci, S., D'Antoni, S., Bonaccorso, C. M., Giuffrida-Stella, A. M., Oostra, B. A., & Catania, M. V. (2005). A Reduced Number of Metabotropic Glutamate Subtype 5 Receptors Are Associated with Constitutive Homer Proteins in a Mouse Model of Fragile X Syndrome. *The Journal of Neuroscience*, 25(39), 8908. <https://doi.org/10.1523/JNEUROSCI.0932-05.2005>
- Goodman, J., Krupnick, J. G., Santini, F., Gurevich, V. V, Penn, R. B., Gagnon, A. W., Keen, J. H., & Benovic, J. L. (1996). β -Arrestin acts as a clathrin adaptor in endocytosis of the β 2- adrenergic receptor. *Nature*, 383(6599), 447–450. <https://doi.org/10.1038/383447a0>
- Goudett, C., Gaven, F., Kniazeff, J., Vol, C., Liu, J., Cohen-Gonsaud, M., Acher, F., Prézeau, L., & Pin, J. P. (2004). Heptahelical domain of metabotropic glutamate receptor 5 behaves like rhodopsin-like receptors. *Proceedings of the National Academy of Sciences of the United States of America*, 101(1), 378. <https://doi.org/10.1073/PNAS.0304699101>
- Grundmann, M., Merten, N., Malfacini, D., Inoue, A., Preis, P., Simon, K., Rüttiger, N., Ziegler, N., Benkel, T., Schmitt, N. K., Ishida, S., Müller, I., Reher, R., Kawakami, K., Inoue, A., Rick, U., Kühl, T., Imhof, D., Aoki, J., ... Kostenis, E. (2018). Lack of beta-arrestin signaling in the absence of active G proteins. *Nature Communications*, 9(1), 1–7. <https://doi.org/10.1038/s41467-017-02661-3>
- Grynkiewicz, G., Poenie, M., & Tsien, R. Y. (1985). A New Generation of Ca²⁺ Indicators with Greatly Improved Fluorescence Properties. *The Journal of Biological Chemistry*, 260(6).
- Guo, W., Molinaro, G., Collins, K. A., Hays, S. A., Paylor, R., Worley, P. F., Szumlanski, K. K., & Huber, K. M. (2016). Selective Disruption of Metabotropic Glutamate Receptor 5-Homer Interactions Mimics Phenotypes of Fragile X Syndrome in Mice. *Journal of Neuroscience*, 36(7), 2131–2147. <https://doi.org/10.1523/JNEUROSCI.2921-15.2016>
- Haas, L. T., Salazar, S. V, Smith, L. M., Zhao, H. R., Cox, T. O., Herber, C. S., Degnan, A. P., Balakrishnan, A., Macor, J. E., Albright, C. F., & Strittmatter, S. M. (2017). Silent Allosteric Modulation of mGluR5 Maintains Glutamate Signaling while Rescuing Alzheimer's Mouse Phenotypes. *Cell Reports*, 20(1), 76–88. <https://doi.org/10.1016/j.celrep.2017.06.023>
- Habrian, C., Latorraca, N., Fu, Z., & Isacoff, E. Y. (2023). Homo- and hetero-dimeric subunit interactions set affinity and efficacy in metabotropic glutamate receptors. *Nature Communications* 2023 14:1, 14(1), 1–10. <https://doi.org/10.1038/s41467-023-44013-4>

- Hagena, H., & Manahan-Vaughan, D. (2022). Role of mGlu5 in Persistent Forms of Hippocampal Synaptic Plasticity and the Encoding of Spatial Experience. *Cells*, 11(21), 3352. <https://doi.org/10.3390/cells11213352>
- Hall, M. P., Unch, J., Binkowski, B. F., Valley, M. P., Butler, B. L., Wood, M. G., Otto, P., Zimmerman, K., Vidugiris, G., Machleidt, T., Robers, M. B., Ne, H., Benink, A., Eggers, C. T., Slater, M. R., Meisenheimer, P. L., Klaubert, D. H., Fan, F., Encell, L. P., & Wood, K. V. (2012). Engineered Luciferase Reporter from a Deep Sea Shrimp Utilizing a Novel Imidazopyrazinone Substrate. *ACS Chem. Biol*, 7, 26. <https://doi.org/10.1021/cb3002478>
- Hamilton, A., Esseltine, J. L., Devries, R. A., Cregan, S. P., & Ferguson, S. S. G. (2014). Metabotropic glutamate receptor 5 knockout reduces cognitive impairment and pathogenesis in a mouse model of Alzheimer's disease. *Molecular Brain*, 7(1). <https://doi.org/10.1186/1756-6606-7-40>
- Hamilton, A., Vasefi, M., Vander Tuin, C., McQuaid, R. J., Anisman, H., & Ferguson, S. S. G. (2016). Chronic Pharmacological mGluR5 Inhibition Prevents Cognitive Impairment and Reduces Pathogenesis in an Alzheimer Disease Mouse Model. *Cell Reports*, 15(9), 1859–1865. <https://doi.org/10.1016/j.celrep.2016.04.077>
- Harmar, A. J. (2001). Protein family review family. *Genome Biology*, 2(12), 1–7. <http://genomebiology.com/2001/2/12/reviews/3013> <http://genomebiology.com/2001/2/12/reviews/3013>
- Harrison, C., & Traynor, J. R. (2003). The [35S]GTPγS binding assay: Approaches and applications in pharmacology. *Life Sciences*, 74(4), 489–508. <https://doi.org/10.1016/j.lfs.2003.07.005>
- Hattori, M., & Ozawa, T. (2014). Split Luciferase Complementation for Analysis of Intracellular Signaling. *Analytical Sciences*, 30, 539–544.
- Helassa, N., Dürst, C. D., Coates, C., Kerruth, S., Arif, U., Schulze, C., Simon Wiegert, J., Geeves, M., Oertner, T. G., & Török, K. (2018). Ultrafast glutamate sensors resolve high-frequency release at Schaffer collateral synapses. *Proceedings of the National Academy of Sciences of the United States of America*, 115(21), 5594–5599. <https://doi.org/10.1073/PNAS.1720648115/-/DCSUPPLEMENTAL>
- Hermans, E., & Challiss, R. A. J. (2001). Structural, signalling and regulatory properties of the group I metabotropic glutamate receptors : prototypic family C G-protein-coupled receptors. *Biochem. J*, 359, 465–484. <http://portlandpress.com/biochemj/article-pdf/359/3/465/707740/bj3590465.pdf>
- Hirose, K., & Chan, P. H. (1993). Blockade of Glutamate Excitotoxicity and Its Clinical Applications. *Neurochemical Research*, 18(4), 479–483.
- Houamad, K. M., Kuijper, J. L., Gilbert, T. L., Haldeman, B. A., O'Hara, P. J., Mulvihill, E. R., Almers, W., & Hagen, F. S. (1991). Cloning, Expression, and Gene Structure of a G Protein-Coupled Glutamate Receptor from Rat Brain. In *Electroenceph. Clin. Neuro-physiol* (Vol. 10, Issue 7). <https://www.science.org>
- Hu, G. M., Mai, T. L., & Chen, C. M. (2017). Visualizing the GPCR Network: Classification and Evolution. *Scientific Reports*, 7(1). <https://doi.org/10.1038/s41598-017-15707-9>
- Hu, J. H., Yang, L., Kammermeier, P. J., Moore, C. G., Brakeman, P. R., Tu, J., Yu, S., Petralia, R. S., Li, Z., Zhang, P. W., Park, J. M., Dong, X., Xiao, B., & Worley, P. F. (2012). Preso1 dynamically regulates group I metabotropic glutamate receptors. *Nature Neuroscience*, 15(6), 836–844. <https://doi.org/10.1038/nn.3103>

- Huang, S., Cao, J., Jiang, M., Labesse, G., Liu, J., Pin, J. P., & Rondard, P. (2011). Interdomain movements in metabotropic glutamate receptor activation. *Proceedings of the National Academy of Sciences of the United States of America*, *108*(37), 15480–15485. <https://doi.org/10.1073/PNAS.1107775108/-/DCSUPPLEMENTAL>
- Hudson, B. D. (2016). Using Biosensors to Study Free Fatty Acid Receptor Pharmacology and Function. *Handbook of Experimental Pharmacology, January*, 251–263. <https://doi.org/10.1007/164>
- Hudson, B. D., Shimpukade, B., Mackenzie, A. E., Butcher, A. J., Padiani, J. D., Christiansen, E., Heathcote, H., Tobin, A. B., Ulven, T., & Milligan, G. (2013). The Pharmacology of TUG-891, a Potent and Selective Agonist of the Free Fatty Acid Receptor 4 (FFA4/GPR120), Demonstrates Both Potential Opportunity and Possible Challenges to Therapeutic Agonism. *MOLECULAR PHARMACOLOGY Mol Pharmacol*, *84*, 710–725. <https://doi.org/10.1124/mol.113.087783>
- Hughes, A. R., & Putney, J. W. (1990). Inositol phosphate formation and its relationship to calcium signaling. *Environmental Health Perspectives*, *84*, 141. <https://doi.org/10.1289/EHP.9084141>
- Ives, A. N., Dunn, H. A., Afsari, H. S., Seckler, H. D. S., Foroutan, M. J., Chavez, E., Melani, R. D., Fellers, R. T., Leduc, R. D., Thomas, P. M., Martemyanov, K. A., Kelleher, N. L., & Vafabakhsh, R. (2022). Middle-Down Mass Spectrometry Reveals Activity-Modifying Phosphorylation Barcode in a Class C G Protein-Coupled Receptor. *Journal of the American Chemical Society*. <https://doi.org/10.1021/jacs.2c10697>
- Jacob, W., Gravius, A., Pietraszek, M., Nagel, J., Belozertseva, I., Shekunova, E., Malyshkin, A., Greco, S., Barberi, C., & Danysz, W. (2009). The anxiolytic and analgesic properties of fenobam, a potent mGlu5 receptor antagonist, in relation to the impairment of learning. *Neuropharmacology*, *57*(2), 97–108. <https://doi.org/10.1016/J.NEUROPHARM.2009.04.011>
- Janetzko, J., Kise, R., Barsi-Rhyne, B., Siepe, D. H., Heydenreich, F. M., Kawakami, K., Masureel, M., Maeda, S., Garcia, K. C., von Zastrow, M., Inoue, A., & Kobilka, B. K. (2022). Membrane phosphoinositides regulate GPCR- β -arrestin complex assembly and dynamics. *Cell*, *185*(24), 4560. <https://doi.org/10.1016/J.CELL.2022.10.018>
- Janíčková, H., Rudajev, V., Zimčík, P., Jakubík, J., Tanila, H., El-Fakahany, E. E., & Doležal, V. (2013). Uncoupling of M1 muscarinic receptor/G-protein interaction by amyloid β (1-42). *Neuropharmacology*, *67*, 272–283. <https://doi.org/10.1016/J.NEUROPHARM.2012.11.014>
- Janicot, R., Maziarz, M., Park, J.-C., Luebbbers, A., Green, E., Zhao, J., Philibert, C., Zhang, H., Layne, M. D., Wu, J. C., & Garcia-Marcos, M. (2024). Direct interrogation of context-dependent GPCR activity with a universal biosensor platform. *BioRxiv*. <https://doi.org/10.1101/2024.01.02.573921>
- Jean-Charles, P.-Y., Kaur, S., & Shenoy, S. K. (2017). GPCR signaling via β -arrestin-dependent mechanisms. *Journal of Cardiovascular Pharmacology*, *70*(3), 142–158. <https://doi.org/10.1097/FJC.0000000000000482>
- Jin, H. L., & Ragolia, L. (2006). AKT Phosphorylation Is Essential For Insulin-induced Relaxation of Rat Vascular Smooth Muscle Cells. *American Journal of Physiology. Cell Physiology*, *291*(6), C1355. <https://doi.org/10.1152/AJPCELL.00125.2006>
- Joly, C., Gomeza, Lsabelle Brabet, J., Curry, K., Bockaert, J., & Pin, J.-P. (1995). Molecular, Functional, and Pharmacological Characterization of the Metabotropic Glutamate Receptor Type 5 Splice

- Variants: Comparison with mGluR1. *The Journal of Neuroscience*, 75(5), 3970–3981.
- Kaar, A., Weir, M. P., & Rae, M. G. (2024). Altered neuronal group 1 metabotropic glutamate receptor- and endoplasmic reticulum-mediated Ca²⁺ signaling in two rodent models of Alzheimer's disease. *Neuroscience Letters*, 823. <https://doi.org/10.1016/J.NEULET.2024.137664>
- Karnam, P. C., Vishnivetskiy, S. A., & Gurevich, V. V. (2021). Structural Basis of Arrestin Selectivity for Active Phosphorylated G Protein-Coupled Receptors. *International Journal of Molecular Sciences*, 22(22). <https://doi.org/10.3390/IJMS222212481>
- Kato, H. K., Kassai, H., Watabe, A. M., Aiba, A., & Manabe, T. (2012). Functional coupling of the metabotropic glutamate receptor, InsP3 receptor and L-type Ca²⁺ channel in mouse CA1 pyramidal cells. *The Journal of Physiology*, 590(Pt 13), 3019. <https://doi.org/10.1113/JPHYSIOL.2012.232942>
- Katz, B., & Miledi, R. (1967). Ionic Requirements of Synaptic Transmitter Release. *Nature*, 215.
- Kawabata, S., Tsutsumi, R., Kohara, A., Yamaguchi, T., Nakanishi, S., & Okada, M. (1996). Control of calcium oscillations by phosphorylation of metabotropic glutamate receptors. *Nature*, 383(6595), 89–92. <https://doi.org/10.1038/383089a0>
- Kazdoba, T. M., Leach, P. T., Silverman, J. L., & Crawley, J. N. (2014). Modeling fragile X syndrome in the Fmr1 knockout mouse. *Intractable & Rare Diseases Research*, 3(4), 118. <https://doi.org/10.5582/IRDR.2014.01024>
- Kenakin, T. (2002). Efficacy at G-protein-coupled receptors. In *Nature Reviews Drug Discovery* (Vol. 1, Issue 2, pp. 103–110). <https://doi.org/10.1038/nrd722>
- Kenny, P. J., Boutrel, B., Gasparini, F., Koob, G. F., & Markou, A. (2005). Metabotropic glutamate 5 receptor blockade may attenuate cocaine self-administration by decreasing brain reward function in rats. *Psychopharmacology*, 179, 247–254. <https://doi.org/10.1007/s00213-004-2069-2>
- Kim, C. H., Braud, S., Isaac, J. T. R., & Roche, K. W. (2005). Protein kinase C phosphorylation of the metabotropic glutamate receptor mGluR5 on serine 839 regulates Ca²⁺ oscillations. *Journal of Biological Chemistry*, 280(27), 25409–25415. <https://doi.org/10.1074/jbc.M502644200>
- Kim, Y. S., Kim, Y. J., Paik, S. K., Cho, Y. S., Kwon, T. G., Ahn, D. K., Kim, S. K., Yoshida, A., & Bae, Y. C. (2009). Expression of Metabotropic Glutamate Receptor mGluR5 in Human Dental Pulp. *Journal of Endodontics*, 35(5), 690–694. <https://doi.org/10.1016/J.JOEN.2009.02.005>
- Kingston, A. E., O'Neill, M. J., Lam, A., Bales, K. R., Monn, J. A., & Schoepp, D. D. (1999). Neuroprotection by metabotropic glutamate receptor agonists: LY354740, LY379268 and LY389795. *European Journal of Pharmacology*, 377(2–3), 155–165. [https://doi.org/10.1016/S0014-2999\(99\)00397-0](https://doi.org/10.1016/S0014-2999(99)00397-0)
- Kliwer, A., Schmiedel, F., Sianati, S., Bailey, A., Bateman, J. T., Levitt, E. S., Williams, J. T., Christie, M. J., & Schulz, S. (2019). Phosphorylation-deficient G-protein-biased μ -opioid receptors improve analgesia and diminish tolerance but worsen opioid side effects. *Nature Communications*, 10(1). <https://doi.org/10.1038/S41467-018-08162-1>
- Ko, S. J., Isozaki, K., Kim, I., Lee, J. H., Cho, H. J., Sohn, S. Y., Oh, S. R., Park, S., Kim, D. G., Kim, C. H., & Roche, K. W. (2012). PKC Phosphorylation Regulates mGluR5 Trafficking by Enhancing Binding of Siah-1A. *The Journal of Neuroscience*, 32(46), 16391. <https://doi.org/10.1523/JNEUROSCI.1964-12.2012>

- Koehl, A., Hu, H., Feng, D., Sun, B., Zhang, Y., Robertson, M. J., Chu, M., Kobilka, T. S., Laermans, T., Steyaert, J., Tarrasch, J., Dutta, S., Fonseca, R., Weis, W. I., Mathiesen, J. M., Skiniotis, G., & Kobilka, B. K. (2019). Structural Insights into Metabotropic Glutamate Receptor Activation. *Nature*, *566*(7742), 79. <https://doi.org/10.1038/S41586-019-0881-4>
- Kolb, P., Kenakin, T., Alexander, S. P. H., Bermudez, M., Bohn, L. M., Breinholt, C. S., Bouvier, M., Hill, S. J., Kostenis, E., Martemyanov, K. A., Neubig, R. R., Onaran, H. O., Rajagopal, S., Roth, B. L., Selent, J., Shukla, A. K., Sommer, M. E., & Gloriam, D. E. (2022). Community guidelines for GPCR ligand bias: IUPHAR review 32. In *British Journal of Pharmacology*. <https://doi.org/10.1111/bph.15811>
- Krebs, H. A. (1935). Metabolism of amino-acids: The synthesis of glutamine from glutamic acid and ammonia, and the enzymic hydrolysis of glutamine in animal tissues. *The Biochemical Journal*, *29*(8), 1951–1969. <http://www.ncbi.nlm.nih.gov/pubmed/16745865> <http://www.pubmedcentral.nih.gov/articlerender.fcgi?artid=PMC1266709>
- Krupnick, J. G., & Benovic, J. L. (1998). The role of receptor kinases and arrestins in G protein-coupled receptor regulation. *Annual Review of Pharmacology and Toxicology*, *38*, 289–319. <https://doi.org/10.1146/annurev.pharmtox.38.1.289>
- Kumar, K. K., Wang, H., Habrian, C., Latorraca, N. R., Xu, J., O'Brien, E. S., Zhang, C., Montabana, E., Koehl, A., Marqusee, S., Isacoff, E. Y., & Kobilka, B. K. (2023). Step-wise activation of a Family C GPCR. *BioRxiv*. <https://doi.org/10.1101/2023.08.29.555158>
- Kunishima, N., Shimada, Y., Tsuji, Y., Sato, T., Yamamoto, M., Kumasaka, T., Nakanishi, S., Jingami, H., & Morikawa, K. (2000). Structural basis of glutamate recognition by a dimeric metabotropic glutamate receptor. *Nature*, *407*(6807), 971–977. <https://doi.org/10.1038/35039564>
- LaCrosse, A. L., May, C. E., Griffin, W. C., & Foster Olive, M. (2024). mGluR5 positive allosteric modulation prevents MK-801 induced increases in extracellular glutamate in the rat medial prefrontal cortex. *Neuroscience*. <https://doi.org/10.1016/J.NEUROSCIENCE.2024.06.016>
- Lambright, D. G., Sondek, J., Bohm, A., Skiba, N. P., Hamm, H. E., & Sigler, P. B. (1996). The 2.0 Å crystal structure of a heterotrimeric G protein. *Nature*, *379*(6563), 311–319. <https://doi.org/10.1038/379311a0>
- Landry, C. R., Levy, E. D., & Michnick, S. W. (2009). Weak functional constraints on phosphoproteomes. *Trends in Genetics : TIG*, *25*(5), 193–197. <https://doi.org/10.1016/J.TIG.2009.03.003>
- Lans, I., Díaz, Ó., Dalton, J. A. R., & Giraldo, J. (2020). Exploring the Activation Mechanism of the mGlu5 Transmembrane Domain. *Frontiers in Molecular Biosciences*, *7*. <https://doi.org/10.3389/fmolb.2020.00038>
- Latorraca, N. R., Sabaat, S., Habrian, C., Bleier, J., Stanley, C., Marqusee, S., & Isacoff, E. Y. (2024). Domain coupling in activation of a family C GPCR. *BioRxiv*. <https://doi.org/10.1101/2024.02.28.582567>
- Lee, S. M., Booe, J. M., & Pioszak, A. A. (2015). Structural insights into ligand recognition and selectivity for classes A, B, and C GPCRs. *European Journal of Pharmacology*, *763*, 196–205. <https://doi.org/10.1016/j.ejphar.2015.05.013>
- Lefkowitz, R. J., & Shenoy, S. K. (2005). Transduction of receptor signals by β -arrestins. In *Science* (Vol. 308, Issue 5721, pp. 512–517). American Association for the Advancement of Science. <https://doi.org/10.1126/science.1109237>
- Levey, A. I., Kitt, C. A., Simonds, W. F., Price, D. L., & Brann, M. R. (1991). Identification and localization of muscarinic acetylcholine receptor proteins in

- brain with subtype-specific antibodies. *Journal of Neuroscience*, 11(10), 3218–3226. <https://doi.org/10.1523/JNEUROSCI.11-10-03218.1991>
- Liauw, B. W.-H., Afsari, H. S., & Vafabakhsh, R. (2021). Conformational rearrangement during activation of a metabotropic glutamate receptor. *Nature Chemical Biology*, 17, 291–297. <https://doi.org/10.1038/s41589-020-00702-5>
- Littmann, T., Ozawa, T., Hoffmann, C., Buschauer, A., & Bernhardt, G. (2018). A split luciferase-based probe for quantitative proximal determination of Gαq signalling in live cells. *Scientific Reports* 2018 8:1, 8(1), 1–10. <https://doi.org/10.1038/s41598-018-35615-w>
- Liu, K., Titus, S., Southall, N., Zhu, P., Inglese, J., Austin, C. P., & Zheng, W. (2008). Comparison on Functional Assays for Gq-Coupled GPCRs by Measuring Inositol Monophosphate-1 and Intracellular Calcium in 1536-Well Plate Format. *Current Chemical Genomics*, 1, 70–78. <https://doi.org/10.2174/1875397300801010070>
- Lohse, M. J., Nuber, S., & Hoffmann, C. (2012). Fluorescence/Bioluminescence Resonance Energy Transfer Techniques to Study G-Protein-Coupled Receptor Activation and Signaling. *Pharmacological Reviews*, 64(2), 299–336. <https://doi.org/10.1124/pr.110.004309>
- Luo, L., Huang, M., Zhang, Y., Wang, W., Ma, X., Shi, H., Worley, P. F., Kim, D. K., Fedorovich, S. V., Jiang, W., & Xu, T. (2020). Disabling phosphorylation at the homer ligand of the metabotropic glutamate receptor 5 alleviates complete Freund's adjuvant-induced inflammatory pain. *Neuropharmacology*, 170(August 2019), 108046. <https://doi.org/10.1016/j.neuropharm.2020.108046>
- Maharana, J., Sarma, P., Yadav, M. K., Saha, S., Singh, V., Saha, S., Chami, M., Banerjee, R., & Shukla, A. K. (2023). Structural snapshots uncover a key phosphorylation motif in GPCRs driving β-arrestin activation. *Molecular Cell*. <https://doi.org/10.1016/J.MOLCEL.2023.04.025>
- Mahato, P. K., Pandey, S., & Bhattacharyya, S. (2015). Differential effects of protein phosphatases in the recycling of metabotropic glutamate receptor 5. *Neuroscience*, 306, 138–150. <https://doi.org/10.1016/j.neuroscience.2015.08.031>
- Makoff, A., Lelchuk, R., Oxer, M., Harrington, K., & Emson, P. (1996). Molecular characterization and localization of human metabotropic glutamate receptor type 4. *Molecular Brain Research*, 37(1–2), 239–248. [https://doi.org/10.1016/0169-328X\(95\)00321-1](https://doi.org/10.1016/0169-328X(95)00321-1)
- Malherbe, P., Kratzeisen, C., Lundstrom, K., Grayson Richards, J., Faull, R. L. M., & Mutel, V. (1999). Cloning and functional expression of alternative spliced variants of the human metabotropic glutamate receptor 8. *Molecular Brain Research*, 67.
- Malik, R. U., Dysthe, M., Ritt, M., Sunahara, R. K., & Sivaramakrishnan, S. (2017). ER/K linked GPCR-G protein fusions systematically modulate second messenger response in cells. *Scientific Reports*, 7(1), 1–13. <https://doi.org/10.1038/s41598-017-08029-3>
- Malik, R. U., Ritt, M., DeVree, B. T., Neubig, R. R., Sunahara, R. K., & Sivaramakrishnan, S. (2013). Detection of G protein-selective G protein-coupled receptor (GPCR) conformations in live cells. *Journal of Biological Chemistry*, 288(24), 17167–17178. <https://doi.org/10.1074/jbc.M113.464065>
- Mann, D., Teuber, C., Tennigkeit, S. A., Schröter, G., Gerwert, K., Kötting, C., & Pai, E. F. (2016). Mechanism of the intrinsic arginine finger in heterotrimeric G proteins. *Proceedings of the National Academy of Sciences of the United*

- States of America*, 113(50), E8041–E8050.
<https://doi.org/10.1073/pnas.1612394113>
- Mann, M., Ong, S. E., Grønborg, M., Steen, H., Jensen, O. N., & Pandey, A. (2002). Analysis of protein phosphorylation using mass spectrometry: Deciphering the phosphoproteome. In *Trends in Biotechnology* (Vol. 20, Issue 6, pp. 261–268). Trends Biotechnol. [https://doi.org/10.1016/S0167-7799\(02\)01944-3](https://doi.org/10.1016/S0167-7799(02)01944-3)
- Mao, L. M., Liu, X. Y., Zhang, G. C., Chu, X. P., Fibuch, E. E., Wang, L. S., Liu, Z., & Wang, J. Q. (2008). Phosphorylation of group I metabotropic glutamate receptors (mGluR1/5) in vitro and in vivo. *Neuropharmacology*, 55(4), 403–408. <https://doi.org/10.1016/j.neuropharm.2008.05.034>
- Mao, L.-M., & Wang, Q. (2016). Phosphorylation of group I metabotropic glutamate receptors in drug addiction and translational research. *Journal of Translational Neuroscience*, 1(1), 17–23.
<http://www.ncbi.nlm.nih.gov/pubmed/28553558>
<http://www.pubmedcentral.nih.gov/articlerender.fcgi?artid=PMC5444875>
- Marsango, S., Ward, R. J., Jenkins, L., Butcher, A. J., Al Mahmud, Z., Dwomoh, L., Nagel, F., Schulz, S., Tikhonova, I. G., Tobin, A. B., & Milligan, G. (2022). Selective phosphorylation of threonine residues defines GPR84-arrestin interactions of biased ligands. *Journal of Biological Chemistry*, 298, 101932. <https://doi.org/10.1016/j.jbc.2022.101932>
- Marton, T. M., Hussain Shuler, M. G., & Worley, P. F. (2015). Homer 1a and mGluR5 phosphorylation in reward-sensitive metaplasticity: A hypothesis of neuronal selection and bidirectional synaptic plasticity. In *Brain Research* (Vol. 1628, pp. 17–28). Elsevier B.V.
<https://doi.org/10.1016/j.brainres.2015.06.037>
- Marvin, J. S., Borghuis, B. G., Tian, L., Cichon, J., Harnett, M. T., Akerboom, J., Gordus, A., Renninger, S. L., Chen, T. W., Bargmann, C. I., Orger, M. B., Schreiter, E. R., Demb, J. B., Gan, W. B., Hires, S. A., & Looger, L. L. (2013). An optimized fluorescent probe for visualizing glutamate neurotransmission. *Nature Methods*, 10(2), 162. <https://doi.org/10.1038/NMETH.2333>
- Marvin, J. S., Scholl, B., Wilson, D. E., Podgorski, K., Kazemipour, A., Müller, J. A., Schoch, S., Quiroz, F. J. U., Rebola, N., Bao, H., Little, J. P., Tkachuk, A. N., Cai, E., Hantman, A. W., Wang, S. S. H., DePiero, V. J., Borghuis, B. G., Chapman, E. R., Dietrich, D., ... Looger, L. L. (2018). Stability, affinity and chromatic variants of the glutamate sensor iGluSnFR. *Nature Methods*, 15(11), 936. <https://doi.org/10.1038/S41592-018-0171-3>
- Masuho, I., Ostrovskaya, O., Kramer, G. M., Jones, C. D., Xie, K., & Martemyanov, K. A. (2015). Distinct profiles of functional discrimination among G proteins determine the actions of G protein-coupled receptors. *Science Signaling*, 8(405). <https://doi.org/10.1126/SCISIGNAL.AAB4068>
- Matthews, C. C., Zielke, H. R., Parks, D. A., & Fishman, P. S. (2003). Glutamate-pyruvate transaminase protects against glutamate toxicity in hippocampal slices. *Brain Research*, 978, 59–64. [https://doi.org/10.1016/S0006-8993\(03\)02765-3](https://doi.org/10.1016/S0006-8993(03)02765-3)
- Matthews, C., Zielke, R., Wollack, B., & Fishman, S. (2000). Enzymatic Degradation Protects Neurons from Glutamate Excitotoxicity. *J. Neurochem*, 75, 1045–1052. <https://doi.org/10.1046/j.1471-4159.2000.0751045.x>
- Maziarz, M., Park, J. C., Leyme, A., Marivin, A., Garcia-Lopez, A., Patel, P. P., & Garcia-Marcos, M. (2020). Revealing the Activity of Trimeric G-proteins in Live Cells with a Versatile Biosensor Design. *Cell*, 182(3), 770–785.e16. <https://doi.org/10.1016/j.cell.2020.06.020>

- McCulloch, T. W., Cardani, L. P., & Kammermeier, P. J. (2023). Signaling specificity and kinetics of the human metabotropic glutamate receptors. *BioRxiv : The Preprint Server for Biology*.
<https://doi.org/10.1101/2023.07.24.550373>
- Meng, J., Xu, C., Lafon, P. A., Roux, S., Mathieu, M., Zhou, R., Scholler, P., Blanc, E., Becker, J. A. J., Le Merrer, J., González-Maeso, J., Chames, P., Liu, J., Pin, J. P., & Rondard, P. (2022). Nanobody-based sensors reveal a high proportion of mGlu heterodimers in the brain. *Nature Chemical Biology*, 18(8), 894–903. <https://doi.org/10.1038/s41589-022-01050-2>
- Michalon, A., Sidorov, M., Ballard, T. M., Ozmen, L., Spooren, W., Wettstein, J. G., Jaeschke, G., Bear, M. F., & Lindemann, L. (2012). Chronic Pharmacological mGlu5 Inhibition Corrects Fragile X in Adult Mice. *Neuron*, 74, 49–56.
<https://doi.org/10.1016/j.neuron.2012.03.009>
- Milanese, M., Bonifacino, T., Torazza, C., Provenzano, F., Kumar, M., Ravera, S., Zerbo, A. R., Frumento, G., Balbi, M., Nguyen, T. P. N., Bertola, N., Ferrando, S., Viale, M., Profumo, A., & Bonanno, G. (2021). Blocking glutamate mGlu5 receptors with the negative allosteric modulator CTEP improves disease course in SOD1G93A mouse model of amyotrophic lateral sclerosis. *British Journal of Pharmacology*, 178(18), 3747–3764.
<https://doi.org/10.1111/bph.15515>
- Miller, L. J., Dong, M., & Harikumar, K. G. (2012). Ligand binding and activation of the secretin receptor, a prototypic family B G protein-coupled receptor. *British Journal of Pharmacology*, 166(1), 18–26. <https://doi.org/10.1111/J.1476-5381.2011.01463.X>
- Minakami, R., Iida, K., Hirakawa, N., & Sugiyama, H. (1995). The Expression of Two Splice Variants of Metabotropic Glutamate Receptor Subtype 5 in the Rat Brain and Neuronal Cells During Development. *Journal of Neurochemistry*, 65(4), 1536–1542. <https://doi.org/10.1046/J.1471-4159.1995.65041536.X>
- Minakami, R., Jinnai, N., & Sugiyama, H. (1997). Phosphorylation and Calmodulin Binding of the Metabotropic Glutamate Receptor Subtype 5 (mGluR5) Are Antagonistic in Vitro. *Journal of Biological Chemistry*, 272(32), 20291–20298.
<https://doi.org/10.1074/JBC.272.32.20291>
- Minakami, R., Katsuki, F., & Sugiyama, H. (1993). A variant of metabotropic glutamate receptor subtype 5: An evolutionally conserved insertion with no termination codon. *Biochemical and Biophysical Research Communications*, 194(2), 622–627. <https://doi.org/10.1006/bbrc.1993.1866>
- Minakami, R., Katsuki, F., Yamamoto, T., Nakamura, K., & Sugiyama, H. (1994). Molecular cloning and the functional expression of two isoforms of human metabotropic glutamate receptor subtype 5. *Biochemical and Biophysical Research Communications*, 199(3), 1136–1143.
<https://doi.org/10.1006/BBRC.1994.1349>
- Mion, S., Corti, C., Neki, A., Shigemoto, R., Corsi, M., Fumagalli, G., & Ferraguti, F. (2001). Bidirectional Regulation of Neurite Elaboration by Alternatively Spliced Metabotropic Glutamate Receptor 5 (mGluR5) Isoforms.
<https://doi.org/10.1006/mcne.2001.0993>
- Mistry, R., Dowling, M. R., & Challiss, R. A. J. (2011). [³⁵S]GTPγS binding as an index of total G-protein and Gα-subtype-specific activation by GPCRs. *Methods in Molecular Biology (Clifton, N.J.)*, 746, 263–275.
https://doi.org/10.1007/978-1-61779-126-0_14
- Mody, M., Petibon, Y., Han, P., Kuruppu, D., Ma, C., Yokell, D., Neelamegam, R., Normandin, M. D., Fakhri, G. El, & Brownell, A.-L. (2021). In vivo imaging of mGlu5 receptor expression in humans with Fragile X Syndrome towards

- development of a potential biomarker. *Scientific Reports*, 11. <https://doi.org/10.1038/s41598-021-94967-y>
- Mollapour, M., Tsutsumi, S., Truman, A. W., Xu, W., Vaughan, C. K., Beebe, K., Konstantinova, A., Vourganti, S., Panaretou, B., Piper, P. W., Trepel, J. B., Prodromou, C., Pearl, L. H., & Neckers, L. (2011). Threonine 22 phosphorylation attenuates Hsp90 interaction with cochaperones and affects its chaperone activity. *Molecular Cell*, 41(6), 672–681. <https://doi.org/10.1016/J.MOLCEL.2011.02.011>
- Møller, T. C., Pedersen, M. F., Van Senten, J. R., Seiersen, S. D., Mathiesen, J. M., Bouvier, M., Bräuner-Osborne, H., & Pedersen, F. (2020). Dissecting the roles of GRK2 and GRK3 in μ -opioid receptor internalization and β -arrestin2 recruitment using CRISPR/ Cas9-edited HEK293 cells. *Scientific Reports*, 10, 17395. <https://doi.org/10.1038/s41598-020-73674-0>
- Monod, J., Wyman, J., & Changeux, J. P. (1965). On the nature of allosteric transitions: A plausible model. *Journal of Molecular Biology*, 12(1), 88–118. [https://doi.org/10.1016/S0022-2836\(65\)80285-6](https://doi.org/10.1016/S0022-2836(65)80285-6)
- Mundell, S. J., Pula, G., McIlhinney, R. A. J., Roberts, P. J., & Kelly, E. (2004). Desensitization and internalization of metabotropic glutamate receptor 1a following activation of heterologous Gq/11-coupled receptors. *Biochemistry*, 43(23), 7541–7551. <https://doi.org/10.1021/bi0359022>
- Murrin, C. L., & Talbot, J. N. (2007). RanBPM, a Scaffolding Protein in the Immune and Nervous Systems. *Journal of Neuroimmune Pharmacology*, 2, 290–295. <https://doi.org/10.1007/s11481-007-9079-x>
- Nakahara, K., Okada, M., & Nakanishi, S. (1997). The metabotropic glutamate receptor mGluR5 induces calcium oscillations in cultured astrocytes via protein kinase C phosphorylation. *Journal of Neurochemistry*, 69(4), 1467–1475. <https://doi.org/10.1046/J.1471-4159.1997.69041467.X>
- Nakai, J., Ohkura, M., & Imoto, K. (2001). A high signal-to-noise Ca²⁺ probe composed of a single green fluorescent protein. *Nature Biotechnology* 2001 19:2, 19(2), 137–141. <https://doi.org/10.1038/84397>
- Namkung, Y., Le Gouill, C., Lukashova, V., Kobayashi, H., Hogue, M., Khoury, E., Song, M., Bouvier, M., & Laporte, S. A. (2016). Monitoring G protein-coupled receptor and β -arrestin trafficking in live cells using enhanced bystander BRET. *Nature Communications*, 7. <https://doi.org/10.1038/ncomms12178>
- Nasrallah, C., Cannone, G., Briot, J., Rottier, K., Berizzi, A. E., Huang, C. Y., Quast, R. B., Hoh, F., Banères, J. L., Malhaire, F., Berto, L., Dumazer, A., Font-Ingles, J., Gómez-Santacana, X., Catena, J., Kniazeff, J., Goudet, C., Llebaria, A., Pin, J. P., ... Lebon, G. (2021). Agonists and allosteric modulators promote signaling from different metabotropic glutamate receptor 5 conformations. *Cell Reports*, 36(9). <https://doi.org/10.1016/j.celrep.2021.109648>
- Nasrallah, C., Rottier, K., Marcellin, R., Compan, V., Font, J., Llebaria, A., Pin, J.-P., Banères, J.-L., & Lebon, G. (2018). Direct coupling of detergent purified human mGlu 5 receptor to the heterotrimeric G proteins Gq and Gs. *Scientific Reports*, 8(4407). <https://doi.org/10.1038/s41598-018-22729-4>
- Neer, E. J., & Clapham, D. E. (1988). Roles of G protein subunits in transmembrane signalling. In *Nature* (Vol. 333, Issue 6169, pp. 129–134). <https://doi.org/10.1038/333129a0>
- Ng, A. N., Salter, E. W., Georgiou, J., Bortolotto, Z. A., & Collingridge, G. L. (2023). Amyloid-beta1-42 oligomers enhance mGlu5R-dependent synaptic weakening via NMDAR activation and complement C5aR1 signaling. *SCIENCE*, 26, 108412. <https://doi.org/10.1016/j.isci.2023.108412>

- Nicoletti, F., Bruno, V., Catania, M. V., Battaglia, G., Copani, A., Barbagallo, G., Ceñ, V., Sanchez-Prieto, J., Spano, P. F., & Pizzi, M. (1999). Group-I metabotropic glutamate receptors: hypotheses to explain their dual role in neurotoxicity and neuroprotection. In *Neuropharmacology* (Vol. 38). www.elsevier.com/locate/neuropharm
- Niswender, C. M., & Conn, P. J. (2010). Metabotropic glutamate receptors: Physiology, pharmacology, and disease. In *Annual Review of Pharmacology and Toxicology* (Vol. 50, pp. 295–322). <https://doi.org/10.1146/annurev.pharmtox.011008.145533>
- Nobles, K. N., Xiao, K., Ahn, S., Shukla, A. K., Lam, C. M., Rajagopal, S., Strachan, R. T., Huang, T. Y., Bressler, E. A., Hara, M. R., Shenoy, S. K., Gygi, S. P., & Lefkowitz, R. J. (2011a). Distinct phosphorylation sites on the β 2-adrenergic receptor establish a barcode that encodes differential functions of β -arrestin. *Science Signaling*, *4*(185). https://doi.org/10.1126/SCISIGNAL.2001707/SUPPL_FILE/4_RA51_SM.PDF
- Nobles, K. N., Xiao, K., Ahn, S., Shukla, A. K., Lam, C. M., Rajagopal, S., Strachan, R. T., Huang, T. Y., Bressler, E. A., Hara, M. R., Shenoy, S. K., Gygi, S. P., & Lefkowitz, R. J. (2011b). Distinct Phosphorylation Sites on the β 2-Adrenergic Receptor Establish a Barcode That Encodes Differential Functions of β -Arrestin. *Science Signaling*, *4*(185), ra51. <https://doi.org/10.1126/SCISIGNAL.2001707>
- Nomura, A., Shigemoto, R., Nakamura, Y., Okamoto, N., Mizuno, N., & Nakanishi, S. (1994). Developmentally regulated postsynaptic localization of a metabotropic glutamate receptor in rat rod bipolar cells. *Cell*, *77*(3), 361–369. [https://doi.org/10.1016/0092-8674\(94\)90151-1](https://doi.org/10.1016/0092-8674(94)90151-1)
- Norisada, J., Fujimura, K., Amaya, F., Kohno, H., Hirata, Y., & Oh-hash, K. (2018). Application of NanoBiT for Monitoring Dimerization of the Null Hong Kong Variant of α -1-Antitrypsin, NHK, in Living Cells. *Molecular Biotechnology*, *60*(8), 539–549. <https://doi.org/10.1007/S12033-018-0092-5>
- Oakes, S. G., Martin, W. J., Lisek, C. A., & Powis, G. (1988). Incomplete hydrolysis of the calcium indicator precursor fura-2 pentaacetoxymethyl ester (fura-2 AM) by cells. *Analytical Biochemistry*, *169*(1), 159–166. [https://doi.org/10.1016/0003-2697\(88\)90267-9](https://doi.org/10.1016/0003-2697(88)90267-9)
- Obrenovich, M. E., Smith, M. A., Siedlak, S. L., Chen, S. G., De Le Torre, J. C., Perry, G., & Aliev, G. (2006). Overexpression of GRK2 in Alzheimer's Disease and in a Chronic Hypoperfusion Rat Model is an Early Marker of Brain Mitochondrial Lesions. *Neurotoxicity Research*, *10*(1), 43–56.
- Ochoa, D., Jarnuczak, A. F., Viéitez, C., Gehre, M., Soucheray, M., Mateus, A., Kleefeldt, A. A., Hill, A., Garcia-Alonso, L., Stein, F., Krogan, N. J., Savitski, M. M., Swaney, D. L., Vizcaíno, J. A., Noh, K. M., & Beltrao, P. (2020). The functional landscape of the human phosphoproteome. *Nature Biotechnology*, *38*(3), 365. <https://doi.org/10.1038/S41587-019-0344-3>
- O'Gorman, S., Fox, D. T., & Wahl, G. M. (1991). Recombinase-Mediated Gene Activation and Site-Specific Integration in Mammalian Cells. *Science*, *251*(4999), 1351–1355. <https://doi.org/10.1126/SCIENCE.1900642>
- Oh, D. J., & Ahn, K. H. (2008). Fluorescent sensing of IP3 with a trifurcate Zn(II)-containing chemosensing ensemble system. *Organic Letters*, *10*(16), 3539–3542. https://doi.org/10.1021/OL801290G/SUPPL_FILE/OL801290G-FILE003.PDF
- Ohnuma, T., Augood, S. J., Arai, H., McKenna, P. J., & Emson, P. C. (1998). Expression of the human excitatory amino acid transporter 2 and metabotropic glutamate receptors 3 and 5 in the prefrontal cortex from normal

- individuals and patients with schizophrenia. *Brain Research. Molecular Brain Research*, 56(1–2), 207–217. [https://doi.org/10.1016/S0169-328X\(98\)00063-1](https://doi.org/10.1016/S0169-328X(98)00063-1)
- Okamoto, N., Hori, S., Akazawa, C., Hayashi, Y., Shigemoto, R., Mizuno, N., & Nakanishi, S. (1994). Molecular characterization of a new metabotropic glutamate receptor mGluR7 coupled to inhibitory cyclic AMP signal transduction. *Journal of Biological Chemistry*, 269(2), 1231–1236. [https://doi.org/10.1016/S0021-9258\(17\)42247-2](https://doi.org/10.1016/S0021-9258(17)42247-2)
- Olsen, C. M., Childs, D. S., Stanwood, G. D., & Winder, D. G. (2010). Operant Sensation Seeking Requires Metabotropic Glutamate Receptor 5 (mGluR5). *PLoS ONE*, 5(11), 15085. <https://doi.org/10.1371/JOURNAL.PONE.0015085>
- Olsen, R. H. J., DiBerto, J. F., English, J. G., Glaudin, A. M., Krumm, B. E., Slocum, S. T., Che, T., Gavin, A. C., McCorvy, J. D., Roth, B. L., & Strachan, R. T. (2020). TRUPATH, an open-source biosensor platform for interrogating the GPCR transducerome. *Nature Chemical Biology*, 16(8), 841–849. <https://doi.org/10.1038/s41589-020-0535-8>
- Olsen, R. H. J., & English, J. G. (2023). Advancements in GPCR biosensors to study GPCR-G Protein coupling. *British Journal of Pharmacology*, 180(11), 1433. <https://doi.org/10.1111/BPH.15962>
- Olsen, J. V., Blagoev, B., Gnad, F., Macek, B., Kumar, C., Mortensen, P., & Mann, M. (2006). Global, In Vivo, and Site-Specific Phosphorylation Dynamics in Signaling Networks. *Cell*, 127(3), 635–648. <https://doi.org/10.1016/j.cell.2006.09.026>
- Pal, A. S., Agredo, A. M., & Kasinski, A. L. (2022). In-Cell Western Protocol for Semi-High-Throughput Screening of Single Clones. *Bio-Protocol*, 12(16). <https://doi.org/10.21769/BIOPROTOCOL.4489>
- Paleologou, K. E., Schmid, A. W., Rospigliosi, C. C., Kim, H. Y., Lamberto, G. R., Fredenburg, R. A., Lansbury, P. T., Fernandez, C. O., Eliezer, D., Zweckstetter, M., & Lashuel, H. A. (2008). Phosphorylation at Ser-129 but Not the Phosphomimics S129E/D Inhibits the Fibrillation of α -Synuclein. *The Journal of Biological Chemistry*, 283(24), 16895. <https://doi.org/10.1074/JBC.M800747200>
- Palmatier, M. I., Liu, X., Donny, E. C., Caggiula, A. R., & Sved, A. F. (2007). Metabotropic Glutamate 5 Receptor (mGluR5) Antagonists Decrease Nicotine Seeking, But Do Not Affect the Reinforcement Enhancing Effects of Nicotine. *Neuropsychopharmacology* 2008 33:9, 33(9), 2139–2147. <https://doi.org/10.1038/sj.npp.1301623>
- Pandey, A. K., Ganguly, H. K., Sinha, S. K., Daniels, K. E., Yap, G. P. A., Patel, S., & Zondlo, N. J. (2023). An Inherent Difference between Serine and Threonine Phosphorylation: Phosphothreonine Strongly Prefers a Highly Ordered, Compact, Cyclic Conformation. *ACS Chemical Biology*, 18(9), 1938–1958. https://doi.org/10.1021/ACSCHEMBIO.3C00068/ASSET/IMAGES/LARGE/CB3C00068_0016.JPEG
- Pandya, N. J., Klaassen, R. V., van der Schors, R. C., Slotman, J. A., Houtsmuller, A., Smit, A. B., & Li, K. W. (2016). Group 1 metabotropic glutamate receptors 1 and 5 form a protein complex in mouse hippocampus and cortex. *Proteomics*, 16(20), 2698–2705. <https://doi.org/10.1002/PMIC.201500400>
- Park, J. M., Hu, J.-H., Milshteyn, A., Zhang, P.-W., Moore, C. G., Park, S., Datko, M. C., Domingo, R. D., Reyes, C. M., Wang, X. J., Etkorn, F. A., Xiao, B., Szumlanski, K. K., Kern, D., Linden, D. J., & Worley, P. F. (2013). A Prolyl-Isomerase Mediates Dopamine-Dependent Plasticity and Cocaine Motor Sensitization. *Cell*, 154, 637–650. <https://doi.org/10.1016/j.cell.2013.07.001>

- Parmentier, M. L., Joly, C., Restituto, S., Bockaert, J., Grau, Y., & Pin, J. P. (1998). The G Protein-Coupling Profile of Metabotropic Glutamate Receptors, as Determined with Exogenous G Proteins, Is Independent of Their Ligand Recognition Domain. *Molecular Pharmacology*, 53(4), 778–786. <https://doi.org/10.1124/MOL.53.4.778>
- Parmentier-Batteur, S., Obrien, J. A., Doran, S., Nguyen, S. J., Flick, R. B., Uslaner, J. M., Chen, H., Finger, E. N., Williams, T. M., Jacobson, M. A., & Hutson, P. H. (2012). Differential effects of the mGluR5 positive allosteric modulator CDPBB in the cortex and striatum following repeated administration. *Neuropharmacology*, 62(3), 1453–1460. <https://doi.org/10.1016/J.NEUROPHARM.2010.11.013>
- Pecknold, J. C., McClure, D. J., Appeltauer, L., Wrzesinski, L., & Allan, T. (1982). Treatment of anxiety using fenobam (a nonbenzodiazepine) in a double-blind standard (diazepam) placebo-controlled study. *Journal of Clinical Psychopharmacology*, 2(2), 129–133.
- Pedersen, M. H., Pham, J., Mancebo, H., Inoue, A., Asher, W. B., & Javitch, J. A. (2021). A novel luminescence-based β -arrestin recruitment assay for unmodified receptors. *Journal of Biological Chemistry*, 296. <https://doi.org/10.1016/j.jbc.2021.100503>
- Perroy, J., Gutierrez, G. J., Coulon, V., Bockaert, J., Pin, J.-P., & Fagni, L. (2001). The C Terminus of the Metabotropic Glutamate Receptor Subtypes 2 and 7 Specifies the Receptor Signaling Pathways*. *Journal of Biological Chemistry*, 276(49), 45800–45805. <https://doi.org/10.1074/jbc.M106876200i>
- Persechino, M., Hedderich, J. B., Kolb, P., & Hilger, D. (2022). Allosteric modulation of GPCRs: From structural insights to in silico drug discovery. In *Pharmacology and Therapeutics* (Vol. 237). <https://doi.org/10.1016/j.pharmthera.2022.108242>
- Pfleger, K. D. G., & Eidne, K. A. (2006). Illuminating insights into protein-protein interactions using bioluminescence resonance energy transfer (BRET). In *Nature methods* (Vol. 3, Issue 3, pp. 165–174). <https://doi.org/10.1038/nmeth841>
- Pieretti, M., Zhang, F., Fu, Y. H., Warren, S. T., Oostra, B. A., Caskey, C. T., & Nelson, D. L. (1991). Absence of expression of the FMR-1 gene in fragile X syndrome. *Cell*, 66(4), 817–822. [https://doi.org/10.1016/0092-8674\(91\)90125-I](https://doi.org/10.1016/0092-8674(91)90125-I)
- Pin, J. P., Waeber, C., Prezeau, L., Bockaert, J., & Heinemann, S. F. (1992). Alternative splicing generates metabotropic glutamate receptors inducing different patterns of calcium release in *Xenopus* oocytes. *Proceedings of the National Academy of Sciences of the United States of America*, 89(21), 10331. <https://doi.org/10.1073/PNAS.89.21.10331>
- Płoska, A., Siekierzycka, A., Cieślak, P., Dobrucki, L. W., Kalinowski, L., & Wierońska, J. M. (2024). The Impact of LY487379 or CDPBB on eNOS Expression in the Mouse Brain and the Effect of Joint Administration of Compounds with NO• Releasers on MK-801- or Scopolamine-Driven Cognitive Dysfunction in Mice. *Molecules*, 29(3), 627. <https://doi.org/10.3390/MOLECULES29030627>
- Price, D. L., Rockenstein, E., Ubhi, K., Phung, V., Maclean-Lewis, N., Askay, D., Cartier, A., Spencer, B., Patrick, C., Desplats, P., Ellisman, M. H., & Masliah, E. (2010). Alterations in mGluR5 expression and signaling in lewy body disease and in transgenic models of alpha-synucleinopathy - implications for excitotoxicity. *PLoS ONE*, 5(11), e14020. <https://doi.org/10.1371/journal.pone.0014020>

- Price, K. L., & Lummis, S. C. R. (2005). FlexStation examination of 5-HT₃ receptor function using Ca²⁺- and membrane potential-sensitive dyes: Advantages and potential problems. *Journal of Neuroscience Methods*, *149*(2), 172–177. <https://doi.org/10.1016/J.JNEUMETH.2005.05.014>
- Prömel, S., Langenhan, T., & Araç, D. (2013). Matching structure with function: The GAIN domain of Adhesion-GPCR and PKD1-like proteins. In *Trends in Pharmacological Sciences* (Vol. 34, Issue 8, pp. 470–478). <https://doi.org/10.1016/j.tips.2013.06.002>
- Pula, G., Mundell, S. J., Roberts, P. J., & Kelly, E. (2004). Agonist-independent internalization of metabotropic glutamate receptor 1a is arrestin- and clathrin-dependent and is suppressed by receptor inverse agonists. *J. Neurochem*, *89*, 1009–1020. <https://doi.org/10.1111/j.1471-4159.2004.02387.x>
- Quiroz, J. A., Tamburri, P., Deptula, D., Banken, L., Beyer, U., Rabbia, M., Parkar, N., Fontoura, P., & Santarelli, L. (2016). Efficacy and safety of basimglurant as adjunctive therapy for major depression: A randomized clinical trial. *JAMA Psychiatry*, *73*(7), 675–684. <https://doi.org/10.1001/jamapsychiatry.2016.0838>
- Rajmohan, R., & Reddy, P. H. (2017). Amyloid Beta and Phosphorylated Tau Accumulations Cause Abnormalities at Synapses of Alzheimer's disease Neurons. *Journal of Alzheimer's Disease : JAD*, *57*(4), 975. <https://doi.org/10.3233/JAD-160612>
- Rang, H. P., Dale, M. M., Ritter, J. M., & Flower, R. J. (2007). *Rang and Dale's Pharmacology* (6th ed.). Churchill Livingstone, Elsevier.
- Renner, M., Lacor, P. N., Velasco, P. T., Xu, J., Contractor, A., Klein, W. L., & Triller, A. (2010). Deleterious Effects of Amyloid β Oligomers Acting as an Extracellular Scaffold for mGluR5. *Neuron*, *66*(5), 739–754. <https://doi.org/10.1016/J.NEURON.2010.04.029>
- Ribeiro, F. M., Ferreira, L. T., Paquet, M., Cregan, T., Ding, Q., Gros, R., & Ferguson, S. S. G. (2009). Phosphorylation-independent regulation of metabotropic glutamate receptor 5 desensitization and internalization by G protein-coupled receptor kinase 2 in neurons. *Journal of Biological Chemistry*, *284*(35), 23444–23453. <https://doi.org/10.1074/jbc.M109.000778>
- Ritter-Makinson, S. L., Paquet, M., Bogenpohl, J. W., Rodin, R. E., Chris Yun, C., Weinman, E. J., Smith, Y., & Hall, R. A. (2017). Group II Metabotropic Glutamate Receptor Interactions with NHERF Scaffold Proteins: Implications for Receptor Localization in Brain. *Neuroscience*, *353*, 58. <https://doi.org/10.1016/J.NEUROSCIENCE.2017.03.060>
- Robbins, M. J., Ciruela, F., Rhodes, A., & McIlhinney, R. A. J. (1999). Characterization of the Dimerization of Metabotropic Glutamate Receptors Using an N-Terminal Truncation of mGluR1. *J. Neurochem*, *72*, 2539–2547. <https://doi.org/10.1046/j.1471-4159.1999.0722539.x>
- Roche, K. W., Tu, J. C., Petralia, R. S., Xiao, B., Wenthold, R. J., & Worley, P. F. (1999). Homer 1b regulates the trafficking of group I metabotropic glutamate receptors. *The Journal of Biological Chemistry*, *274*(36), 25953–25957. <https://doi.org/10.1074/JBC.274.36.25953>
- Rodien, P., Brémont, C., Sanson, M.-L. R., Parma, J., Van Sande, J., Costagliola, S., Luton, J.-P., Vassart, G., & Duprez, L. (1998). Familial gestational hyperthyroidism caused by a mutant thyrotropin receptor hypersensitive to human chorionic gonadotropin. *The New England Journal of Medicine*, *339*(25), 1823–1826. <https://doi.org/10.1056/NEJM199812173392505>
- Rodriguez, A. L., Nong, Y., Sekaran, N. K., Alagille, D., Tamagnan, G. D., & Conn, P. J. (2005). A close structural analog of 2-methyl-6-(phenylethynyl)-pyridine acts as a neutral allosteric site ligand on metabotropic glutamate receptor

- subtype 5 and blocks the effects of multiple allosteric modulators. *Molecular Pharmacology*, 68(6), 1793–1802. <https://doi.org/10.1124/mol.105.016139>
- Rohrer, D. K., Desai, K. H., Jasper, J. R., Stevens, M. E., Regula, D. P., Barsh, G. S., Berstein, D., & Kobilka, B. K. (1996). Targeted disruption of the mouse beta1-adrenergic receptor gene: developmental and cardiovascular effects. *Proceedings of the National Academy of Sciences of the United States of America*, 93(14), 7375. <https://doi.org/10.1073/PNAS.93.14.7375>
- Romano, C., Miller, J. K., Hyrc, K., Dikranian, S., Mennerick, S., Takeuchi, Y., Goldberg, M. P., & O'Malley, K. L. (2001). Covalent and noncovalent interactions mediate metabotropic glutamate receptor mGlu5 dimerization. *Molecular Pharmacology*, 59(1), 46–53. <https://doi.org/10.1124/mol.59.1.46>
- Romano, C., Smout, S., Miller, J. K., & O'Malley, K. L. (2002). Developmental regulation of metabotropic glutamate receptor 5b protein in rodent brain. *Neuroscience*, 111(3), 693–698. [https://doi.org/10.1016/S0306-4522\(02\)00042-8](https://doi.org/10.1016/S0306-4522(02)00042-8)
- Romano, C., Yang, W. L., & O'Malley, K. L. (1996). Metabotropic glutamate receptor 5 is a disulfide-linked dimer. *Journal of Biological Chemistry*, 271(45), 28612–28616. <https://doi.org/10.1074/jbc.271.45.28612>
- Rook, J. M., Xiang, Z., Lv, X., Ghoshal, A., Dickerson, J. W., Bridges, T. M., Johnson, K. A., Foster, D. J., Gregory, K. J., Vinson, P. N., Thompson, A. D., Byun, N., Collier, R. L., Bubser, M., Nedelcovych, M. T., Gould, R. W., Stauffer, S. R., Daniels, J. S., Niswender, C. M., ... Conn, P. J. (2015). Biased mGlu5-Positive Allosteric Modulators Provide InVivo Efficacy without Potentiating mGlu5 Modulation of NMDAR Currents. *Neuron*, 86(4), 1029–1040. <https://doi.org/10.1016/j.neuron.2015.03.063>
- Rose, M., Dütting, E., & Enz, R. (2008). Band 4.1 proteins are expressed in the retina and interact with both isoforms of the metabotropic glutamate receptor type 8. *Journal of Neurochemistry*, 105(6), 2375–2387. <https://doi.org/10.1111/J.1471-4159.2008.05331.X>
- Ross, A. H., Baltimore, D., & Eisen, H. N. (1981). Phosphotyrosine-containing proteins isolated by affinity chromatography with antibodies to a synthetic hapten. *Nature*, 294(5842), 654–656. <https://doi.org/10.1038/294654a0>
- Santos, R., Ursu, O., Gaulton, A., Patrícia Bento, A., Donadi, R. S., Bologa, C. G., Karlsson, A., Al-Lazikani, B., Hersey, A., Oprea, T. I., & Overington, J. P. (2017). A comprehensive map of molecular drug targets. *Nature Publishing Group*. <https://doi.org/10.1038/nrd.2016.230>
- Sartorius, L. J., Nagappan, G., Lipska, B. K., Lu, B., Sei, Y., Ren-Patterson, R., Li, Z., Weinberger, D. R., & Harrison, P. J. (2006). Alternative splicing of human metabotropic glutamate receptor 3. *Journal of Neurochemistry*, 96(4), 1139–1148. <https://doi.org/10.1111/j.1471-4159.2005.03609.x>
- Sauer, B. (1994). Site-specific recombination: developments and applications. *Current Opinion in Biotechnology*, 5, 521–527.
- Scarpa, M., Molloy, C., Jenkins, L., Strellis, B., Budgett, R. F., Hesse, S., Dwomoh, L., Marsango, S., Tejada, G. S., Rossi, M., Ahmed, Z., Milligan, G., Hudson, B. D., Tobin, A. B., & Bradley, S. J. (2021). Biased M1 muscarinic receptor mutant mice show accelerated progression of prion neurodegenerative disease. *Proceedings of the National Academy of Sciences of the United States of America*, 118(50). <https://doi.org/10.1073/pnas.2107389118>
- Schools, G. P., & Kimelberg, H. K. (1999). mGluR3 and mGluR5 are the predominant metabotropic glutamate receptor mRNAs expressed in hippocampal astrocytes acutely isolated from young rats. *Journal of*

- Neuroscience Research*, 58(4), 533–543. [https://doi.org/10.1002/\(SICI\)1097-4547\(19991115\)58:4<533::AID-JNR6>3.0.CO;2-G](https://doi.org/10.1002/(SICI)1097-4547(19991115)58:4<533::AID-JNR6>3.0.CO;2-G)
- Schulz, H. L., Stohr, H., & Weber, B. H. F. (2002). Characterization of three novel isoforms of the metabotropic glutamate receptor 7 (GRM7). *Neuroscience Letters*, 326(1), 37–40. [https://doi.org/10.1016/S0304-3940\(02\)00306-3](https://doi.org/10.1016/S0304-3940(02)00306-3)
- Seebahn, A., Dinkel, H., Mohrlüder, J., Hartmann, R., Vogel, N., Becker, C. M., Sticht, H., & Enz, R. (2011). Structural characterization of intracellular C-terminal domains of group III metabotropic glutamate receptors. *FEBS Letters*, 585(3), 511–516. <https://doi.org/10.1016/J.FEBSLET.2010.12.042>
- Seebahn, A., Rose, M., & Enz, R. (2008). RanBPM is expressed in synaptic layers of the mammalian retina and binds to metabotropic glutamate receptors. *FEBS Letters*, 582(16), 2453–2457. <https://doi.org/10.1016/J.FEBSLET.2008.06.010>
- Seeman, P. (2013). Are dopamine D2 receptors out of control in psychosis? *Progress in Neuro-Psychopharmacology and Biological Psychiatry*, 46, 146–152. <https://doi.org/10.1016/J.PNPBP.2013.07.006>
- Seifert, R., & Wenzel-Seifert, K. (2002). Constitutive activity of G-protein-coupled receptors: cause of disease and common property of wild-type receptors. *Naunyn-Schmiedeberg's Archives of Pharmacology*, 366(5), 381–416. <https://doi.org/10.1007/S00210-002-0588-0>
- Sengmany, K., Singh, J., Stewart, G. D., Conn, P. J., Christopoulos, A., & Gregory, K. J. (2017). Biased allosteric agonism and modulation of metabotropic glutamate receptor 5: Implications for optimizing preclinical neuroscience drug discovery. *Neuropharmacology*, 115, 60–72. <https://doi.org/10.1016/j.neuropharm.2016.07.001>
- Seven, A. B., Barros-Álvarez, X., de Lapeyrière, M., Papasergi-Scott, M. M., Robertson, M. J., Zhang, C., Nwokonko, R. M., Gao, Y., Meyerowitz, J. G., Rocher, J. P., Schelshorn, D., Kobilka, B. K., Mathiesen, J. M., & Skiniotis, G. (2021a). G-protein activation by a metabotropic glutamate receptor. *Nature*, 595(7867), 450–454. <https://doi.org/10.1038/s41586-021-03680-3>
- Shaner, N. C., Lambert, G. G., Chammas, A., Ni, Y., Cranfill, P. J., Baird, M. A., Sell, B. R., Allen, J. R., Day, R. N., Israelsson, M., Davidson, M. W., & Wang, J. (2013). A bright monomeric green fluorescent protein derived from *Branchiostoma lanceolatum*. *Nature Methods*, 10(5), 407–409. <https://doi.org/10.1038/nmeth.2413>
- Shigemoto, R., Kinoshita, A., Wada, E., Nomura, S., Ohishi, H., Takada, M., Flor, P. J., Neki, A., Abe, T., Nakanishi, S., & Mizuno, N. (1997). Differential presynaptic localization of metabotropic glutamate receptor subtypes in the rat hippocampus. *The Journal of Neuroscience: The Official Journal of the Society for Neuroscience*, 17(19), 7503–7522. <https://doi.org/10.1523/JNEUROSCI.17-19-07503.1997>
- Shigemoto, R., Nomura, S., Ohishi, H., Sugihara, H., Nakanishi, S., & Mizuno, N. (1993). Immunohistochemical localization of a metabotropic glutamate receptor, mGluR5, in the rat brain. *Neuroscience Letters*, 163(1), 53–57. [https://doi.org/10.1016/0304-3940\(93\)90227-C](https://doi.org/10.1016/0304-3940(93)90227-C)
- Shimomura, O., Johnson, F. H., & Saiga, Y. (1962). Extraction, purification and properties of aequorin, a bioluminescent protein from the luminous hydromedusan, *Aequorea*. *Journal of Cellular and Comparative Physiology*, 59, 223–239. <https://doi.org/10.1002/JCP.1030590302>
- Sivaramakrishnan, S., & Spudich, J. A. (2011). Systematic control of protein interaction using a modular ERK α -helix linker. *PNAS*, 108. <https://doi.org/10.1073/pnas.1116066108/-/DCSupplemental>

- Soave, M., Kellam, B., Woolard, J., Briddon, S. J., & Hill, S. J. (2020). NanoBiT Complementation to Monitor Agonist-Induced Adenosine A1 Receptor Internalization. *SLAS Discovery*, 25(2), 186–194. https://doi.org/10.1177/2472555219880475/ASSET/IMAGES/LARGE/10.1177_2472555219880475-FIG5.JPEG
- Spellmann, I., Rujescu, D., Musil, R., Mayr, A., Giegling, I., Genius, J., Zill, P., Dehning, S., Opgen-Rhein, M., Cerovecki, A., Hartmann, A. M., Schäfer, M., Bondy, B., Müller, N., Möller, H. J., & Riedel, M. (2011). Homer-1 polymorphisms are associated with psychopathology and response to treatment in schizophrenic patients. *Journal of Psychiatric Research*, 45(2), 234–241. <https://doi.org/10.1016/J.JPSYCHIRES.2010.06.004>
- Srinivasan, S., Lubrano-Berthelier, C., Govaerts, C., Picard, F., Santiago, P., Conklin, B. R., & Vaisse, C. (2004). Constitutive activity of the melanocortin-4 receptor is maintained by its N-terminal domain and plays a role in energy homeostasis in humans. *The Journal of Clinical Investigation*, 114(8), 1158–1164. <https://doi.org/10.1172/JCI21927>
- Sterne-Marr, R., Tesmer, J. J. G., Day, P. W., Stracquatano, R. A. P., Cilente, J. A. E., O'Connor, K. E., Pronin, A. N., Benovic, J. L., & Wedegaertner, P. B. (2003). G Protein-coupled Receptor Kinase 2/Gaq/11 Interaction. *Journal of Biological Chemistry*, 278(8), 6050–6058. <https://doi.org/10.1074/JBC.M208787200>
- Stockhaus, J., Nagatani, A., Halfter, U., Kay, S., Furuya, M., & Chua, N.-H. (1992). Serine-to-alanine substitutions at the amino-terminal region of phytochrome A result in an increase in biological activity. *Genes & Development*, 6, 2364–2372.
- Stoppel, L. J., Auerbach, B. D., Senter, R. K., Preza, A. R., Lefkowitz, R. J., & Bear, M. F. (2017). β -Arrestin2 Couples Metabotropic Glutamate Receptor 5 to Neuronal Protein Synthesis and Is a Potential Target to Treat Fragile X. *Cell Reports*, 18(12), 2807–2814. <https://doi.org/10.1016/j.celrep.2017.02.075>
- Stowell, J. N., & Craig, A. M. (1999). Axon/Dendrite Targeting of Metabotropic Glutamate Receptors by Their Cytoplasmic Carboxy-Terminal Domains. *Neuron*, 22(3), 525–536. [https://doi.org/10.1016/S0896-6273\(00\)80707-2](https://doi.org/10.1016/S0896-6273(00)80707-2)
- Strange, P. G. (2008). Agonist binding, agonist affinity and agonist efficacy at G protein-coupled receptors. In *British Journal of Pharmacology* (Vol. 153, Issue 7, pp. 1353–1363). <https://doi.org/10.1038/sj.bjp.0707672>
- Strange, P. G. (2010). Use of the GTP γ S ([35 S]GTP γ S and Eu-GTP γ S) binding assay for analysis of ligand potency and efficacy at G protein-coupled receptors. *British Journal of Pharmacology*, 161(6), 1238. <https://doi.org/10.1111/J.1476-5381.2010.00963.X>
- Su, L. Da, Wang, N., Han, J., & Shen, Y. (2021). Group 1 Metabotropic Glutamate Receptors in Neurological and Psychiatric Diseases: Mechanisms and Prospective. In *Neuroscientist*. <https://doi.org/10.1177/10738584211021018>
- Sugiyama, H., Ito, I., & Hirono, C. (1987). A new type of glutamate receptor linked to inositol phospholipid metabolism. *Nature*, 325(6104), 531–533. <https://doi.org/10.1038/325531A0>
- Szumliński, K. K., Beltran, J., van Doren, E., Leonardo Jimenez Chavez, C., Domingo-Gonzalez, R. D., Reyes, C. M., Ary, A. W., Lang, A., Guo, W., Worley, P. F., & Huber, K. M. (2023). Evidence for Phosphorylation-Dependent, Dynamic, Regulation of mGlu5 and Homer2 in Expression of Cocaine Aversion in Mice. *ENeuro*, 10(4). <https://doi.org/10.1523/ENEURO.0423-22.2023>

- Szumlini, K. K., Dehoff, M. H., Kang, S. H., Frys, K. A., Lominac, K. D., Klugmann, M., Rohrer, J., Griffin, W., Toda, S., Champtiaux, N. P., Berry, T., Tu, J. C., Shealy, S. E., During, M. J., Middaugh, L. D., Worley, P. F., & Kalivas, P. W. (2004). Homer proteins regulate sensitivity to cocaine. *Neuron*, *43*(3), 401–413. <https://doi.org/10.1016/j.neuron.2004.07.019>
- Szumlini, K. K., Herbert, J. N., Mejia Espinoza, B., Madory, L. E., & Scudder, S. L. (2023). Alcohol-drinking during later life by C57BL/6J mice induces sex-and age-dependent changes in hippocampal and prefrontal cortex expression of glutamate receptors and neuropathology markers. *Addiction Neuroscience*, *7*, 100099. <https://doi.org/10.1016/j.addicn.2023.100099>
- Tesmer, V. M., Kawano, T., Shankaranarayanan, A., Kozasa, T., & Tesmer, J. J. G. (2005). Structural biology: Snapshot of activated G proteins at the membrane: The Gαq-GRK2-Gβγ complex. *Science*, *310*(5754), 1686–1690. https://doi.org/10.1126/SCIENCE.1118890/SUPPL_FILE/TESMER.SOM.PDF
- Tessari, M., Pilla, M., Andreoli, M., Hutcheson, D. M., & Heidbreder, C. A. (2004). Antagonism at metabotropic glutamate 5 receptors inhibits nicotine- and cocaine-taking behaviours and prevents nicotine-triggered relapse to nicotine-seeking. *European Journal of Pharmacology*, *499*(1–2), 121–133. <https://doi.org/10.1016/J.EJPHAR.2004.07.056>
- Thal, D. M., Yeow, R. Y., Schoenau, C., Huber, J., & Tesmer, J. J. G. (2011). *Molecular Mechanism of Selectivity among G Protein-Coupled Receptor Kinase 2 Inhibitors*. <https://doi.org/10.1124/mol.111.071522>
- The Dutch-Belgian Fragile X Consortium, Bakker, C. E., Verheij, C., Willemsen, R., van der Helm, R., Oerlemans, F., Vermey, M., Bygrave, A., Hoogeveen, A. T., Oostra, B. A., Reyniers, E., De Boule, K., D’Hooge, R., Cras, P., van Velzen, D., Nagels, G., Martin, J. J., De Deyn, P. P., Darby, J. K., & Willems, P. J. (1994). Fmr1 knockout mice: A model to study fragile X mental retardation. *Cell*, *78*(1), 23–33. [https://doi.org/10.1016/0092-8674\(94\)90569-X](https://doi.org/10.1016/0092-8674(94)90569-X)
- Thomsen, C., Pekhletski, R., Haldeman, B., Gilbert, T. A., O’Hara, P., & Hampson, D. R. (1997). Cloning and Characterization of a Metabotropic Glutamate Receptor, mGluR4b. *Neuropharmacology*, *36*(1), 21–30.
- Tian, X., Kang, D. S., & Benovic, J. L. (2014). β-Arrestins and G protein-coupled receptor trafficking. In *Handbook of Experimental Pharmacology* (Vol. 219, pp. 173–186). https://doi.org/10.1007/978-3-642-41199-1_9
- Tobin, A. B. (2008). G-protein-coupled receptor phosphorylation: Where, when and by whom. *British Journal of Pharmacology*, *153*(SUPPL. 1), 167–176. <https://doi.org/10.1038/sj.bjp.0707662>
- Tobin, A. B., Butcher, A. J., & Kong, K. C. (2008). Location, location, location...site-specific GPCR phosphorylation offers a mechanism for cell-type-specific signalling. In *Trends in Pharmacological Sciences* (Vol. 29, Issue 8, pp. 413–420). <https://doi.org/10.1016/j.tips.2008.05.006>
- Trinh, P. N. H., May, L. T., Leach, K., & Gregory, K. J. (2018). Biased agonism and allosteric modulation of metabotropic glutamate receptor 5. In *Clinical Science* (Vol. 132, Issue 21, pp. 2323–2338). <https://doi.org/10.1042/CS20180374>
- Trinquet, E., Bouhelal, R., & Dietz, M. (2011). Monitoring Gq-coupled receptor response through inositol phosphate quantification with the IP-One assay. *Expert Opinion on Drug Discovery*, *6*(10), 981–994. <https://doi.org/10.1517/17460441.2011.608658>
- Trivedi, R. R., & Bhattacharyya, S. (2012). *Constitutive internalization and recycling of metabotropic glutamate receptor 5 (mGluR5)*. <https://doi.org/10.1016/j.bbrc.2012.09.040>

- Tsuji, Y., Shimada, Y., Takeshita, T., Kajimura, N., Nomura, S., Sekiyama, N., Otomo, J., Usukura, J., Nakanishi, S., & Jingami, H. (2000). *Cryptic Dimer Interface and Domain Organization of the Extracellular Region of Metabotropic Glutamate Receptor Subtype 1**. <https://doi.org/10.1074/jbc.M003226200>
- Tu, J. C., Xiao, B., Naisbitt, S., Yuan, J. P., Petralia, R. S., Brakeman, P., Doan, A., Aakalu, V. K., Lanahan, A. A., Sheng, M., & Worley, P. F. (1999). Coupling of mGluR/Homer and PSD-95 complexes by the Shank family of postsynaptic density proteins. *Neuron*, 23(3), 583–592. [https://doi.org/10.1016/S0896-6273\(00\)80810-7](https://doi.org/10.1016/S0896-6273(00)80810-7)
- Tu, J. C., Xiao, B., Yuan, J. P., Lanahan, A. A., Leoffert, K., Li, M., Linden, D. J., & Worley, P. F. (1998). Homer Binds a Novel Proline-Rich Motif and Links Group 1 Metabotropic Glutamate Receptors with IP3 Receptors. *Neuron*, 21(4), 717–726. [https://doi.org/10.1016/S0896-6273\(00\)80589-9](https://doi.org/10.1016/S0896-6273(00)80589-9)
- Turrigiano, G. (2012). Homeostatic Synaptic Plasticity: Local and Global Mechanisms for Stabilizing Neuronal Function. *Cold Spring Harbor Perspectives in Biology*, 4(1). <https://doi.org/10.1101/CSHPERSPECT.A005736>
- Uehling, D. E., Joseph, B., Chung, K. C., Zhang, A. X., Ler, S., Prakesch, M. A., Poda, G., Grouleff, J., Aman, A., Kiyota, T., Leung-Hagesteijn, C., Konda, J. D., Marcellus, R., Griffin, C., Subramaniam, R., Abibi, A., Strathdee, C. A., Isaac, M. B., Al-Awar, R., & Tiedemann, R. E. (2021). Design, Synthesis, and Characterization of 4-Aminoquinazolines as Potent Inhibitors of the G Protein-Coupled Receptor Kinase 6 (GRK6) for the Treatment of Multiple Myeloma. *Cite This: J. Med. Chem*, 64, 11129–11147. <https://doi.org/10.1021/acs.jmedchem.1c00506>
- Uematsu, K., Heiman, M., Zelenina, M., Padovan, J., Chait, B. T., Aperia, A., Nishi, A., & Greengard, P. (2015). Protein kinase A directly phosphorylates metabotropic glutamate receptor 5 to modulate its function. *Journal of Neurochemistry*, 132(6), 677–686. <https://doi.org/10.1111/jnc.13038>
- Ueno, H., Ito, R., Abe, S. I., Ogino, H., Maruyama, M., Miyashita, H., Miyamoto, Y., Moritoh, Y., Tsujihata, Y., Takeuchi, K., & Nishigaki, N. (2019). GPR40 full agonism exerts feeding suppression and weight loss through afferent vagal nerve. *PloS One*, 14(9). <https://doi.org/10.1371/JOURNAL.PONE.0222653>
- Um, J. W., Kaufman, A. C., Kostylev, M., Heiss, J. K., Stagi, M., Takahashi, H., Kerrisk, M. E., Vortmeyer, A., Wisniewski, T., Koleske, A. J., Gunther, E. C., Nygaard, H. B., & Strittmatter, S. M. (2013). Metabotropic Glutamate Receptor 5 Is a Coreceptor for Alzheimer A β Oligomer Bound to Cellular Prion Protein. *Neuron*, 79(5), 887–902. <https://doi.org/10.1016/j.neuron.2013.06.036>
- Valerio, A., Ferraboli, S., Paterlini, M., Spano, P. F., & Barlati, S. (2001). Identification of novel alternatively-spliced mRNA isoforms of metabotropic glutamate receptor 6 gene in rat and human retina. *Gene*, 262(1–2), 99–106. [https://doi.org/10.1016/S0378-1119\(00\)00547-3](https://doi.org/10.1016/S0378-1119(00)00547-3)
- van Senten, J. R., Møller, T. C., Moo, E. Von, Seiersen, S. D., & Bräuner-Osborne, H. (2022). Use of CRISPR/Cas9-edited HEK293 cells reveals that both conventional and novel protein kinase C isozymes are involved in mGlu5a receptor internalization. *Journal of Biological Chemistry*, 298(10), 102466. <https://doi.org/10.1016/j.jbc.2022.102466>
- Vendruscolo, L. F., Vendruscolo, J. C. M., Whiting, K. E., Acri, J. B., Volkow, N. D., & Koob, G. F. (2024). The mGlu5 receptor negative allosteric modulator mavoglurant reduces escalated cocaine self-administration in male and

- female rats. *Psychopharmacology*, 1–11. <https://doi.org/10.1007/S00213-024-06634-5/FIGURES/4>
- Vincent, K., Cornea, V. M., Jong, Y. J. I., Laferriere, A., Kumar, N., Mickeviciute, A., Fung, J. S. T., Bandegi, P., Ribeiro-Da-Silva, A., O'Malley, K. L., & Coderre, T. J. (2016). Intracellular mGluR5 plays a critical role in neuropathic pain. *Nature Communications* 2016 7:1, 7(1), 1–13. <https://doi.org/10.1038/ncomms10604>
- Wang, J., He, Y., Chen, X., Huang, L., Li, J., You, Z., Huang, Q., Ren, S., He, K., Schibli, R., Mu, L., Guan, Y., Guo, Q., Zhao, J., & Xie, F. (2024). Metabotropic glutamate receptor 5 (mGluR5) is associated with neurodegeneration and amyloid deposition in Alzheimer's disease: A [18F]PSS232 PET/MRI study. *Alzheimer's Research & Therapy*, 16(9). <https://doi.org/10.1186/s13195-024-01385-z>
- Ward, R. J., Alvarez-Curto, E., & Milligan, G. (2011). Using the Flp-In™ T-Rex™ system to regulate GPCR expression. *Methods in Molecular Biology*, 746, 21–37. https://doi.org/10.1007/978-1-61779-126-0_2/FIGURES/4
- Weiss, J. M., Morgan, P. H., Lutz, M. W., & Kenakin, T. P. (1996). The cubic ternary complex receptor-occupancy model. III. resurrecting efficacy. *Journal of Theoretical Biology*, 181(4), 381–397. <https://doi.org/10.1006/JTBI.1996.0139>
- Wenthur, C. J., Gentry, P. R., Mathews, T. P., & Lindsley, C. W. (2014). Drugs for Allosteric Sites on Receptors. *Annual Review of Pharmacology and Toxicology*, 54, 165. <https://doi.org/10.1146/ANNUREV-PHARMTOX-010611-134525>
- Whitaker, M., & Patel, R. (1990). Calcium and cell cycle control. *Development (Cambridge, England)*, 108(4), 525–542. <https://doi.org/10.1242/DEV.108.4.525>
- Winship, I. R., Dursun, S. M., Baker, G. B., Balista, P. A., Kandratavicius, L., Maia-de-Oliveira, J. P., Hallak, J., & Howland, J. G. (2019). An Overview of Animal Models Related to Schizophrenia. *Canadian Journal of Psychiatry. Revue Canadienne de Psychiatrie*, 64(1), 5. <https://doi.org/10.1177/0706743718773728>
- Wong, T. S., Li, G., Li, S., Gao, W., Chen, G., Gan, S., Zhang, M., Li, H., Wu, S., & Du, Y. (2023). G protein-coupled receptors in neurodegenerative diseases and psychiatric disorders. *Signal Transduction and Targeted Therapy* 2023 8:1, 8(1), 1–57. <https://doi.org/10.1038/s41392-023-01427-2>
- Woods, N. M., Cuthbertson, K. S. R., & Cobbold, P. H. (1986). Repetitive transient rises in cytoplasmic free calcium in hormone-stimulated hepatocytes. *Nature* 1986 319:6054, 319(6054), 600–602. <https://doi.org/10.1038/319600a0>
- Wooten, D., Christopoulos, A., & Sexton, P. M. (2013). *Emerging paradigms in GPCR allostery: implications for drug discovery*. <https://doi.org/10.1038/nrd4052>
- Woszczek, G., Fuerst, E., & Maguire, T. J. A. (2021). FLIPR Calcium Mobilization Assays in GPCR Drug Discovery. *Methods in Molecular Biology*, 2268, 193–205. https://doi.org/10.1007/978-1-0716-1221-7_13
- Wreggett, K. A., Lander, D. J., & Irvine, R. F. (1990). Two-stage analysis of radiolabeled inositol phosphate isomers. *Methods in Enzymology*, 191(C), 707–718. [https://doi.org/10.1016/0076-6879\(90\)91043-6](https://doi.org/10.1016/0076-6879(90)91043-6)
- Xia, Y., Xia, Y., Prokop, S., Prokop, S., Prokop, S., Prokop, S., Gorion, K. M. M., Gorion, K. M. M., Kim, J. D., Kim, J. D., Sorrentino, Z. A., Sorrentino, Z. A., Bell, B. M., Bell, B. M., Manaois, A. N., Manaois, A. N., Chakrabarty, P., Chakrabarty, P., Chakrabarty, P., ... Giasson, B. I. (2020). Tau Ser208

- phosphorylation promotes aggregation and reveals neuropathologic diversity in Alzheimer's disease and other tauopathies. *Acta Neuropathologica Communications*, 8(1). <https://doi.org/10.1186/S40478-020-00967-W>
- Xiao, B., Cheng Tu, J., & Worley, P. F. (2000). Homer: a link between neural activity and glutamate receptor function. *Current Opinion in Neurobiology*, 10(3), 370–374. [https://doi.org/10.1016/S0959-4388\(00\)00087-8](https://doi.org/10.1016/S0959-4388(00)00087-8)
- Xu, B., O'Donnell, A. H., Kim, S.-T., & Kastan, M. B. (2002). Phosphorylation of Serine 1387 in Brca1 Is Specifically Required for the Atm-mediated S-Phase Checkpoint after Ionizing Irradiation. *Cancer Research*, 62, 4588–4591. <https://aacrjournals.org/cancerres/article/62/16/4588/509179/Phosphorylation-of-Serine-1387-in-Brca1-Is>
- Xu, C., Zhou, Y., Liu, Y., Lin, L., Liu, P., Wang, X., Xu, Z., Pin, J. P., Rondard, P., & Liu, J. (2024). Specific pharmacological and Gi/o protein responses of some native GPCRs in neurons. *Nature Communications* 2024 15:1, 15(1), 1–14. <https://doi.org/10.1038/s41467-024-46177-z>
- Yan, Q. J., Rammal, M., Tranfaglia, M., & Bauchwitz, R. P. (2005). Suppression of two major Fragile X Syndrome mouse model phenotypes by the mGluR5 antagonist MPEP. *Neuropharmacology*, 49, 1053–1066. <https://doi.org/10.1016/j.neuropharm.2005.06.004>
- Yanagawa, M., Yamashita, T., & Shichida, Y. (2009). Activation Switch in the Transmembrane Domain of Metabotropic Glutamate Receptor. *Molecular Pharmacology*, 76(1), 201–207. <https://doi.org/10.1124/MOL.109.056549>
- Yang, D., Zhou, Q., Labroska, V., Qin, S., Darbalaei, S., Wu, Y., Yuliantie, E., Xie, L., Tao, H., Cheng, J., Liu, Q., Zhao, S., Shui, W., Jiang, Y., & Wang, M. W. (2021). G protein-coupled receptors: structure- and function-based drug discovery. In *Signal Transduction and Targeted Therapy* (Vol. 6, Issue 1). <https://doi.org/10.1038/s41392-020-00435-w>
- Young, S. R., Bianchi, R., & Wong, R. K. S. (2008). Signaling mechanisms underlying group I mGluR-induced persistent AHP suppression in CA3 hippocampal neurons. *Journal of Neurophysiology*, 99(3), 1105–1118. <https://doi.org/10.1152/JN.00435.2007>
- Young, S. R., Chuang, S. C., Zhao, W., Wong, R. K. S., & Bianchi, R. (2013a). Persistent Receptor Activity Underlies Group I mGluR-Mediated Cellular Plasticity in CA3 Neuron. *Journal of Neuroscience*, 33(6), 2526–2540. <https://doi.org/10.1523/JNEUROSCI.3338-12.2013>
- Young, S. R., Chuang, S. C., Zhao, W., Wong, R. K. S., & Bianchi, R. (2013b). Persistent Receptor Activity Underlies Group I mGluR-Mediated Cellular Plasticity in CA3 Neuron. *Journal of Neuroscience*, 33(6), 2526–2540. <https://doi.org/10.1523/JNEUROSCI.3338-12.2013>
- Youssef, E. A., Berry-Kravis, E., Czech, C., Hagerman, R. J., Hessler, D., Wong, C. Y., Rabbia, M., Deptula, D., John, A., Kinch, R., Drewitt, P., Lindemann, L., Marcinowski, M., Langland, R., Horn, C., Fontoura, P., Santarelli, L., Quiroz, J. A., & Study Group, F. (2017). Effect of the mGluR5-NAM Basimglurant on Behavior in Adolescents and Adults with Fragile X Syndrome in a Randomized, Double-Blind, Placebo-Controlled Trial: FragXis Phase 2 Results. *Neuropsychopharmacology*, 43, 503–512. <https://doi.org/10.1038/npp.2017.177>
- Zhang, B., Li, S., & Shui, W. (2022). Post-Translational Modifications of G Protein-Coupled Receptors Revealed by Proteomics and Structural Biology. *Frontiers in Chemistry*, 10, 199. <https://doi.org/10.3389/fchem.2022.843502>
- Zhang, H., Jiang, X., Ma, L., Wei, W., Li, Z., Chang, S., Wen, J., Sun, J., & Li, H. (2022). Role of A β in Alzheimer's-related synaptic dysfunction. *Frontiers in*

Cell and Developmental Biology, 10.

<https://doi.org/10.3389/FCELL.2022.964075>

Zhang, J. H., Chung, T. D. Y., & Oldenburg, K. R. (1999). A Simple Statistical Parameter for Use in Evaluation and Validation of High Throughput Screening Assays. *Journal of Biomolecular Screening*, 4(2), 67–73.

<https://doi.org/10.1177/108705719900400206>

Zhou, X., Vink, M., & Das, A. T. (2006). Optimization of the Tet-On system for regulated gene expression through viral evolution. *Gene Therapy*, 13, 1382–1390. <https://doi.org/10.1038/sj.gt.3302780>